INVESTIGATION OF SELECTED AUTOPHAGIC PROTEINS AND THE EFFECT OF TPSI-GFP EXPRESSION

Mowafag F. Elazzouzi

A thesis submitted in partial fulfilment of the requirements of
Sheffield Hallam University
for the degree of Doctor of Philosophy

أَلَمْ تَرَ أَنَّ اللَّهَ أَنزَلَ مِنَ السَّمَاء مَاء فَأَخْرَجْنَا بِهِ ثَمَرَاتٍ مُّخْتَلِفًا أَلْوَانُهَا وَمِنَ الْجِبَالِ جُدَدٌ بِيضٌ وَحُمْرٌ مُّخْتَلِفٌ أَلْوَانُهَا وَغَرَابِيبُ سُودٌ(27) وَمِنَ النَّاسِ وَالدَّوَابِّ وَالأَنْعَامِ مُخْتَلِفٌ أَلْوَانُهُ كَذَلِكَ إِنَّمَا يَخْشَى اللَّهَ مِنْ عِبَادِهِ الْعُلَمَاء إِنَّ اللَّهَ عَزِيزٌ غَفُورٌ(28) سورة فاطر

Do you not see that Allah sends down rain from the sky, and we produce thereby fruits of varying colors? And in the mountains are tracts, white and red of varying shades and [some] extremely black (27). And among people and moving creatures and grazing livestock are various colors similarly. Only those fear Allah, from among His servants, who have knowledge. Indeed, Allah is Exalted in Might and Forgiving (28). Fatir

Dedication

For my beloved prophet MOHAMED peace be upon him

And also

For Mowafag's family:
father, mother, wife, children, brothers and sisters

Abstract

Normally, the balance between the production and degradation of cellular proteins is necessary for the cell to exist. One of the most important pathways by which the largest number of cytosolic and misfolded proteins is degraded is the autophagy-lysosome pathway. A defect in this process may result in accumulation and aggregation of proteins leading to cellular toxicity and subsequently neurodegenerative diseases. Previous work by Anderson (2003) with a truncated presenillin 1 construct, in HEK293 cell line showed structural changes in the cell in the early stages of autophagy. However, it seems that the autophagic process had failed to clear the presenilin-1 aggregates as would be expected in the normal state and appeared to lead to cell death. The work presented in this thesis primarily attempts to investigate, in term of subcellular localization, the influence of truncated PS1, expressed in HEK293 cells, on selected autophagy regulators (mTOR, raptor and LC3 proteins) and subsequently on the autophagy process.

To investigate this, many different commercial antibodies were characterized against whole cell lysates from three different cell lines (NRK, MCF-7 and HEK293) using western blotting to obtain specific antibodies for mTOR, raptor and LC3. Then, the selected antibodies were used in dual label immunocytochemistry with mitochondrial antibody and wheat germ agglutinin (as a Golgi marker) to determine the subcellular localizations of mTOR, raptor and LC3 in non-autophagic HEK293 cells. To study the behaviour of the proteins of interest during autophagy of untransfected cells, HEK293 cells were rapamycin treated or serum starved. To compare the observed results with the behaviour of the proteins after the transfection, a truncated PS1-GFP construct was transiently transfected into HEK293 cells. Also, the subcellular localizations of the proteins were determined by dual label ICC.

The data obtained suggests that in non-autophagic HEK293 cells, mTOR appears to be localized to mitochondria, raptor to the cytoplasm and LC3 to Golgi apparatus. Rapamycin treatment and serum starvation have the same influence on the behaviour of these proteins. In both cases, mTOR remained localized to mitochondria (no effect), raptor protein partially moved from the cytoplasm to the perinuclear area (similar to mitochondrial distribution) and some of the LC3 protein diffused to the cytoplasm, while most of it remained localized to the Golgi apparatus. Following the transfection, the observable data suggest that interactions between truncated PS1 and mTOR, raptor and LC3 might be occurring. It seems that truncated PS1 has no influence on the subcellular localizations of mTOR and raptor proteins (similar to mitochondrial distribution). However, in the case of LC3 protein, it seems that the protein has partially moved from the Golgi apparatus to interact with truncated PS1 in a new subcellular localization which is similar to the subcellular localizations of mTOR and raptor. The suggested interactions between truncated PS1 and mTOR, raptor and LC3 may dysregulate mTOR signalling pathway, prevent recruitment of mTOR substrates by raptor or block the fusion between autophagosomes and lysosomes via LC3. The results of this thesis indicate that further investigations into the interactions between PS1 and the proteins of interest especially LC3 are warranted.

Table of Contents

List of figures

Chapter 1

Chapter 2

Chapter 3

Chapter 5

Chapter 6

List of tables

Chapter 2

Chapter 3

Abbreviations

4E-BP1	Eukaryotic initiation factor 4E-binding protein 1
AD	Alzheimer's disease
Akt	Protein kinase B (PKB), also known as Akt
Ambra	Activating molecule in Beclin1-regulated autophagy
AMPK	The AMP-activated protein kinase
AP	Alkaline phosphatase
APP	Amyloid precursor protein
APS	Ammonium persulfate
Atg1	Autophagy related gene 1
ATM	Ataxia telangiectasia mutated
Avo1	Adheres voraciously to TOR2 protein 1
Aβ	β-amyloid
BCIP	5-Bromo 4-Chloro 3'-Indolyphosphate p-Toluidine salt
Bcl-2	B-cell lymphoma 2
Bcl-XL	B-cell lymphoma-extra large
BIF-1	Endophilin B1
BIT61	61 kDa binding partner of TOR2 protein
BSA	Bovine serum albumin
CAPS	(3-[cyclohexylamino]-1-propane-sulfonic acid)
CMA	Chaperone-mediated autophagy
DAPI	4,6-Diamidino-2-phenylindole
DMSO	Dimethyl sulfoxide
DTT	Dithiothreitol
EDTA	Ethylenediaminetetraacetic acid
ELISA	Enzyme-linked immunosorbent assay
ER	Endoplasmic reticulum
FAD	Familial Alzheimer's disease
FATC	C-terminal end of the PIK-related kinases
FcRs	Fc receptors
FCS	Foetal calf serum
FIP200	Focal adhesion kinase family interacting protein of 200kDa
FKBP12	FK506 binding protein 12
FKBP38	FK506 bindingprotein 38
FoxO3	Fork head transcription factors of O group
FRAP	FKBP-Rapamycin Associated Protein
FRB	FKBP12-rapamycin binding domain

GABARAP	γ-aminobutyric-acid-type-A ($GABA_A$)-receptor-associated protein
GAP	GTPase Activating Protein
GATE 16	Golgi-associated ATPase enhancer of 16 kDa
GFP	Green Fluorescent protein
GWAS	Genome-wide association studies
GβL	G protein β-like
HD	Huntington's disease
HEAT	Huntington, Elongation Factor 3, PR65/A, TOR
Hu	Human
ICC	Immunocytochemistry
IF	Immunofluorescence
IGF-1	Insulin/insulin-like growth factor
IHC	Immunohistochemistry
IP	Immunoprecipitation
Jnk1	Jun N-terminal kinase 1
kDa	Kilodaltons
KOG1	Kontroller of growth protein 1
Lamp2a	Lysosomal membrane receptor
LB	Luria-Bertani media
LC3	Microtubule-associated protein light chain 3
LST8	Lethal with SEC13 protein 8
MAP	Microtubule-associated protein
MEME	Minimum Essential Medium Eagle
Mk	Monkey
mLST8	Mammalian lethal with SEC13 protein 8
Ms	Mouse
mTOR	Mammalian target of rapamycin
mTORC1	Mammalian target of rapamycin complex 1
mTORC2	Mammalian target of rapamycin complex 2
NBR1	Neighbor Of BRCA1 Gene 1
NBT	Nitro- Blue Tetrazolium
NF-kB	Nuclear factor kappa-light-chain-enhancer of activated B cells
P62/SQSTM1	p62 protein, also called sequestosome 1 (SQSTM1), is a ubiquitin-binding scaffold protein
P70 S6K	S6, ribosomal protein S6; $p70^{S6K}$, 70 kDa S6 kinase
PAS	Pre-autophagosomal structure
PD	Parkinson's disease
PDK1	phosphoinositide-dependent kinase 1

PE	phosphatidylethanolamine
Pg	pig
PI	Phosphatidylinositol
PI3K	Phosphoinositide 3-kinase
PI3P	Phosphatidyl inositol triphosphate
PIKK	Phosphatidylinositol 3-kinase-related kinases
PKB	Protein kinase B
PRAS40	Proline-rich AKT substrate 40 kDa
PRR5	Proline-rich protein 5 (Protor)
PS1	Presenillin 1
PTEN	Phosphatase and tensin homolog
PVDF	Polyvinylidene difluoride
Rab7	RAS-related GTP-binding proteins
Raptor	Regulatory-associated protein of mTOR
Rat	Rat
REDD1	Regulated in development and DNA damage 1
Rheb	Ras homolog enriched in brain
Rictor	rapamycin-insensitive companion of mTOR
RNC	Raptor N-terminal conserved
ROS	Reactive oxygen species
S6K1	Ribosomal protein S6 kinase 1
SDS-PAGE	Sodium Dodecyl Sulphate Polyacrylamide Gel Electrophoresis
Sin1	Stress-activated map kinaseHH-interacting protein 1
siRNA	Small interfering RNA
SOC	Super optimal broth with catabolite repression
TAE	Tris base, acetic acid and EDTA
TBS	Tris-buffered saline
TBST	Tris-buffered saline tween 20
TCO89	89 kDa TOR complex 1 protein
TEMED	tetramethylethylenediamine
TOR	Target of rapamycin
TSC1	Tuberous sclerosis complex gene 1
TSC2	Tuberous sclerosis complex 2
TTRAP	TRAF and TNF receptor-associated protein
Ulk	UNC-51 like kinase
UPS	Ubiquitin -proteasome system
Uth1p	Youth protein 1
UV	Ultraviolet

UVRAG	UV radiation resistance-associated gene protein
VDAC	voltage-dependent anion channel
Vps34	Vesicular protein sorting 34
WB	Western Blot
WD40	WD or beta-transducin repeats are short ~40 amino acid motifs
WGA	Wheat germ agglutinin

Acknowledgment

A PhD study, both autonomous and cooperative, is as much a self-sustained project as it is a learning experience. I may have carried out the greater part of the work described in this thesis myself, but I doubt I would have achieved it without the help and support of a large number of people to whom I should willingly express my sincere gratitude. I will do my best to recall as many as of them here.

First and foremost is, of course, Almighty Allah for all the grants he bestowed on me and making my dreams come true. My supervisor, David Parkinson, has definitely been the leading light throughout the entire research project. Thank you for relentless guidance, unbroken support, inspiration and supplying me with interests, whilst being patient, understanding and diligent. I am immensely grateful to the neuroimmuno group, for valuable advice, suggestion and criticism during monthly meetings.

I would like to kindly acknowledge the generous contribution of David Owen who has dealt with some of my ICC slides and produced some nice confocal pictures. There are a number of PhD fellows who deserve a special mention, to Esadawi Abuneeza, Haytham Dahlawi, Khaled Alshamaki, Yasin Al-luaibi, Natruedee Potiwat, Lisa Ferguson, Umarat Srisawat and Timea Eva Illes-Toth. I am most deeply indebted to them for always making me feel relaxed, being there for an entertainment or coffee or prayer, but most of all for being my dear friends over the last three years.

Also, thank you to Professor Nicola Woodroofe for her valuable advice and support. I wish to extend heartfelt appreciations to Marguerite Lyons, Sarah Nile and Daniel English, I will forever be grateful for your time and kindness shown during my stay in the BMRC. Words of credits should also go to all the members of the BMRC. It has been constantly a pleasant and excellent atmosphere to work in. Thank you to all my friends in Libya; especially Mohamed Shennieb and Abobaker Affan for their financial support during the difficult circumstances after the Libyan revolution.

Lastly but not the least, my family: father, mother, wife, children, brothers and sisters, as always, have been superb. Words can't possibly describe how much tribute I must pay to you for your endless patience, tolerance, care, motivation, support and love. This not only enabled me to survive during the recent terrible events in Libya but also would encourage me to take on any future challenge. Surely, I wouldn't have reached this point without your blessings and herculean sacrifices which I can never repay. Thank you from down deep in my heart and soul.

Chapter 1

General Introduction

1.1 AUTOPHAGY

Autophagy (from the Greek meaning "eating of self ") was first proposed by Christian de Duve over 40 years ago (Glick *et al.*, 2010). This term was based on the observed degradation of mitochondria and other intracellular structures inside the lysosomes of rat liver perfused with glucagon (Deter and De Duve, 1967). The balance between the formation and degradation of cellular proteins is necessary for the cell to exist. The pathways by which the largest number of cytosolic and misfolded proteins is degraded are through the ubiquitin proteasome system (UPS) and autophagy-lysosome pathway (ALP) (Ciechanover, 2005; Rubinsztein, 2006). A fault, problem or lack in either of these processes may result in accumulation and aggregation of proteins leading to cellular toxicity and subsequently neurodegeneration as seen in Parkinson's disease, Alzheimer's disease, Huntington's disease, amyotrophic lateral sclerosis and other related protein conformation disorders (Pan *et al.*, 2008). Despite the importance of autophagy being well recognized in mammalian systems, the important discovery of how autophagy is regulated and executed at the molecular level has been made in yeast (Klionsky, 2007). At the present time, 32 different genes related to autophagy have been identified in yeast (Nakatogawa et al, 2009). Based on how intracellular cargo is delivered to lysosomes, autophagy can be divided into three basic forms: macroautophagy, microautophagy and chaperon-mediated autophagy (Cuervo et al., 2004; Levine and Klionsky, 2004).

Macroautophagy: usually referred to as autophagy, is activated by several stress conditions such as nutrient starvation, toxin exposure, infection or oxidative stress (He and Klionsky, 2009). Autophagy is a multistep process, including the formation of double membrane structures called autophagosomes. After that, the autophagosomes fuse with lysosomes to produce autolysosomes where their contents are degraded by lysosomal enzymes (Takeuchi *et al.*, 2004). At the end, degradation products are

recycled to supply energy and amino acids needed by the cell (Pan et al, 2008). A large number of autophagy related genes have been recognized to work at different stages of the process, one of the most important regulators of the process is mTOR (Mammalian target of rapamycin) which can inhibit autophagy-related gene 1(Atg1) leading to suppression of macroautophagy (Hands et al, 2009).

Microautophagy: unlike macroautophagy, microautophagy happens when the lysosomes directly engulf cytoplasm by invaginating the lysosomal membrane to sequestrate cytosolic components (Garcia-Arencibia *et al.*, 2010).

Chaperone-mediated autophagy: is a process in which a specific protein binds to a molecular chaperone (heat-shock protein, hsp70) to form a complex which subsequently binds to the lysosomal membrane receptor (Lamp2a) leading to the translocation of substrate across the lysosomal membrane (Pan *et al.*, 2008).

1.2 THE BASIC AUTOPHAGY MACHINERY

As summarised in Figure 1.1, autophagy starts with an isolation membrane called a phagophore. Although the exact origin of the phagophore is controversial, it probably arises from the lipid bilayer contributed by the endoplasmic reticulum (ER) and/or the trans-Golgi network and endosomes (Axe *et al.*, 2008). The phagophore increases in size to completely surround and engulf intracellular cargo, such as protein aggregates, ribosomes and organelles, leading to sequestering the cargo in a double-membrane autophagosome (Mizushima, 2007).

The autophagosome then fuses with the lysosome, promoting the degradation of the autophagosomal contents by the acid proteases which are present in the lysosome. After that, via the permeases and transporters of the lysosome, the degradation products such as amino acids are exported back to the cytoplasm for re-use.

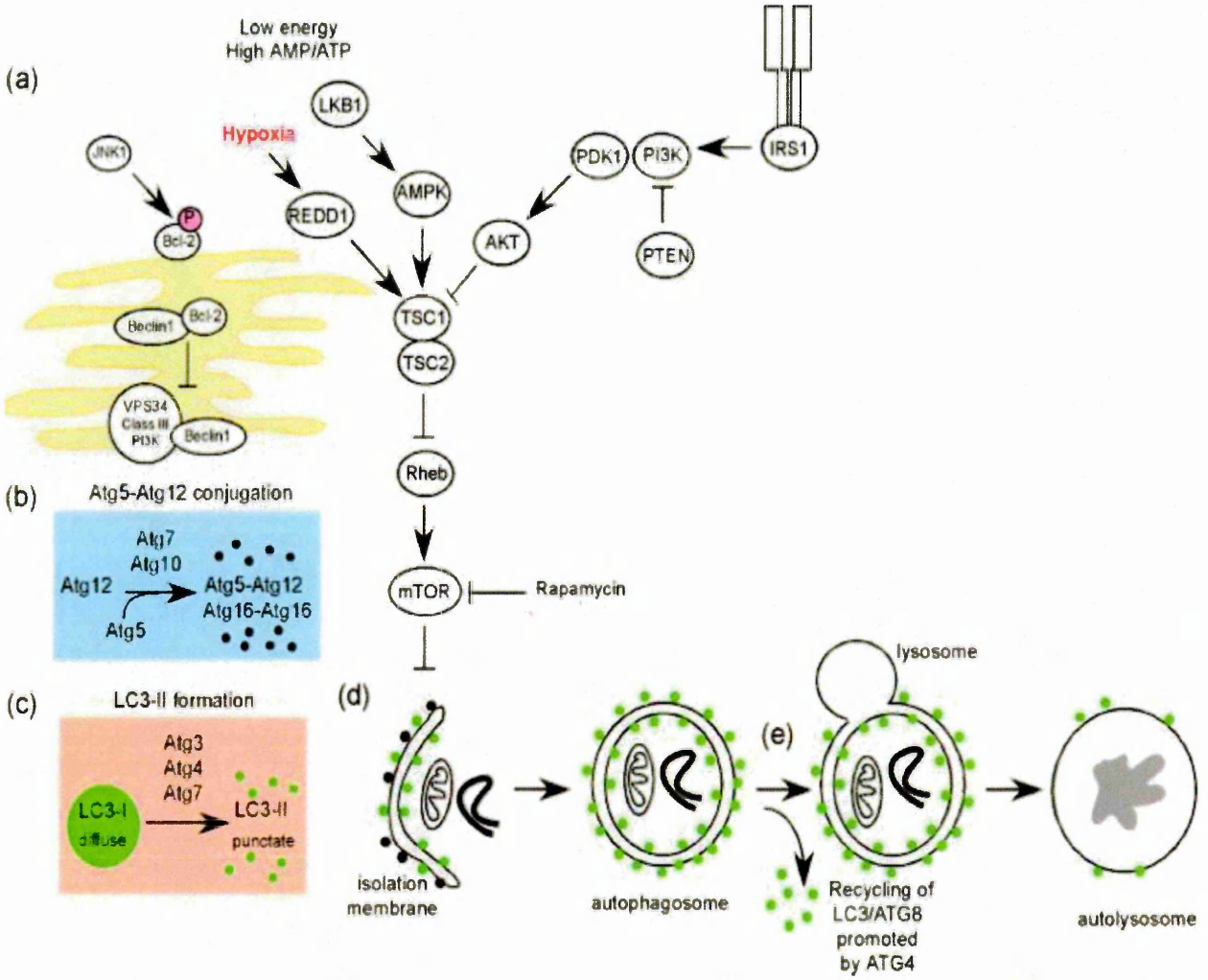

Figure 1.1 Molecular and signalling pathways regulating autophagy. Autophagy is a multistep self-degradative process: (a) regulation of phagophore initiation by Beclin-1/VPS34 at the ER and other membranes under the influence of stress signalling pathways; (b) conjugation of Atg5–Atg12, interaction with Atg16L and multimerization at the phagophore; (c) LC3 processing and insertion into the extending phagophore membrane; (d) catch of random or selective cargo for degradation, elongation and completion of the autophagosome accompanied by recycling of some LC3-II/*ATG8* by *ATG4*, (e) fusion of the autophagosome with the lysosome for cargo degradation by lysosomal proteases (Glick *et al.*, 2010).

Therefore, autophagy is considered as a cellular recycling process that in addition to the degradation of non-functional proteins and organelles can also play an important role in promoting energy efficiency via ATP generation (Mizushima, 2007).

At the molecular level, autophagy can be divided into five main stages which are:

(1) The formation or nucleation of the phagophore.

(2) Atg5-Atg12 conjugation.

(3) Processing of LC3.

(4) Cargo for degradation.

(5) Fusion of autophagosome with the lysosome (Glick *et al.*, 2010).

1.2.1 Formation of the phagophore membrane

In yeast, the formation of the phagophore membrane begins around a cytosolic structure called the pre-autophagosomal structure (PAS). However, in mammals there is no evidence for a PAS (Klionsky, 2007). The formation of the phagophore membrane in mammalian cells appears to start primarily from the ER (Yla-Anttila *et al.*, 2009) in dynamic state of balance with other cytosolic membrane structures, such as the trans-Golgi network and late endosomes (Axe *et al.*, 2008) and possibly even membrane derived from the nuclear envelope under some conditions (English *et al.*, 2009). The ER source is more feasible because it, along with its ribosomes, is involved in protein synthesis. The presence of many Atg proteins close to the ER also suggests that ER plays an important role as a membrane source for autophagosome formation (Hayat, 2015).

However, given the relative lack of transmembrane proteins in autophagosomal membranes, it is not yet possible to completely rule out *de novo* membrane formation

from cytosolic lipids in mammalian cells (Glick *et al.*, 2010). In yeast, during the phagophore formation, the activity of the Atg1 kinase in a complex with Atg13 and Atg17 is required, and this may control the transmembrane protein Atg9 recruitment by encouraging the recruitment of lipid to the expanding phagophore (Klionsky, 2007; Garcia-Arencibia *et al.*, 2010). Energy-sensing TOR kinase has a role to play in controlling this step. TOR kinase phosphorylates Atg13 preventing it from interacting with Atg1 and initiating autophagy sensitive to growth factor and nutrient availability (Glick *et al.*, 2010). More recent data, however, suggest that Atg13 is always in a complex with Atg1 (Kraft *et al.* 2012), which would be in agreement with the interactions of the homologous proteins in higher eukaryotes (Reggiori and Klionsky, 2013).

The mammalian homologue of Atg1 (Ulk-1) is very important for autophagy in maturing reticulocytes (Kundu *et al.*, 2008). However, it still not clears whether Ulk-1 or Ulk-2 (a second Atg1 homologue) has a role in promoting autophagy in mammalian systems (Glick et al., 2010). In mammalian cells, the role of class III Phosphoinositide 3-kinase (PI-3 kinases), especially Vps34 (vesicular protein sorting 34) and it's binding to Atg6/Beclin-1, in the formation of phagophore and autophagy is relatively well established. Vps34 participates in many different membrane sorting processes in the cell but especially in autophagy when connected to Beclin-1 and other regulatory proteins (Backer, 2008).

In addition, regulatory proteins such as uv radiation resistance-associated gene protein (UVRAG), endophilin B1 (BIF-1), Atg14L and activating molecule in Beclin1-regulated autophagy (Ambra) complex with Vps34 and Beclin-1 at the ER and nucleated phagophore to promote autophagy (Liang *et al.*, 2006; Fimia *et al.*, 2007), while other regulatory proteins such as Rubicon and Bcl-2 complex with Vps34 and Beclin-1 to inhibit autophagy (Pattingre *et al.*, 2005; Matsunaga *et al.*, 2009).

Supporting this, recently, among others, UV radiation resistance-associated gene (UVRAG), Bax-interacting factor 1 (Bif-1)/Endophilin B1, Run domain Beclin-1 interacting and cysteine- rich containing protein (Rubicon), activating molecule in Beclin 1 regulated autophagy1 (Ambra1), high-mobility group protein B1(HMGB1), and nuclear receptor-binding factor 2 (NRBF2) have been shown to regulate Beclin-1–VPS34 binding or their participation in autophagic activities (Kang *et al.*, 2011; Wirth *et al.*, 2013; Lu *et al.*, 2014).

Vps34 is the only one amongst the PI3-kinases that using phosphatidylinositol (PI) as substrate to produce phosphatidyl inositol triphosphate (PI3P), which is necessary in the elongation of the phagophore and the recruitment of other Atg proteins such as Atg9 to the phagophore (Xie and Klionsky, 2007; Polson *et al.*, 2010; Tooze *et al.*, 2010; Wirth et al., 2013).

One of the regulatory events that is well-characterized is the interaction of Beclin-1 with Bcl-2, which prevents the interaction of Beclin-1 with Vps34 (Pattingre *et al.*, 2005). Thus, in autophagy, the activity of Beclin-1 is inhibited via it's interaction with Bcl-2 (and Bcl-X_L) at the ER (Maiuri *et al.*, 2007). The interaction between Beclin-1 and Bcl-2 is mediated by the BH3 domain in Beclin-1 and this interaction is prevented through Jnk1-mediated phosphorylation of Bcl-2 in response to starvation-induced signalling, thereby allowing autophagy to proceed (Wei *et al.*, 2008). Thus, Bcl-2 has a dual role to play in the determination of cell viability that may depend on its subcellular position: (a) at the mitochondria, Bcl-2 plays a pro-survival role in inhibiting the release of cytochrome c, thereby blocking apoptosis, while (b) at the ER, it plays a role in the inhibition of autophagy through the interaction with Beclin-1 which can result in non-apoptotic cell death (Pattingre *et al.*, 2005).

The cytoprotective function of autophagy is mediated in many circumstances by negative modulation of apoptosis. Apoptotic signaling, in turn, serves to inhibit autophagy (Gordy and He, 2012). The connection between Beclin-1 and Bcl-2 is not the only way to regulate the crosstalk between autophagy and apoptosis, the cleavage of Atg5 by calpain is another way, where this cleavage blocks the activity of Atg5 in autophagy and results in its translocation to the mitochondria, where interaction with Bcl-XL causes the release of cytochrome c, activation of caspase and finally apoptosis (Yousefi *et al.*, 2006; Gordy and He, 2012).

1.2.2 Atg5-Atg12 conjugation

Ubiquitin is a small (8.5 kDa) regulatory protein that has been found in almost all tissues of eukaryotic organisms (Wilkinson, 2005). Ubiquitination is a post-translational modification where ubiquitin is attached to a substrate protein. The addition of ubiquitin can affect proteins in many ways: It can signal for their degradation via the proteasome, alter their cellular location, affect their activity, and promote or prevent protein interactions (Mukhopadhyay and Riezman, 2007).

Extension of autophagosomal membranes is regulated by 2 ubiquitin-like conjugation pathways, with both LC3 and Atg12 resembling an ubiquitin structure (Geng and Klionsky, 2008). One involves Atg7 and Atg10 acting as E1 and E2 enzymes, sequentially conjugating with Atg12 via glycine-cysteine thioester bonds, eventually conjugating Atg12 to Atg5 at a lysine residue through an isopeptide bond (Glick *et al.*, 2010). Then, the conjugated Atg12- Atg5 binds in pairs with Atg16L dimers in order to produce a multimeric Atg5-Atg12-Atg16L complex association with the extending phagophore (Lee, 2012). The connection of Atg5-Atg12-Atg16L complexes is thought to cause a curvature in the growing phagophore by asymmetric recruitment of processed LC3B-II. This complex associates with the autophagosomal membrane at an early step

and dissociates from the autophagosomes upon completion of autophagy (Barth *et al.*, 2010).

1.2.3 LC3 processing

The second ubiquitination-like reaction involves the conjugation of microtubule-associated protein 1 light chain 3 (MAP1-LC3/Atg8) to the lipid phosphatidylethanolamine (PE). LC3 is cleaved at its C terminus by Atg4 to form the cytosolic LC3-I with exposed carboxyterminal glycine, which is conjugated with PE through the action of Atg7 (E1-like) and Atg3 (E2-like) to generate LC3-II (Tanida *et al.*, 2004). LC3-II is bound to both sides of the membrane of autophagosomes, and it remains membrane bound even after fusion with lysosomes (Tanida *et al.*, 2004). The presence of LC3 on both the internal and external surfaces of autophagosome has a role to play in both hemifusion of membranes and in selecting cargo for degradation (Glick *et al.*, 2010). Then, LC3-II on the cytosolic face of autophagosomes can be recycled (to LC3-I) by Atg4, while the LC3-II on the inner face of the membrane is degraded (Tanida *et al.*, 2004). The increase in LC3 synthesis and processing during autophagy make it a key read-out of autophagy levels in cells (Barth *et al.*, 2010).

1.2.4 Cargo degradation

Generally, autophagy appears to engulf the cytosol indiscriminately. For this reason, it was believed that autophagy is a random process, especially when electron micrographs showed autophagosomes with different contents including ER, mitochondria and Golgi membranes (Eskelinen, 2008). However, much evidence has shown that the growing phagophore membrane has the ability to communicate selectively with protein aggregates and organelles. It has been suggested that ubiquitinated proteins can be re-cognized by adaptor proteins, p62/SQSTM1 (sequestosome 1), NBR1 (neighbour of Brca1 gene 1) NDP52 (nuclear dot protein 52), and Optineurin, through an ubiquitin

associated domain (UBA), and brought to autophagosomes through binding of these adaptor proteins to LC3 via their LC3-interaction regions (LIR) (Johansen and Lamark, 2011; Rogove *et al.*, 2014). In yeast, Uth1p and Atg32 have been recognized to play a role in selective uptake of mitochondria in a process called mitophagy (Kim *et al.*, 2007; Kirkin et al., 2009).

1.2.5 Fusion of the autophagosome with the lysosome

After the fusion of the expanding ends of the phagophore membrane to form an autophagosome, the next step in maturation in this process is fusion with the lysosome to produce an autolysosome (Mizushima, 2007). It has been suggested that before the fusion with the lysosome, the autophagosome fuses with early and late endosomes and both deliver cargo and components of the membrane fusion machinery and decrease the pH of the autophagic vesicle before delivery of lysosomal acid proteases (Eskelinen, 2005). Fusion firstly requires movement of the autophagosome into endosomes or lysosomes along microtubules using dynein-dynactin complex (Ravikumar *et al.*, 2005; Jahresis *et al.*, 2008). Therefore, cytoskeletal complexes are important facilitators of the autophagic process (Lee, 2012), since agents such as nocadazole block the fusion of the autophagosome with the lysosome (Webb *et al.*, 2004). There is some ambiguity about this part of the process. However, this aspect requires the small G protein Rab7 in its GTP-bound state (Gutierrez *et al.*, 2004; Jager *et al.*, 2004), and also the presenilin protein that is involved in Alzheimer's disease (Eskelinen, 2005). It has been shown that mTOR localization to the lysosomes is an important regulator of autophagosomal–lysosomal fusion, and mTOR inhibition by Torin1 stimulates fusion (Zhou *et al.*, 2013). Other components such as microtubules and DNA damage-regulated autophagy modulator 1 (DRAM1) are required for, or promote, autophagosomal-lysosomal fusion (Webb *et al.*, 2004; Zhang *et al.*, 2013).

Within the lysosome, cathepsin proteases B and D are needed for autophagosome turnover and also for autolysosome maturation (Koike *et al.*, 2005). For functional autophagy, Lamp-1 and Lamp-2 in the lysosome are important because it was revealed that deletion of these proteins in mice has an inhibitory effect on the maturation of autolysosomes (Tanaka et al, 2000).

mTOR is an important component of a complex that regulates autophagy through the mTOR complex 1 (mTORC1) composed of mTOR, raptor, mLST8 and PRAS40 (Hara *et al.*, 2002, and Peterson *et al.*, 2009). Raptor acts as a scaffold protein inside the complex, responsible for identifying and binding to the mTORC1 substrates.

1.3 MAMMALIAN TARGET OF RAPAMYCIN (mTOR)

Nutrient starvation, stress, or growth factor deficiencies are conditions that cause eukaryotic cells to change their metabolic processes to survive. One of the first changes in the cellular metabolic processes is inhibition of growth and induction of autophagy to optimize the usage of limited energy supplies. Among the many different components participating in the regulation of autophagy and growth, TOR is a key component that coordinately controls the balance between growth and autophagy in response to cellular physiological conditions and environmental stress (Jung *et al.*, 2010).

1.3.1 mTOR domain structure

TOR is a serine/threonine protein kinase with a large molecular size of approximately 300 kDa (Noda and Ohsumi, 1998; Scott *et al.*, 2004). TOR was first described in 1991 as a target protein of the anti-fungal and immunosuppressant agent rapamycin (Heitman et al., 1991). Rapamycin binds to the FK506 binding protein 12 (FKBP12) to produce a complex that interacts and inhibits many different functions regulated by TOR (Loewith et al., 2006). TOR belongs to the phosphatidylinositol kinase related kinase (PIKK) family (Bhaskar and Hay, 2007; Loewith *et al.*, 2006). Members of the PIKK family

contain a catalytic carboxy-terminal domain that has similarities with the catalytic domains of phosphatidylinositol-3 and phosphatidylinositol-4 kinases (Pattingre *et al.*, 2008). Four functional domains are conserved in TOR proteins including the central FAT [FKBP-Rapamycin Associated Protein (FRAP), Ataxia telangiectasia mutated (ATM), TRAF and TNF receptor-associated protein (TTRAP)] domain, the FRB (FKBP12-rapamycin binding domain) domain, the kinase domain and at the C-terminal part of the protein the FATC domain. It has been suggested that these two domains may interact to expose the catalytic domain. The FATC domain is essential for TOR kinase activity (Pattingre *et al.*, 2008) (Figure 1.2). The inhibition of TOR activity under the influence of nutrient starvation has been considered to be the crucial step for autophagy induction in eukaryotic cells (Noda and Ohsumi, 1998; Scott *et al.*, 2004).

1.3.2 mTOR function

Several studies have demonstrated many important functions of TOR in yeast and higher eukaryotes, placing the TOR protein at a central position in the signalling network that controls cell growth. The function of TOR in yeast and eukaryotic cells includes regulation of translation, metabolism and transcription in response to nutrients and growth factors (Jung *et al.*, 2010). The different cellular functions of TOR have made it a subject of considerable interest in the study of cancer, metabolism, longevity and neurodegenerative diseases.

In yeast, the activity of TOR is controlled by the availability of nutrients such as nitrogen and carbon (Wullschleger et al., 2006). In a similar way, in mammalian cells, the activity of mTOR is regulated by the levels of available amino acids and glucose (Hara *et al.*, 1998; Inoki *et al.*, 2003). The understanding of TOR regulation has significantly increased since the discoveries of TOR binding partners. There are two TOR proteins in *Saccharamyces cerevisiae*; TOR1 and TOR2. The two TOR proteins

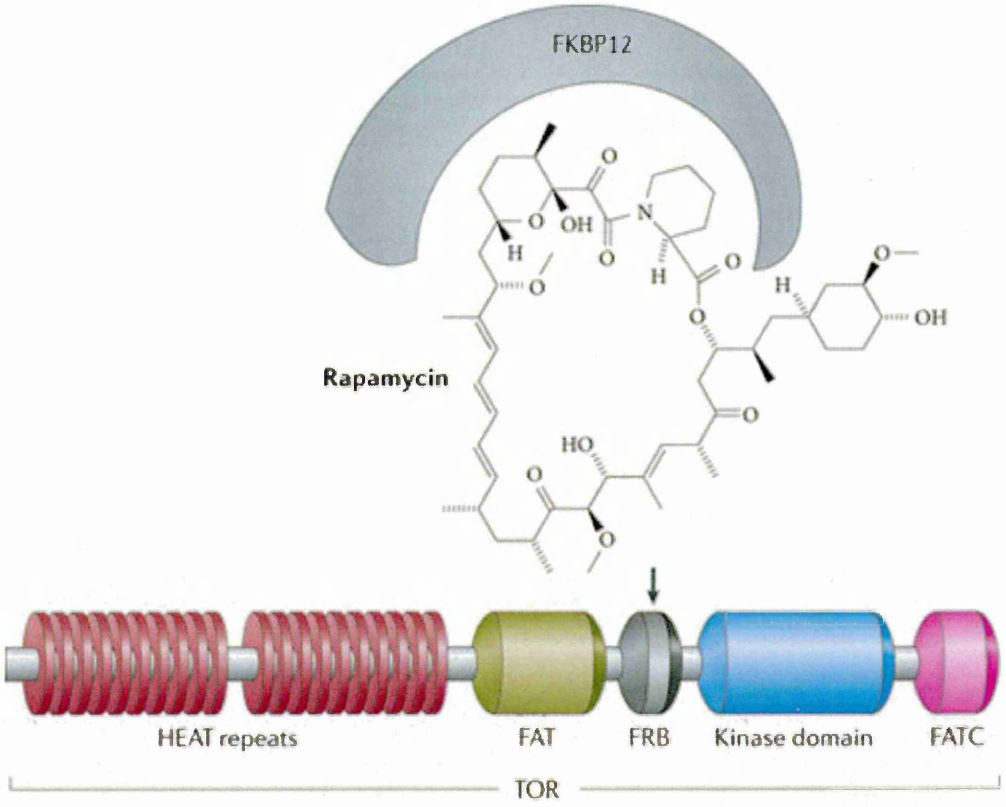

Figure 1.2 Domain structure of TOR.The N-terminus of mTOR composed of tandem HEAT repeats that are required for protein-protein interactions. The C-terminus of the protein contains FAT and FATC domains that modulate the activity of the kinase domain; FAT stands for FRAP, ATM, TRRAP which belong to the same family as TOR, phosphoinositide kinase-related (PIKK) family. In addition FRB domain (FK506-binding protein 12 (FKBP12)-rapamycin binding domain) which is the site where rapamycin binds (Benjamin *et al.*, 2011).

bind to KOG1, LST8 and TCO89, but TOR2 also binds lethal with SEC13 protein 8 (LST8), Avo1, Avo2, Avo3, and 61 kDa binding partner of TOR2 protein (BIT61) to produce a separate protein complex (Wullschleger et al., 2006; Loewith et al., 2002). Similarly, the mammalian target of rapamycin (mTOR) exists in two different complexes: mTORC1 and mTORC2 (Figure 1.3).

mTORC1 is composed of raptor (KOG1 ortholog), which is involved in recruiting substrates for phosphorylation by the kinase domain of mTOR (Wang and Proud, 2011), GβL/mLst8, proline-rich Akt substrate 40 kDa (PRAS40) and DEP domain-containing mTOR-interacting protein (DEPTOR).

mTORC2 (mTOR complex 2) is composed of rapamycin insensitive companion of mTOR (rictor) (Avo3 ortholog), GβL/mLst8, Sin1 (Avo1 ortholog), Proline-rich protein 5 (PRR5)/protor and DEPTOR (Hara et al., 2002, and Peterson et al., 2009).

The TORC1 complex, which contains KOG1, and the mammalian mTORC1, which contains raptor, are key regulators of translation and ribosome biogenesis in yeast and mammalian cells, respectively. They are also responsible for autophagy induction in response to starvation (Jung *et al.*, 2010). On the other hand, mTORC2, the rapamycin-insensitive complex participates in the regulation of phosphorylation and activation of Akt/PKB, protein kinase C, and serum-and glucocorticooid-induced protein kinase 1 (Sarbassov *et al.*, 2005; Garcia-Martinez and Alessi, 2008). Because mTORC1 is positively regulated by Akt, it is possible to speculate that mTORC2 may work as a negative regulator of autophagy. Indeed, autophagy and atrophy in skeletal muscle cells were induced by the inhibition of mTORC2 via fasting condition (Mammucari *et al.*, 2007, and Zhao *et al.*, 2007). However, the induction of autophagy through the inhibition of mTORC2 is mediated mainly by FoxO3, a transcription factor downstream of Akt, which has a role to play in the expression of autophagy genes (Figure 1.3) (Jung *et al.*, 2010).

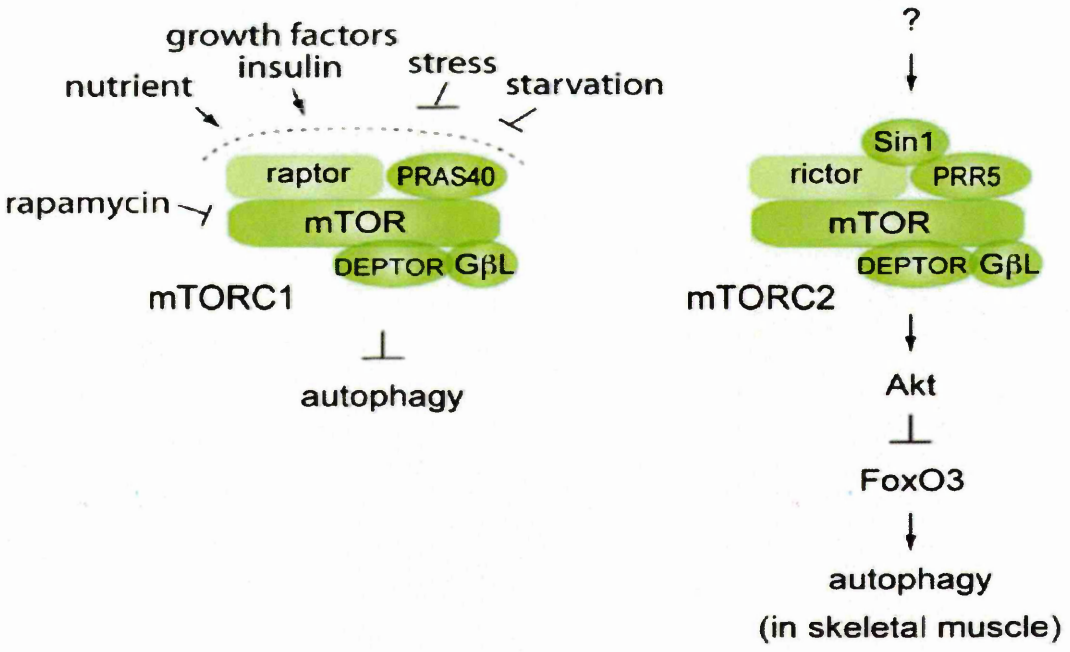

Figure 1.3 mTORC1 and mTORC2 complexes, and their components. mTORC1 is composed of mammalian target of rapamycin (mTOR), regulatory-associated protein of mTOR (raptor), proline-rich AKT substrate 40 kDa (PRAS40), DEP domain-containing mTOR-interacting protein (DEPTOR) and G protein β-like (GβL). mTORC1 is the protein complex that induces autophagy in response to nutrient starvation, stress and reduced growth factor signaling. mTORC2 is composed of mTOR, rapamycin-insensitive companion of mTOR (rictor), proline-rich protein 5 (PRR5), stress-activated map kinaseHH-interacting protein 1(Sin1), DEPTOR and GβL. mTORC2 controls autophagy through protein kinase B (Akt)- Fork head transcription factors of O group (FoxO3) in skeletal muscle cells under fasting condition (Jung *et al.*, 2010).

mTORC1 is also an important mediator of growth factor signalling to activate autophagy. The signalling of the growth factor that controls mTORC1 usually involves the insulin/insulin-like growth factor (IGF-1)-PI3K (phosphoinositide 3-kinase class I)-Akt pathway, which negatively regulates the induction of autophagy (Jung *et al.*, 2010). The pathway of the insulin/IGF-1 involves positive and negative regulators of mTORC1 signalling. The positive regulators include phosphoinositide-dependent kinase 1 (PDK1) and Ras homolog enriched in brain (Rheb), while the negative regulators include phosphatase and tensin homolog (PTEN) and tuberous sclerosis complex 2 (TSC2). TSC2 works in a complex with tuberous sclerosis complex 1 (TCS1) that behaves as a GTPase activating protein (GAP) for the small GTPase Rheb and the activity of GAP is controlled by Akt through the mediation of TSC2 phosphorylation (Manning *et al.*, 2002; Inoki *et al.*, 2002). The Akt-dependent phosphorylation results in dissociation of TSC1/2 from the lysosome, where Rheb is localized and promoting Rheb activation (Menon et al., 2014). Since GTP-bound Rheb is a potent mTORC1 activator, inhibition of TSC1/2 by AKT-dependent phosphorylation results in mTORC1 activation (Saucedo *et al.*, 2003; Stocker *et al.*, 2003).

In addition, Akt directly phosphorylates and inhibits PRAS40, an mTORC1 component that negatively regulates the complex's kinase activity, leading to mTORC1 activation (Vander *et al.*, 2007; Woo *et al.*, 2007; Sancak et al., 2007; Wang *et al.*, 2007).

Autophagy can be also induced by cellular stresses through mTORC1. Low cellular energy levels or hypoxia activate TSC1/2 to inhibit mTORC1 activation. The AMP-activated protein kinase (AMPK) is a sensor of cellular energy levels and is activated by a high AMP/ATP ratio. AMPK phosphorylates TSC2 and presumably increases the TSC1/2 GAP activity (Inoki *et al.*, 2003; Sofer *et al.*, 2005). Moreover, AMPK directly phosphorylates raptor, resulting in decreased mTORC1 activity through allosteric inhibition (Gwinn *et al.*, 2008).

It has been demonstrated that REDD1(regulated in development and DNA damage 1) can participate in the response of mTORC1 and autophagy to the stress in the endoplasmic reticulum (ER) which is connected to the unfolded protein response and inflammatory signalling (Whitney *et al.*, 2009). This gives an impression that there is a tight link between mTOR and mitochondrial function (Kim *et al.*, 2002; Desai *et al.*, 2002). It has been suggested that the inhibitory effect of the reactive oxygen species (ROS) on the mitochondrial function might in some way stimulate the mitochondrial autophagy (mitophagy) in a manner dependent upon mTORC1 (Jung *et al.*, 2010). The discovery that mTORC1 is found in proximity of mitochondria and is inhibited by oxidative stress and mitochondrial dysfunction, raises the possibility that mTORC1 participates in the mechanism through which damaged mitochondria induce autophagy (Kim *et al.*, 2002; Desai *et al.*, 2002).

1.3.2.1 The regulation of autophagy related gene 1 (Atg1) by TOR in yeast

This section will focus on the mTORC1 downstream signalling pathway by which mTORC1 regulates the machinery of autophagy. Firstly, how does TOR regulate the autophagy machinery in yeast? The first signalling component downstream of TOR in the pathway of autophagy is Atg1, an evolutionarily-conserved serine/threonine kinase (Jung *et al.*, 2010). Atg1 has an important role to play which may be the most upstream step in the initial stages of autophagy induction such as the nucleation (the early event when membrane structures are initiated) and formation of the pre-autophagosome structures (PAS) (Noda and Ohsumi, 1998; Straub *et al.*, 1997, Matsuura *et al.*, 1997).

In yeast, based on the nutrient status or TOR activity, Atg1 interacts with autophagy proteins such as Atg13, Atg17, Atg29 and Atg31 (Kamada *et al.*, 2000; Funakoshi *et al.*, 1997; Kawamata *et al.*, 2008, Kabeya *et al.*, 2005; Kabeya *et al.*, 2009) (Figure 1.4a). Activation of Atg1 and induction of autophagy require Atg13 (Kamada *et al.*, 2000).

Atg17 is very important for Atg1 and other autophagy proteins to be localized on the PAS (Suzuki *et al.*, 2007; Sekito *et al.*, 2009). Under nutrient starvation, Atg17 interacts with other autophagy components such as Atg1, Atg13, Atg29 and Atg31, but the interaction between Atg13 and Atg17 is essential for Atg1 kinase activity and autophagosome formation (Figure 1.4a) (Kabeya *et al.*, 2005; Cheong *et al.*, 2005). In addition, Atg17 plays an important role by recruiting Atg9 to the PAS in a manner dependent upon Atg1 (Sekito *et al.*, 2009).

In yeast, Atg13 is phosphorylated by TOR at a number of residues leading to the decrease of the affinity between Atg1 and its binding proteins resulting in autophagy repression (Kamada *et al.*, 2000; Kawamata *et al.*, 2008; Kabeya *et al.*, 2005). Following the inhibition of TOR activity by nutrient starvation, Atg13 is de-phosphorylated and the hypo-phosphorylated form of the protein acts to stimulate Atg1, Atg17 and other important autophagy factors to be localized on the PAS (Kamada et al., 2010). The interaction between the three important autophagy components (Atg1, Atg13 and Atg17) under the influence of rapamycin treatment or nutrient starvation enhances the kinase activity of Atg1 that is required for autophagosome formation. It has been suggested that the Atg1 complex is an important node of the signalling pathway through which TOR triggers the events of autophagy in yeast (Jung et al., 2010).

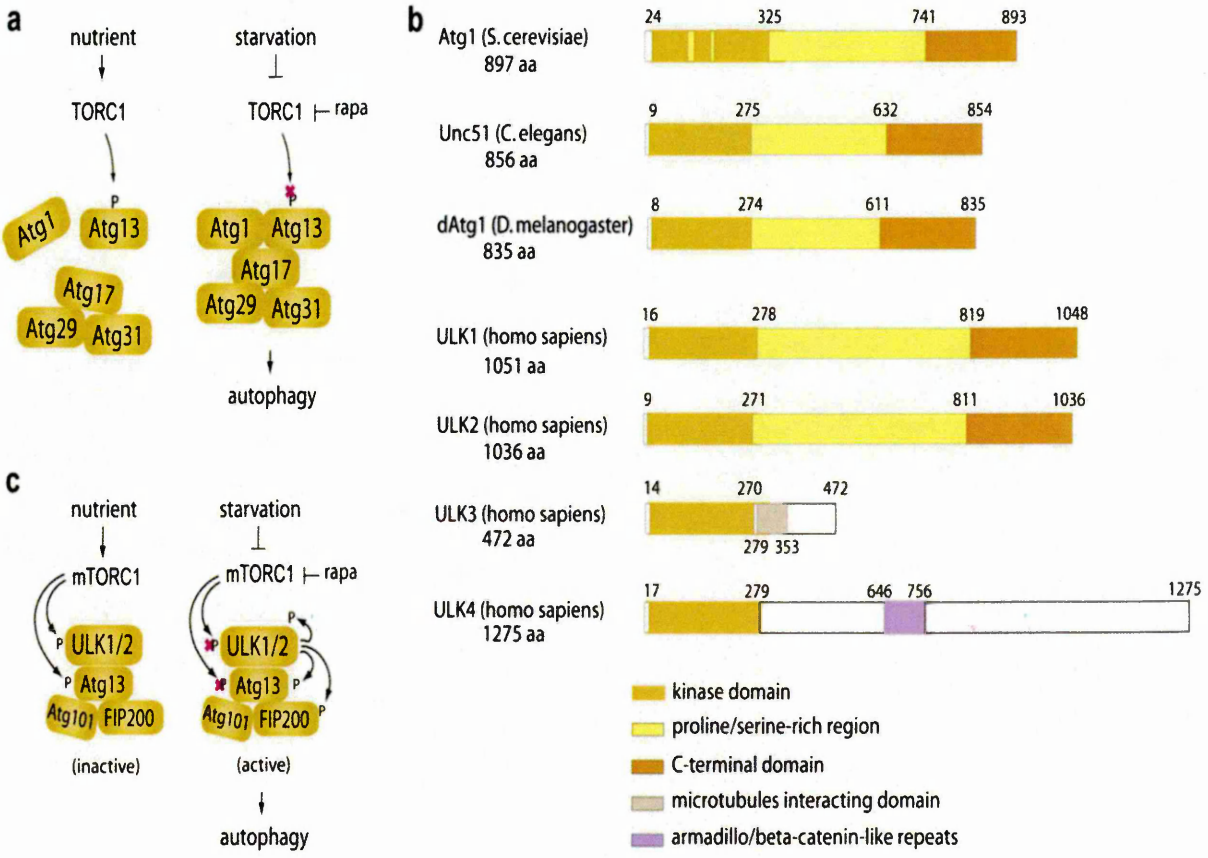

Figure 1.4 Comparison of the autophagy related gene 1(Atg1)/ UNC-51 like kinase (ULK) machinery between yeast and higher eukaryotes. (a) Current model for the regulation of Atg1 complex by TOR in *S. cerevisiae*. Atg13 phosphorylated at multiple residues by TOR leading to autophagy inhibition because of the disruption of the complex. (b) Comparison of the domain structures of *S. cerevisiae* Atg1, *C. elegans* UNC51, *D. melanogaster* Atg1, and *Homo sapiens* ULK1, ULK2, ULK3 and ULK4. (c) Regulation of phosphorylation of ULK1/2 complexes via mTORC1under the influence of nutrient levels. mTORC1 phosphorylates ULK1/2 and Atg13 and inhibits the kinase activity of ULK1/2 under high nutrient conditions. Under starvation, mTORC1 suppresses the phosphorylation of ULK complex, releasing ULK from mTORC1 inhibition, which subsequently induces ULK to phosphorylate Atg13, focal adhesion kinase family interacting protein of 200kDa (FIP200) and itself (Jung *et al.*, 2010).

1.3.2.2 The regulation of mammalian Atg1 (ULK) by mTOR

In mammalian cells, the counterpart of Atg1 is known as ULK (UNC-51 like kinase). The first member of the ULK family proteins (ULK1) was recognized as a homologue of *C.elegans* UNC-51, the gene named following a mutational phenotype "UNCoordinated locomotion" connected with defects in the mutant worm (Yan *et al.*, 1998; Kuroyanagi *et al.*, 1998). After that, ULK2 was recognized in mouse as a second member of the gene family and cloned (Yan *et al.*, 1999). The structure of the domain demonstrated unique features having the N-terminal kinase domain, the middle proline/serine-rich domain, and the C-terminal domain involved in protein-protein interaction (Figure 1.4b). The sequence similarity between ULK1 and *C.elegans* UNC-51 is 41%, and the sequence similarity between ULK1 and *S. Cerevisiae* Atg1 is 29%. In regard to ULK2, it demonstrates 33% amino acid identity to UNC-51 (Kabeya *et al.*, 2005).

There are at least two additional Atg1 homologues in the human genome: ULK3 and ULK4. There is no proline/serine-rich region in the middle of both ULK3 and ULK4 similar to that of ULK1 and ULK2. Also, the C-terminal domain that is present in ULK1 and ULK2 are missing in both ULK3 and ULK4. The middle region in ULK3 is predicted to interact with microtubules, and the middle region of ULK4 contains a protein-protein interaction motif of armadillo/beta-catenin-like repeats (Figure 1.4b) (Jung *et al.*, 2010). The C-terminal regions of ULK3 and ULK4 are completely different from ULK1 and ULK2. However, the kinase domains of ULK3 and ULK4 demonstrate high sequence similarity, 52% and 41% to that of ULK1, respectively (Jung et al., 2010).

It has been revealed that ULK1, ULK2 and ULK3 participate in the pathways of autophagy (Chan *et al.*, 2007; Young *et al.*, 2009). It has also been demonstrated that ULK1 is recognized as a kinase that has the ability to control autophagy (Chan *et al.*,

2007). In addition, a study by Hara *et al* (2008) revealed that overexpression of the kinase-dead mutants of ULK1 and ULK2 resulted in autophagy suppression in NIH3T3 mouse embryonic fibroblasts. Furthermore, a study utilizing HeLa and HEK293 cells has shown that when ULK1 and ULK2 were silenced from these cells, the activity of the autophagy process in the cells was inhibited (Jung *et al.*, 2009). In terms of colocalisation, a study has revealed that ULK3 is co-localized with Atg12, the ubiquitin-like protein participates in the production of the autophagic isolation membrane under the influence of reduced amino acid levels and serum depletion (Young *et al.*, 2009).

The limited information about Atg13, Atg17, Atg29 and Atg31 homologues in mammalian cells has made the autophagy induction mechanisms difficult to study. A putative mammalian homologue of Atg13 was predicted by a gapped-blast homologue search (Meijer *et al.*, 2007). Different studies have demonstrated that the predicted mammalian homologue of Atg13 interacts with ULK1 and ULK2 and plays a crucial role in the formation of autophagosomes (Jung *et al.*, 2009; Chan *et al.*, 2009; Mercer *et al.*, 2009) (Figure 1.4c).

It has been proposed that FIP200 (focal adhesion kinase family interacting protein of 200kDa) is a counterpart of Atg17 in mammalian cells. The protein was recognized as one that interacts with ULK1 and ULK2 and plays an essential role in the process of autophagosome formation (Hara *et al.*, 2008) (Figure 1.4c). FIP200 performs the same function as Atg17 in yeast; however, they have little sequence similarity (Hara *et al.*, 2008). A recently identified protein named ATG101 appears to bind to Atg13 (Mercer *et al.*, 2009; Hosokawa *et al.*, 2009) (Figure 1.4c). It was shown that ATG101 interacts with ULK1 in an ATG13-dependent manner and plays an important role in the formation of autophagosomes (Mercer *et al.*, 2009; Hosokawa *et al.*, 2009).

Many research groups have demonstrated that mTOR, similar to yeast TOR, has the ability to phosphorylate mammalian ATG13 (Jung *et al.*, 2009; Ganley *et al.*, 2009; Hosokawa *et al.*, 2009). Certainly, mTORC1 could phosphorylate not only ATG13 but also ULK1 and ULK2 *in vitro* (Jung *et al.*, 2009; Ganley *et al.*, 2009; Hosokawa *et al.*, 2009) (Figure 1.4c). It has been shown that mTORC1 inhibition by rapamycin or starvation, the process known to induce autophagy, has led to de-phosphorylation of ULK1, ULK2 and ATG13 in human cells (Jung *et al.*, 2009; Ganley *et al.*, 2009; Hosokawa *et al.*, 2009). Based on the results obtained from these studies, it has been suggested that ULK1, ULK2 and ATG13 would be direct effectors of mTORC1. On the other hand, FIP200 phosphorylation inversely correlated with mTORC1 activity (Jung *et al.*, 2009). This inverse relationship implies that the phosphorylation of FIP200 is stimulated when ULK1 and ULK2 are in active forms. Certainly, ULK1 and ULK2 could phosphorylate FIP200 *in vitro* (Jung *et al.*, 2009). In addition, the binding between ULK1, ULK2 and ATG13 was essential for the phosphorylation of FIP200 by ULK1 and ULK2 in cells, and therefore suggests that the interaction between FIP200 and ULK via ATG13 is necessary for the phosphorylation of FIP200 by ULK (Jung *et al.*, 2009).

The interaction between Atg1 and Atg13 is regulated by nutrient starvation in yeast. However, in mammalian cells, the interaction between ULK1 and ATG13 is not affected by starvation or rapamycin treatment (Jung *et al.*, 2009; Hosokawa *et al.*, 2009) (Figure 1.4c). It has been revealed that the association between mTORC1 and ULK1 complex is very strong under nutrient-enriched conditions (Hosokawa *et al.*, 2009).

This result is in agreement with the findings that mTORC1 stimulates ULK1 phosphorylation under nutrient-enriched conditions (Jung *et al.*, 2009; Ganley *et al.*, 2009; Hosokawa *et al.*, 2009). So, it has been suggested that the recruitment of ULK1

complex to mTORC1 under nutrient-enriched conditions may facilitate the phosphorylation of ULK1 complex by mTOR resulting in inhibition of ULK1 function (Jung *et al.*, 2010).

In yeast, TOR stimulates hyperphosphorylation of Atg13 and inhibits the kinase activity of Atg1 (Kamada *et al.*, 2000), so, it was expected that a similar mechanism would occur with the mammalian homologues. In mammalian cells, mTORC1 phosphorylates Ser758 (Ser757 in mouse) of ULK1, preventing the interaction and phosphorylation of ULK1 by AMPK, which is essential for ULK1 activation. Thus, the initiation of autophagy by ULK is reciprocally regulated by mTORC1 and AMPK in response to dynamic changes in cellular nutrients and energy levels (Kim *et al.*, 2011). In addition, another layer of ULK1 regulation by mTORC1 has been suggested in which mTORC1 inhibits ULK1 stability by inhibitory phosphorylation of autophagy/beclin 1 regulator 1 (AMBRA1) (Nazio *et al.*, 2013).

Indeed, mTOR regulated the kinase activity of ULK1 and ULK2 (Hara *et al.*, 2008; Jung *et al.*, 2009; Ganley *et al.*, 2009; Hosokawa *et al.*, 2009) (Figure 1.4c). It has been demonstrated that inhibition of mTOR by leucine deprivation or rapamycin treatment has led to enhance the kinase activity of ULK1 and ULK2 and stimulates the phosphorylation of ATG13 and FIP200 and autophosphorylation of ULK under starvation conditions (Jung *et al.*, 2009; Ganley *et al.*, 2009; Hosokawa *et al.*, 2009).

On the other hand, the kinase activity of ULK1 was reduced when mTORC1 was activated by overexpression of Rheb (Jung *et al.*, 2009; Ganley *et al.*, 2009; Hosokawa *et al.*, 2009). In line with these results, ULK-dependent phosphorylation of FIP200 as well as ULK autophosphorylation became more apparent under the condition of mTORC1 inhibition. These findings support the notion that mTORC1 has the ability to

regulate the kinase activity of ULK and thereby mTORC1 is able to suppress the induction of autophagy (Jung *et al.*, 2010) (Figure 1.4c).

In regard to ULK function and cellular localization, it has been suggested that mTORC1 might regulate the function of ULK through altering its cellular localization. Several studies have revealed that inhibition of mTORC1 by nutrient starvation has promoted the localization of ULK1, ULK2 and ATG13 to the autophagic isolation membrane (Scott *et al.*, 2007; Chan *et al.*, 2007; Chan *et al.*, 2009; Hosokawa *et al.*, 2009). In support of this result, a study utilizing HeLa cells revealed that, following rapamycin treatment, ULK1 accumulated in membrane fractions of the cells (Jung *et al.*, 2009). All the studies mentioned above have emphasised that ULK complexes work as a crucial node through which nutrient and growth factor signalling and stress response pathways are transmitted to the autophagy process via mTORC1.

1.4 REGULATORY ASSOCIATED PROTEIN OF mTOR (RAPTOR)

mTOR, when connected to raptor, mLST8 and PRAS40, forms the mTOR Complex 1 (mTORC1) (Kim *et al.*, 2002; Loewith *et al.*, 2002; Vander Haar *et al.*, 2007; Sancak *et al.*, 2007). Raptor works as a scaffold protein inside the complex, and is responsible for identifying and binding to the substrates of mTORC1 (Hara *et al.*, 2002; Schalm *et al.*, 2003). mTORC1 receives signals derived from growth factors, energy and nutrient levels to regulate the activity and phosphorylation of two crucial downstream substrates which participate in the translation of the protein, known as ribosomal protein S6 kinase 1(S6K1) and eukaryotic initiation factor 4E-binding protein 1(4E-BP1). Low levels of cellular amino acids down regulate mTORC1 signalling, which decreases the synthesis of the protein and stimulates the process of autophagy (Dunlop *et al.*, 2011).

1.4.1 Raptor structure

All raptor homologues have an N-terminal domain known as RNC (for raptor N-terminal conserved) that consists of three blocks with at least 67% - 79% sequence similarity (Kim *et al.*, 2002). Following the RNC domain, all raptor homologues have three HEAT repeats, which are then followed by seven WD40 repeats (WD or beta-transducin repeats are short ~40 amino acid motifs) in the C-terminal third of the protein (Figure 1.5) (Kim *et al.*, 2002; Yonezawa *et al.*, 2004). It has also been reported that human and mouse raptor exhibited 96.9% identity in the amino acid sequence (Yonezawa *et al.*, 2004).

1.4.2 Raptor function

Raptor serves as a scaffold for the mTOR signalling pathway (Hara *et al.*, 2002). It has been revealed that over expression of recombinant mTOR in HEK293 cells showed 5-6 times higher kinase activity toward 4EBP1 *in vitro* when coexpressed with raptor (Hara *et al.*, 2002). This result demonstrates that raptor must be continuously connected with mTOR to enhance the kinase activity of mTOR toward 4EBP1 (Hara *et al.*, 2002). The same study also revealed that reduction in the expression of endogenous raptor by RNA interference led to reduction in the mTOR-catalyzed 4EBP1 phosphorylation *in vitro*, supporting the key role of raptor in the signalling pathway of mTOR. In a similar way, the kinase activity of mTOR toward P70α also increased in the presence of raptor *in vitro*, and this enhancement is lost when raptor is reduced *in vitro* (Hara *et al.*, 2002).

Independently of its connection with mTOR, the raptor polypeptide is able to bind directly to 4EBP1 and P70α (Hara *et al.*, 2002). mTOR has the ability to enter a ternary complex with raptor and either 4EBP1 or P70α. This supports the notion that raptor works as a scaffold for mTOR and positively regulates the reaction of mTOR kinase toward 4EBP1 and P70α (Hara *et al.*, 2002).

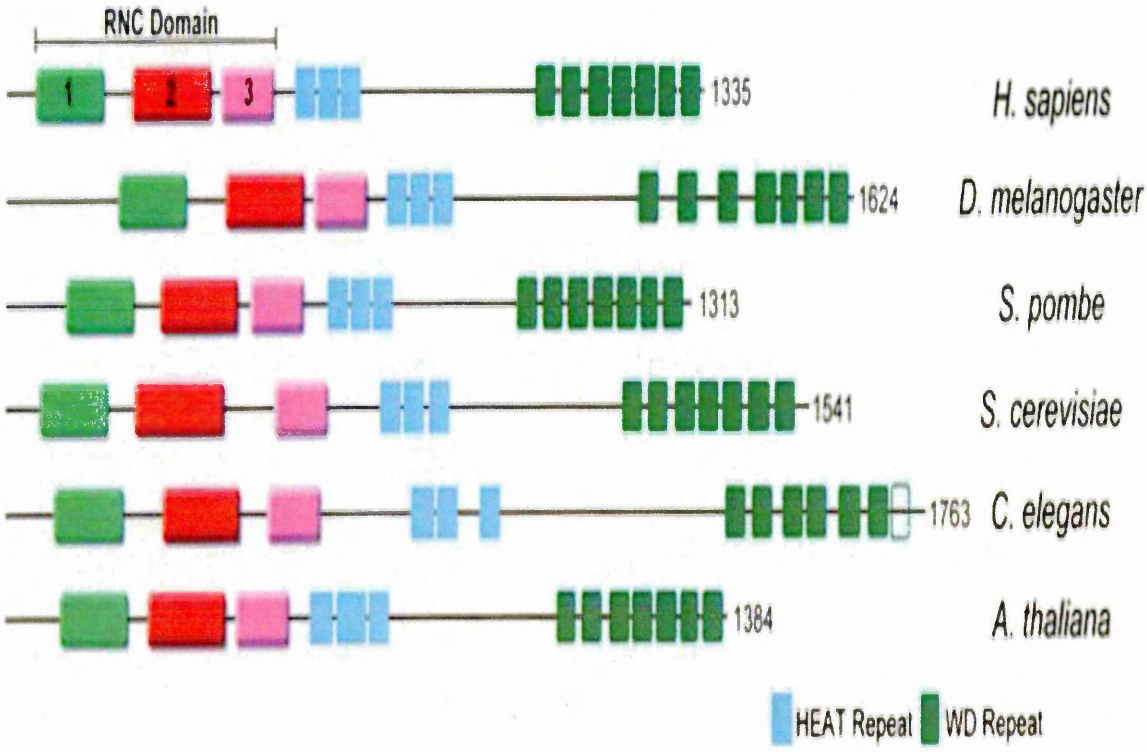

Figure 1.5 Raptor and its homologues. The N-terminal domain of all raptor homologues known as RNC domain. RNC stands for raptor N-terminal conserved, and consists of three blocks with at least 67% - 79% sequence similarity. In addition to RNC, all raptor homologs contain three HEAT (Huntington, Elongation Factor 3, PR65/A, TOR) repeats followed by seven WD40 repeats in the C-terminal third of the protein. The accession numbers for the raptor homologs are: *D. melanogaster* (AAF46122), *S. pombe* (P87141), *S. cerevisiae* (P38873), *C. elegans* (T19183), and *A. Thaliana* (NP_187497) (Kim *et al.*, 2002).

Raptor mediates mTOR signalling pathway in intact cells (Hara *et al.*, 2002). Overexpression of raptor unexpectedly led to dose-dependent inhibition of the phosphorylation and activation of 4EBP1 and P70α respectively. In addition, a deletion mutant of raptor lacking the C-terminal 437 residues including WD repeat also caused similar inhibitory effects (Hara *et al.*, 2002).

Scaffold protein when overexpressed usually leads to inhibition of signalling *in vivo*. This occurs because the excess scaffold may associate with incomplete sets of signalling elements, causing an uncoupling of signal transmission (Hara *et al.*, 2002). Hara *et al* (2002) revealed that mutant raptor does not bind mTOR and binds only weakly to 4EBP1. Thus, the inhibitory effect of overexpressed mutant raptor (and possibly wild type raptor) may not be caused by binding to mTOR or 4EBP1 and thereby disrupting the ternary signalling complex of mTOR-raptor-4EBP1; rather, mutant and wild-type raptor may sequester an unknown molecule that is essential for the intact mTOR signalling pathway, and this may occur by binding via the highly conserved regions in the N-terminus (Hara *et al.*, 2002).

As reported above in the mTOR section 1.3.2.1, in yeast, Atg1 forms a complex with Atg13, Atg17, Atg29 and Atg31, (Funakoshi *et al.*, 1997; Kamada *et al.*, 2000) and plays an initial role in the induction of autophagy. The mammalian complex which is equivalent to this yeast complex consists of ULK1, ATG13, FIP200 and ATG101 (Hosokawa *et al.*, 2009; Mercer *et al.*, 2009). Also, as mentioned above, ULK1 is a serine/threonine kinase which promotes autophagy signalling. It has been shown that the association between mTORC1 and ULK1-ATG13-FIP200 complex occurs through the binding of raptor with ULK1 (Hosokawa *et al.*, 2009; Lee *et al.*, 2010a). It has also been revealed that through raptor interaction with ULK1-ATG13-FIP200 complex, mTORC1 phosphorylates both ULK1 and ATG13, which represses the kinase activity

of ULK1 (Hosokawa *et al.*, 2009; Jung *et al.*, 2009; Ganley *et al.*, 2009). Thus, when amino acids are available and mTORC1 is active, autophagy is inhibited as a consequence of ULK1 inhibition by mTORC1-mediated phosphorylation. Conversely, under conditions of starvation or mTORC1 downregulation, mTORC1 de-phosphorylates ULK1, and as a result, ULK1 is activated by autophosphorylation. Thereby, allowing the phosphorylation of ATG13 and FIP200 by ULK1 and initiation of autophagy (Dunlop *et al.*, 2011).

Biochemical changes between anabolic processes such as protein synthesis and catabolic processes such as autophagy in cells must be tightly regulated. Two studies have shown that ULK1 negatively controls S6K1 in Drosophila (Lee *et al.*, 2007; Scott *et al.*, 2007) and mammalian cells (Lee *et al.*, 2007), suggesting a possible crosstalk between ULK1 and the mTORC1 pathway (Dunlop *et al.*, 2011). This suggests that there is a complex interplay of signal transduction between mTORC1 and the autophagic ULK1-ATG13-FIP200 complex, which coordinates whether protein synthesis or autophagy becomes dominant (Dunlop *et al.*, 2011). It has been revealed that following ULK1 overexpression in HEK293 cells, ULK1 has directly phosphorylated raptor on multiple sites and inhibited the signalling of mTORC1 by impeding substrate binding. For this reason, while mTORC1 represses ULK1 and autophagy induction during nutrient sufficiency, a negative feedback loop was proposed. It has been proposed that ULK1 induces the phosphorylation of raptor, impairs docking of substrate to raptor and represses the signalling of mTORC1 during nutrient limitation (Dunlop *et al.*, 2011).

1.5 MICROTUBULE-ASSOCIATED PROTEIN 1 LIGHT CHAIN 3 (LC3)

LC3 was recognised originally as a protein that co-purified with microtubule-associated protein (MAP) 1A and 1B from rat brain (Mann and Hammarback, 1994). LC3 shows

28% amino acid identity with Atg8 which is essential for yeast autophagy (Liang *et al.*, 1999). A study of Atg8 has suggested that the protein plays a crucial role in autophagosome formation (Kirisako *et al.*, 1999). At least three families of mammalian Atg8-related proteins have been identified: microtubule-associated protein 1 light chain 3 (LC3); Golgi-associated ATPase enhancer of 16 kDa (GATE 16); and γ-aminobutyric-acid-type-A ($GABA_A$)-receptor-associated protein (GABARAP). Each family sometimes has subfamilies, and three human LC3 subfamilies (LC3A, LC3B and LC3C) have been identified (He *et al*, 2003). LC3 localizes to autophagosomal membranes, and based on this observation, LC3 is thought to be an orthologue of yeast Atg8 (Kabeya *et al.*, 2004).

1.5.1 LC3 processing and function

It has been revealed that there are two forms of LC3 molecules in cells: one that is in the cytoplasmic form and is processed into a second form associated with the membrane of autophagosomes (Kabeya *et al.*, 2000). These forms are known as LC3-I (18 kDa) and LC3-II (16 kDa) (Kabeya *et al.*, 2000). The same group have also revealed that both LC3-I and LC3-II are derived from the same mRNA. After translation, the unprocessed form of LC3 (proLC3) is proteolytically cleaved by Atg4, resulting in the formation of LC3-I with a carboxyterminal exposed glycine. Following autophagy induction, the exposed glycine of LC3-I is conjugated by Atg7, Atg3, and by Atg12-Atg5-Atg16L multimers to the highly lipophilic phosphatidylethanolamine (PE) moiety to produce LC3-II (Mizushima, 2007; Nakatogawa *et al.*, 2009) (Figure 1.6). The PE group causes LC3-II to integrate into lipid membranes at the phagophore and autophagosomes. At the autophagosome, LC3-II has been shown to perform two functions: the first is selecting cargo for degradation, and the second is promoting membrane tethering and fusion (Nakatogawa *et al.*, 2007). This is supporting a possible role in the fusion of autophagosomes with other membrane compartments, such as endosomes or

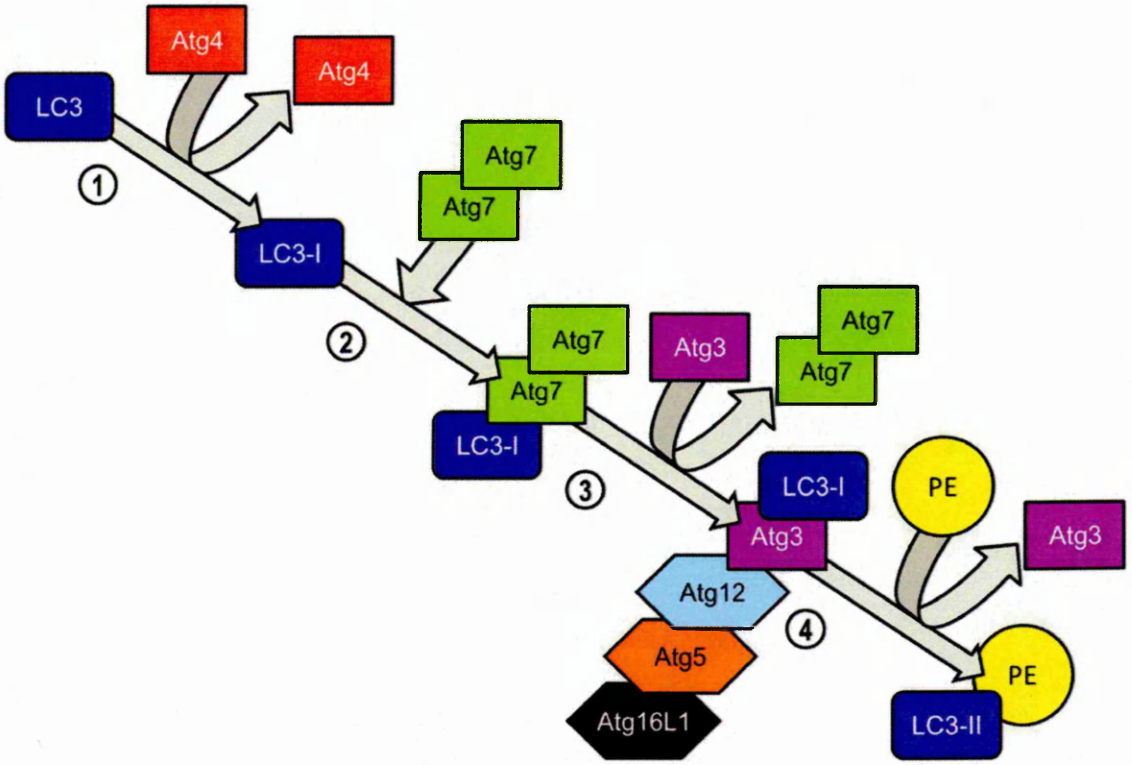

Figure 1.6 processing of Microtubule-associated protein light chain 3 (LC3). Immediately after synthesis, (1) the C-terminus of LC3 is cleaved by Atg4 to produce a soluble LC3-I with C-terminal glycine. (2) Atg7 acts as ubiquitin-activating (E1) and binds to the exposed C-terminus of LC3-I before recruiting Atg3 via its N-terminal domain. (3) During the interaction between Atg3 and Atg7, LC3-I is transferred to Atg3 and Atg7 leaves the LC3-I complex. (4) The conjugation between LC3-I and the lipid phosphatidylethanolamine (PE) results in the production of LC3-II in a reaction catalyzed by Atg3. The lipidation of LC3-I enhances through the binding of Atg5-Atg12-Atg16L1 to Atg3.The newly produced LC3-II is incorporated into the elongating isolation membrane. The conversion of LC3-I to LC3-II is reversible (Eri *et al.*, 2013).

mitochondria (Barth *et al.*, 2010). Interestingly, Atg8/LC3-PE is deconjugated, again by Atg4. The cycle of conjugation and deconjugation is very important for the normal progression of autophagy (Kirisako *et al.*, 2000). It has been reported that LC3-II is the only well-characterized protein that is specifically localized to the autophagic structures throughout the process from phagophore to lysosomal degradation (Nakatogawa *et al.*, 2009).

Based on the importance of LC3 processing for autophagosome formation and function, antibodies to LC3-I and LC3-II are widely used in western blotting techniques to monitor autophagy (Karim *et al.*, 2007; Tanida *et al.*, 2008; Mizushima and Yoshimori, 2007). As previously reported, LC3 is expressed as three isoforms in mammalian cells, LC3A, LC3B and LC3C; however LC3B is only the isoform that correlates with the number of autophagic vesicles. For this reason, it is recommended to utilize anti-LC3B antibodies for analysis of autophagosomes formation (Barth *et al.*, 2010).

1.6 AUTOPHAGY AND DISEASE

The large number of physiological functions performed by autophagy provides a good reason why alterations in this process either in term of autophagy protein function or subcellular localisation, result in cellular malfunctioning and often cell death (Sridhar *et al.*, 2012). This has formed the basis for the contribution of autophagy to the pathogenesis of several human diseases. The common pathological conditions in which autophagy has been shown to be altered are: cancer, immune and infectious diseases, heart dysfunction and neurodegeneration (Sridhar *et al.*, 2012).

In cancer, for instance, it has been revealed that Beclin-1 (ATG 6), a core component of the autophagosome nucleation complex, is mono-allelically deleted in human breast, ovarian and prostate cancer (Liang *et al.*, 1999), and recently, it has also been revealed that the Beclin 1 gene is mono-allelically deleted in most cases of sporadic human

cancers (Gong *et al.*, 2013; Fu *et al.*, 2013). It has been suggested that autophagy prevents tumorigenesis through limiting necrosis and inflammation, inducing cell cycle arrest and preventing instability of the genome (Degenhardt *et al.*, 2006). However, because of the role of autophagy in the cell survival mechanism, it has been argued that autophagy may encourage drug resistance and adaptation of tumour cells to stress (Amaravadi *et al.*, 2007).

With regards to immune and infectious diseases, a genome-wide association study (GWAS) has reported that there is a connection between the mutation T330A in ATG16L (Atg16L binds in pairs with the conjugated Atg12- Atg5 dimers to produce a multimeric Atg5-Atg12-Atg16L complex (Figure 1.1b) which is crucial for the extending phagophore (Lee, 2012)), and Crohn's disease, a condition that causes inflammation of the digestive system (Hampe *et al*, 2007).

In addition, autophagic inhibition may lead to insufficient induction of tolerance against commensals or self-antigens in the gut (Rioux *et al.*, 2007); also it may affect antimicrobial protein production by Paneth cells (epithelial cells of the small intestine) (Cadwell *et al.*, 2008). This autophagic role in the establishment and maintenance of tolerance has suggested a possible role for autophagy in autoimmunity (Lunemann and Munz, 2009). It is known that autophagy contributes to apoptotic cell clearance (Qu *et al.*, 2007), and the failure in the clearance of apoptoic cells has been proposed to result in autoimmune diseases, such as systemic lupus erythematosus (Bratton and Henson, 2005).

It has been revealed that mutations of P62/SQSTM linked to Paget's disease, lead to abnormal turnover of bone leading to bone deformation, arthritis and nerve injury (Ralston, 2008). Osteoclasts in such patients demonstrate deregulation of NF-kB

signalling and ubiquitinated proteins accumulate, consistent with a main role for autophagy in normal bone development and function (Glick *et al.*, 2010).

With regards to heart diseases, it has been reported that inactivation of Lamp-2 is the genetic cause of the lesion associated with Danon disease in humans, an X-linked disease that results in cardiomyocyte hypertrophy and autophagosome accumulation in heart muscle (Glick *et al.*, 2010). This thesis focuses on the relation between autophagy and neurodegenerative diseases.

1.6.1 Autophagy and neurodegenerative diseases

In neurons of some neurodegenerative diseases, abnormal accumulation of autophagosomes or autolysosomes was observed (Lee, 2012). Despite this, it is not obvious whether the accumulation of autophagic vacuoles in degenerating neurons is a sign of increased autophagic flux. In fact, the increase in the number of autophagosomes or autolysosomes could be caused by either increased autophagic vacuoles formation or impaired autophagic vacuoles clearance (Lee, 2012). It has been reported that the sustained failure of the balance between the formation and degradation of autophagosomes results in autophagic stress (Chu, 2006). Either the cells failed to control excessive demand of autophagy or failed to remove autophagic vacuoles as a result of defects in fusion or lysosomal degradation could result in autophagic stress which is associated with neurodegenerative diseases (Lee, 2012).

Intracellular protein aggregates is one of the features that are shared by a number of neurodegenerative diseases (Bredesen et al., 2006). Initial studies have revealed the accumulation of autophagic vacuoles in the brains of Alzheimer's disease (AD), Parkinson's disease (PD) and Huntington's disease (HD) patients (Rubinsztein, 2006, Levine and Kroemer, 2008).

As the bulk degradative nature of autophagy would promote the removal of the intracellular protein aggregates, great efforts have been devoted to understanding whether autophagy may be induced to eliminate these aggregated proteins, and whether the presence of aggregates may be attributed to malfunctioning of the autophagic pathway (Cheung and Ip, 2011).

Many studies have suggested that aggregation of the toxic species may actually be neuroprotective (Rubinsztein, 2006), autophagy may still be important for removing the oligomeric form of the toxic proteins (Cheung and Ip, 2011). Supporting the protective role of autophagy, it has been revealed that transgenic animals with neural-specific deletion of Atg5 and Atg7 develop neurodegeneration, accompanied by the presence of inclusion bodies (Hara *et al.*, 2006; Komatsu *et al.*, 2006). Nonetheless, although it has been observed that elevated autophagy would facilitate the degradation of protein aggregates in HD, PD and AD (Rubinsztein, 2006; Mizushima *et al.*, 2008), other studies have revealed that each neurodegenerative disease may have different extents of autophagy deregulation, at different stages in the pathway of autophagy (Cheung and Ip, 2011).

In Huntington's disease, it is believed that the toxicity of the mutant huntingtin (Htt) protein is caused by the intraneuronal aggregates of the N-terminal fragments, the typical pathological hallmark of HD. Autophagic alterations were first observed in post-mortem brains of HD patients (Tellez-Nagel *et al.*, 1974). Mutant Htt accumulation was proposed to induce the endosomal-lysosomal pathway and contribute to an autophagic process of cell death (Son *et al.*, 2012). The involvement of autophagy in HD was further demonstrated by mTOR sequestration in polyglutamine aggregates in cell models, transgenic mice and human brains (Son *et al.*, 2012). This sequestration inhibits the kinase activity of mTOR leading to autophagy induction. The induced autophagy

protects against the toxicity of polyglutamine (Son *et al.*, 2012). It has been revealed that induction of autophagy through inhibition of mTOR by rapamycin has attenuated the Htt accumulation and cell death in a cellular model of HD, and when autophagy was inhibited the opposite effect was observed (Ravikumar *et al.*, 2004).

Despite the observed neuroprotective effect of autophagy activation in HD models, the precise mechanism that underlies autophagic dysfunction in HD is poorly understood. However, it has been proposed that the inefficient engulfment of cytosolic components by autophagosomes is responsible for the general decrease in turnover of these components and accumulation of Htt in HD cells. A study using cellular and mouse models of HD and also HD patient's cells, has revealed that the autophagic vacuoles in the HD cells failed to recognize the cytosolic cargo. The formation of the autophagic vacuoles was at normal rates and removal by lysosomes was also at the normal rate, however, autophagosomes failed to efficiently trap cytosolic cargo in their lumen (Martinez-Vincente *et al.*, 2010).

In Parkinson's disease, death of dopaminergic neurons in the substantia nigra is associated with accumulation of α-synuclein within inclusions known as Lewy bodies (Hashimoto and Masliah, 1999). It has been demonstrated that α-synuclein, the major constituents of Lewy bodies, is degraded by both macroautophagy (autophagy) and chaperone-mediated autophagy (CMA) (Webb *et al.*, 2003; Cuervo *et al.*, 2004; Vogiatzi *et al.*, 2008; Mak *et al.*, 2010). Impaired clearance of α-synuclein aggregates may play a crucial role in PD pathogenesis (Bendiske and Bahr, 2003; Cuervo *et al.*, 2004). It has been suggested that α-synuclein aggregates interfere with the autophagy mechanisms resulting in neurodegeneration (Cuervo *et al.*, 2004; Meredith *et al.*, 2002; Nakajima *et al.*, 2005; Rideout *et al.*, 2004; Rockenstein *et al.*, 2005; Stefanis *et al.*, 2001). Mutant forms of α-synuclein found in familial PD patients, and also the oxidized

forms of α-synuclein found in sporadic PD have been shown to block autophagy, and α-synuclein contains a consensus sequence for CMA targeting (Cuervo *et al.*, 2004; Martinez-Vicente *et al.*, 2008). Studies utilising neuronal cell cultures (Xilouri et al., 2009) and transgenic mice, have revealed that overexpression of α-synuclein is connected with autophagic impairment and neurodegeneration that is reversed by expression of Beclin-1 (Spencer *et al.*, 2009). Other studies have suggested that progressive accumulation of α-synuclein aggregates interferes with the fusion of lysosomes and formation of autophagosomes (Cuervo et al., 2004; Martinez-Vicente et al., 2008; Xilouri et al., 2009). Taken together, these lines of evidence suggest that in PD, specific molecular defects in the pathway of autophagy may play a role in the pathogenesis of this disease (Kragh *et al.*, 2012).

In Alzheimer's disease (AD) (the most common form of dementia) the presence of senile plagues composed of β-amyloid (Aβ) aggregates, and intracellular neurofibrillary tangles containing hyperphosphorylated tau, are characteristic features (Vassar *et al.*, 1999). The deregulation of autophagy was initially connected to AD when a study utilizing electron microscopy revealed the accumulation of autophagic vacuoles in the brains of AD patients (Nixon *et al.*, 2005; Yu *et al.*, 2005). It has been reported that autophagy activation is increased after Aβ stimulation and also in APP/PS1 mice (APPPS1 mice contain human transgenes for both APP bearing the Swedish mutation and PSEN1 containing an L166P mutation which exhibits a partial loss to γ-secretase function and resistant to γ-secretase modulation by nonsteroidal anti-inflammatory drugs), an AD mouse model (Yu *et al.*, 2005; Hung *et al.*, 2009; Wang *et al.*, 2010). Interestingly, strong evidence has shown that during autophagy, Aβ is generated in the autophagic vacuoles, suggesting that autophagy activation in AD brains may exacerbate the pathogenesis of AD through increasing the levels of Aβ (Yu *et al.*, 2005; Nixon *et al.*, 2007). It has been shown that autophagic vacuoles are efficiently removed in

healthy neurons; whereas clearance of autophagic vacuoles is impaired in AD brains (Boland *et al.*, 2008). In addition, knock down of presenilin-1 (PS1), a gene mutated in familial AD, results in defects in clearance of autophagic vacuoles, acidification of lysosomes and also decreased lysosomal proteolytic activity (Lee *et al.*, 2010b). Importantly, expression of PS1 mutants associated with early-onset AD also leads to similar abnormality in the autophagic-lysosomal pathway (Lee *et al.*, 2010b). Different studies have reported that despite the observed generation of Aβ in autophagosomes, autophagy is also involved in the degradation of APP and Aβ (Caccamo *et al.*, 2010; Jaeger *et al.*, 2010; Vingtdeux *et al.*, 2010). Moreover, it was demonstrated that autophagy is involved in the modulation of tau protein levels and fragmentation (Berger *et al.*, 2006; Wang *et al.*, 2009). The soluble and aggregated forms of tau are degraded by autophagy and the inhibition of autophagy increased the aggregation and toxicity of tau (Berger et al., 2006; Wang et al., 2009).

1.7 PROTEIN LOCALISATION AND FUNCTION

The correct localisation of a protein within a cell is crucial to allow them to perform their functions effectively. Approximately half of the proteins synthesized by a cell have to be transported into, or across, at least one cellular membrane to reach their functional destination (Chacinska *et al.*, 2009). The regulation of the trafficking of the protein relies on encoded information within the sequence of the protein and occurs through two mechanisms: co-translational and post-translational translocation (Rapoport, 2007). Co-translational translocation is found in all cells and is used for the translocation of secretory proteins, and also for most membrane protein integration (Rapoport, 2007). In most cells, some proteins are transported after completion of their synthesis. This pathway of translocation is known as post-translational translocation. Post-translational translocation appears to be used by a larger proportion of proteins in simpler organisms,

such as bacteria and yeast, because the growth in these simple organisms is very fast and translocation does not always keep pace with translation (Rapoport, 2007).

Subcellular localisation controls the access of proteins to interacting partners and the post-translational machinery and facilitates the proteins integration into functional biological networks (Hung and Link, 2011).

Abnormal protein localisation can be caused by a mutation, altered expression of cargo proteins or transport receptors or by deregulation of components of the trafficking machinery and has been linked to human diseases as diverse as Alzheimer's disease, kidney stones and cancer (Hung and Link, 2011). Deregulation of protein trafficking can cause incorrect localization of proteins and hence result in loss of function, and also misregulation or an adverse effect at the wrong location. Abnormalities in the subcellular localization of proteins that are necessary for the signaling, metabolic or structural properties of the cell can lead to disorders that involve biogenesis, protein aggregation, cell metabolism or signaling (Hung and Link, 2011).

An example of incorrect localisation of protein via alterations of the trafficking machinery has been documented for the nuclear pore complex (NPC). Alterations in this complex have been linked to several genetic diseases (Chahine and Pierce, 2009). For example, mutations in some components of NPC, such as the nucleoporin p62 protein and ALADIN (alacrima achalasia adrenal insufficiency neurologic disorder) are thought to be the reason behind the neurodegenerative diseases infantile bilateral striatal necrosis and triple A syndrome, respectively (Basel-Vanagaite *et al.*, 2006; Kiriyama *et al.*, 2008). The mutations in some components of the NPC can reduce the permeability of the nuclear envelope and has an influence on the export of *Hsp70* mRNA and import of HSP70 protein. Also, mutation in ALADIN prevents nuclear entry of the DNA repair

proteins aprataxin and DNA ligase I, leading to increased DNA damage followed by cell death (Kiriyama *et al.*, 2008).

Incorrect localisation of proteins via alterations in targeting signals due to genetic alterations that have an influence on protein targeting signals, have been linked to several metabolic diseases that are characterized by defects in functions of specific organelles, such as lysosomal or peroxisomal functions (Djordjevic *et al.*, 2010). In addition to changing the localisation signal of a protein, some disease related mutations can lead to incorrect localisation of a protein via protein sequestration. For example, it has been revealed that mutations in the LMNA (lamin A/C) gene, the cause of laminopathies, cause incorrect localization of the DNA-binding transcriptional repressor zinc finger protein 239 (ZNF239). The mutant protein (pathogenic lamin A/C) sequesters ZNF239 into nuclear aggregates, and this sequestration is thought to deregulate ZNF239 target genes (Dreuillet *et al.*, 2008).

With regards to the incorrect localisation of signaling proteins, because proteins cannot diffuse as fast as small molecule second messengers (such as cyclic AMP, cyclic GMP, inositol triphosphate, diacylglycerol and calcium), the subcellular localisation of signaling proteins near their downstream targets is crucial (Scott and Pawson, 2009). Signaling protein translocation gives a signal over a large distance or between components of a cell. A fault in this signaling arrangement has been demonstrated to be involved in tumorigenesis, tumor growth and metastasis (Kau *et al.*, 2004; Wang and Hung, 2005). To perform their function, some important tumor suppressor proteins need to be localised to the nucleus, however, their localisation to the cytoplasm works as an inactivation mechanism and causes uncontrolled cell proliferation and the onset of disease. Consequently, this incorrect localization of these nuclear proteins to the

cytoplasm has been suggested as a mechanism for the inactivation of tumor suppressors (Kau *et al.*, 2004; Salmena and Pandolfi, 2007).

1.7.1 Autophagy and Protein localisation

In autophagy, the re-localisation of mammalian homologue of yeast Atg18 (WIPI2) to the omegasome (pre-autophagosome)-anchored phagophore plays an important role in LC3 lipidation and autophagosome formation (Polson *et al.*, 2010). The re-localisation of Atg18 occurs by the aid of Atg1 kinase complex and the autophagy specific Vps34 lipid kinase complex (Suzuki *et al.*, 2007). Polson *et al.*, (2010) demonstrated that in mammalian cells, WIPI2 is amongst one of the early components of the process of autophagy and moves to sites of autophagosome formation in response to PtdIns3P, where it colocalizes with double FYVE domain-containing protein (DFCP1), Atg16L and ULK1. They revealed that re-localisation of WIPI2 to these structures is dependent on the production of PtdIns3P and is required for their maturation (DFCP1, Atg16L and ULK1) and for LC3 lipidation. This explains the importance of lipid phosphorylation by PI3Kinase. It seems that WIPI2 plays an important role in the maturation of these proteins through maintaining their distribution on the omegasome membrane to perform their function in the maturation of the omegasome to autophagosome. It has been revealed that after WIPI2 deletion, DFCP1 redistributes to punctate structures, and these structures failed to produce LC3-positive autophagosomes, or mature. Thus, it has been hypothesized that WIPI2 works downstream of DFCP1 and is required for the maturation of the omegasome (Polson *et al.*, 2010).

It is also thought that Atg18, WIPI1 and WIPI2 that have PtdIns3P binding domains exist in a cytosolic pool and re-localise to the pre-autophagosomal structure (PAS) or autophagosome by direct interaction with PtdIns3P. This re-localisation of these proteins is an indication that there is a link between autophagic protein localisation and

their function. So, the suggested interaction between tPS1 and mTOR, raptor and LC3 in the present study may result in re-localisation of these proteins causing a change in their function leading to an autophagic failure.

Vps34 (amongst the PI3Kinases) has the ability to phosphorylate the 3' position of the inositol head group of phosphatidylinositol (PtdIns) to produce PtdIns3P (Polson *et al.*, 2010). In yeast, an autophagy-specific complex was formed by the combination of Vps34 with Vps15, Vps30/Atg6 and Atg14. The Vps34-autophagy specifc PtdIns3P can be recognized by Atg18p, Atg21 and Ygr223p. The mammalian homologue of yeast Vps34 complex is produced by the combination of hVps34 with p150, Beclin 1 and ATG14L. The importance of creating and regulating the autophagy-specific pool of PtdIns3P in mammals was discovered by the recognition of a PtdIns3P phosphatase, Jumpy, (Vergne *et al.*, 2009), that dephosphorylates PtdIns3P on phagophores and autophagosomes in order to negatively regulate the formation of autophagosomes. Furthermore, it has been demonstrated that a double FYVE domain-containing protein (DFCP1) binds to ER membrane domains where PtdIns3P pools are produced under starvation resulting in omegasome formation (Axe *et al.*, 2008). Polson *et al.*, (2010) also demonstrated that both WIPI1 and WIPI2 share common ancestry with Atg18 and they are the mammalian orthologue of Atg18. In addition, they proposed that the function of WIPI2 and DFCP1 are connected, and they hypothesized that WIPI2 works as a downstream target of DFCP1 and is needed for the maturation of the omegasome.

In 2010, Sancak *et al.,* demonstrated that for the mTORC1 (an autophagy key regulator) to be activated by amino acids requires the re-localisation from an un-defined cytoplasmic location to the lysosomal surface in a Rag-Ragulator dependent manner. To regulate cell growth, mTORC1 requires signals from growth factors, intracellular energy levels and amino acid availability, and in some different diseases, the

deregulation of this signaling pathway has been observed (Guertin and Sabatini, 2007). For growth factors and energy sensing, mTORC1 receives signals from the TSC1 and TSC2 complex through the regulation of GTP-loading state of Rheb, a Ras-related GTP-binding protein. After the interaction with GTP, Rheb has the ability to interact and activate mTORC1 (Laplante and Sabatini, 2009). However, in the case of amino acid sensing, the Rag GTPases, are the amino acid-specific regulators of the mTORC1 pathway (Kim *et al.*, 2008; Sancak *et al.*, 2008).

There are four mammalian Rag proteins: RagA, RagB, RagC, and RagD. These four Rag proteins form heterodimers consisting of RagA or RagB with RagC or RagD. RagA and RagB, like RagC and RagD, are highly similar to each other and are functionally redundant (Sancak *et al.*, 2008). It has been revealed that in HEK293T cells, the presence of amino acids, mTOR and raptor co-localized with LAMP2 (lysosomal marker) (Eskelinen, 2006) and this localisation is dependent on the Rag GTPases. Sancak *et al* also showed that; mTORC1 binds to the Rag heterodimers in an amino acid-dependent manner, with the Rag GTPases working as an amino acid-regulated docking site for mTORC1 on lysosomes (Sancak *et al.*, 2010).

Rag GTPases do not have lipid modification signals in their amino acid sequence that might play a role in the recruitment of Rag to lysosomal membranes. It was believed that unknown Rag-interacting proteins are required for localisation of the Rag GTPases to lysosomes and play a role in mTORC1 signaling. It has been revealed that three small proteins called MP1, p14, and p18 (Ragulator) were behined the localisation of Rag GTPases to the lysosomes and a complex consisting of Ragulator, a Rag heterodimer, and mTORC1 can exist in cells (Sancak *et al.*, 2010). It has been revealed that in HEK-293T cells with p14, p18, or MP1 knockdown, amino acids failed to induce the recruitment of mTOR to the lysosomal suface, where mTOR was found in the

cytoplasm in both amino acid starved and stimulated cells. This confirms the essential role of Rag proteins in the translocation of mTORC1 to the lysosomes, and also reveals that all Ragulator subunits are essential and needed for lysosomal targeting of the Rag GTPases and mTORC1 (Sancak *et al.*, 2010). The disruption of the localisation of mTORC1 to the lysosomes results in mTORC1 inactivation. For instance, nutrient depletion and lysosomal stress converge on the v-ATPase-Ragulator-RagGTPase system, and lead to the detachment of mTORC1 from the lysosome and inactivation. Inactivation of mTORC1 stops anabolic reaction and improves cellular degradation (Efeyan *et al.*, 2012). In addition, it has been revealed that disruption of mTORC1 localisation to the lysosome due to a partial loss of function of Ragulator, which is responsible on the recruitment of mTORC1 to the lysosome through Rags, has caused a human disease known as hypoactive mTORC1 signaling, and this disease is characterized by stunted growth, immunodeficiency and albinism (Bohn *et al.*, 2007).

The importance of mTOR localisation has also been documented where the sequestration of mTOR with HD (Huntington disease) aggregates impaired its kinase activity and induced autophagy (Ravikumar *et al.*, 2004). This sequestration decreased soluble mTOR levels and as a result, the mTOR phosphorylation of S6K1 and BP1 was reduced and S6K1-driven translation decreased (Ravikumar *et al.*, 2004). In addition, the presence of mutant htt (huntingtin) has led to production of a greater number of autophagosomes, and therefore, it has been suggested that sequestration of mTOR by htt aggregates could increase autophagosome numbers by limiting mTOR availability (Ravikumar *et al.*, 2004).

It is very clear from the mechanisms described above that there is a link between autophagic protein localisation and their function. Based on this information, the present study was an investigation of subcellular localisation of selected autophagy proteins in

non-autophagic, autophagic and tPS1 transfected HEK293 cells. The present study investigated the movement and subcellular localisation of selected autophagy proteins (mTOR, raptor and LC3) in autophagic and non-autophagic cells. Then, the observed result was compared with the results obtained after the transfection of HEK293 cells with truncated protein presenilin-1 (PS1) (the most common genetic cause of Alzheimer's disease) to investigate if the normal movement and subcellular localisation of the selected proteins was interrupted by the truncated PS1 aggregates leading to autophagic failure.

1.8 THE ROLE OF PS1 AND AUTOPHAGY

In 2010, Lee *et al.,* demonstrated that autophagy requires the Alzheimer's disease (AD)-related (PS1) and that PS1 mutations lead to a disruption in the autophagic pathway. PS-1 is a ubiquitous transmembrane protein needed for lysosomal turnover of autophagic and endocytic protein cargo. Lee *et al.*, (2010b) revealed that PS1 holoprotein, present in the ER, works as an ER chaperone to facilitate maturation and targeting of the v-ATPase V0a1 subunit to lysosomes. This step is crucial for lysosomal acidification, protease activation, and autophagic/lysosomal cargo degradation. In WT cells, the v-ATPase V0a1 subunit (as a marker of proton pump function in lysosomes) was localised to LAMP-2-positive compartments. However, in PS1 (-/-) cells, v-ATPase was concentrated in a perinuclear region (Lee *et al.*, 2010b). This shows the importance of normal PS1 in the correct localisation of v-ATPase to the lysosome to play its role in the lysosomal acidification.

The v-ATPases are multisubunit complexes that are composed of a membrane-bound subcomplex V0 and a cytosolic V1 subcomplex. Lee *et al.*, (2010b) demonstrated that in the immature form of v-ATPase, the V0a1 subunit is unglycosylated, and to be N-glycosylated, v-ATPase V0a1 subunit requires a physical interaction with PS1. This N-

glycosylation is needed for the subunit to be efficiently delivered to lysosomes. It has also been shown that v-ATPase V0a1 subunit was posttranslationally N-glycosylated, and the function was lost after the deletion of PS1. Also, they demonstrated that the PS1 effects on autophagy are not dependent on gamma secretase activity. Of particular clinical significance, Lee *et al.*, (2010b) have also shown that PS1 mutations that cause early-onset familial Alzheimer's disease (FAD) has prevented the same lysosomal/autophagic functions that are more severely affected in PS1 KO cells (PS1 knockout mouse).

Previous work showed that a truncated presenillin 1 construct, when transfected into fibroblast cell line (HEK293 cells), stimulated the early stages of autophagy, as shown by structural changes within the cell seen by electronic microscopy (Anderson, PhD thesis). However, the autophagic process did not appear to go to completion as would be expected in the normal state, because the presenillin 1 aggregates persisted in the cells and were not removed, and appeared to lead to cell death.

1.9 HYPOTHESIS

In addition to a lysosomal acidification defect, truncation or mutation of PS1 (the most common genetic cause of Alzheimer's disease) results in intracellular autophagy protein movement interruption, leading to their incorrect subcellular localisations, causing an autophagic failure leading to protein aggregation inside the cells.

1.10 THE AIMS AND OBJECTIVES OF THIS RESEARCH:

Since presenillin 1 mutations are the most common genetic cause of Alzheimer's disease, and defects in autophagy have been implicated in degenerative diseases, and as many published localisation studies have revealed that there is a connection between autophagy proteins localisation and their function, the aims of this project are:

1. To characterize antibodies to selected protein components of the autophagy pathway (mTOR, raptor and LC3) for their utility in detecting the expression and determining the subcellular localization of these proteins in cultured cells.

2. To establish the transient expression of a truncated presenillin 1 protein construct in cultured cells that previous work has shown leads to an aborted autophagic response.

3. To investigate and determine the subcellular localization of selected autophagy proteins using the methods described in (1) and (2) above to determine if the cause for the aborted autophagy can be identified.

Chapter 2

Materials and Methods

2.1 INTRODUCTION

This chapter describes the details of the experimental procedures applied throughout the course of this research. Further details of the materials and methods exploited for specific experiments are presented in the relevant chapter.

2.2 Cell culture

The cell lines that have been used in this study were a normal rat kidney (NRK) cell line (gift from Professor David Parkinson), a human breast cancer (MCF-7) cell line (European Collection of Cell Cultures) and a human embryonic kidney (HEK293) cell line (European Collection of Cell Cultures).

2.2.1 Culture of cells from frozen stock

Cells were stored in 10 % (v/v) dimethyl sulfoxide (DMSO) (Sigma, UK) in foetal calf serum in liquid N_2, and once thawed were propagated in specific culture medium for these cell lines.

The media used in this research is Eagle's Minimum Essential Medium (EMEM) (Lonza, UK) supplemented with 10 % (v/v) foetal bovine serum (FBS) (Sigma-Aldrich, UK), 1 % (v/v) non-essential amino acids of 10 mM (Sigma-Aldrich, UK), 1 % (v/v) sodium pyruvate of 100 mM (Sigma-Aldrich, UK), 1 % (v/v) penicillin (100 I.U/ml) (Sigma-Aldrich, UK), 1 % (v/v) streptomycin (100µg/ml) (Sigma-Aldrich, UK) and 2 mM L-glutamine (Sigma-Aldrich, UK).

The vial containing frozen cells (for all used cell lines) was warmed to 37 °C. The contents of the vial were transferred to a 50 ml tube and 5 ml of media was added to the cells drop wise to reduce the toxicity of DMSO. The cells were cultured by dividing the contents of the tubes into culture flasks containing media according to the appropriate

density that determined by a haemocytometer. The cells were incubated in a humidified environment at 37°C under 5 % CO_2 atmosphere for 3 days.

Cells were allowed to reach 80-90 % confluence before being sub-cultured. Next, the cells were rinsed with serum free media (EMEM) to remove any trace of serum. The adherent cells were re-suspended by trypsinisation with 0.5 % trypsin and 0.2 % Ethylenediaminetetraacetic acid (EDTA) solution (Sigma-Alrich, UK) (3 ml for 25 cm^2 flask) and incubated at 37 °C for 5 minutes. Trypsinisation was then stopped by neutralising trypsin/EDTA with 3 mL complete media, which was mixed with the cell suspension by gentle pipetting and then transferred to a sterile 15 mL centrifuge tube. Suspended cells were then centrifuged at 1000 rpm to pellet the cells, and the supernatant was aspirated to remove the trypsin/EDTA containing medium. The cell pellet was then re-suspended in a known volume of fresh pre-warmed culture medium, and cells counted if required for experimental purposes, or suspended in the appropriate amount of complete media and seeded at a 1:10 split ratio to further propagate cells. Cell lines were used between passages 4 and 15.

2.2.2 Cell counting

Cells were centrifuged at 200 g for 10 minutes and supernatant discarded. The cells pellet was resuspended in 1 ml of complete media and mixed gently by pipeting up and down. Cells were counted using a haemocytometer and the number of the cells in the central and four corner squares of the middle square (25 small squares) of the counting area were counted. Then the number of cells per ml was calculated using the following equation: Cell concentration per ml = Total cell count in 5 squares x 5 x 10^4. The counted cells were further diluted to the densities required for experimental procedures.

2.3 Protein Extraction

2.3.1 Whole cell lysate

The cells were sub-cultured in 6-well plates and left in the incubator at 37 °C until confluent. After aspiration of the media from the wells of 6-well plate, 3 ml of ice cold serum free media (EMEM) (Lonza, UK) containing protease inhibitor cocktail (10/100 µl) (Sigma, UK) were added to each well in order to wash the cells. After aspiration of the wash, 500 µl of sample buffer containing 10 mM of DTT and protease inhibitor cocktail were added to each well. The protein extract was then collected from each well into 1.5 ml Eppendorf tubes and heated in thermal-lok 4-position dry heat bath at 60°C for 10 minutes. After that, the DNA in the extract was sheared by moving it up and down in the tube with a pipette fitted with a blue tip for 20 times. Then, 25 µl of fresh iodoacetamide (20 mM) was added to each tube and incubated for 1 hour at room temperature. Then, the samples were ready to be run on the SDS-PAGE.

2.4 Tris-glycine polyacrylamide gel preparation:

The most commonly employed type of gel electrophoresis is sodium dodecyl sulphate-polyacrylamide gel electrophoresis (SDS-PAGE) (Laemmli, 1970). SDS-PAGE is a technique used to separate proteins according to the molecular weight. Polyacrylamide gels for SDS-PAGE were prepared in different percentages based on the molecular weights of the proteins of interest (Laemmli, 1970).

2.4.1 Resolving gels

Glass plates thoroughly cleaned with washing-up detergent, rinsed, dried, assembled into cassettes and then mounted in the casting stand. Based on the desired acrylamide percentage and total volume, the following table was used, (Table 2.1).

Table 2.1: Acrylamide percentages in tris-glycine resolving gels

	Percentages (%)	6	6.5	7	7.5	10
10 ml	30 % acrylamide (ml)	2	2.167	2.333	2.5	3.333
	d-water (ml)	3	2.833	2.667	2.5	1.667

In the whole study, mini-gels (8 x 10 cm, BioRad) of 1 mm thickness were prepared. After the selection of the desired acrylamide percentage, for instance, 6 % acrylamide gel; 2 ml of 30 % (v/v) acrylamide, 3 ml of distilled water, 2.5 ml of 60 % (v/v) glycerol, 2.5 ml of 4x resolving buffer, 100 µl of 10 % (w/v) SDS, 100 µl 5 % (v/v) tetramethylethylenediamine (TEMED) and 100 µl 5 % (w/v) ammonium persulfate (APS) were added to the same tube. Immediately after the addition of APS, 3.2 ml of the gel mixture was pipetted between the glass plates and overlaid with distilled water and allowed to polymerize for 1 hour.

2.4.2 Stacking gels

The stacking solution was prepared by adding 2 ml of 2x stack acrylamide, 1 ml of 60 % (v/v) glycerol, 1 ml 4x stacking buffer (0.5 M tris.HCL pH 6.8), 40 µl of 10 % (w/v) SDS, 40 µl of 5% (v/v) TEMED and 40 µl of 5% (v/v) APS. The layer of distilled water over the resolving gel was aspirated. Immediately the glass plates were filled with stacking solution to the top and the Teflon comb was inserted and the gel allowed to polymerize for 1 hour.

2.5 Tris-tricine polycrylamide gel preparation:

According to Schagger and Von Jagow (1987), these gels were used to separate low molecular weight proteins and peptides down to 4 kDa. In this project, these different gels were used to detect LC3 proteins (18 and 16 kDa).

2.5.1 Resolving gels

Glass plates were prepared as above (Section 2.4.1). 10 % tris-tricine gels were prepared by adding of 3 ml 30 % (v/v) acrylamide to 3 ml 3M Tris, pH 8.45 to 3 ml of 60 % (v/v) glycerol or 3.2 g urea and mixed. Then, 90 µl of 10 % (w/v) SDS, 90 µl of 5% (v/v) TEMED and 90 µl of APS were added, mixed and immediately loaded in to the cassette and overlaid with distilled water and allowed to polymerize for 1 hour.

2.5.2 Stacking gels

The stacking solution was prepared by adding of 2 ml of 2 x stack acrylamide to 1 ml of 60 % (v/v) glycerol to 1 ml of 3M tris at pH 8.45 and mixed. Then, 40 µl of 10 % (w/v) SDS, 40 µl of 5 % (v/v) TEMED and 40 µl of 5 % (w/v) APS were added. The layer of distilled water over the resolving gel was aspirated. Immediately the glass plates were filled with stacking solution to the top and Teflon comb was inserted and the solution allowed to polymerize for 1 hour.

2.6 Western blotting

Western blotting is a widely used analytical technique for the detection of specific proteins in a given sample of tissue homogenate or cell extract (Kurien and Scofield, 2006). It uses gel electrophoresis to separate native proteins by three-dimensional structures or denatured proteins by the length of the polypeptide chain. These separated proteins are then transferred onto a membrane where they are probed with antibodies specific to the target protein. Specific antibody binding is then detected using a range of methods, most commonly chemiluminescence with an enzyme-labelled secondary antibody, or a fluorescently labelled secondary antibody.

2.6.1 Sodium Dodecyl Sulphate Polyacrylamide Gel Electrophoresis (SDS-PAGE)

Protein samples (18 µl / well) were fractionated on different percentages (6 %-10 %) of gels using SDS-PAGE. Protein samples were prepared as above (Section 2.3.1). The gels were placed into an electrophoresis tank containing electrode buffer (running buffer) which was prepared by adding of 6 g of Tris, 28.8 g of glycine and 2 g of SDS to 2 L of d-water. Protein sample was loaded per well along with 10 µl of molecular weight marker (7-215 kDa) (BioRad, UK) or multicolor high range protein ladder (40-300 kDa) (Thermo Scientific, UK), and electrophoresis carried out at 100 V for approximately 3 hrs, until the dye front reached the bottom of the gel.

2.6.2 Protein electroblotting

Following electrophoresis, the proteins were electroblotted onto nitrocellulose membranes (Hybond-c, GE Healthcare, UK) at 100 V for 1h with an ice insert as follows: first, the transfer tank was filled with cold transfer buffer (2.2 g of CAPS in 900 ml of d-water and then 100 ml of MeOH was added, pH 10.3), and then an ice pack was inserted into the tank. The gel was removed from the plate into a large weighing boat containing cold transfer buffer. Blotting paper and nitrocellulose membrane were soaked in transfer buffer for 5 minutes and the blotting sandwich was made according to the following order; black (cathode -ve), sponge, two blotting papers, gel, membrane, two blotting papers, sponge and white (anode +ve) for each gel. The blotting sandwich was placed into the transfer tank and the proteins were electroblotted at 100 V and 0.2A for 1h.

2.6.3 Immunoprobing

Membranes were incubated for at least 30 minutes in 5% (w/v) non-fat skimmed milk in Tris-buffered saline (TBS) (15 mM Tris, 140 mM NaCl in d-water, pH 7.4) containing

0.01 % (v/v) Tween 20 (TBST) (Sigma, UK) to block non-specific binding of antibody. Blots were then washed 3 times for 5 minutes each in TBST.

The primary antibodies (Tables 3.1, 3.2 and 3.3) were then diluted to appropriate concentrations in TBS-T with 5 % (w/v) non-fat skimmed milk and incubated overnight at 4°C with gentle shaking. For negative controls, primary antibody was omitted, and the membrane was incubated with TBS-T with 5 % (w/v) non-fat skimmed milk alone. The next day, the membranes were washed as above to remove any unbound antibody. Alkaline phosphatase (AP)-linked secondary antibody (Donkey anti-rabbit IgG) (Cell signalling technology, UK) were then diluted (1:1000) in TBS-T and placed onto the blots and incubated for 1 hour with gentle agitation. The membrane was then washed 3 times for 5 minutes each in TBS followed by 1 time for 5 minutes in d-water.

Development of the blots was carried out using substrate solution prepared by adding 6 ml of Alkaline phosphatase (AP) buffer to 60 µl of 15 mg/ml 5-Bromo 4-Chloro 3'-Indolyphosphate p-Toluidine salt (BCIP) (Sigma-Alrich, UK) and 60 µl of 30 mg/ml nitroblue tetrazolium (NBT) (Sigma-Alrich, UK) for each membrane and then the membrane incubated with the solution for 30-60 minutes. The reaction was stopped by washing the membranes in d-water. The blots were then visualised using the naked eye and scanned (Epson Expression 1680 pro).

2.6.4 Molecular weight calculation for unknown protein samples

The molecular weight of an unknown protein can either be estimated using the prestained molecular weight marker as a guide to identify the molecular weight of the protein of interest, or using a graph, shown in figure (2.1). The graph uses the molecular weight standards; the log10 for each band of the known molecular weight marker was taken, and then plotted against the R_f values. The R_f value is the distance a specific

sample travels (mm) divided by the distance the tracking dye travels, which was the bromophenol blue (mm).

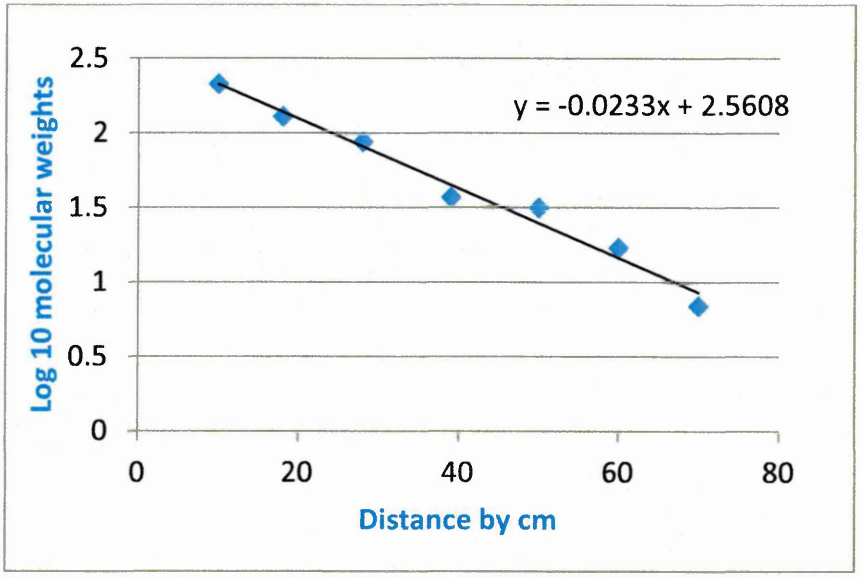

Figure 2.1 to determine molecular weight of unknown protein on SDS PAGE/WB

The equation in figure 2.1 y = - 0.023x + 2.560, was used. The R_f value of the protein of interest was substituted for y and rearranged. The obtained value was the log 10 of the molecular weight, in order to find the molecular weight of the protein the anti log was taken.

2.7 IMMUNOCYTOCHEMISTRY

Antibodies are routinely used to detect the cellular localisation of proteins (or antigens) in cells, tissues or biological fluids. The detection of an antigen using antibodies in cultured cells is referred to as immunocytochemistry (ICC).

Prior to antibody application the cells and/or tissues are subjected to fixation, permeabilisation and if necessary blocking. Fixation preserves both the cellular and subcellular structure in addition to the antigenicity of the antigen(s) of interest. Fixatives either form cross-linkages to preserve the tissue structure *e.g.* aldehydes such as

glutaraldehyde or formalin, or remove lipids and dehydrate cells whilst precipitating proteins or fixing them in their usual cellular localisation *e.g.* organic solvents such as acetone, ethanol or methanol (Delves *et al.*, 2006).

A blocking step is often employed using bovine serum albumin (BSA) or serum from the species in which the secondary antibody is made. This prevents non-specific binding of the labelled secondary antibody and particularly binding to endogenous Fc receptors (FcRs) present on the surface of some cells (Buchwalow *et al.*, 2011).

There are two types of immunofluorescence: direct and indirect. In the direct method of immunofluorescence, the primary antibody directed against the antigen of interest is directly conjugated with a fluorochrome. Although this method involves fewer steps, the technique is limited as only a limited number of antibodies can access the antigen of interest leading to low sensitivity. Based on this, indirect immunofluorescence is often the preferred method utilised.

In this research work, indirect immunocytochemistry was used to reveal the subcellular localisation of autophagy proteins of interest utilising single and double-label techniques.

2.7.1 Indirect immunocytochemistry

2.7.1.1 Preparation of cover slips

For cover slip sterilization, one cover slip was dropped into each well of a 24 well plate and incubated in 70 % (v/v) ethanol for 30 minutes. Following this, the ethanol was aspirated and the plate left open inside the laminar hood for 30 minutes to dry. Then the cover slips were washed with sterile EMEM media (Lonza, UK) and media aspirated to remove the residual ethanol, before adding the cells to the wells to grow on the cover slips. To support the attachment in the case of HEK293 cells, cover slips were coated with poly-L-lysine (1 µg/ml) (Sigma, UK) first. After the ethanol dried, the cover slips were washed with sterile distilled water and 250 µl of poly-L-lysine (1 µg/ml) per well

were added and incubated for 30 minutes inside the hood. Then the poly-L-lysine was aspirated and the cover slips washed again with sterile distilled water. Then the cells were seeded into the 24-well plate at a density of 0.5 x 10^5 cells/ml in complete media (500 µl per well) and left to adhere to the cover slips for 48 hours in an incubator at 37 ºC containing 95 % air and 5 % CO2.

2.7.1.2 Fixation

Methanol (-20 ºC) was used as it can both fix and permeabilise cells (Jamur and Oliver, 2010) prior to immunocytochemistry without chemical modification of antigens. The media was aspirated from the wells and the cells washed with cold medium lacking FBS. Cells were then fixed with methanol at the same volume as used for medium (500 µl) and incubated for 10 minutes at room temperature. Following this, the methanol was aspirated and the cells washed with TBS containing 0.02 % (w/v) sodium azide.

2.7.1.3 Addition of primary antibodies

Following fixation, the cells were blocked with 5 % (v/v) normal serum (from animal used for secondary antibody) (Sigma-Alrich, UK) in TBS (filtered by syringe filter and centrifuged 1000 rpm for 5 minutes), 500 µl per well, for 30 minutes at room temperature to reduce background. Cells were stained for mitochondria, mTOR, raptor and LC3A/B with specific antibodies (Table 2.2). Preliminary experiments were performed to determine the optimum concentration for ICC, with each antibody diluted within a range recommended by the supplier. The primary antibodies were diluted in the same blocking solution and incubated overnight at 4 ºC. The negative controls with the primary antibody omitted were incubated in the block solution only.

2.7.1.4 Addition of secondary antibodies

The primary antibody solution was aspirated and the cells were washed 3 times in TBS containing 0.02 % (w/v) sodium azide, to remove any unbound antibody, for 5

minutes each. In order to detect any bound antibody, secondary antibodies, Alexa Fluor 488® conjugated to chicken anti-mouse IgG (for mouse monoclonal antibodies) or Alexa Fluor 594® conjugated to donkey anti-rabbit IgG (for rabbit monoclonal antibodies) were then applied. The secondary antibodies were diluted in blocking buffer and 500 µl per well was added and incubated in the dark for 45 minutes at room temperature. The secondary antibody dilutions used in this experiment are shown in (Table 2.2). Following this, cells were washed three times in TBS containing 0.02 % (w/v) sodium azide, to remove any unbound secondary antibody, for 5 minutes each. To stain the cell nuclei blue, 4,6-Diamidino-2-phenylindole (DAPI) 1 µg/ml (Sigma, UK) was added in the first wash for 5 minutes and the unbound DAPI was removed by the second and third washes.

2.7.1.5 Slide preparation

Slides were labelled appropriately and a small drop of Fluoromount-G (Southern Biotechnology Associates, UK) was dropped on to the slide. The cover slip was taken from the well with a bent syringe needle and forceps and cells down onto the Fluoromount-G drop. Slides were left to dry in the fridge and examined on the second day using an upright Olympus BX60 fluorescent microscope, equipped with a Cool-Snap Pro (Cybernetics) digital camera to acquire images into Labworks™ where they were saved without further manipulation or confocal microscopy (Axiovert 200M, laser unit: ZESS LSM 510 Laser Module).

Table 2.2: Details of primary and secondary antibodies used for immunocytochemical detection of mTOR, raptor, LC3A/B and Mitochondria

Primary antibodies				
Immunogen	**Species**	**Clonality**	**Dilution**	**Source**
mTOR	Rabbit	Monoclonal	**1:100** 1:200	Millipore, UK
Raptor	Rabbit	Monoclonal	1:100 **1:50**	Cell Signaling Technology, UK
LC3 A/B	Rabbit	Monoclonal	**1:100** 1:200	Millipore, UK
Mitochondria	Mouse	Monoclonal	1:100 **1:200**	Millipore, UK
Secondary antibodies				
Immunogen	**Species**	**Conjugate**	**Dilution**	**Source**
Rabbit IgG	Donkey	Alexa fluor® 594	1:100	Life technologies, UK
Mouse IgG	Chicken	Alexa fluor® 488	1:100	Life technologies, UK

Key: mTOR; mammalian target of rapamycin, Raptor; regulatory associated protein of mTOR, LC3; microtubule-associated protein 1 light chain 3.

The optimal antibody titre was determined in preliminary experiments. The optimum concentration for each antibody used in this thesis is highlighted in bold.

2.8 DNA MANIPULATION

DNA vector encode for truncated PS1 (N-terminal fragment) fused to the N-terminus of GFP was synthesized by Life Technologies, UK to be used in transfection of HEH293 cells. For vector multiplication, the vector was transformed into the *E. coli* strain NEB 5-α (competent cells) (New England BioLabs, UK) and extracted using QIAprep Spin Miniprep kits (Qiagen, UK). To confirm the presence of the vector in the extraction, restriction enzymes were used to digest the vector according to the cloning sites provided by the supplier (Life Technologies. UK).

2.8.1 Expression vector:

The synthetic gene PS1282EGFPa was assembled from synthetic oligonucleotides and/or PCR products. The fragment was cloned into pcDNA 3.1(+) _A009 using *HindIII* and *Xhol* cloning sites (Figure 2.2). The plasmid DNA was purified from transformed bacteria and concentration determined by UV spectroscopy. The final construct was verified by sequencing. The sequence within the used restriction sites was 100 % accurate as supplied by the manufacturer (Life Technologies, UK).

pcDNA™3.1(+) is a 5.4 kb vector derived from pcDNA™3 and designed for high-level stable and transient expression in mammalian hosts. High level stable and non-replicative transient expression can be carried out in most mammalian cells. The vector contains human cytomegalovirus (CMV) immediate-early promoter for high-level expression in a wide range of mammalian cells, multiple cloning sites in the forward (+) and reverse (–) orientations to facilitate cloning, neomycin resistance gene for selection of stable cell lines, SV40 origin for episomal replication and simple vector rescue in cell lines expressing the large T antigen (*i.e.*, COS-1 and COS-7), Ampicillin resistance gene and pUC origin for selection and maintenance in *E. coli* (Life Technology, UK).

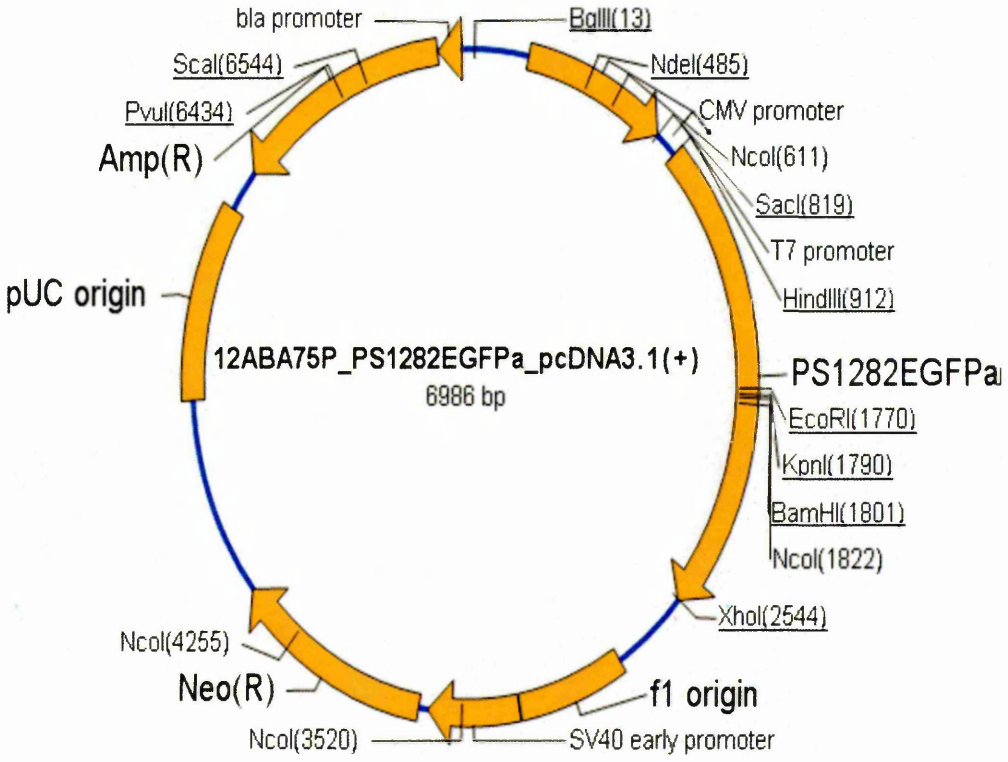

Figure 2.2: N-terminal fragment of PS-1 fused to GFP

Designation: *E.coli* K 12 (dam+dcm+tonA rec-).

Gene name: PS1282EGFPa.

Gene size: 1638 bp.

Vector backbone: pcDNA3.1 (+)-A009.

Cloning sites: *HindIII* / *XhoI.*

2.8.2 Competent cells

The *E. coli* strain NEB 5-α (High Efficiency) (New England BioLabs, UK) was routinely exploited for production of stock plasmids.

2.8.3 Transformation

A tube containing 0.05 ml of chemically competent NEB 5-α competent *E.coli* cells was thawed on ice for 10 minutes, and then 1 µl of plasmid DNA (Life Technology, UK) at an approximate concentration of 100 ng was transferred into the cells mixture. The tube was gently agitated prior to being incubated on ice for 30 minutes. Cells were heat shocked at 42 °C for exactly 30 seconds then returned to ice for a further 5 minutes. After adding 950 µl of super optimal broth with catabolite repression (SOC) at RT, cells were allowed to recover by incubating the tube at 37 °C, for 60 minutes with shacking at 250 rpm. When cells were purchased as competent cells, transformations were carried out according to the procedure described by the manufacturer. To select out the transformed cells, 100 µl of undiluted, 1:10 diluted, 1:100 diluted and 1:1000 diluted transformation reactions were plated out on antibiotic (Amp)-selective LB-agar plate and incubated at 37°C overnight. In order to extract the plasmid DNA, a single colony was selected and incubated with 5 ml of LB broth in a shaker at 37°C for 16 hours.

2.8.4 Growth media and solutions

2.8.4.1 Luria-Bertani media (LB media)

To 250 ml of deionised water, 5 g of LB media powder (ready to use) (Oxoid, UK) were added. The media solution was maintained at pH 7.0, and then sterilised by autoclaving at 121 °C for 20 minutes. LB-agar was produced by adding 3.75 g bacto-agar (Oxoid, UK) to the media prior to autoclaving.

2.8.4.2 Antibiotic selection: Ampicillin

A 1000 x stock solution of ampicillin was produced by dissolving ampicillin sodium salt (Melford, UK) in water at a concentration of 100 mg/ ml and filter sterilised with a 0.2 μm syringe filter (Sigma-Alrich, UK). Aliquots (1ml) of the stock solution were kept at -20 °C until needed when they were gently thawed and added to culture media at a final concentration of 100 μg/ml.

2.8.5 Plasmid minipreps

Plasmid DNA was extracted from 5 ml overnight growths in Luria Bertani (LB) medium using QIAprep Spin Miniprep kits (Qiagen, UK) according to the protocol provided by the supplier. The purified plasmid was stored at -20 °C.

2.8.6 Estimation of DNA concentration

The concentration of the plasmid was determined using the optical absorbance at 260 nm. The purity of the plasmid was assessed by comparing the ratio of absorbance at 260 nm and 280 nm as a pure DNA sample has a ratio of approximately 2. All absorbance measurements were taken on a Nano-Drop ND1000 spectrophotometer (Bio-Rad).

2.9 AGAROSE GEL ELECTROPHORESIS

2.9.1 Running buffer (TAE buffer)

To a liter of deionised water, 4.84 g of Tris hydroxymethylamine, 1 % (v/v) of glacial acetic acid and 1 mM of EDTA (pH 8.0) were added.

2.9.2 Loading dye

Bromophenol blue	0.25 % (w/v)
Xylene cyanol	0.25 % (w/v)
Glycerol	30 % (v/v)

2.9.3 DNA bp standards

GeneRuler 1 kbp DNA ladder (Fermentas Life Sciences) was prepared and used according to the manufacturer's protocol. The ladder has 14 fragments of 10000, 8000, 6000, 5000, 4000, 3500, 3000, 2500, 2000, 1500, 1000, 750, 500 and 250 base pairs.

2.9.4 Preparation of 1 % (w/v) agarose gel

A 1 % (w/v) agarose gel was prepared by adding 1 g electrophoresis grade agarose to 100 ml TAE buffer in a loosely stoppered conical flask. The solution was gently heated until all the agarose had melted and then allowed to cool. The gel solution was poured into the gel tray of a Biorad mini sub DNA tank up to 1 cm in height. 1.5 µl ethidium bromide (5 mg/ml) was introduced into the gel solution and mixed. The well comb was carefully inserted and the gel allowed to set. The gel was placed in the gel tank and submerged in TAE buffer.

2.9.5 Electrophoresis

Samples were prepared with a ratio of 2:1 (DNA solution: loading buffer) and 8 µl was loaded onto the gel. The gel was electrophoresed at constant voltage of 100 V for 1 hour. The electrophoretic pattern was photographed utilising a UVP epi chemi II dark room using Labworks software version 4.0.

2.10 TRANSFECTION

2.10.1 Transient transfection

HEK293 cells were transfected in a 24-well plate. The cells were cultured on cover slips (13 mm) as above (2.7.1.1). Cell density was 50,000 cells per well. In this experiment, X-tremeGENE 9 DNA Transfection Reagent (Roche, UK) was used. Cells were incubated at 37 °C in 500 µl per well complete MEME media (Lonza, UK) and allowed reach 50 % confluence before transfection.

DNA complex was prepared as follows: X-tremeGENE 9 DNA Transfection Reagent (Roche, UK), DNA and media (antibiotic and serum free media) were allowed to equilibrate to 15 °C. According to the supplier (Roche, UK), to form a complex, the minimum amount for the reaction between X-tremeGENE 9 DNA Transfection Reagent and DNA is 100 µl. So in a 100 µl reaction, a ratio of 3:1 (transfection reagent: DNA) were used. 3 µl of transfection reagent and 1 µg of DNA were diluted in 100 µl of serum, antibiotic free media and incubated for 30 minutes at room temperature.

The plate was removed from the incubator and the complete media was aspirated and replaced with antibiotic free growth media (500 µl). According to the protocol, 25 µl per well of the transfection complex was added in a drop wise manner. The plate was replaced in the incubator for 24 hours at 37 °C.

As mentioned above, the HEK293 cells were cultured on a cover slip in the well and because green fluorescent protein (GFP) was conjugated to the gene of interest in the construct, cells expressing the construct were fixed and examined under the fluorescence microscope.

After 24 hours, the plate was removed from the incubator, the growth media was aspirated and the cells were fixed with ice cold methanol for 10 minutes (section 2.7.1.2). The slides were prepared as described above (section 2.7.1.5) and the cells were examined under the fluorescence and confocal microscopes. The green fluorescent colour produced by correctly folded GFP inside the cell is an indicator of successful transfection.

Chapter 3

Antibody Characterisation

3.1 INTRODUCTION

The number of antibodies available commercially grows ever larger. Maybe as a result, quality control is not always what it could and should be. Investigators must be aware of potential mistakes and take steps to assure themselves that the specificity of each antibody is as advertised (Couchman, 2009).

The use of immunocytochemistry and immunohistochemistry has become ubiquitous in many scientific fields. Now, a large number of published papers uses immunocytochemistry or immunohistochemistry, and some papers use ten or more antibodies to investigate issues of colocalization or cell typing. This way of dealing with these types of techniques has produced a large amount of new information, but also a large amount of misinformation (Clifford B, 2005).

The Journal of comparative neurology has reported that the Journal has received distressed communications from authors, who have had to withdraw papers because an antibody against a novel marker was found to stain tissue in knockout animals, who lack the protein of interest (Clifford, 2005).

Many researchers use multiple antibodies from different companies and compare staining patterns. This is a very good approach; especially if the antibodies are monoclonal and polyclonal antibodies and they recognize different epitopes on the antigen of interest (Couchman, 2009).

In the present study, different antibodies from different sources against autophagy proteins of interest (mTOR, raptor and LC3) were characterised utilizing western blotting. Anti-mTOR and anti-raptor antibodies were tested against protein extracted from three untreated and untransfected cell lines: normal rat kidney (NRK) cell line, human breast cancer (MCF-7) cell line and human embryonic kidney (HEK293) cell line. Anti-LC3 antibodies were tested against proteins extracted from rapamycin treated

HEK293 cell line in order to detect the two forms of LC3 (LC3-I and LC3-II), produced as a result of autophagy induction under the influence of rapamycin treatment.

3.2 MATERIALS AND METHODS

All the primary antibodies that have been characterised in this study and the ones that were selected to be used in this project are shown in the three tables below: anti-mTOR antibodies (table 3.1), anti-raptor antibodies (table 3.2) and anti-LC3 antibodies (table 3.3). In the case of anti-LC3 antibody characterisation, the proteins used were extracted from rapamycin treated (different concentrations for different times) HEK293 cells.

Table 3.1: The primary rabbit anti-mTOR antibodies used in this study

Clonality	Applications	Species Reactivity	Immunogen	Company
polyclonal	ICC, IHC-Fr, IP, WB.	Hu, Ms, Rat.	Synthetic peptide human-represents a portion of human Mammalian Target of Rapamycin encoded in part by exons 5 and 6.	Abcam (ab2732)
polyclonal	ICC/IF, WB.	Hu, Ms.	Synthetic 15 amino acid peptide from the N terminus of human TOR.	Abcam (ab25880)
polyclonal	ELISA, IP, WB.	Hu, Ms, Rat.	Synthetic peptide corresponding to the C-terminal of human TOR protein.	Abcam (ab83495)
Polyclonal	IP, WB.	Hu, Ms, Rat, MK	Synthetic peptide corresponding to residues surrounding Ser2481 of human TOR.	Cell Signaling Technology (2972)
Polyclonal	IP, WB, IH (P).	Hu, R (M).	Recombinant GST fusion protein corresponding to amino acids 1223-1290 of human mTOR.	Millipore (07-1415).
Monoclonal	FC, IC, IH (P), IP, WB.	Hu, Ms, Rat.	KLH-conjugated synthetic peptide corresponding to the C-terminal region of human mTOR.	Millipore (04-385).

Table 3.2: The primary rabbit anti-raptor antibodies used in this study

Clonality	Applications	Species Reactivity	Immunogen	Company
Polyclonal	IP, WB.	Hu	KLH conjugated linear peptide corresponding to human raptor at the N-terminus.	Millipore (09-217)
Polyclonal	WB.	Hu, Ms, Rat	A synthetic peptide corresponding to amino acids encoded within exon 26 of human raptor.	Calbiochem (ST1048).
Monoclonal	IP, WB.	Hu, Ms, Rat, MK	Synthetic peptide corresponding to the sequence of human raptor.	CellSignaling Technology (2280)

Table 3.3: The primary rabbit anti-LC3 antibodies used in this study

Clonality	Applications	Species Reactivity	Immunogen	Predicted molecular Weight	Company
Polyclonal LC3 antibody	WB, IF, IHC-P, IP	Hu, Ms, Rat	A synthetic peptide made to an N-terminal portion of the human LC3 protein sequence (between residues 1-100).	17,19kDa	Novus Biological (NB100-2220)
Monoclonal LC3B antibody	WB, IP, IHC-P, IF-IC, F.	Hu, Ms, Rat, (Mk, B, Pg)	Synthetic peptide corresponding to residues near the N terminus of LC3B.	14,16 kDa	CellSignaling Technology (D11)XP (3868)
Monoclonal LC3A/B antibody	WB, IH (P), IC, IP, FC.	Hu, Ms, Rat	Synthetic peptide corresponding to the N-terminus of human LC3A/B.	16 kDa	Millipore (MABC176)

3.2.1 Cell culture and protein extraction

Cell culture, protein extraction and western blot were conducted by the methods described in chapter 2 (Sections: 2.2, 2.3 and 2.6). Additional experiments (mTOR knock down using mTOR siRNA, peptide competition and negative controls) were conducted to confirm the identity of some bands produced by the two rabbit polyclonal anti-mTOR antibodies (ab 83495) and (ab 25880) (Abcam, UK).

3.2.2 siRNA experiment for mTOR knockdown

RNA interference is the process of sequence-specific, post transcriptional gene silencing in animals and plants, induced by double-stranded RNA that triggers the degradation of complementary mRNA (Gunter and Tuschi, 2004). To confirm the identity of the bands at 42 kDa, siRNA experiments to knockdown mTOR gene expression were conducted. The two polyclonal anti-mTOR antibodies (ab 83495) and (ab 25880) were used to detect mTOR in this experiment.

In this experiment, only NRK cells were used. SignalSilence mTOR siRNA kit (10μM in 150 μl) (Cell Signalling Technology, UK) was used. The transfection reagent used was X-treme GENE siRNA transfection reagent (1 ml) (Roche, UK). The proteins extracted from un-transfected NRK cells, NRK cells transfected with mTOR siRNA I and II (200 nM) and NRK cells treated with transfection reagent only were loaded (18μl/well) on to 7.0 % polyacrylamide gels.

The difference between siRNA I and II is that they target different regions of the mRNA. Both of them target the open reading frame, but siRNA I is about 1000 nucleotides more 5̀ than the second. In the siRNA experiment, the NRK cells were cultured in t25 flasks containing EMEM media (Lonza, UK) and left in the incubator at 37 °C until 80 % confluent. Next, the cells were trypsinised and the suspension was aspirated. Then, the cells were centrifuged at 200g for 10 minutes at RT. The media was discarded and

the cell pellets were re-suspended in 1 ml of fresh serum and antibiotic free EMEM media. 20µl sample from the solution was taken for cell counting using a haematocytometer. Cells were seeded into 6-well plates at a density of 2×10^5 (2 ml serum and antibiotic free medium/well) and allowed to adhere for 24 h. Subsequently, the cells were transfected by adding the complex (transfection reagent: siRNA) to each well (siRNA, 200 nM/well) according to the siRNA manufacturer protocol. Some wells contained un-transfected cells and others had cells treated with transfection reagent only as a control. Then the cells were returned to the incubator and allowed to grow until confluent. Protein was extracted from the cells as described in chapter 2 (section 2.3) and examined by western blotting.

3.2.3 Peptide competition experiment for mTOR antibody (ab83495)

Peptide competition experiment was also performed to confirm the identity of the same bands detected on WB. The protein extraction from the NRK cells and western blot were performed as described in chapter 2 (Sections: 2.3 and 2.6). Only, the polyclonal anti-mTOR antibody (ab 83495) was used in this experiment. In order to block the primary antibody (ab83495), peptide (sequence derived from C-terminus of human TOR protein, covering from 2400-2470 aa) corresponding to the immunogen (ab 99156) (0.20 mg/ml) (Abcam, UK) was used.

In this experiment, blocking peptide (100µl) (0.20 mg/ml) was incubated with the primary antibody (1µl) (0. 50 mg/ml) in 1.5 ml of 5 % non-fat skimmed milk in Tris-buffered saline (TBS) at RT for 1 hour before incubation with the membrane for 90 minutes at room temperature.

3.2.4 Negative control for mTOR antibody (ab83495)

In the case of negative control experiments, only secondary antibodies were incubated with the membrane. The secondary antibody was goat anti-rabbit labelled with alkaline

phosphatase (AP) (Cell signalling technology, UK). To identify any false positive results, proteins extracted from NRK cells were loaded (18µl/well) on two 7% polyacrylamide gels and immunoblotted onto two nitrocellulose membranes. The first membrane was incubated with primary antibody (1:1000) overnight at 4°C, and then incubated with the secondary antibody (1:1000) for 1hr at RT. The other membrane was incubated only with the secondary antibody (1:1000) for 1hr at RT.

3.3 RESULTS

3.3.1 mTOR expression

The proteins used to assess the specificity of the antibodies were extracted from three different cell lines which are: NRK, MCF-7 and HEK293. Six different anti-mTOR antibodies from different suppliers were characterised, (table 3.1). Also, alongside antibody characterisation, optimisation was performed in terms of fixation and antibody dilution. For example, different percentages of polyacrylamide gels ranging from 6 to 7.5 % were prepared in order to obtain the optimal gel percentage to separate bands for such a large protein (mTOR) at 289 kDa.

3.3.1.1 The Polyclonal anti-mTOR antibody (ab2732)

The polyclonal anti-mTOR antibody (ab2732) stained non-specific bands for mTOR (approximately at 129 and at 88 kDa) on 6.5 % polycarylamide gel utilizing NRK protein extract (Figure 3.1). After that and because mTOR is a large protein, 6% polyacrylamide gels were used. In this western blot, the antibody (ab2732) detected two bands: one at approximately 270 kDa which is close to that expected for mTOR at 289 kDa. However, there was another band at approximately 115 kDa in cell extracts both: with and without protease inhibitor cocktail, (Figure 3.2). For this reason, this antibody (ab2732) was excluded and was not used to determine the subcellular localization of mTOR by immunocytochemistry.

3.3.1.2 The Polyclonal anti-mTOR antibodies (ab83495) and (ab25880)

After the failure of the first antibody to detect the correct molecular weight band for mTOR, two more anti-mTOR antibodies (different immunogens) from the same company (Abcam, UK) were obtained and characterised. The antibodies are: (ab83495) and (ab25880).

According to the anti-mTOR antibodies supplier (Abcam) bands should be detected by ab 83495 at molecular size approximately 298 kDa and by ab 25880 at molecular size approximately more than 204 kDa.

On a 7 % polyacrylamide gel using NRK extraction, the two antibodies (ab83495) and (ab25880) detected bands at high molecular weight, approximately 135 kDa, but less than 298 and 204 kDa, while the major bands stained by the two antibodies were at approximately 42 kDa (Figures 3.3 and 3.4).

The above experiment was repeated using the same gel percentage and the same result was obtained (data not shown). In addition, the experiment was also repeated using lower gel percentage (6.5 %) and both antibodies (ab83495) and (ab25880) produced the same staining as before (Figures 3.5 and 3.6).

3.3.1.2.1 siRNA experiment for mTOR knockdown

From these results, it appears that the result is reproducible and the band detected at approximately 42 kDa, especially by ab83495, is strong and clear. Therefore, to confirm the identity of the band, siRNA experiments to knockdown mTOR gene expression were conducted (figures 3.7 and 3.8). By using the same anti-mTOR antibodies, the immuno blot shows that the two antibodies: (ab83495) and (ab25880), failed to detect any band in the lanes (4, 5, 8 and 9) that represent the transfected cells lanes (i.e the lanes where mTOR has knocked down)

Western blot analysis for actin (18µl/well) demonstrated the presence of actin in all samples loaded at similar levels, acting as a loading control. The monoclonal anti-actin antibody produced a band at 42 kDa (figure 3.9).

3.3.1.2.2 Peptide competition experiment for mTOR antibody (ab83495)

The result of the previous experiment (mTOR knockdown) suggested that the lower molecular weight bands might be generated from mTOR, and therefore another confirmation experiment was required. Peptide competition experiment in which the primary antibody is blocked by the corresponding peptides before incubation with the membrane was used. In this experiment, the primary antibody (ab83495) was blocked by the corresponding peptide (ab99156).

Western blot result in (figure 3.10) shows that the antibody was blocked and the bands disappeared, as can be seen in lanes 5 and 6 when compared with the other lanes.

3.3.1.2.3 Negative control experiment for mTOR antibody (ab83495)

To exclude any false positive result, protein extracted from NRK (18µl/well) was used as a negative control to assess non-specific binding of the secondary antibodies. The result revealed no non-specific bands detected by the secondary antibodies in the absence of the primary antibodies as can be seen in lanes 5 and 6 when compared with lanes 2 and 3 where primary antibodies were used before the secondary antibody (figure 3.11).

To test for mTOR degradation during extraction, the same protein extraction (with and without protease inhibitors cocktail) was performed. The western blot analysis (Figures 3.12 and 3.13) revealed that both antibodies stained faintly bands for mTOR at the correct molecular weight (approximately 289 kDa). However, the antibodies especially (ab38495) also stained very strong and clear bands at approximately 70 kDa on the same membrane.

It has been reported that the human breast cancer cell line MCF-7 is a good model to study mTOR. For this reason, MCF-7 cells were obtained, and again the same antibodies were tested against the protein extracted from MCF-7 cells. The protein was extracted from MCF-7 cells with and without protease inhibitor cocktail. The western blot results showed that the antibodies (ab83495) and (ab25880) stained the same bands that were seen in the previous experiment (bands at approximately 289 and 70 kDa) with extra bands at approximately 170 and 130 kDa in case of ab83495 (Figure 3.14) and (Figure 3.15).

3.3.1.3 Rabbit polyclonal anti-mTOR antibody (2972)

The previous three different commercial anti-mTOR antibodies from the same company (Abcam, UK) were characterised. All of the antibodies failed to detect a single band at the appropriate molecular weight for mTOR full length protein on different percentages of polyacrylamide gels. For this reason, using anti-mTOR antibodies from different suppliers was considered. Rabbit polyclonal anti-mTOR antibody (2972) (Cell Signaling Technology, UK) was obtained. The antibody was tested against protein extracted from NRK, MCF-7 and HEK293 cells (Figure 3.16) and (Figure 3.17) on 6 % polyacrylamide gels. The antibody produced the correct molecular weight bands for mTOR with the three cell lines at approximately 289 kDa. However, the antibody also stained faintly other bands at approximately 250 and 180 kDa on the same membrane. For this reason, also this antibody was excluded from the project.

3.3.1.4 Rabbit polyclonal anti-mTOR antibody (07-1415)

Another rabbit polyclonal anti-mTOR antibody (07-1415) (Millipore, UK) was obtained. The antibody also was tested against protein extracted from two cell lines, NRK and MCF-7. The proteins were separated on 6 % polyacrylamide gel. The western blot result showed staining of multiple bands in both cell lines (Figure 3.18). Some of these bands

were at the correct molecular size of full length mTOR, but the other bands were at different molecular weights. Also, because of the multiple band detection, this antibody was excluded from the study.

3.3.1.5 Rabbit monoclonal anti-mTOR antibody (04-385)

All the anti-mTOR antibodies that were previously characterised were polyclonal antibodies. The shared characteristic between these polyclonal antibodies is the production of multiple bands. For this reason, a rabbit monoclonal anti-mTOR antibody (04-385) (Millipore, UK) was obtained. The monoclonal antibody was tested against proteins extracted from three different cell lines (NRK, MCF-7 and HEK293). The proteins were separated on 6 % polyacrylamide gels. The western blot results revealed that the antibody detected only one band at the correct molecular weight of full length mTOR (289 kDa) with the three cell lines (Figures 3.19 and 3.20). Based on this result, this rabbit monoclonal anti-mTOR antibody was selected to be used in the determination of the subcellular localization of mTOR protein in the present study. While, all the other previously characterised polyclonal anti-mTOR antibodies were excluded from the research.

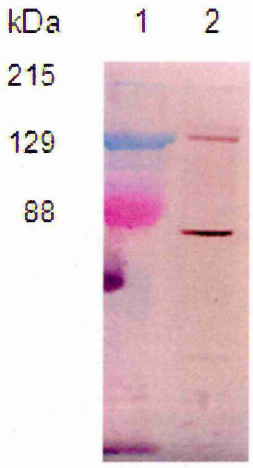

Figure 3.1 Western blot analysis for mTOR expression by NRK cells, protein sample (18µl/well) was loaded and analyzed by polyclonal anti-mTOR antibody (ab2732) on 6.5% polyacrylamide gel. Lane 1 prestained protein marker. Lane 2 protein extracted from NRK cells.

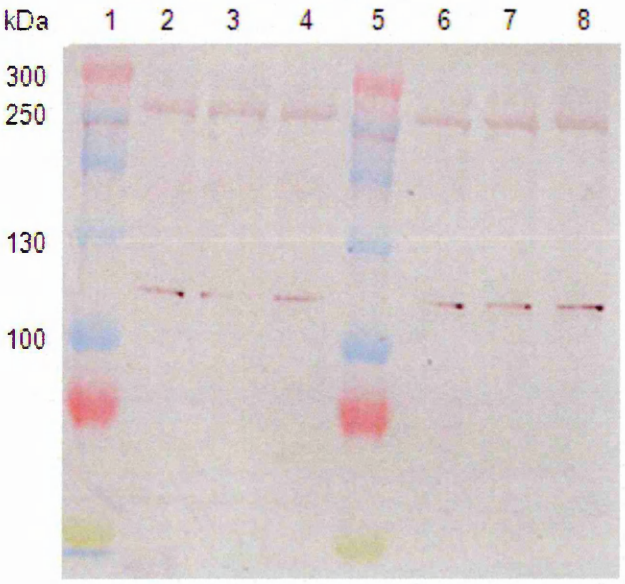

Figure 3.2 Western blot analysis for mTOR expression by NRK cells, protein sample (18µl/well) was loaded and analyzed by polyclonal anti-mTOR antibody (ab2732) on 6.0% polyacrylamide gel. Lanes 1 and 5 multicolor high range protein ladder. Lanes 2-4 protein extracted from NRK cells without protease inhibitor cocktail. Lanes 6-8 protein extracted from NRK cells with protease inhibitor cocktail.

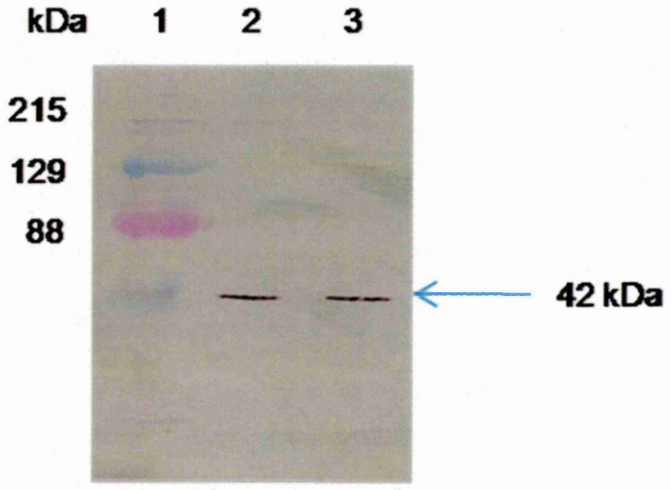

Figure 3.3 Western blot analysis for mTOR expression by NRk cells, Protein samples (18µl/well) were loaded and analyzed by using polyclonal anti-mTOR antibodies (ab83495) on 7.0 % polyacrylamide gel. Lane 1 is molecular marker. Lanes 2-3 Protein extracted from NRK cell line.

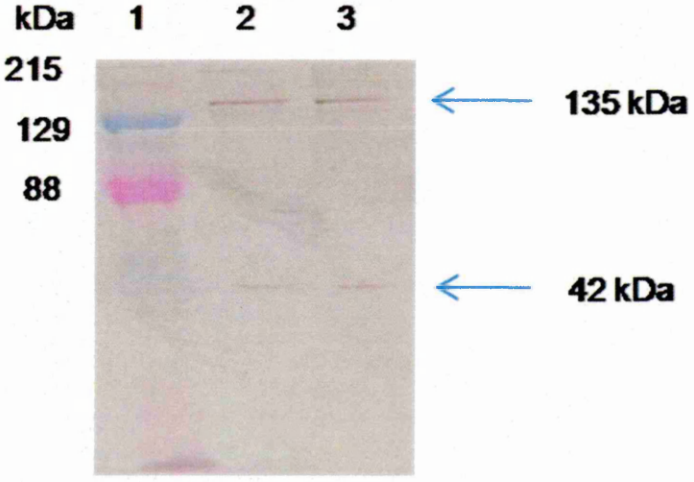

Figure 3.4 Western blot analysis for mTOR expression by NRK cells, Protein samples (18µl/well) were loaded and analyzed by using polyclonal anti-mTOR antibodies (ab25880) on 7.0 % polyacrylamide gel. Lane 1 is molecular marker. Lanes 2-3 Protein extracted from NRK cell line.

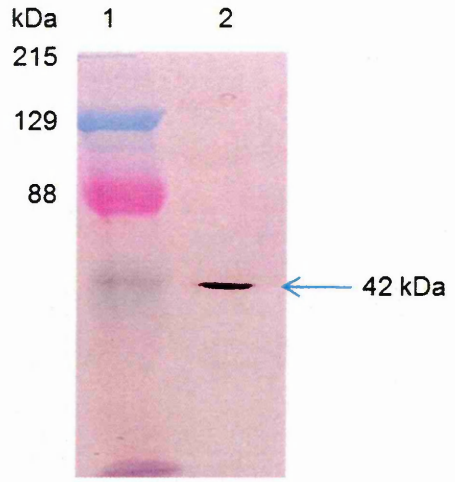

Figure 3.5 Western blot analysis for mTOR expression by NRk cells, Protein samples (18µl/well) were loaded and analyzed by using polyclonal anti-mTOR antibodies (ab83495) on a 6.5 % polyacrylamide gel. Lane 1 is molecular marker. Lane 2 Protein extracted from NRK cell line.

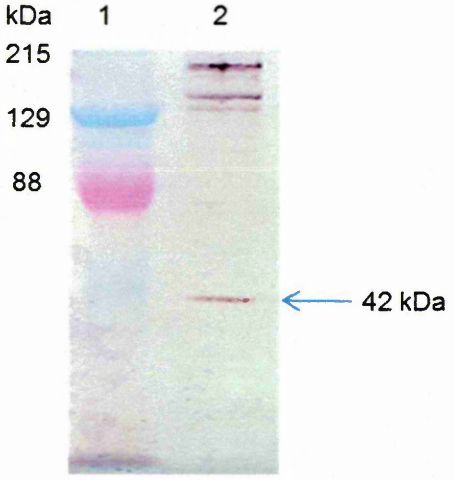

Figure 3.6 Western blot analysis for mTOR expression by NRK cells, Protein samples (18µl/well) were loaded and analyzed by using polyclonal anti-mTOR antibodies (ab25880) on a 6.5 % polyacrylamide gel. Lane 1 is molecular marker. Lane 2 Protein extracted from NRK cell line.

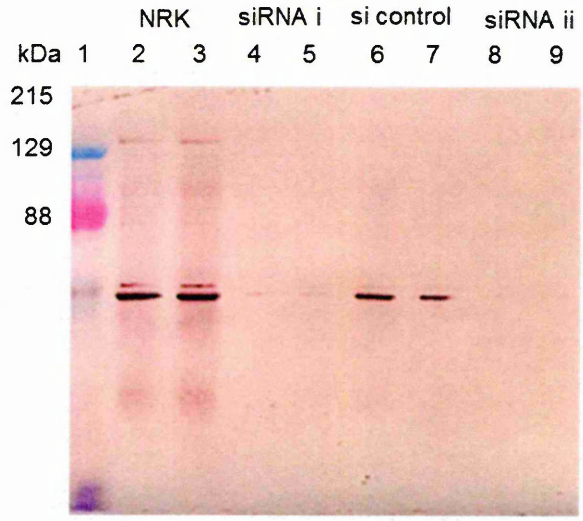

Figure 3.7 mTOR knocked down. Western blot analysis for mTOR expression by NRK cells, Protein samples (18µl/well) were loaded on 7 % gels and analyzed using polyclonal anti-mTOR antibodies (83495). Lanes 2-3 Protein extracted from untreated NRK cells, lanes 4-5 Protein extracted from NRK cells treated with mTOR siRNA I, lanes 6-7 Protein extracted from NRK cells treated with transfection reagent only, Lanes 8-9 protein extracted from NRK cells transfected with mTOR siRNA II and lane 1 is molecular weight markers.

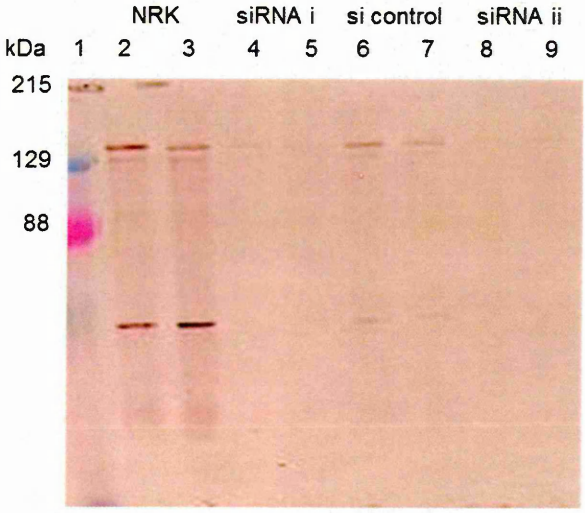

Figure 3.8 mTOR knocked down. Western blot analysis for mTOR expression by NRK cells, Protein samples (18µl/well) were loaded on 7 % gels and analyzed using polyclonal anti-mTOR antibodies (25880). Lanes 2-3 Protein extracted from untreated NRK cells, lanes 4-5 Protein extracted from NRK cells treated with mTOR siRNA I, lanes 6-7 Protein extracted from NRK cells treated with transfection reagent only, Lanes (8-9) protein extracted from NRK cells transfected with mTOR siRNA II and lane 1 is molecular weight markers.

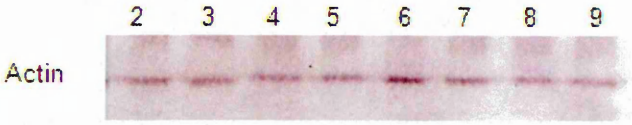

Figure 3.9 Western blot analysis for actin expression by NRK cells, Protein samples (18µl/well) were loaded on 7.0 % gels and analyzed by using polyclonal rabbit anti-actin antibodies. Lanes 2-3 Protein extracted from untransfected NRK cells, lanes 4-5 Protein extracted from NRK cells transfected with mTOR siRNA I, lanes 6-7 Protein extracted from NRK cells treated with transfection reagent only, Lanes 8-9 protein extracted from NRK cells transfected with mTOR siRNA II.

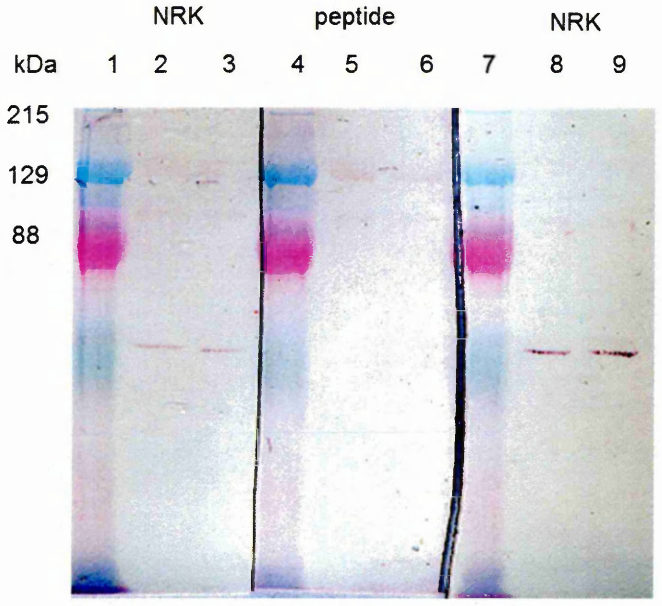

Figure 3.10 Peptide competitions.Western blot analysis for mTOR expression by NRK cells, Protein samples (18µl/well) were loaded and analyzed by using polyclonal anti-mTOR antibodies (ab83495). Lanes 2-3 Protein extracted from NRK cells, lanes 5-6 Protein extracted from NRK cells, but polyclonal anti-mTOR primary antibodies were blocked by corresponding peptide, lanes 8-9 Protein extracted from NRK cells, and Lanes 1-4-7 are molecular markers.

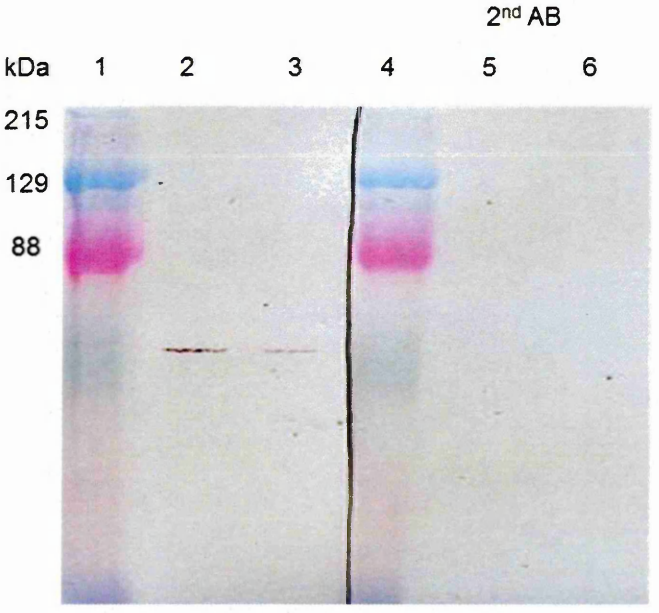

Figure 3.11 negative control for mTOR. Protein samples (18µl/well) were loaded. (Western blot analysis without primary anti-mTOR antibodies). Lanes 2-3 protein extracted from NRK cells, primary and secondary antibodies were used, lanes 5-6 proteins extracted from NRK cells, only secondary antibodies were used and lanes 1-4 are molecular markers.

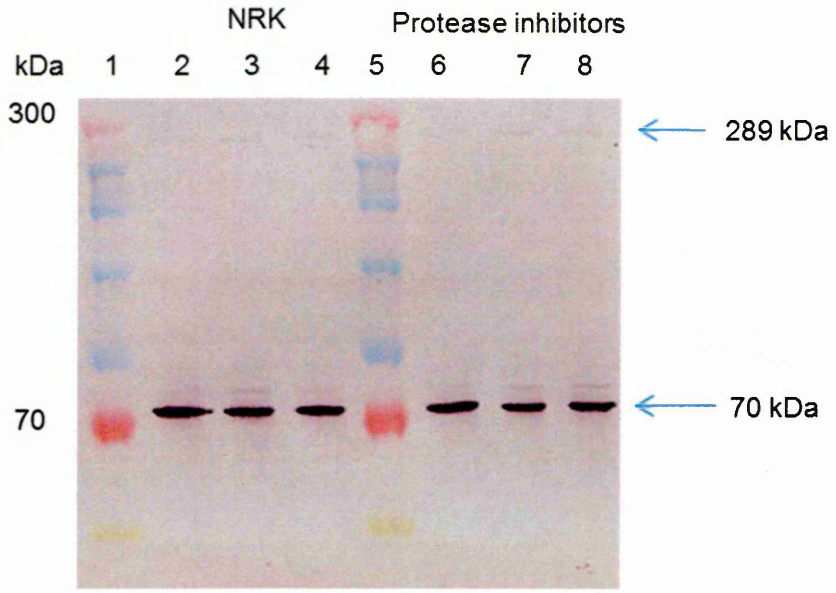

Figure 3.12 Western blot analysis for mTOR expression by NRK cells, Protein samples (18µl/well) were loaded and analyzed by using polyclonal anti-mTOR antibodies (ab83495). Lanes 2-4 Protein extracted from NRK cells without protease inhibitor cocktail. Lanes 6-8 Protein extracted from NRK cells with protease inhibitors cocktail. Lanes 1 and 5 are multicolor high range protein ladder.

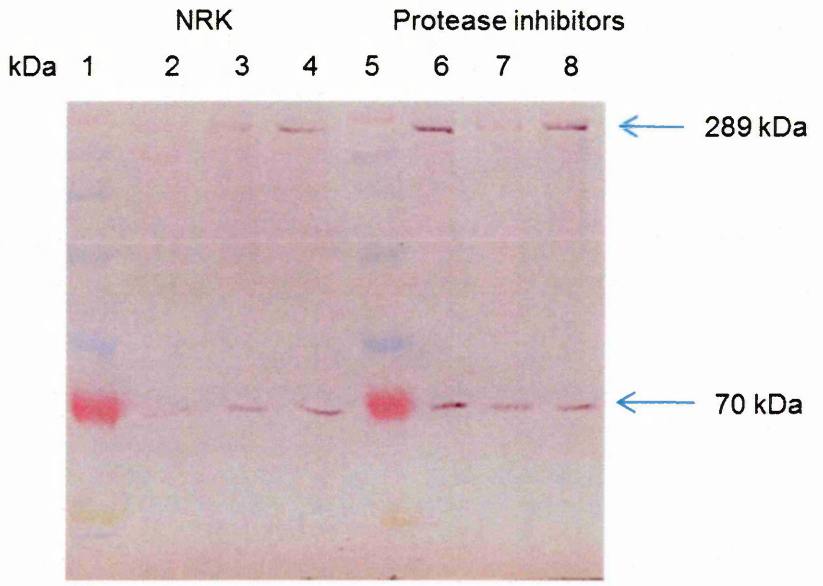

Figure 3.13 Western blot analysis for mTOR expression by NRK cells, Protein samples (18µl/well) were loaded and analyzed by using polyclonal anti-mTOR antibodies (ab25880). Lanes 2-4 Protein extracted from NRK cells without protease inhibitors cocktail. Lanes 6-8 Protein extracted from NRK cells with protease inhibitors cocktail. Lanes 1 and 5 are multicolor high range protein ladder.

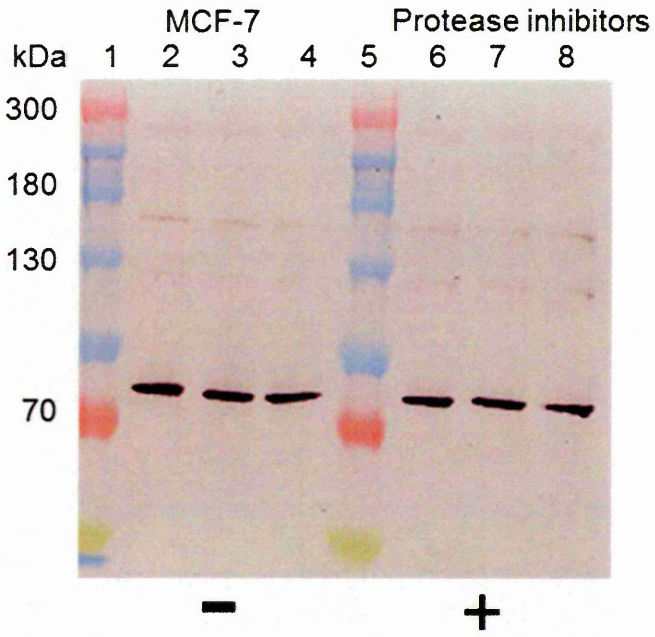

Figure 3.14 Western blot analysis for mTOR expression by MCF-7 cells, Protein samples (18µl/well) were loaded and analyzed by using polyclonal anti-mTOR antibodies (ab83495). Lanes 2-4 Protein extracted from MCF-7 cells without protease inhibitors cocktail. Lanes 6-8 Protein extracted from MCF-7 cells with protease inhibitor cocktail. Lanes 1 and 5 are multicolor high range protein ladder.

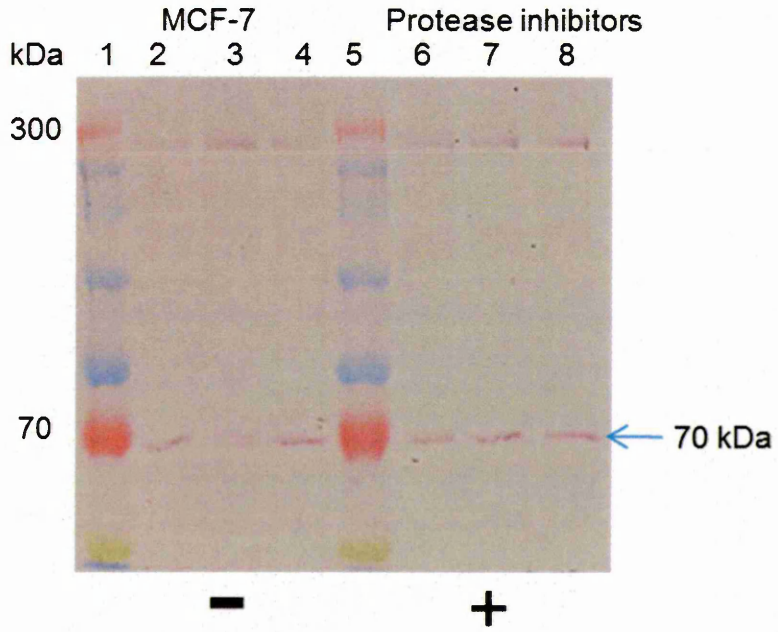

Figure 3.15 Western blot analysis for mTOR expression by MCF-7 cells, Protein samples (18µl/well) were loaded and analyzed by using polyclonal anti-mTOR antibodies (ab25880). Lanes 2-4 Protein extracted from MCF-7 cells without protease inhibitor cocktail. Lanes 6-8 Protein extracted from MCF-7 cells with protease inhibitor cocktail. Lanes 1 and 5 are multicolor high range protein ladder.

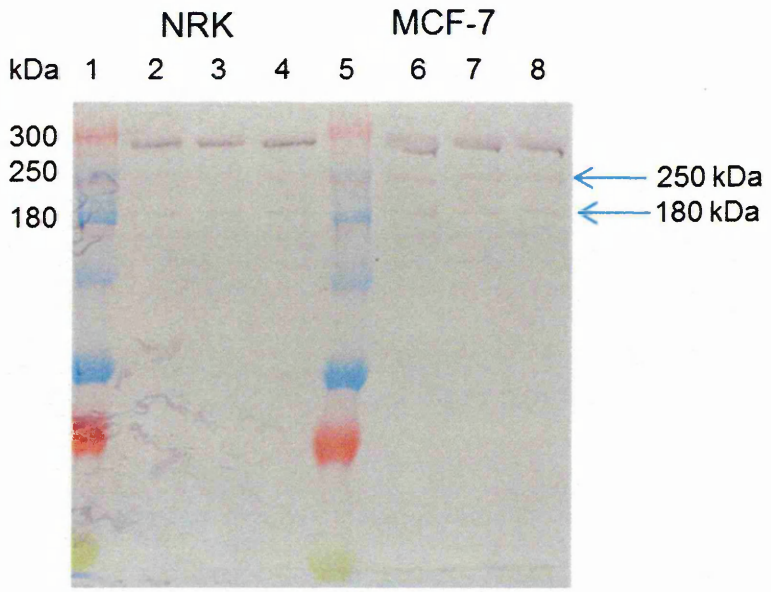

Figure 3.16 Western blot analysis for mTOR expression by NRK and MCF-7 cells, Protein samples (18µl/well) were loaded and analyzed by using polyclonal anti-mTOR antibodies (2972) (Cell Signaling Technology, UK). Lanes 2-4 Protein extracted from NRK cells with protease inhibitor cocktail. Lanes 6-8 Protein extracted from MCF-7 cells with protease inhibitor cocktail. Lanes 1 and 5 are multicolour high range protein ladder.

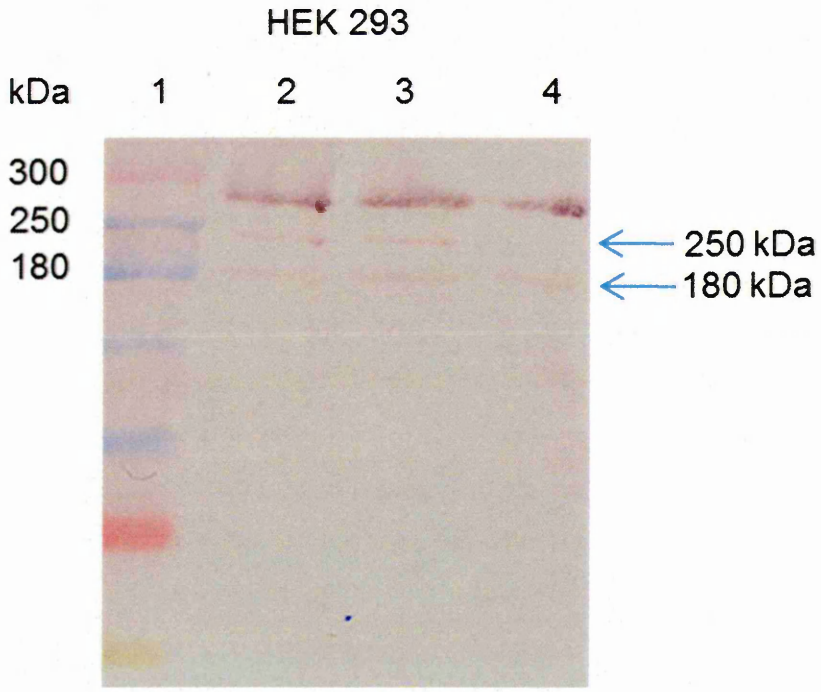

Figure 3.17 Western blot analysis for mTOR expression by HEK293 cells, Protein samples (18µl/well) were loaded and analyzed by using polyclonal anti-mTOR antibodies (2972) (Cell signaling technology, UK). Lanes 2-4 Protein extracted from HEK293 cells with protease inhibitors cocktail. Lane 1 is multicolour high range protein ladder.

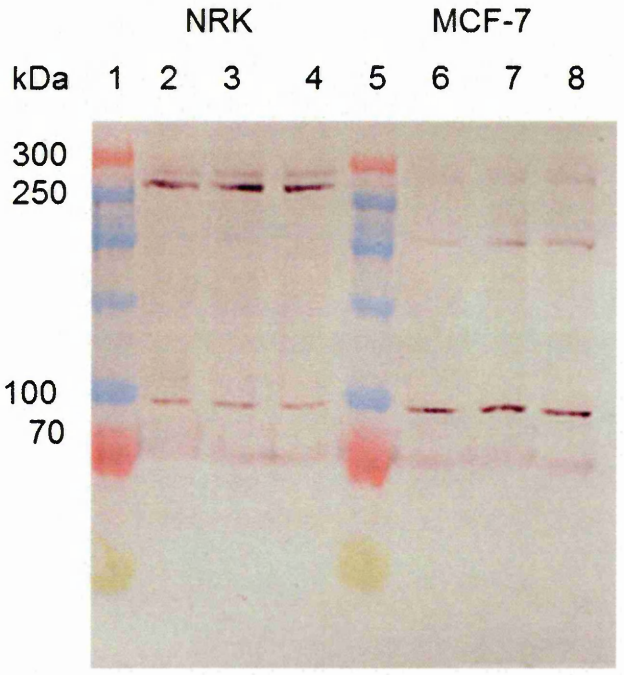

Figure 3.18 Western blot analysis for mTOR expression by NRK and MCF-7 cells, Protein samples (18µl/well) were loaded and analyzed by using polyclonal anti-mTOR antibodies (07-1415) (Millipore, UK). Lanes 2-4 Protein extracted from NRK cells with protease inhibitors cocktail. Lanes 6-8 Protein extracted from MCF-7 cells with protease inhibitor cocktail. Lanes 1 and 5 are multicolour high range protein ladder.

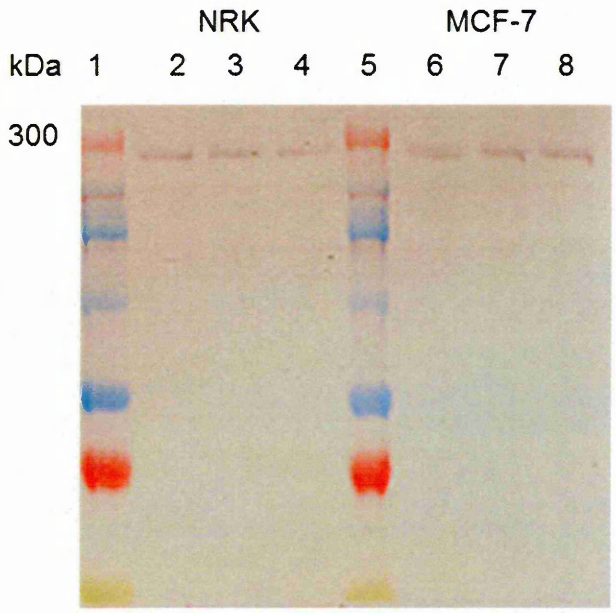

Figure3.19 Western blot analysis for mTOR expression by NRK and MCF-7 cells, Protein samples (18µl/well) were loaded and analyzed by using monoclonal anti-mTOR antibodies (04-385 Millipore, UK). Lanes 2-4 Protein extracted from NRK cells with protease inhibitor cocktail. Lanes 6-8 Protein extracted from MCF-7 cells with protease inhibitor cocktail. Lanes 1 and 5 are multicolour high range protein ladder.

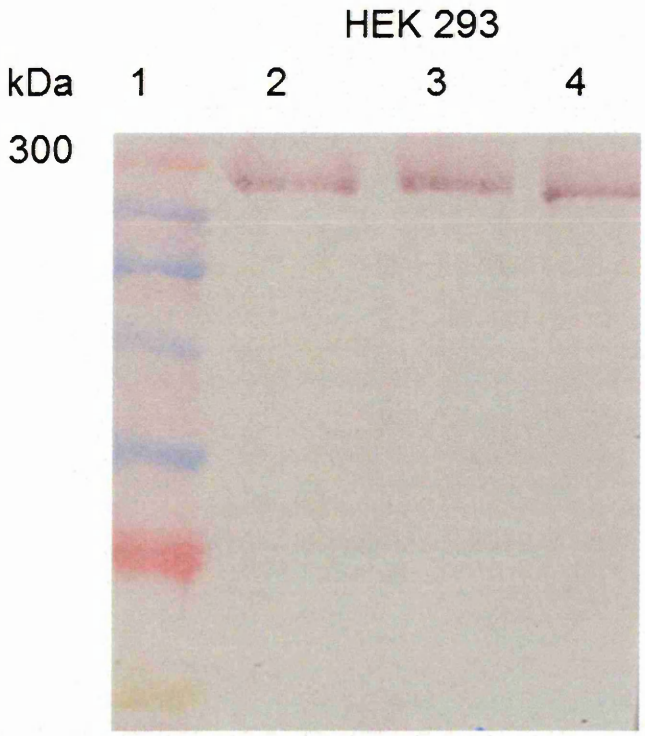

Figure 3.20 Western blot analysis for mTOR expression by HEK293cells, Protein samples (18µl/well) were loaded and analyzed by using monoclonal anti-mTOR antibodies (04-385 Millipore, UK). Lanes 2-4 Protein extracted from HEK293 cells with protease inhibitor cocktail. Lanes 1 is multicolour high range protein ladder.

3.3.2 Raptor expression:

Using the same strategy as used for anti-mTOR antibodies, anti-raptor antibodies were characterised. Three different anti-raptor antibodies from different suppliers were obtained (table 3.2). During anti-mTOR antibodies characterisation, the results showed that the rabbit monoclonal anti-mTOR antibody was more specific than the polyclonal ones in detecting mTOR full length protein. Based on this information, it was decided to obtain anti-raptor antibodies which were either polyclonal or monoclonal. These anti-raptor antibodies were tested against proteins extracted from three different cell lines (NRK, MCF-7 and HEK293). For this western blot analysis, 7 % polyacrylamide gels were used.

3.3.2.1 The polyclonal anti-raptor antibodies (ST1048) and (09-217)

According to the suppliers, the raptor protein detected by these antibodies was at molecular weight of 150 kDa. The western blot result revealed that anti-raptor (ST1048) (Calbiochem, UK) antibody, when tested against protein extracted from HEK293 cells, stained multiple bands at different molecular sizes including one at the expected 150 kDa molecular weight for raptor (Figure 3. 21). The other anti-raptor (09-217) (Millipore, UK) antibody, when tested against the same protein extraction, produced two bands. One of these bands is very near to the correct molecular weight of raptor (Figure 3.22). Because of the production of multiple bands, it was difficult to utilize these two antibodies in the determination of the subcellular localization of raptor by ICC. So, these two antibodies were excluded from the project.

3.3.2.2 The monoclonal anti-raptor antibody (2280): see (table 3.2).

After the failure of the previous two polyclonal anti-raptor antibodies to detect only one band for raptor at the right molecular size, the monoclonal anti-raptor (2280) (Cell Signalling Technology, UK) antibody was tested. According to the supplier, this

antibody should detect a band at molecular weight 150 kDa. Firstly, the antibody was tested against protein extracted from NRK cells. After the separation of the protein on 7 % polyacrylamide gel, the western blot demonstrated that the antibody detected only one band at 150 kDa (Figure 3.23). To confirm the result, in the same experiment circumstances, the antibody was tested against proteins extracted from the other two cell lines (MCF-7 and HEK293). The western blot result revealed that the antibody has also stained only one band for raptor at the right molecular weight in both cell lines (Figures 3.24 and 3.25). From these results in the present study, it seems that monoclonal antibodies are more specific in western blot analysis than polyclonal antibodies. Based on these results, this antibody (2280) was selected to be used in the determination of raptor subcellular localization, while the other two polyclonal antibodies were excluded.

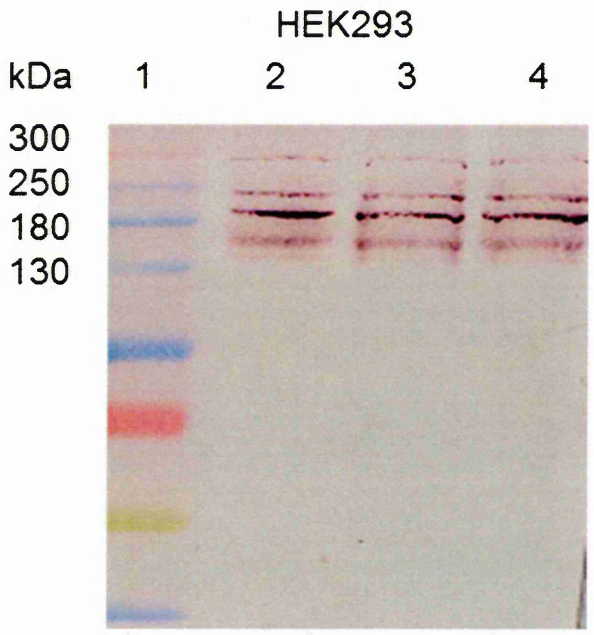

Figure 3.21 Western blot analysis for raptor expression by HEK293 cells, Protein samples (18µl/well) were loaded and analyzed by using polyclonal anti-raptor antibodies (ST1048, Calbiochem, UK). Lanes 2-4 protein extracted from HEK293 cells with protease inhibitors cocktail. Lane 1 is multicolor high range protein ladder.

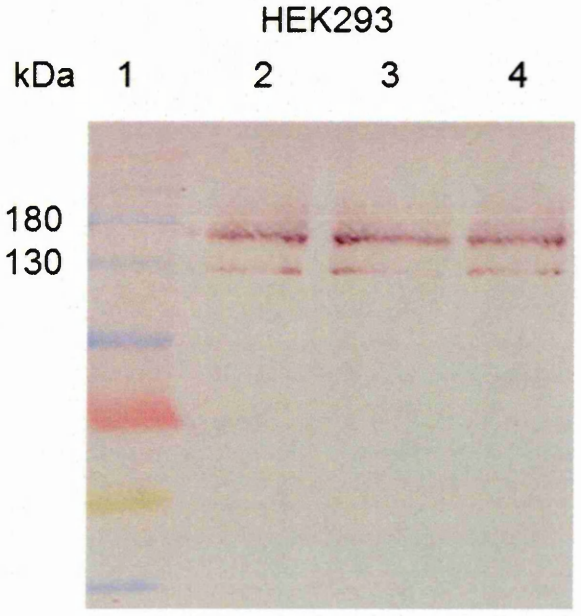

Figure 3.22 Western blot analysis for raptor expression by HEK293 cells, Protein samples (18µl/well) were loaded and analyzed by using polyclonal anti-raptor antibodies (09-217, Millipore, UK). Lanes 2-4 protein extracted from HEK293 cells with protease inhibitors cocktail. Lane 1 is multicolor high range protein ladder.

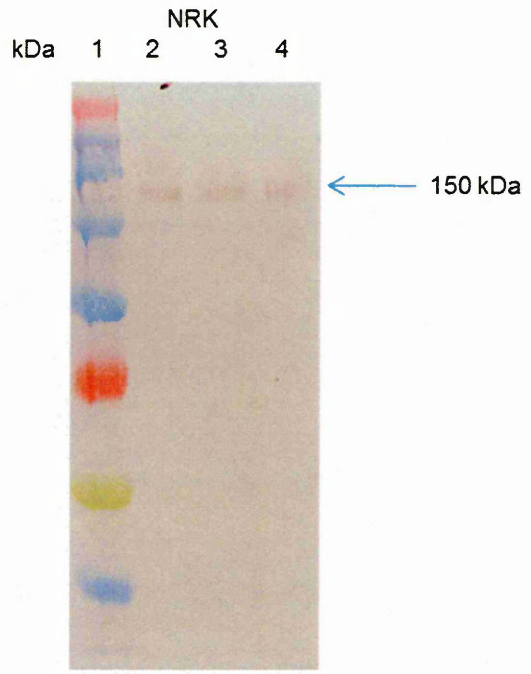

Figure 3.23 Western blot analysis for raptor expression by NRK cells, Protein samples (18µl/well) were loaded and analyzed by using monoclonal anti-raptor antibodies (2280 Cell Signaling Technology, USA). Lanes 2-4 Protein extracted from NRK cells with protease inhibitors cocktail. Lane 1 is multicolor high range protein ladder.

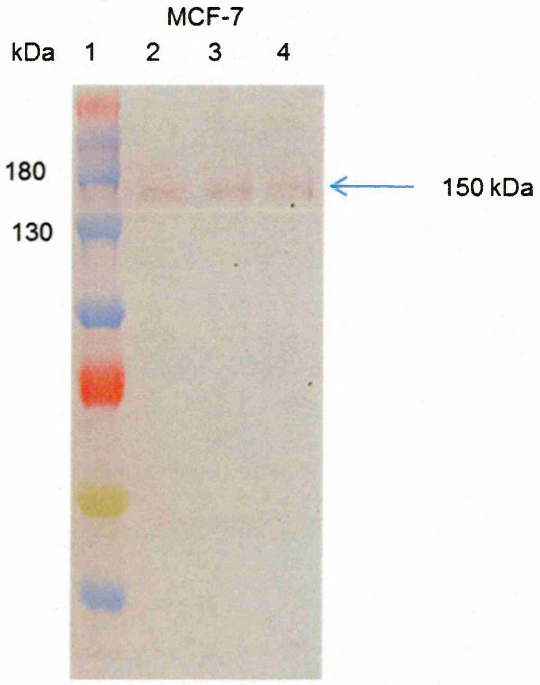

Figure 3.24 Western blot analysis for raptor expression by MCF-7 cells, Protein samples (18µl/well) were loaded and analyzed by using monoclonal anti-raptor antibodies (2280 Cell Signaling Technology, USA). Lanes 2-4 Protein extracted from MCF-7 cells with protease inhibitors cocktail. Lanes 1 is multicolor high range protein ladder.

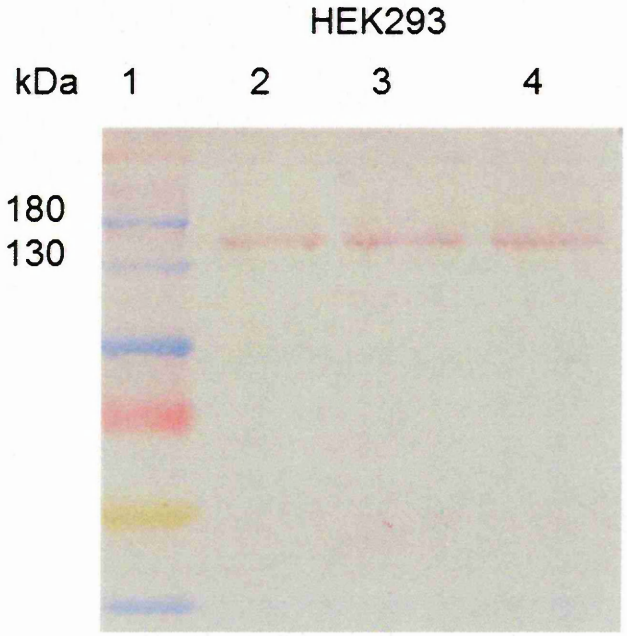

Figure 3.25 Western blot analysis for raptor expression by HEK293 cells, Protein samples (18µl/well) were loaded and analyzed by using monoclonal anti-raptor antibodies (2280 Cell Signaling Technology, USA). Lanes 2-4 Protein extracted from HEK293 cells with protease inhibitors cocktail. Lane 1 is multicolor high range protein ladder.

3.3.3 LC3 expression:

The characterisation of anti-LC3 antibodies was more difficult than the characterisation of anti-mTOR and anti-raptor antibodies. LC3 is now widely used to monitor autophagy. One approach is to detect LC3 conversion (LC3-I to LC3-II) by immunoblot analysis. Pro-LC3, which is neither LC3-I nor LC3-II, is not detected under normal conditions because it is processed by Atg4 into LC3-I immediately after synthesis (Kabeya et al., 2000). Although the molecular weight of LC3-II is larger than that of LC3-I due to the addition of PE, LC3-II migrates faster than LC3-I in SDS-PAGE possibly because of its extreme hydrophobicity. Since LC3-II itself is degraded by autophagy, LC3 immunoblotting is sometimes interpreted inappropriately (Mizushima and Yoshimori, 2007). It so difficult to decide whether the antibody used does not work properly or the experiment needs further optimization. For instance, the type and gel percentage need to be changed or gel ingredients need to be replaced. In the present study, three different anti-LC3 antibodies from different companies were obtained (table 3.3). The antibodies were tested against proteins extracted from HEK293 cells. But this time, the cells were firstly treated with different concentrations of rapamycin for different times to induce autophagy.

3.3.3.1 The polyclonal anti-LC3 (NB100-2220):

According to the supplier, this polyclonal antibody should detect two bands for LC3-I and LC3-II at molecular weights 17 and 19 kDa respectively. The antibody was tested against proteins extracted from rapamycin treated HEK293 cells. Because LC3 is a low molecular weight protein, the extracted proteins were separated on 10% tris-glycine polyacrylamide gels. The western blot result has showed a large number of bands (Figure 3. 26), which could imply specificity issues. For this reason, the antibody was excluded from the project.

3.3.3.2 The monoclonal anti-LC3B (D11) XP (3868):

A monoclonal anti-LC3 antibody was tested against proteins extracted from rapamycin treated HEK293 cells. But this time, the extracted proteins were separated on 10% tris-tricine gel (Schagger and von Jagow, 1987). According to the supplier, two bands for LC3-I and LC3-II should be detected by the antibody at molecular weights 14 and 16 kDa respectively. The western blot result revealed that the antibody detected two bands (Figure 3.27). However, one of these bands is at a higher molecular size than expected, while the other one is near the expected size, but not separated into two bands (LC3-I and LC3-II). In the present study, this is the first observation of a monoclonal antibody producing multiple bands. Production of multiple bands led to the exclusion of this antibody from the present research.

3.3.3.3 Rabbit monoclonal anti-LC3A/B (MABC176):

This antibody was examined against proteins extracted from rapamycin treated HEK293 cells. Also, the extracted proteins were run on 10% tris-tricine gels. The western blot demonstrated that the antibody detected only one strong band at the expected molecular weight. However, this band did not separate to produce the two LC3 forms (LC3-I and LC3-II) (data not shown). This result was promising because the detected strong band was at the correct molecular size and tends to be separated into two bands. This suggested an optimization may be required. Western blot analysis was performed many times under a range of conditions in order to detect LC3-I and LC3-II. Finally, by replacing glycerol with urea during the preparation of the resolving gel, and also by decreasing of the antibody concentration from 1:1000 to be 1: 2000, the antibody succeeded in detecting LC3-I and LC3-II consistently at the correct molecular weight (Figure 3. 28). Based on this result, the antibody was selected to be used in the determination of the subcellular localization of LC3 protein.

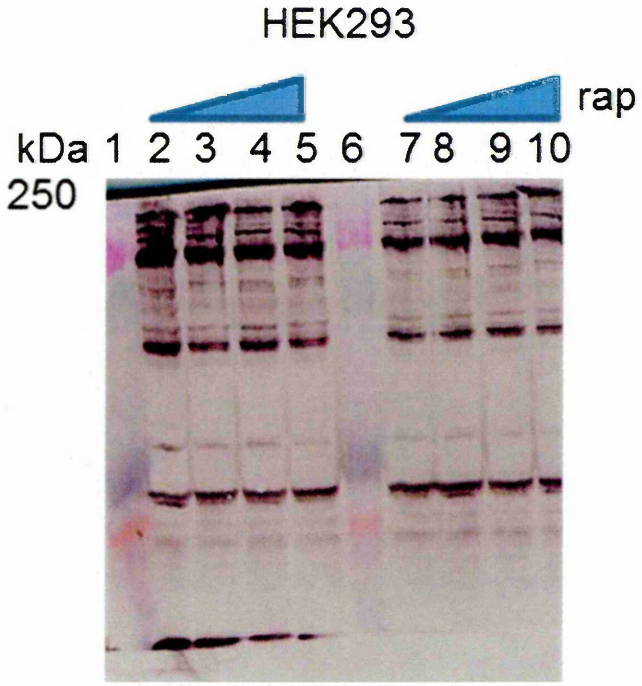

Figure 3.26 Western blot analysis for LC3 expression by HEK293 cells, Protein samples (18µl/well) were loaded and analyzed by using polyclonal anti-LC3 antibody (NB100-2220) (Novus Biologicals, US). Lanes 3, 4 and 5 HEK293 treated with 10nM, 30nM and 50nM of rapamycin respectively for 16 hrs. Lanes 8, 9 and 10 HEK293 treated with 1000nM, 2000nM and 3000nM of rapamycin respectively for 72hrs. Proteins extracted from HEK293 cells with protease inhibitor cocktail. Lanes 2 and 7 untreated HEK293. Lanes 1and 6 are molecular marker.

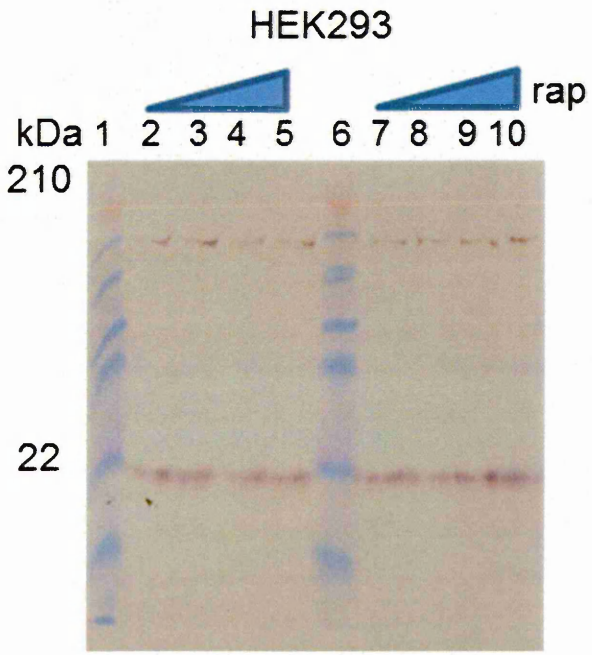

Figure 3.27 Western blot analysis for LC3 expression by HEK293 cells, Protein samples (18µl/well) were loaded and analyzed by using monoclonal anti-LC3B antibody (D11)XP (3868) (Cell Signaling Technology, US). Lanes 3, 4 and 5 HEK293 treated with 10nM, 30nM and 50nM of rapamycin respectively for 16 hrs. Lanes 8, 9 and 10 HEK293 treated with 1000nM, 2000nM and 3000nM of rapamycin respectively for 72hrs. Protein extracted from HEK293 cells with protease inhibitor cocktail. Lanes 2 and 7 untreated HEK293. Lanes 1and 6 are molecular weight marker.

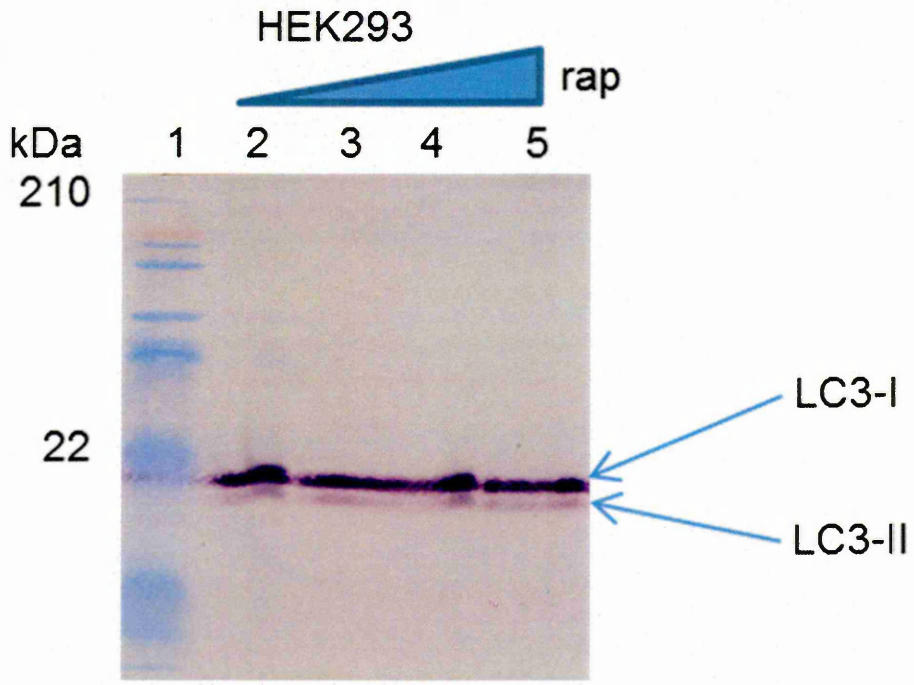

Figure 3.28 Western blot analysis for LC3 expression by HEK293 cells, Protein samples (18µl/well) were loaded and analyzed by using monoclonal anti-LC3B antibody (LC3A/B) (MABC176, Millipore, UK). Lanes 3, 4 and 5 HEK293 treated with 50nM, 200nM and 500nM of rapamycin respectively for 16 hrs. Lane 2 untreated HEK293. Lane 1 is molecular marker. Protein extracted from HEK293 cells with protease inhibitor cocktail.

3.4 DISCUSSION

Antibodies can provide a great deal of critical information about a specific protein under both normal and disease conditions, including localisation and quantification of expression with respect to biological state, post-translational modifications and function within a specific cell (Solache et al., 2013). User experience has shown that high quality antibodies are most often a combined result of effective strategies for immunogen design, immunisation, screening, purification, validation and finally customer usage and feedback (Solache et al., 2013). Many commercially available antibodies on the market today have not been rigorously tested and have only been analysed via a single method (Bordeaux et al., 2010).

For this reason, the antibodies that have been selected to be used in the present study to detect the subcellular localisation of autophagy proteins of interest were re-characterised utilizing western blot technique. Validation by western blotting is best performed using multiple cell or tissue lysates to determine the range of detectable endogenous protein expression in various cells and tissues (Solache et al., 2013). In the present study, the selected antibodies were tested against three different cell lysates (NRK, MCF-7 and HEK293 cells).

Western blotting is a primary validation step that is routinely used to determine whether a specific antibody recognises the denatured target antigen. The observation of a single band that corresponds to the target's molecular weight indicates specificity for the target antigen. However, the presence of multiple bands or a band exhibiting an unexpected molecular weight does not necessarily indicate lack of specificity. These bands may represent the same target antigen with post-translational modifications, breakdown products or splice variants (Solache et al., 2013).

For instance, the case of the polyclonal anti-mTOR antibodies (ab25880) and (ab83495) characterised in this project. By utilizing different cell lysates (NRK and MCF-7), the

antibodies have detected multiple bands at different molecular sizes including ones at expected 289 kDa molecular weight for mTOR especially with MCF-7 cell lysate (Figures 3.12, 3.13, 3.14 and 3.15). To confirm the identity of the detected bands, mTOR in NRK cells was knocked down by mTOR siRNA, the primary antibodies were blocked by the corresponding peptides and the secondary antibodies were used without primaries as a negative control. All the results (Figures 3.7, 3.8, 3.10 and 3.11) revealed that the previously observed multiple bands might be belonging to the mTOR protein. The polyclonal anti-mTOR antibodies (ab25880) and (ab83495) have failed to detect the multiple bands when mTOR was knocked down, also the same primary antibodies failed to stain any bands when blocked by their corresponding peptides. In addition, no bands were produced by the secondary antibody alone. However, such observations should raise concerns for using these antibodies for further experiments. For this reason, the antibodies were excluded from the study.

Although in some cases high-quality and reliable results can be obtained with crude polyclonal antisera, in other cases even the most highly purified polyclonal antibody preparations (i.e., affinity-purified antibody preparations) may contain antibodies with reactivity against closely related antigenic sequences, and this cross reactivity contributes to or even dominates the observed signal (Rhodes and Trimmer, 2006).

All the polyclonal antibodies that have been characterized in the present study have produced the same observation (multiple bands) and failed to produce a single band for the autophagy proteins of interest. The main goal from the commercial antibody characterisation in the present study was to select the appropriate antibodies that are able to detect only one band for the proteins of interest to utilize them in the ICC. For this reason, all of the polyclonal antibodies were excluded from the present research.

The project focused on the characterisation of the monoclonal antibodies. Monoclonal antibodies are produced from single clones of fused cells producing immunoglobulins (Bordeaux et al., 2010). Consistent with this, in the present study, four monoclonal antibodies were characterised. Three of the monoclonal antibodies were specific; they detected a single band at the expected molecular weights 289 kDa, 150 kDa and 16 kDa for mTOR, raptor and LC3 proteins respectively (Figures 3.20, 3.25 and 3.28). However, the clones of the monoclonal antibodies may be grown in host animals where the ascites fluid containing the secreted antibody is collected (Ramos-Vara, 2005; Saper and Sawchenko, 2003).

Therefore, these antibody preparations may be contaminated by antibodies other than the monoclonal antibody of interest. A study by Spicer et al.(1994) demonstrated that seven of 20 monoclonal antibody preparations (35%) they analyzed had staining patterns localized to the Golgi cisternae unrelated to the antigenic specificity of the antibody, and that five of these cross-reactive antibodies failed to even stain the antigen of interest (Spicer et al., 1994).

It has also been reported that antibody validation has shown similar lack of specificity, even in monoclonal antibodies (Bordeaux et al., 2010). This may be in consistence with the fourth monoclonal antibody characterised in the present study. The monoclonal anti-LC3B (D11) (3868) failed to stain only the expected molecular size bands, but it recognized another band at the wrong molecular weight. For this reason this antibody was excluded from the study, while the other three monoclonal antibodies were selected to detect the subcellular localisation of mTOR, raptor and LC3 autophagy proteins in HEK293 cells utilizing ICC.

In the case of ICC, it has been reported that an antibody may recognise a protein that is fully denatured but cannot detect the same protein in its natural conformation; therefore, this antibody would work well for use in western blotting but not for

immunoprecipitation or other applications that require detection of native protein and *vice versa*. Additionally, it is impossible to predict how an antibody will perform when using different sample sources, or when variations are introduced into sample preparation protocols (Solache et al., 2013).

In addition, it has been demonstrated that western blotting cannot be an absolute standardization for antibody binding in IHC or other assays, where the antigen is in its native conformation (Bordeaux et al., 2010). Furthermore, the native versus denatured conformation is further complicated by methods used to fix tissue. Epitopes that are not exposed in the native proteins can be exposed in fixed tissue and *vice versa*, even though they may not be truly denatured. Thus, an antibody could recognize one epitope in fresh tissue, but when applied to fixed tissue recognize another epitope (Saper and Sawchenko, 2003).

However, a database, AbMiner, was published by Major et al. (2006). This database is a resource for information including the immunogen, vendor, and antigen on over 600 commercially available monoclonal antibodies that the group validated via WB against pooled cell lysates from each of the NCI-60 cell lines. Based on this database, it was reported that an antibody was considered validated if it produced a band (or bands) of the expected molecular weight(s) for the target protein (Major et al., 2006).

3.5 CONCLUSION

Antibodies have become a critical research tool within the scientific community and are routinely used in a number of applications. Most commercial antibodies available today have not been rigorously tested, however, and there are no universally accepted validation guidelines or standards to which manufacturers must adhere, leaving suppliers to develop their own internal validation specifications. In the present study, the commercial antibodies were re-characterised utilizing western blot technique. A mixture of twelve commercial polyclonal and monoclonal antibodies against autophagy

proteins of interest (mTOR, raptor and LC3) was characterised. The antibodies were tested against three different cell lysates (NRK, MCF-7 and HEK293 cells). The western blot results have revealed that the monoclonal antibodies are more specific than the polyclonal ones. During the characterisation and optimization processes, only three monoclonal antibodies were succeeded to detect the only expected molecular weight bands for mTOR, raptor and LC3. The selected three monoclonal antibodies are: rabbit monoclonal anti-mTOR antibody 04-385 (Millipore, UK), rabbit monoclonal anti-raptor antibody 2280 (Cell signalling technology, UK) and rabbit monoclonal anti-LC3A/B antibody MABC176 (Millipore, UK) see (Tables 3.1, 3.2 and 3.3), see (Figures 3.20, 3.25 and 3.28) respectively.

The remaining antibodies were excluded from the study, while the selected three monoclonal antibodies were utilized to detect the subcellular localization of mTOR, raptor and LC3 in HEK293 cells.

Chapter 4

Immunocytochemistry of mTOR, Raptor and LC3 and Effect of Rapamycin or Serum Starvation

4.1 INTRODUCTION

Proteins are able to reside in two or more subcellular locations simultaneously or travel across two or more subcellular location sites. This characteristic of proteins, making them unique in their biological functionality, is of particular interest (Chou, 2013). This part of the project was focused on the determination of the subcellular localizations of some important autophagy proteins in order to understand their behaviour under different cellular conditions. The subcellular localization of mTOR, raptor and LC3, which are key regulators of autophagy process, were determined in non-autophagic and autophagic cells by immunocytochemistry. The effects of autophagy induced by starvation or rapamycin treatment were examined. As mentioned in chapter one, it is known that autophagy is aborted in neurodegenerative diseases such as Alzheimer's disease and also a mutation in PS-1 is the common genetic cause of this disease. Thus, does the mutated PS-1 contribute to aborted autophagy?

The main purpose of this is to build knowledge about the behaviour of mTOR, raptor and LC3 in non-autophagic or autophagic cells in the normal state where there is no genetic defect in the cells. This might help in discovering of any changes in the subcellular localization of these proteins after the transfection of the cells with truncated PS-1. This may reveal the reason behind the failure of autophagy in clearing of the protein aggregation inside the cells of degenerative diseases.

4.2 MATERIALS AND METHODS

4.2.1 Cell culture:

Cells were cultured on cover slips in 24-well plates as described in chapter 2. In this project, MCF-7 cells were used as a model to study mTOR.

4.2.2 Rapamycin treatment:

In the case of HEK293 cell line, cells were un-treated or treated with different concentrations of rapamycin for different times. 1 mg of rapamycin (Sigma, UK) was dissolved in 1 ml of dimethyl sulfoxide (DMSO) (Sigma, UK) to obtain 1000,000 nM of rapamycin and 100 % (v/v) of DMSO as a stock solution.

The volume of the media used per well of 24-well plate was 500 µl and the cells seeded onto the plates at a density of (0.5×10^5) cells per well. Working solutions were prepared from the stock solution by dilution in serum-free media and added to the media per well to obtain the required final concentration. In this project, HEK293 cells were treated with six different concentrations of rapamycin for two different periods of time. First; the cells were treated with 10, 30 and 50 nM of rapamycin for 16 hours and the concentration of DMSO was fixed at 0.005 % (v/v) with the three concentrations. Second; high concentrations of rapamycin were applied for longer time. The cells were treated with 1000, 2000 and 3000 nM of rapamycin for 72 hours and DMSO concentration was 0.3 % (v/v).

4.2.3 Serum Starvation:

In the present study, autophagy was also induced by serum starvation. Serum starvation has been used as a tool to study autophagy and other molecular mechanisms by many researchers (Pirkmajer and Chibalin, 2011). In a study of the role of astrocyte elevated gene-1 (AEG-1) in autophagy induction, it was revealed that AEG-1 promotes cell survival by autophagy in normal cells grown under serum starvation conditions (Bhutia *et al.*, 2010). In addition, autophagy was induced by serum starvation in human lung cancer cell line (H1299), human colon cancer cell line (HCT116) and human cervical carcinoma cell line (Hela) to determine whether FoxO1 is a direct factor in the autophagic process. This determination was through the measurement of autophagy biological markers; p62 degradation and LC3-II accumulation (Zhao *et al.*, 2010).

Nutrient starvation is a typical trigger of autophagy, based on this, unavailability of any type of essential nutrients is able to induce autophagy (Mizushima, 2007). Apart from amino acid deprivation, serum starvation results in lack of growth factors which impacts on induction of autophagy. It has been demonstrated that the endocrine system, especially insulin has the ability to manage autophagy regulation *in vivo*. It has also been revealed that other hormones and growth factors are able to regulate autophagy (Mizushima, 2007). It is well known that serum starvation has the ability to induce autophagy in many different types of cultured cells (Mizushima, 2007). Haematopoietic growth factor interleukin-3 (IL-3) suppressed autophagy via regulation of nutrient availability (Mizushima, 2007). Signals of insulin/growth factors are thought to converge on mTOR, which is the main regulator of nutrient signaling (Mizushima, 2007). In this case, the signaling by growth factors controls mTORC1 expression and subsequently regulates autophagy induction (Jung *et al.*, 2010). (See page 16).

According to the method described in Pirkmajer and Chibalin, (2011), HEK293 cells were starved in serum-free MEME media (Lonza, UK) for different periods of time. The cells were cultured on prepared cover slips (Sigma, UK) in three different 24-well plates. The cells were seeded into the plates at a density of ($0.5x10^5$) cells per well in 500 µl complete medium. The plates were labelled as plate 1, 2 and 3 and incubated for 24 hours to allow cells attachment. After that, the complete media was aspirated from the wells of the three plates except the contol wells. The cells were washed with serum-free media to remove all traces of serum and the complete media was replaced with serum-free media. Then, to induce autophagy by serum starvation, the plates 1, 2 and 3 were re-incubated at 37°C for 2, 6 and 24 hours respectively. Then, the plates were collected at different time points and the cells were prepared for ICC.

4.2.4 Immunocytochemistry:

Immunocytochemistry to determine the subcellular localisation of mTOR, raptor and LC3 was performed exactly as described in chapter 2. In the case of using wheat germ agglutinin (Sigma, UK) to stain the Golgi apparatus together with anti-LC3 antibody at the same time, 5 µg/ml of WGA was added to the well of a 24-well plate at the same time with the secondary antibody but this time in 500 µl of BSA and incubated for 45 minutes at room temperature and then washed in the same way as above.

4.3 RESULTS

4.3.1 Mammalian Target of Rapamycin (mTOR)

4.3.1.1 ICC of mTOR in un-treated MCF-7 and HEK293 cells:

After the antibody characterisation, a specific anti-mTOR antibody was selected for the subcellular localization of the protein to assess the endogenous mTOR expression and localisation in autophagic and non-autophagic HEK293 cells. MCF-7 cells were used initially because it has been reported that MCF-7 cells are good cells to express mTOR.

Non-autophagic MCF-7 cells showed mTOR expression mainly in the perinuclear region (Figure 4.1). The distribution of the protein around the nucleus is very similar to the distribution of the mitochondria. To determine if mTOR was present on the mitochondria, an anti-mitochondrial antibody was obtained and used to detect the distribution of the mitochondria in the same cells. The similarity in the distributions of the mitochondria and mTOR was confirmed by dual label ICC. mTOR staining is rather weak, in contrast to antibody to mitochondria, thus it is difficult to detect the co-localisation seen in (D). However, there is little red fluorescence detected in D suggesting proteins are colocalised (Figure 4.2). ICC showed that the endogenous mTOR was expressed in the perinuclear area of non-autophagic HEK293 cells. Also, the subcellular localization of the protein was similar to the distribution of the

mitochondria as mentioned above. By using dual label ICC, it appears that mTOR may localize with the mitochondria. Although there is some colocalisation of mTOR to the mitochondria, this is not complete as many mitochondria are single stained green particularly in perinuclear region. Overlapping of mTOR in D is not punctate, which casts some doubt on the specificity of this localisation (Figure 4.3).

4.3.1.2 ICC of mTOR in rapamycin treated HEK293 cells:

HEK293 cells were treated with rapamycin in order to induce autophagy through mTOR inhibition. This step is to investigate and study the behaviour of mTOR in HEK293 cells that undergoing autophagy and compare it with the behaviour of the protein in both; the non-autophagic HEK293 and also in HEK293 that transfected with tPS-1. To ensure autophagy occurrence, HEK293 cells were treated with different rapamycin concentrations for different periods of times. The cells were treated with 10nM, 30nM and 50nM of rapamycin for 16 hours and also treated with 1000nM, 2000nM and 3000nM for 72 hours. The images of the dual label ICC of mTOR in both experiments showed the same results (Figures 4.4 and 4.5). From the obtained results, it seems that even in the case of autophagy, mTOR did not move to any other part of the cell, but was still mostly localized to the mitochondria. To ensure that this result was not an artefact, all the appropriate controls were performed. The HEK293 cells were treated with rapamycin dissolved in the vehicle (DMSO) or with vehicle alone. The cells were stained with the two secondary antibodies (chicken anti-mouse and donkey anti-rabbit) only with or without rapamycin. To avoid cross reaction, the cells were stained with the two secondary antibodies with each single primary antibody used in the experiment.

4.3.1.3 ICC of mTOR in starved HEK293 cells:

Many researchers have used serum starvation as a tool to study molecular mechanisms involved in protein degradation, cellular stress response, autophagy, and apoptosis

and/or to simulate particular pathological conditions (Pirkmajer and Chibalin, 2011). Protein synthesis and cell growth are regulated by the mTOR pathway, which is in turn indirectly dependent on nutrient, growth factor, and energy availability (Pirkmajer and Chibalin, 2011). The activity of TOR is inhibited under nutrient starvation, which is known as a crucial step for autophagy induction in eukaryotes (Scott *et al.*, 2004).

In the present study, HEK293 cells were starved in serum-free media for different periods of time (for 2, 6 and 24 hrs) to induce autophagy through mTOR inhibition. The purpose of this experiment was to study the behaviour of mTOR in starvation-induced autophagy, and observe if the distribution of mTOR protein is different from what has been seen in the rapamycin-induced autophagy.

Dual label ICC on serum starved HEK293 cells (for 2, 6 and 24 hrs) demonstrated the same results, with mTOR expressed in the perinuclear area. mTOR did not change its previous subcellular localisation under the influence of serum starvation and also mostly localized to the mitochondria (Figure 4.6). This indicates that there is no difference in the movement of mTOR during autophagy under both conditions (rapamycin or starvation-induced).

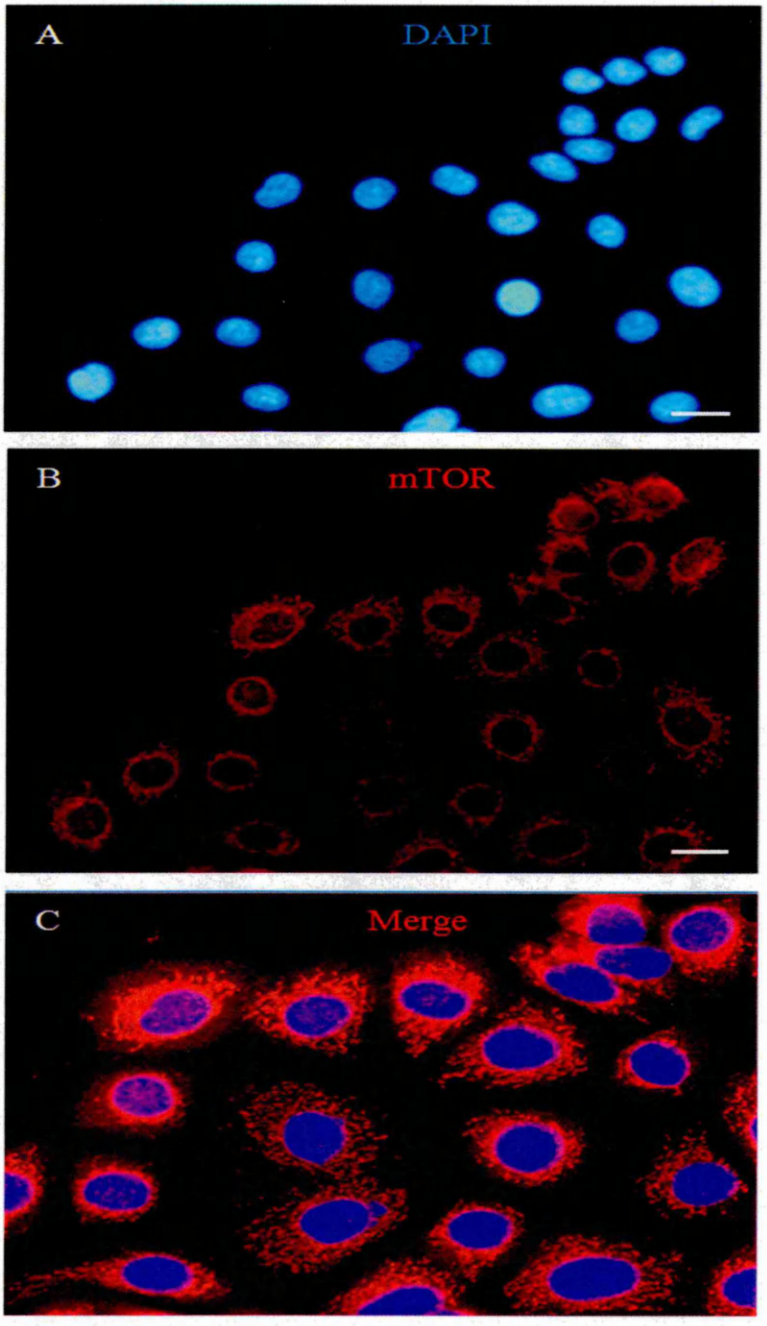

Figure 4.1 Single label immunofluorescence for mTOR in MCF-7 cells. Cells were fixed in cold methanol and labelled for (A) Nuclei, counterstained with DAPI (B) mTOR using primary monoclonal rabbit anti-human mTOR antibody (Millipore, 04-385) and secondary antibody Alexa fluor 594 donkey anti-rabbit IgG (C) Merge (cropped zoomed image). Scale bar: 10μm

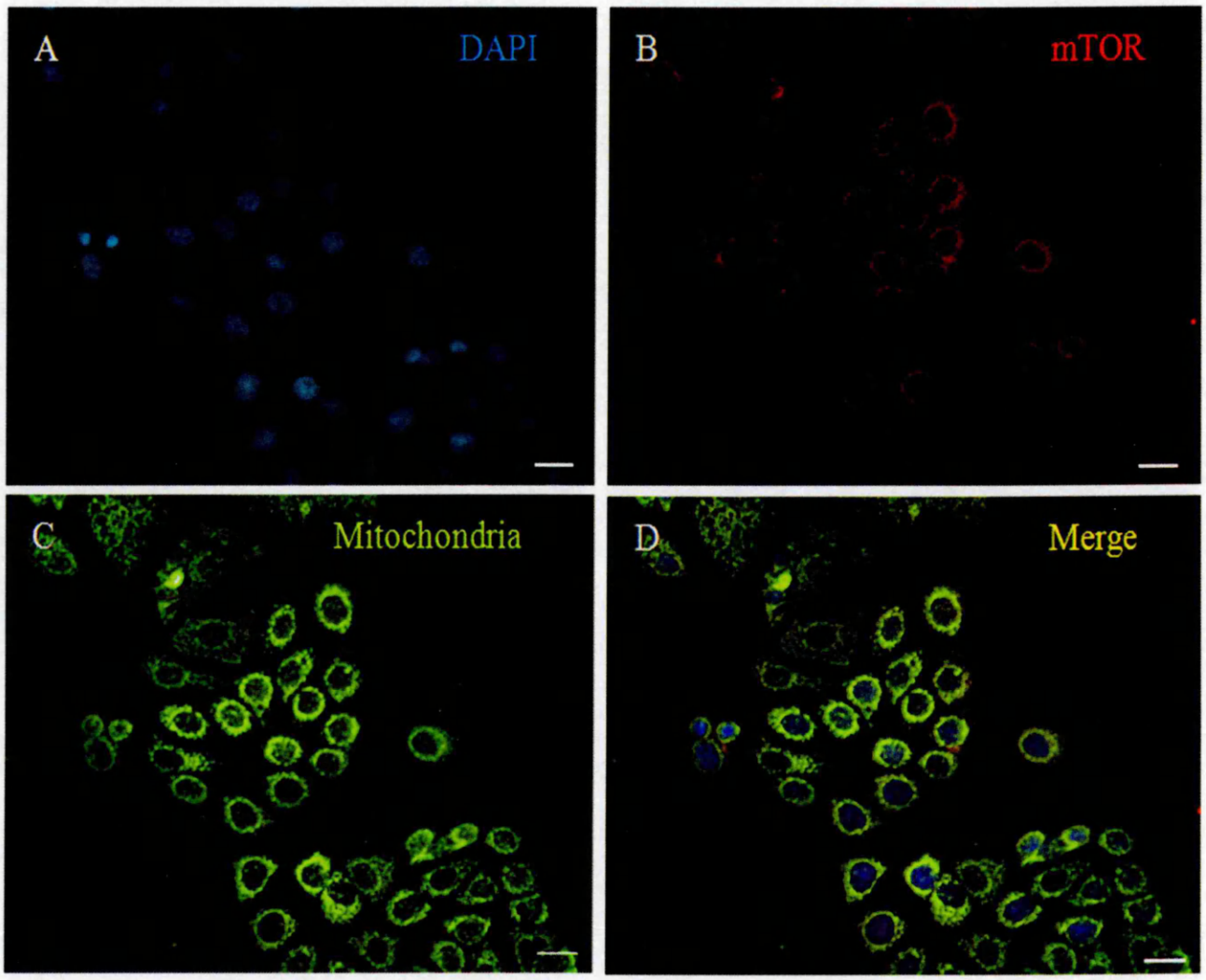

Figure 4.2 Dual label immunofluorescence for mTOR and mitochondria in MCF-7 cells. Cells were fixed in cold methanol and labelled for (A) Nuclei, counterstained with DAPI (B) mTOR using primary monoclonal rabbit anti-human mTOR antibody (Millipore, 04-385) and secondary antibody Alexa fluor 594 donkey anti-rabbit IgG (C) mitochondria using primary monoclonal mouse anti-mitochondria antibody (Millipore, UK) and secondary antibody Alexa fluor 488 chicken anti-mouse IgG (D) Merge. Scale bar: 10μm

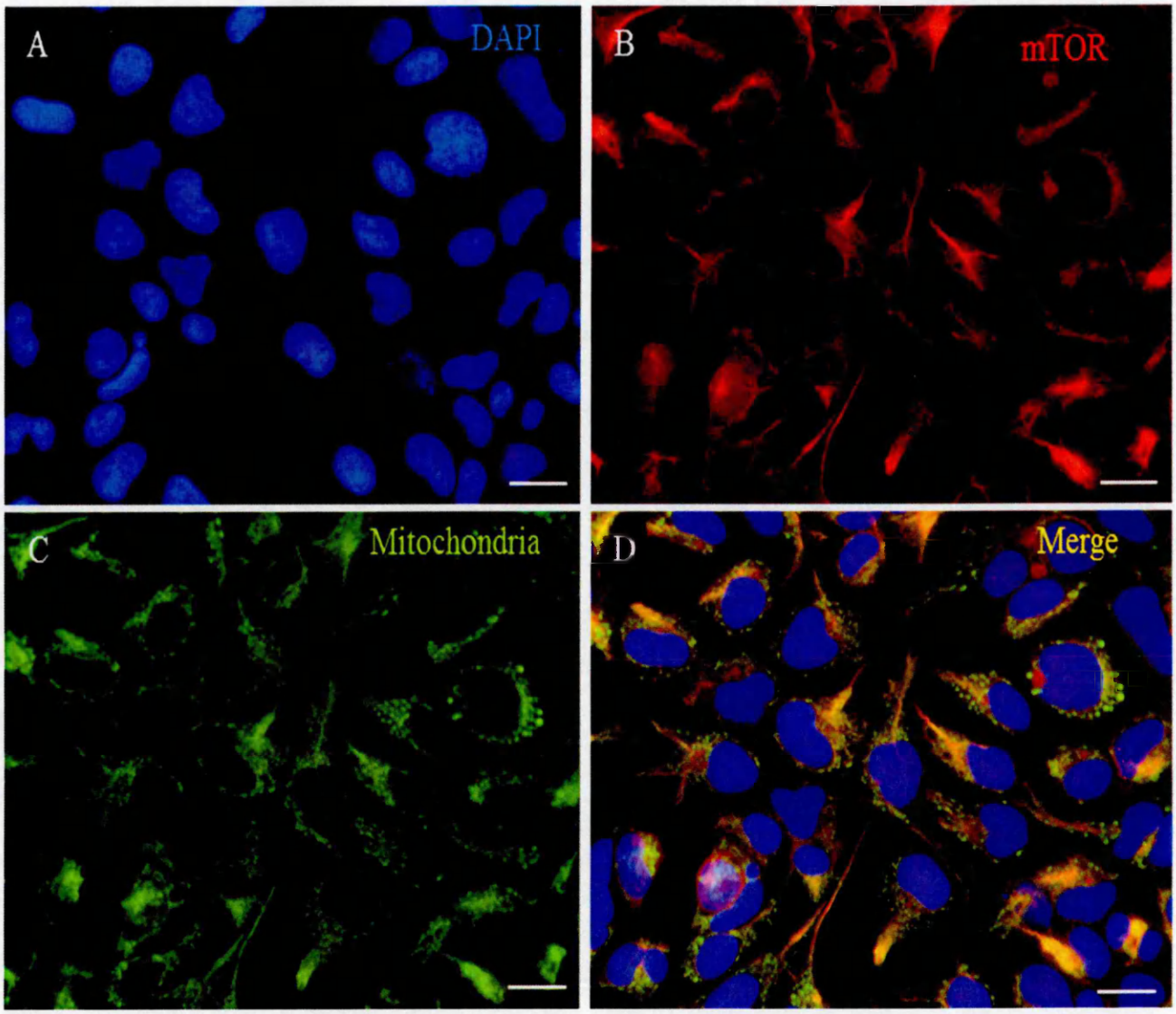

Figure 4.3 Dual label immunofluorescence for mTOR and mitochondria in HEK293 cells. Cells were fixed in cold methanol and labelled for (A) Nuclei, counterstained with DAPI (B) mTOR using primary monoclonal rabbit anti-human mTOR antibody (Millipore, 04-385) and secondary antibody Alexa fluor 594 donkey anti-rabbit IgG (C) mitochondria using primary monoclonal mouse anti-mitochondria antibody (Millipore, UK) and secondary antibody Alexa fluor 488 chicken anti-mouse IgG (D) Merge. Scale bar: 10μm

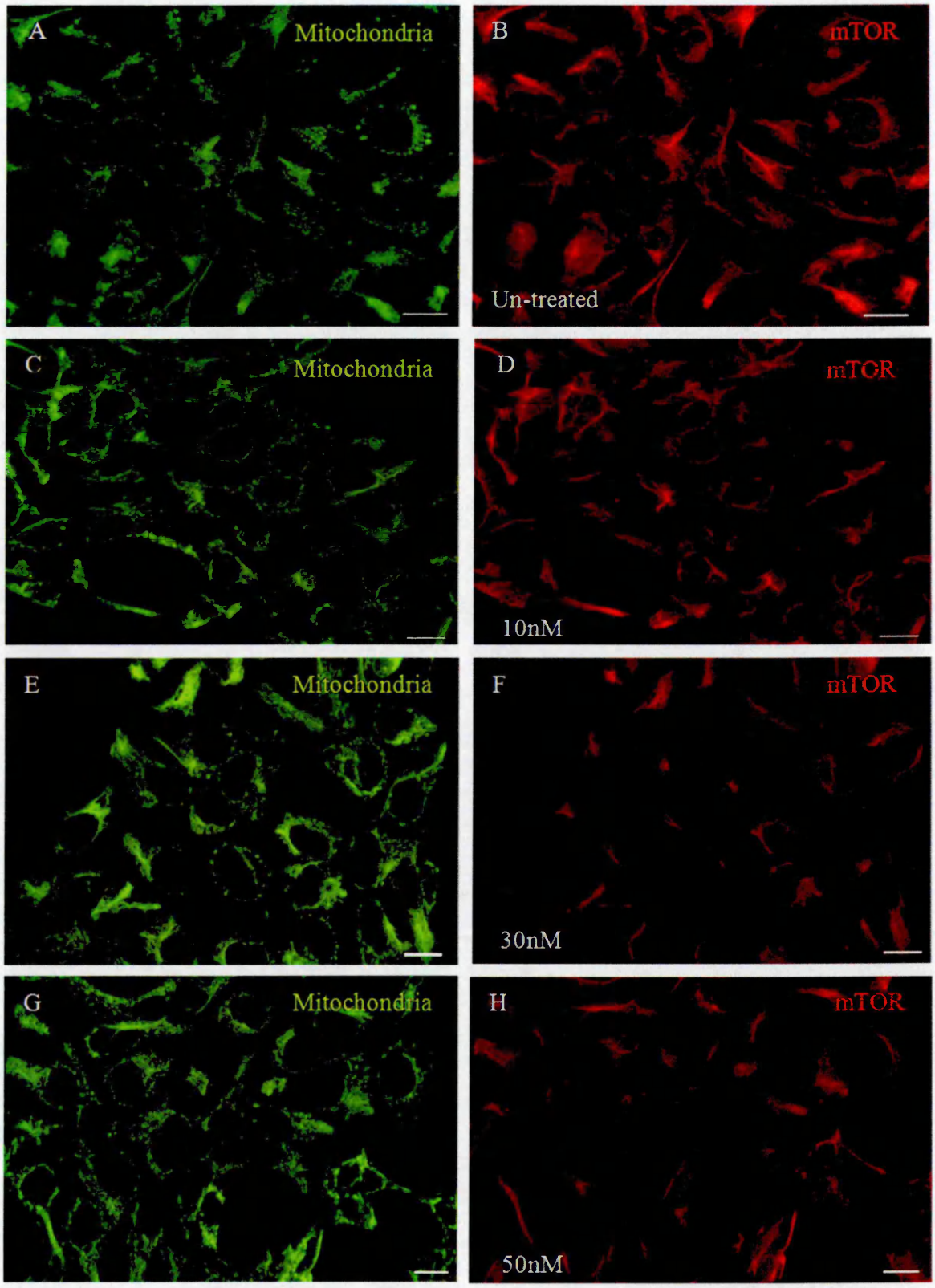

Figure 4.4 Dual label immunofluorescence for mTOR and mitochondria in 16 hours rapamycin treated HEK293 cells. Cells were fixed in cold methanol and labelled for mTOR using primary monoclonal rabbit anti-human mTOR antibody (Millipore, 04-385) and secondary antibody Alexa fluor 594 donkey anti-rabbit IgG and for mitochondria using primary monoclonal mouse anti-mitochondria antibody (Millipore, UK) and secondary antibody Alexa fluor 488 chicken anti-mouse IgG in HEK293 treated with (A, B) control, (C, D) 10nM of rapamycin, (E, F) 30nM of rapamycin, (G, H) 50 nM of rapamycin. Scale bar: 10μm

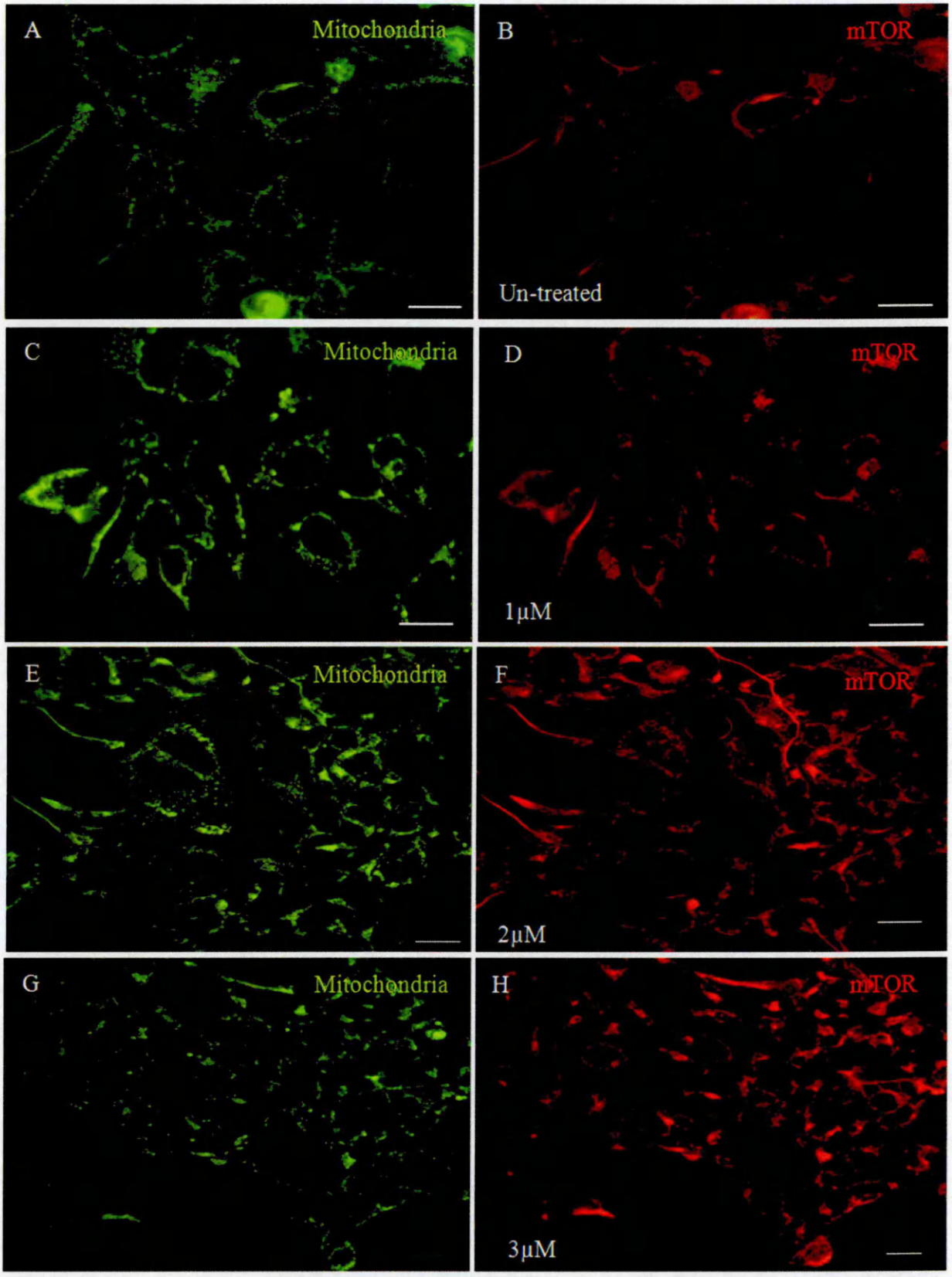

Figure 4.5 Dual label immunofluorescence for mTOR and mitochondria in 72 hours rapamycin treated HEK293 cells. Cells were fixed in cold methanol and labelled for mTOR using primary monoclonal rabbit anti-human mTOR antibody (Millipore, 04-385) and secondary antibody Alexa fluor 594 donkey anti-rabbit IgG (Red) and for mitochondria using primary monoclonal mouse anti-mitochondria antibody (Millipore, UK) and secondary antibody Alexa fluor 488 chicken anti-mouse IgG (Green) in HEK293 treated with (A, B) control, (C, D) 1μM of rapamycin, (E, F) 2μM of rapamycin, (G, H) 3μM of rapamycin. Scale bar: 10μm

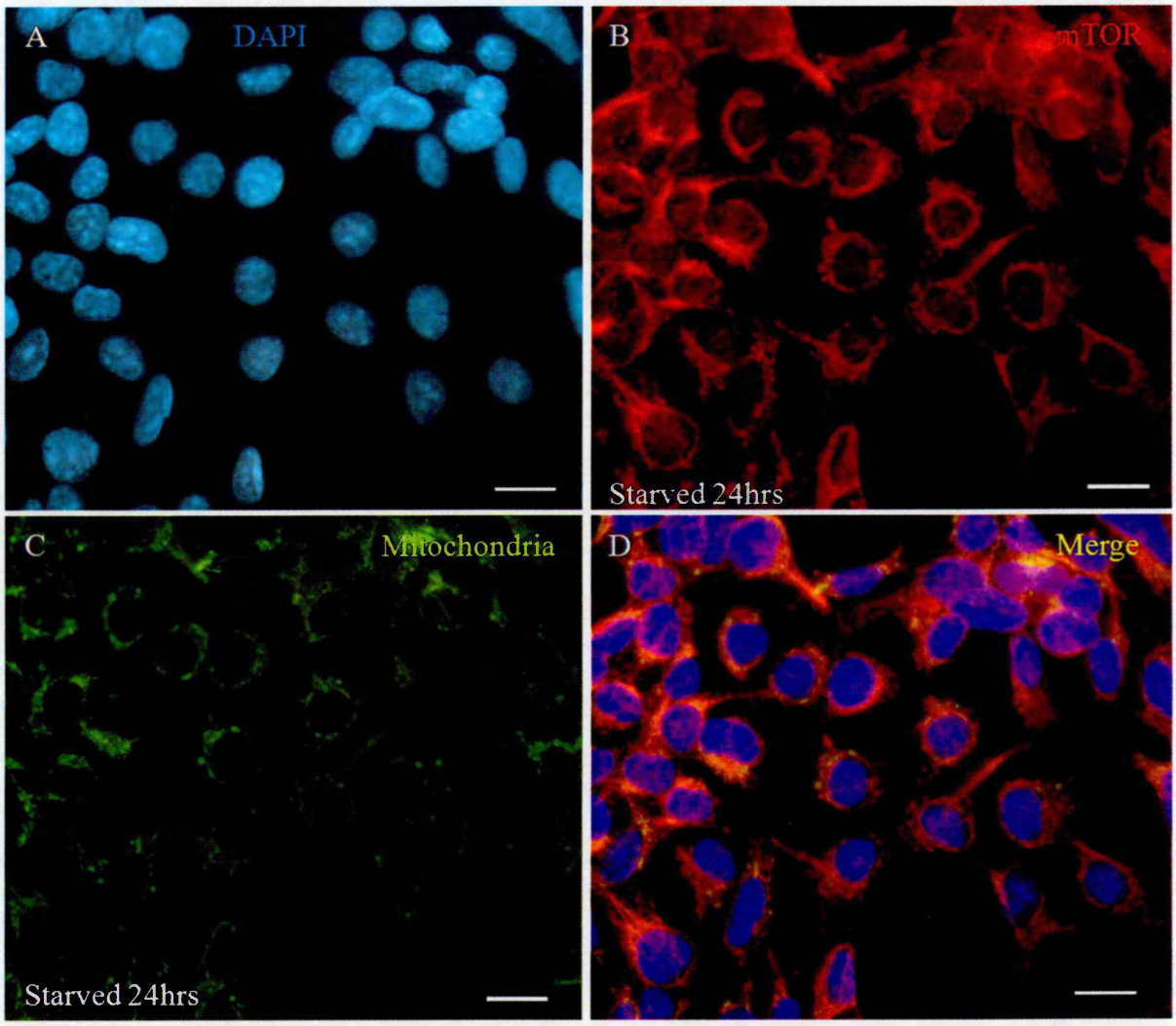

Figure 4.6 Dual label immunofluorescence for mTOR and mitochondria in 24 hours serum starved HEK293 cells. Cells were starved in serum free media for 24 hours and then fixed in cold methanol and labelled for (A) Nuclei, counterstained with DAPI (B) mTOR using primary monoclonal rabbit anti-human mTOR antibody (Millipore, 04-385) and secondary antibody Alexa fluor 594 donkey anti-rabbit IgG (C) mitochondria using primary monoclonal mouse anti-mitochondria antibody (Millipore, UK) and secondary antibody Alexa fluor 488 chicken anti-mouse IgG (D) Merge. Scale bar: 10μm

4.3.2 Regulatory associated protein of mTOR (Raptor)

4.3.2.1 ICC of Raptor in HEK293 cells:

As for mTOR, a specific anti-raptor antibody was selected and used in the determination of the subcellular localization of raptor in autophagic and non-autophagic HEK293 cells. By fluorescence microscopy, the dual label ICC (anti-raptor and anti-mitochondria antibodies) of HEK293 demonstrated that the majority of raptor staining is in the cytoplasm and some of the protein was localized to the mitochondria with the presence of some diffuse raptor staining in the perinuclear region (Figure 4.7).

4.3.2.2 ICC for Raptor expression in rapamycin treated HEK293 cells:

Rapamycin was used to induce autophagy through mTOR inhibition. HEK293 cells were treated with varying concentrations of rapamycin for varying periods of time (see section 4.2.2). The result revealed that, after rapamycin treatment, some of raptor protein has moved toward the perinuclear area. However, the raptor staining appears as single punctate spots within each cell with some diffuse cytoplasmic staining remaining. This change in the subcellular localization of raptor is very clear with the highest concentrations of rapamycin in both experiments (Figures 4.8 and 4.9). The changed distribution of the protein was similar to the distribution of the mitochondria. However, in both figures it seems that raptor already present in the perinuclear area was not localized to the mitochondra.

4.3.2.3 ICC of Raptor in starved HEK293 cells:

HEK293 cells were serum starved for different periods of time (2, 6 and 24 hrs) in order to induce autophagy. The result shows that serum starvation has the same effect as rapamycin on the distribution of raptor protein. After starvation, the protein changed distribution, and some of the protein moved toward the perinuclear region to appear in a new subcellular localization, which is similar to the distribution of mitochondria. However, it is not complete overlap as single red staining seen in D (Figure 4.10). Similar to the previous figures (4.8 and 4.9), it seems that some diffuse cytoplasmic staining remaining and raptor spots that present in the perinuclear area were not localized to the mitochondria. This observation indicates that under the influence of both: rapamycin treatment or serum starvation, mTOR drives and regulates the autophagic process in the same way.

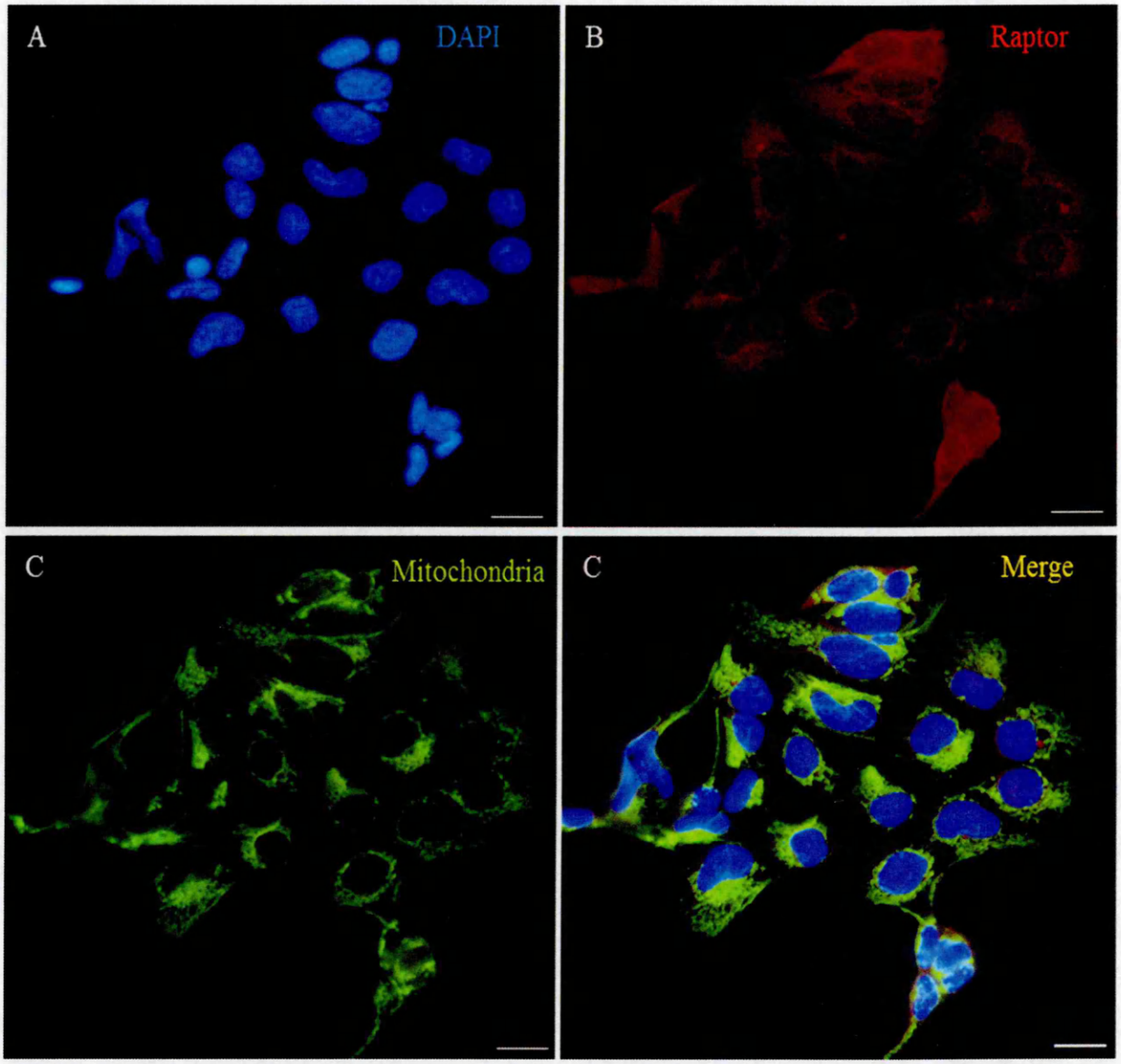

Figure 4.7 Dual label immunofluorescence for raptor and mitochondria in HEK293 cells. Cells were fixed in cold methanol and labelled for (A) Nuclei, counterstained with DAPI (B) raptor using primary monoclonal rabbit anti-human raptor antibody (CellSignaling Technology, 2280) and secondary antibody Alexa fluor 594 donkey anti-rabbit IgG (C) mitochondria using primary monoclonal mouse anti-mitochondria antibody (Millipore, UK) and secondary antibody Alexa fluor 488 chicken anti-mouse IgG (D) Merge. Scale bar: 10μm

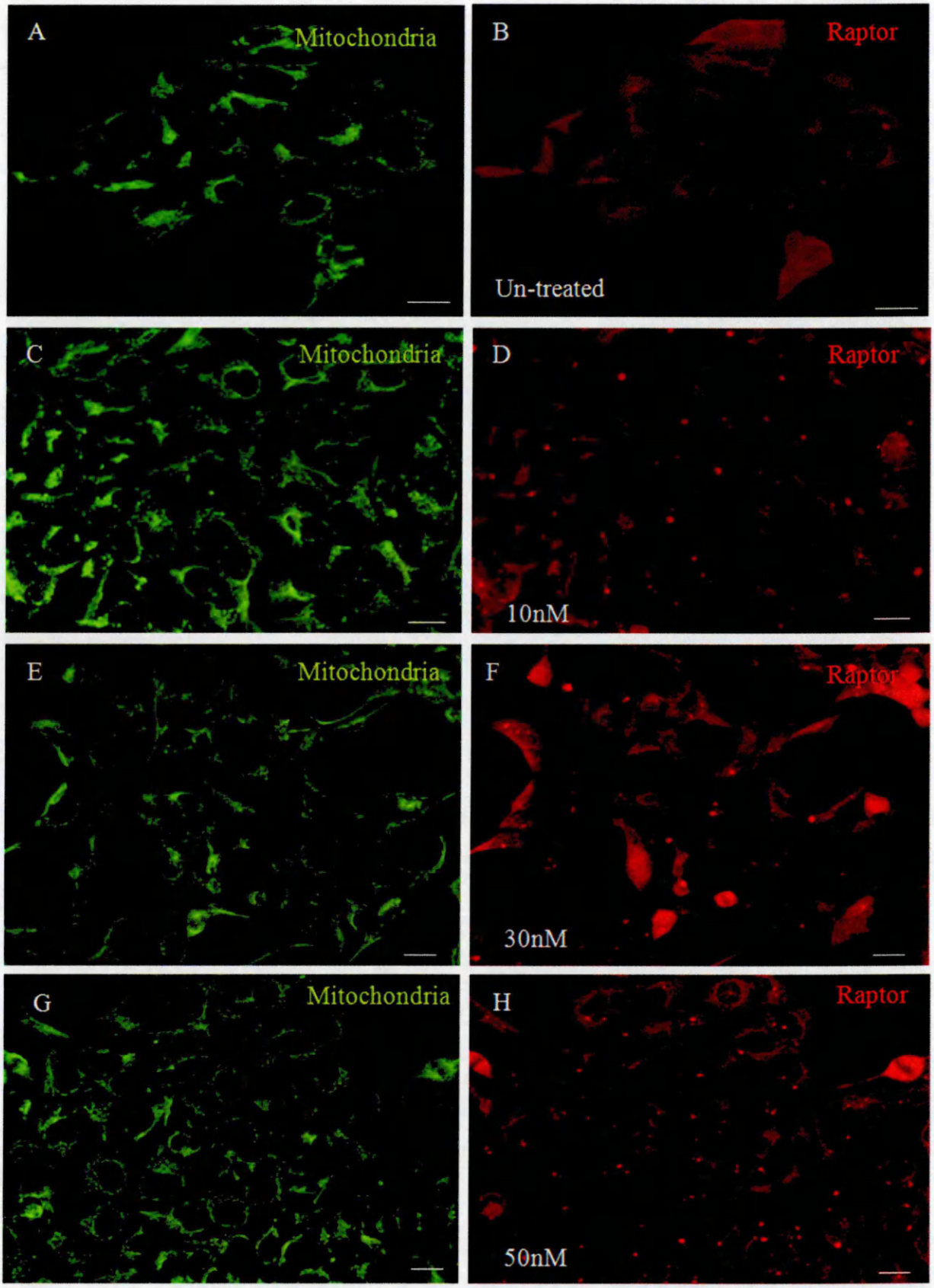

Figure 4.8 Dual label immunofluorescence for raptor and mitochondria in 16 hours rapamycin treated HEK293 cells. Cells were fixed in cold methanol and labelled for raptor using primary monoclonal rabbit anti-human raptor antibody (CellSignaling Technology, 2280) and secondary antibody Alexa fluor 594 donkey anti-rabbit IgG (Red) and for mitochondria using primary monoclonal mouse anti-mitochondria (Millipore, UK) antibody and secondary antibody Alexa fluor 488 chicken anti-mouse IgG (Green) in HEK293 treated with (A, B) control, (C, D) 10nM of rapamycin, (E, F) 30nM of rapamycin, (G, H) 50 nM of rapamycin. Scale bar: 10μm

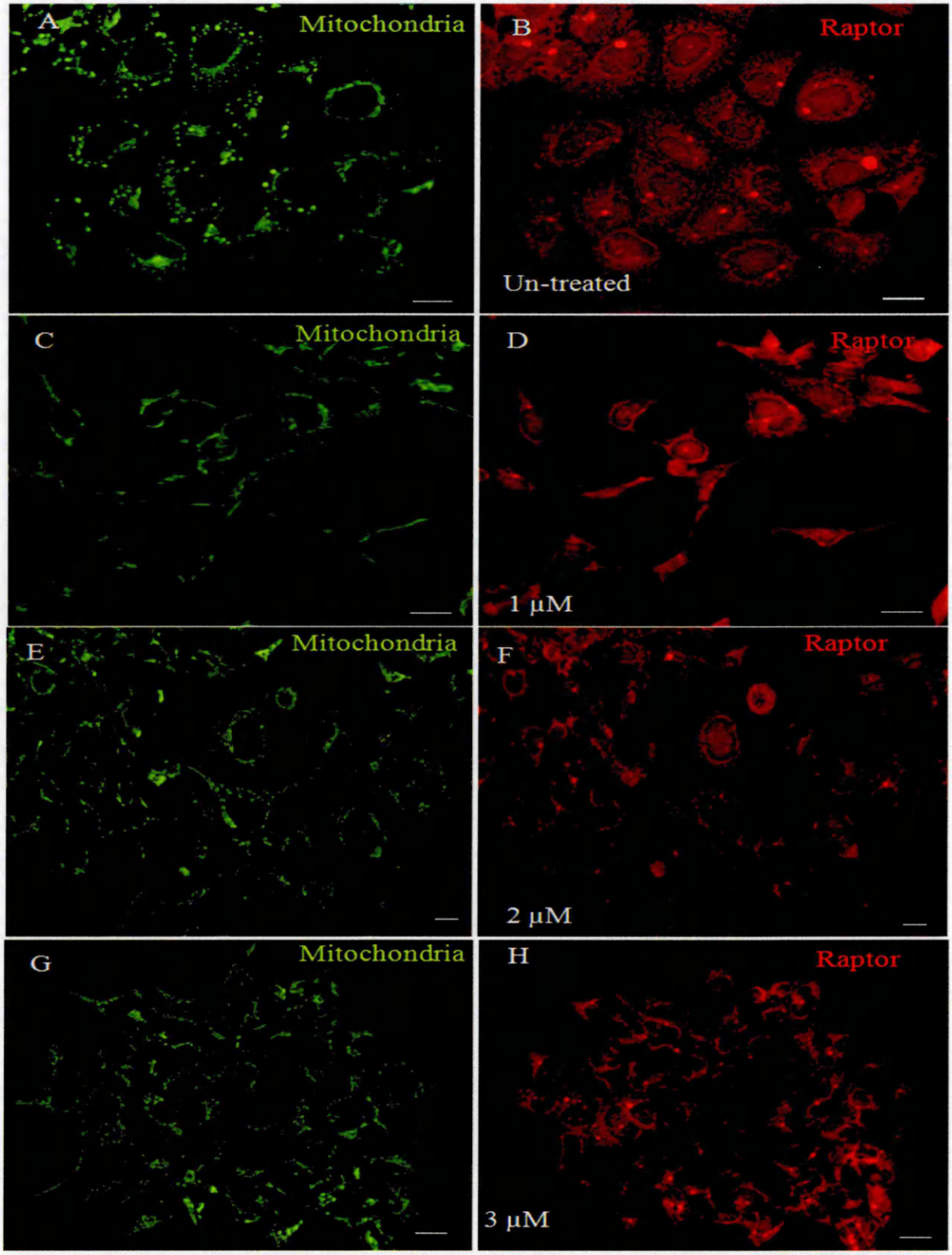

Figure 4.9 Dual label immunofluorescence for raptor and mitochondria in 72 hours rapamycin treated HEK293 cells. Cells were fixed in cold methanol and labelled for raptor using primary monoclonal rabbit anti-human raptor antibody (CellSignaling Technology, 2280) and secondary antibody Alexa fluor 594 donkey anti-rabbit IgG (Red) and for mitochondria using primary monoclonal mouse anti-mitochondria (Millipore, UK) antibody and secondary antibody Alexa fluor 488 chicken anti-mouse IgG (Green) in HEK293 treated with (A, B) control, (C, D) 1µM of rapamycin, (E, F) 2µM of rapamycin, (G, H) 3µM of rapamycin. Scale bar: 10µm

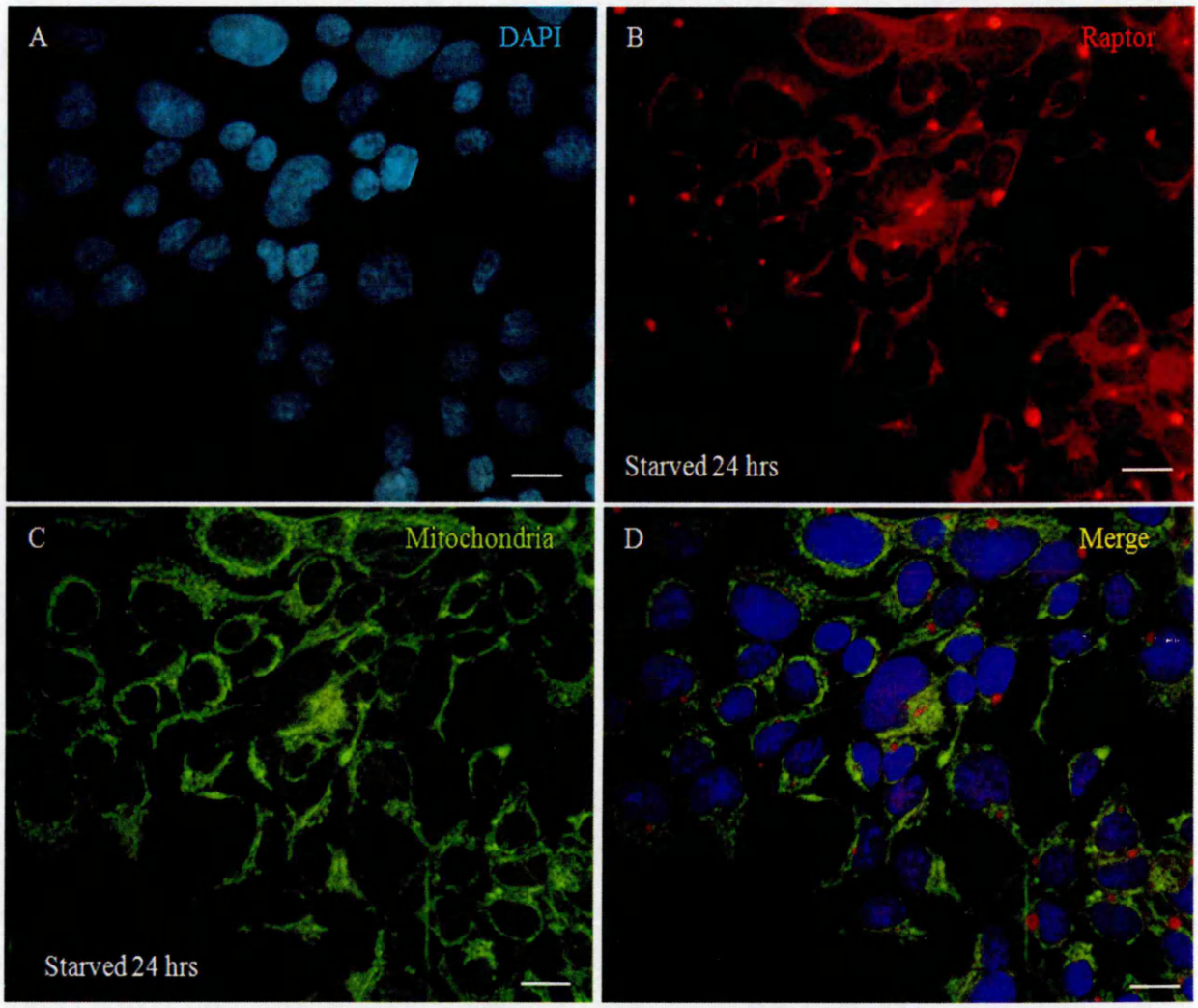

Figure 4.10 Dual label immunofluorescence for raptor and mitochondria in 24 hours serum starved HEK293 cells. Cells were starved in serum free media for 24 hours and then fixed in cold methanol and labelled for (A) Nuclei, counterstained with DAPI (B) raptor using primary monoclonal rabbit anti-human raptor antibody (CellSignaling Technology, 2280) and secondary antibody Alexa fluor 594 donkey anti-rabbit IgG (C) mitochondria using primary monoclonal mouse anti-mitochondria antibody (Millipore, UK) and secondary antibody Alexa fluor 488 chicken anti-mouse IgG (D) Merge. Scale bar: 10μm

4.3.3 Microtubule-associated protein 1 light chain 3 (LC3)

4.3.3.1 ICC of LC3 in HEK293 cells:

LC3 is now widely used to monitor autophagy (Mizushima, 2004; Kirkegaard *et al.*, 2004 and Klionsky *et al.*, 2007). One approach is to detect LC3 conversion (LC3-I to LC3-II) by immunoblot analysis because the amount of LC3-II is clearly correlated with the number of autophagosomes (Kabeya *et al.*, 2000). However, LC3-II itself is degraded by autophagy, making interpretation of the results of LC3-II immunoblotting problematic. The present study focused on using LC3 as an autophagy indicator, and the subcellular localization of it to investigate the behaviour of the protein during autophagy induced by different methods.

In the present study, a specific anti-LC3 antibody was selected by western blot after autophagy induction. The antibody successfully stained LC3-I and LC3-II at the expected molecular sizes. The ICC of endogenous LC3 HEK293 cells demonstrated that the subcellular localization of the protein appears to localise to the Golgi apparatus (Figure 4.11).

To confirm the LC3 localisation to the Golgi apparatus, wheat germ agglutinin (WGA) was utilized to stain the Golgi apparatus. The dual label ICC showed that the subcellular localization of LC3 is similar to the distribution of Golgi apparatus. However, image D showed that there is some red staining not localised to the Golgi apparatus indicating that there is not total overlap (Figure 4.12). To confirm this result, confocal microscopy was used. The obtained confocal images also indicate that LC3 is only partially localized to Golgi apparatus (Figure 4.13).

To avoid artefactual results, several controls were performed. The HEK293 cells were stained with the primary antibody and WGA at the same time and then with the secondary antibody. The cells were also stained with WGA alone (no primary anti-

LC3A/B antibody) and then with the secondary antibody. The secondary antibodies were incubated with the WGA in a tube at RT for 30 min before adding them to the cells already stained with the primary antibody. The cells were stained with the secondary antibody and the WGA at the same time (no incubation) but without the primary antibody. All the controls showed that the observed results are not artefacts.

4.3.3.2 ICC of LC3 in rapamycin-treated HEK293 cells:

To study the behaviour of LC3 during normal autophagy and compare it with the behaviour of the protein in interrupted autophagy, HEK293 cells were treated with 50 nM rapamycin for 16 hours to induce autophagy. The images obtained revealed that a very small proportion of the LC3 protein diffuses in the cytoplasm, while the majority of the protein did not move but remained localized to the Golgi apparatus (Figure 4.14).

4.3.3.3 ICC of LC3 in serum starved HEK293 cells:

To compare the influence of rapamycin treatment and serum starvation on LC3 behaviour, HEK293 cells were starved in serum-free media for 24 hours to induce autophagy. The dual label ICC revealed that rapamycin treatment or starvation has the same influence on LC3 behaviour. During serum starvation induced autophagy, it seems that the majority of LC3 protein still localized to the Golgi apparatus and a very small proportion of the protein diffused to the cytoplasm (Figure 4.15).

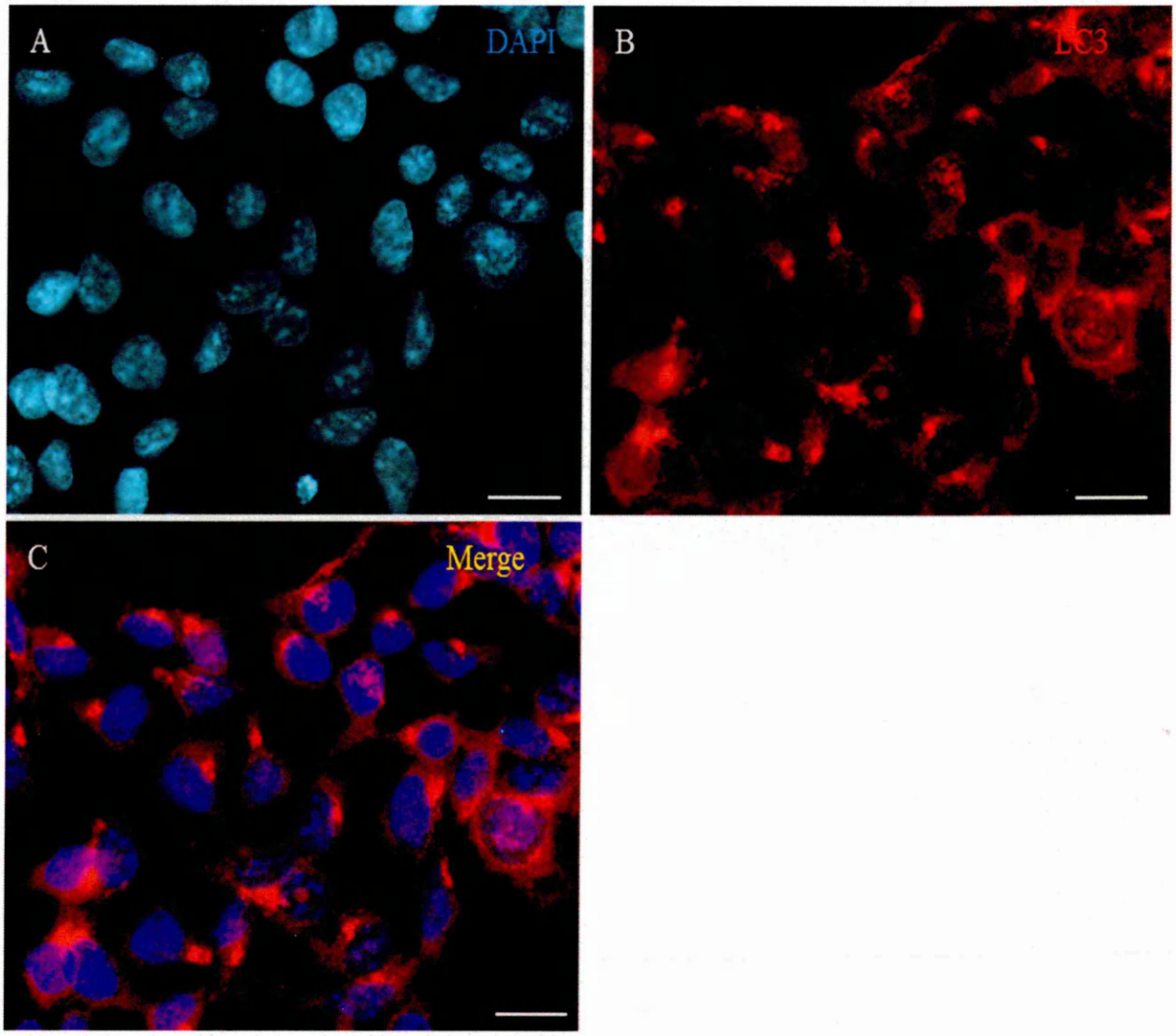

Figure 4.11 Single label immunofluorescence for LC3 in HEK293 cells. Cells were fixed in cold methanol and labelled for (A) Nuclei, counterstained with DAPI (B) LC3 using primary monoclonal rabbit anti-human LC3A/B antibody (Millipore, MABC176) and secondary antibody Alexa fluor 594 donkey anti-rabbit IgG (C) Merge. Scale bar: 10μm

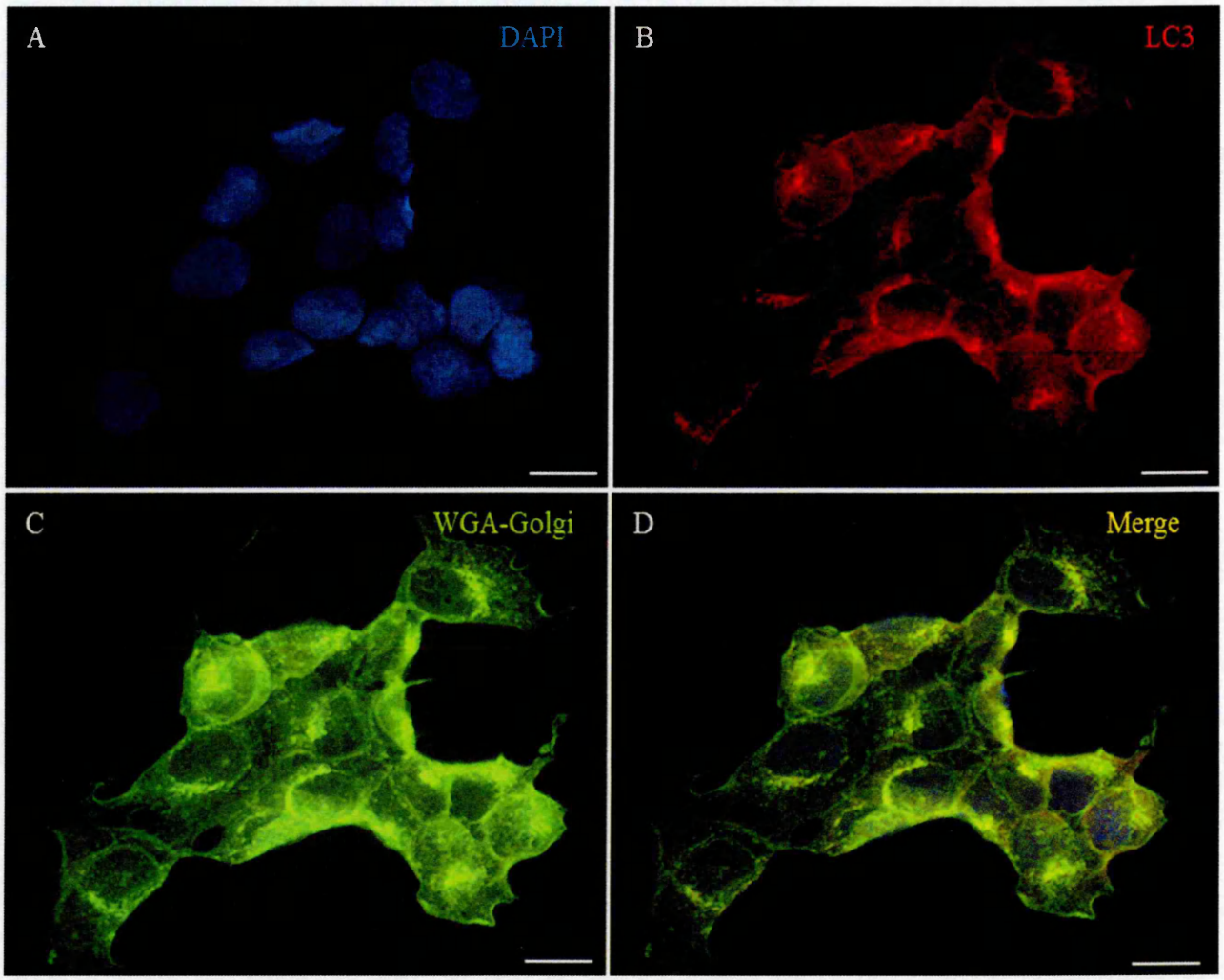

Figure 4.12 Dual label immunofluorescence for LC3 and Golgi apparatus in HEK293 cells. Cells were fixed in cold methanol and labelled for (A) Nuclei, counterstained with DAPI (B) LC3 using primary monoclonal rabbit anti-human LC3A/B antibody (Millipore, MABC176) and secondary antibody Alexa fluor 594 donkey anti-rabbit IgG (C) Golgi apparatus using 5µg/ml WGA (D) Merge. Scale bar: 10µm

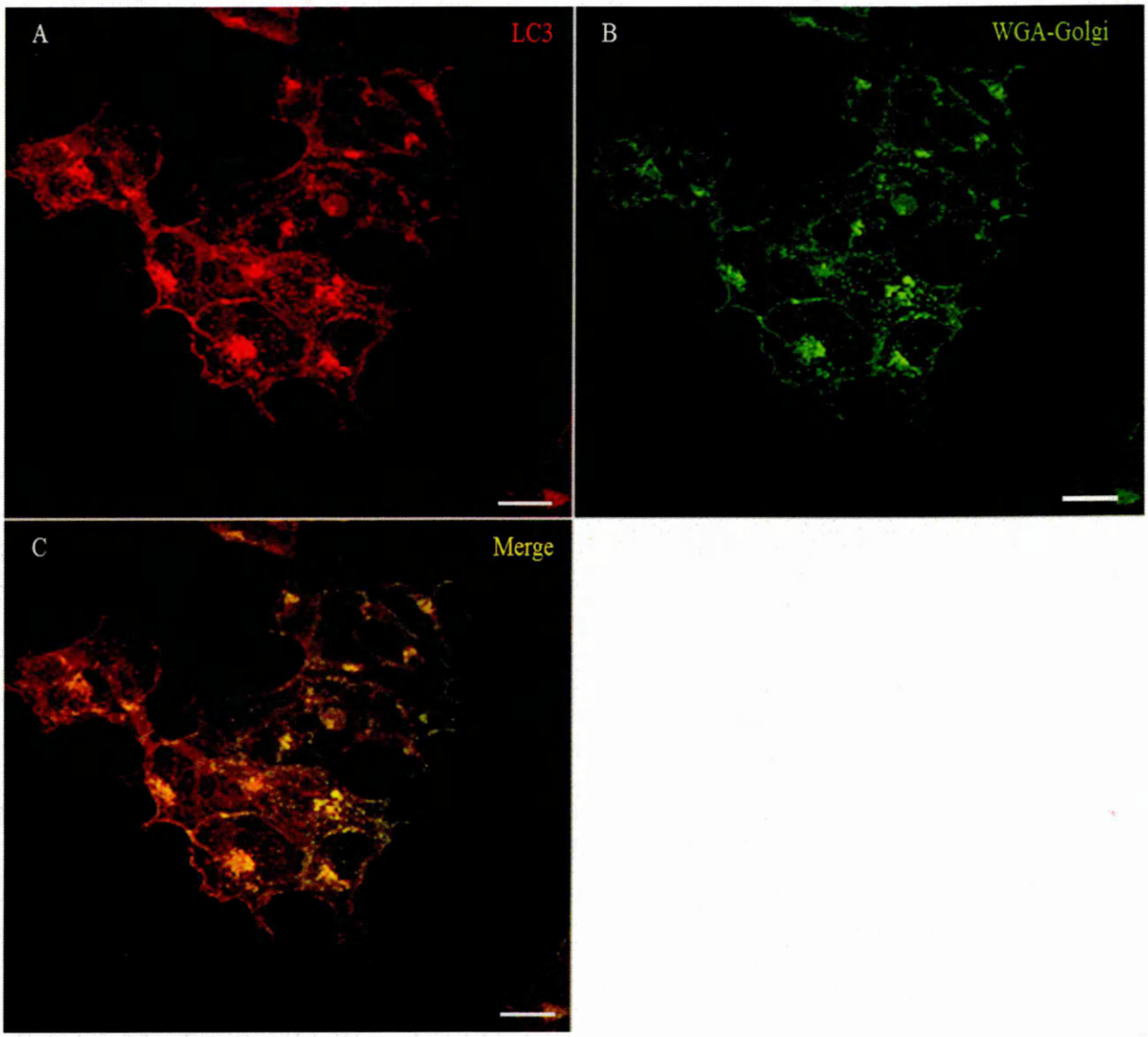

Figure 4.13 Dual label immunofluorescence for LC3 and Golgi apparatus in HEK293 cells, (confocal image). Cells were fixed in cold methanol and labelled for (A) LC3 using primary monoclonal rabbit anti-human LC3A/B antibody (Millipore, MABC176) and secondary antibody Alexa fluor 594 donkey anti-rabbit IgG (B) Golgi apparatus using 5μg/ml WGA (C) Merge. Scale bar: 10μm

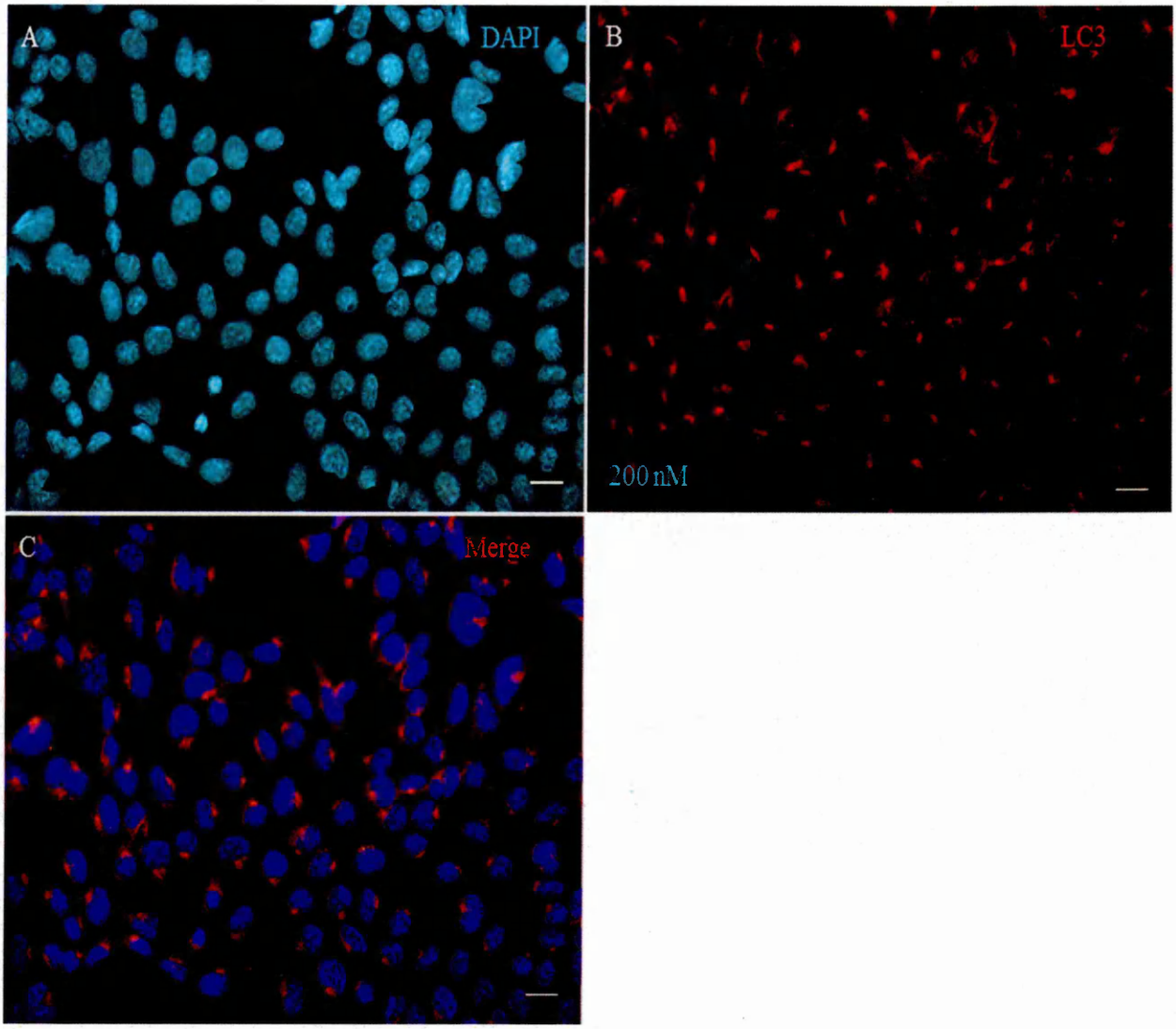

Figure 4.14 Single label immunofluorescence for LC3 in 16 hours rapamycin treated HEK293 cells. Cells were fixed in cold methanol and labelled for (A) Nuclei, counterstained with DAPI (B) LC3 using primary monoclonal rabbit anti-human LC3A/B antibody (Millipore, MABC176) and secondary antibody Alexa fluor 594 donkey anti-rabbit IgG in 200nM rapamycin treated HEK293 (C) Merge. Scale bar: 10μm

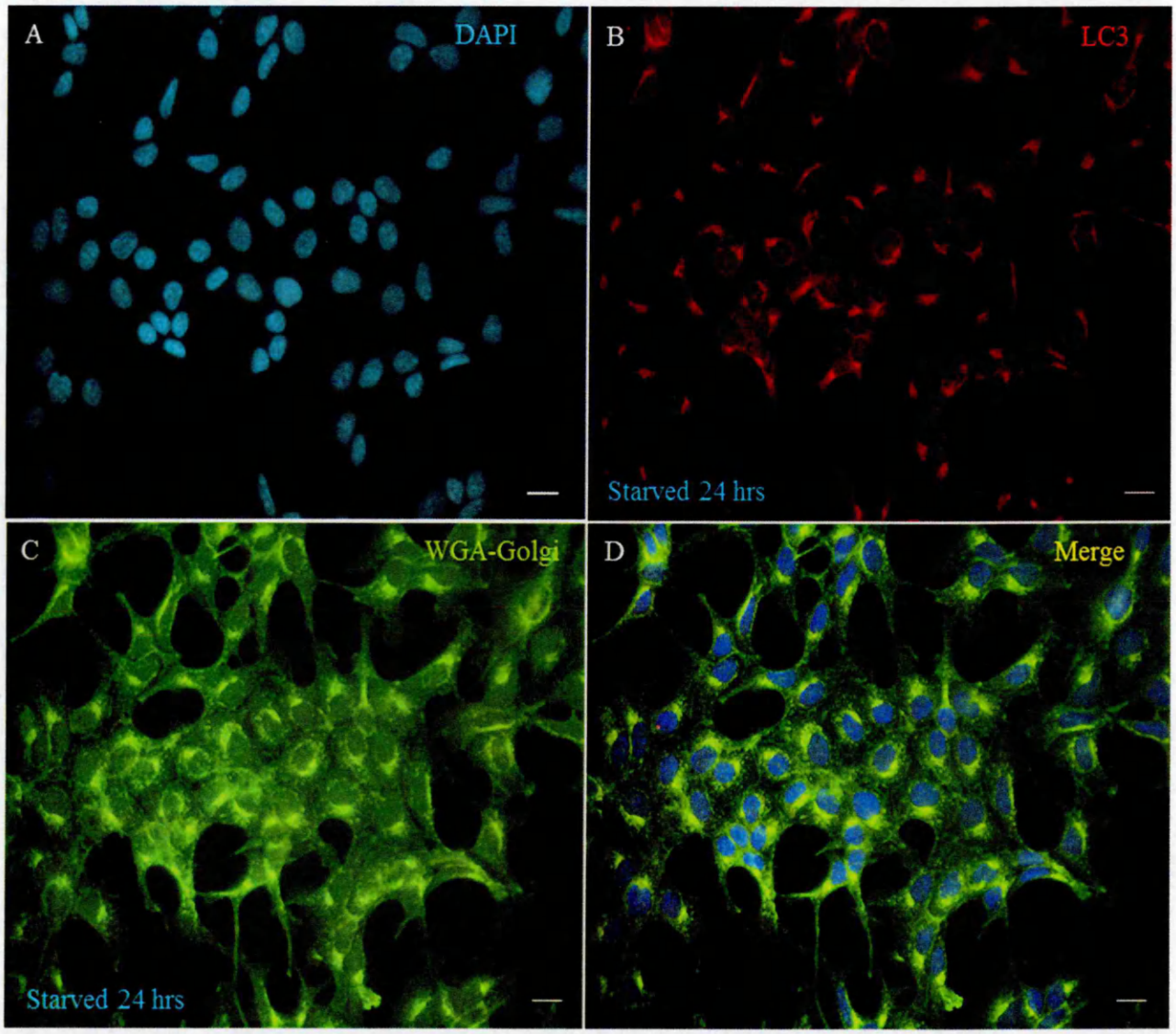

Figure 4.15 Dual label immunofluorescence for LC3 and Golgi apparatus after 24 hours serum starvation in HEK293 cells. Cells were starved in serum free media for 24 hours and then fixed in cold methanol and labelled for (A) Nuclei, counterstained with DAPI (B) LC3 using primary monoclonal rabbit anti-human LC3A/B antibody (Millipore, MABC176) and secondary antibody Alexa fluor 594 donkey anti-rabbit IgG (C) Golgi apparatus using 5µg/ml WGA (D) Merge. Scale bar: 10µm

4.4 DISCUSSION

4.4.1 Mammalian Target of Rapamycin (mTOR)

The present study has shown that endogenous mTOR proteins are predominantly localized to mitochondria in MCF-7 and HEK293 cell lines, as judged by dual label ICC. To ensure the specificity of the antibody used for these experiments, the monoclonal anti-mTOR antibody that produced this result was selected from seven different anti-mTOR antibodies from different suppliers after a characterisation process by western blot (chapter 3). The antibody stained bands at the right molecular size of mTOR (289 kDa) using proteins from whole cell lysate of three different cell lines (NRK, MCF-7 and HEK293 cell lines) (Figures 3.19 and 3.20). The anti-mitochondrial antibody that was used in this experiment was a mouse antibody to a surface of intact mitochondria.

This result is in agreement with the findings of Desai *et al.* (2002). They reported that a large portion of FRAP/mTOR associates with the mitochondrial outer membrane. They proved their results through several confirmational experiments. They reported that P70S6K of human T cell line (kit-225) was markedly dephosphorylated and lost its kinase activity within minutes after treatment of these cells with mitochondrial inhibitors. This result indicates that dysfunctional mitochondria signal to P70S6K in an mTOR-dependent manner. In addition, they used Jurkat cells to perform subcellular fractionation. Four distinct fractions were obtained. These four fractions were: nuclear, heavy membrane, cytosolic and vesicular proteins. These proteins were probed for presence of marker proteins and mTOR. The result showed the presence of mTOR in both the heavy membrane pellet and the cytosolic fraction. Then, they purified the mitochondria from the heavy membrane pellet by utilizing sucrose density gradient-ultra centrifugation. The result demonstrated that mTOR cofractionates with the purified mitochondria and rapamycin treatment had no effect on this association. Furthermore, by using immnuofluorescence confocal microscopy and immunoelectron microscopy,

the same group using 3T3 cells proved the co-localization of mTOR to the mitochondrial outer membrane or exposed on the surface of mitochondria.

Moreover, it has been shown that Rheb activates mTORC1 by antagonising its endogenous inhibitor, FKBP38 (Bai *et al.*, 2007). Under growth factor deprivation or amino acid starvation condition, FKBP38 binds directly to mTOR and down regulates mTORC1 activity. When amino acids and growth factors are present, Rheb interacts with FKBP38 and releases mTORC1 for activation (Ma *et al.*, 2008).

A study by the same group (Ma *et al.*, 2008) using HEK293 and HeLa cells demonstrated that the majority of Rheb is co-localized with mitotracker, suggesting that the protein is localized with mitochondria. The localization of Rheb with the mitochondria is also consistent with the fact that Rheb directly interacts with FKBP38, which has been reported to be a mitochondrial protein (Shirane and Nakayama, 3003; Portier and Taglialatela, 2006).

After fractionation analysis, Ma et al., 2008 reported that at least a portion of mTOR is localized to mitochondria, where Rheb and FKBP38 reside. This result is supported by previous findings showing that mTOR localized with outer membrane of mitochondria (Desai *et al*, in 2002). Given that mitochondria is the major metabolic organelle, co-localization of mTOR, Rheb, and FKBP38 on mitochondria is consistent with the role of mTORC1 in nutrient, energy, and oxygen sensing (Ma *et al.*, 2008).

Furthermore, a study on the subcellular localization of mTOR in Jurkat cells and HEK293 cells utilizing cellular fractionation technique revealed that mTOR in an mTORC1 complex is associated with the mitochondrial channel VDAC (Schieke *et al.*, 2006; Ramanathan and Schreiber, 2009).

However, several studies investigating the mTOR localization have demonstrated that mTOR is localized to other organelles. For example, a recent study (Yadav *et al.*, 2013) using fluorescence lifetime imaging has reported that the main localization of mTOR

appeared to be located in the perinuclear region in the Golgi and ER. Three different cell lines (HEK293, CHO and HeLa cells) were transiently transfected with EGFP tagged at either end of mTOR. Cells were examined for expression 24h and 48h after transfection. HEK293 and HeLa cells showed mTOR expression mainly in the cytoplasm with some detectable but weak presence within the cell nucleus.

In addition, a study conducted by Rosner and Hengstschlager (2008) in HEK293, NIH3T3, IMR-90, MRC-5 and WI-38 cells using subcellular fractionation revealed that mTOR was highly abundant in the nucleus but mTORC1 integrity was higher in the cytoplasm.

Moreover, it has been reported that mTOR is localized to lysosomes. A study in HEK293T cells utilizing paraformaldehyde (PFA) fixation and confocal imaging to investigate the subcellular localization of mTOR revealed that amino acids stimulate mTOR translocation from the cytoplasm to the lysosome in a Rag-and Ragulator-dependent manner and showed that Rheb, Ragulator and Rags are at the lysosome independently of amino acids (Sancak *et al.*, 2008, 2010; Bar-Peled *et al.*, 2012).

The present study demonstrated that mTOR is localized to mitochondria in MCF-7 and HEK293 cells. The distribution of mTOR in the perinuclear area of these cells was in a punctate pattern and was very similar to the distribution of the mitochondria as investigated using an anti-mitochondrial antibody. Thus, it seems that mTOR has been found at several cellular locations by different groups, even in the same cell lines. However, it is necessary to consider the issues that related to a protein or complex subcellular determination. The antibodies that are used in these studies might be non-specific. In addition, tagged proteins can show different localisation. Moreover, the different fixation and lysis methods can also influence the subcellular localization of a protein. The isolated organelles can be contaminated with other organelles (Betz and Hall, 2013). Furthermore, in regard to mTOR, the determination of one component of

the complex in an organelle does not necessarily reflect the presence of the entire complex in that organelle. Also, the most important issue that should be considered, especially when dealing with a very complicated signalling pathway such as mTOR pathway, is nutrient, stress, and cell cycle status. Using different cell lines should be also taken into account (Betz and Hall, 2013).

Modulation of cell signalling can change the subcellular localization of important components of the corresponding pathways (Drenan *et al.*, 2004). Based on this concept, in the present study, HEK293 cells were treated with varying rapamycin concentrations for varying periods of times to induce autophagy via mTOR inhibition to study if there is a change in the subcellular localization of mTOR in cells undergoing autophagy. The result showed that there was no change in the location of mTOR by showing that mTOR still localized to mitochondria. In terms of localisation, this result indicates that mTOR was not affected by rapamycin treatment. However, it might be that the observed mTOR in this study is mTORC2 and not mTORC1. This is because it is well known that mTORC2 is rapamycin insensitive (Sarbassov *et al.*, 2004). However, it has been reported that prolonged rapamycin treatment also inhibits and reduces the levels of mTORC2 (Sarbassov et al., 2006). For this reason, in the present study, HEK293 cells were treated with low concentrations of rapamycin for short period of time (16 hours) to influence mTORC1 and also the cells treated with high concentrations of rapamycin for long period of time (three days) to influence mTORC2. However, the results showed that in both cases, mTOR still localized to mitochondria and did not move to any other organelles. These results indicate that, in terms of subcellular localization, it seems that mTORC1 and mTORC2 were not influenced by rapamycin treatment. These results are also in agreement with the findings of a study conducted by Yadav *et al.* (2013). By utilizing of GFP/FRET-FLIM approach, Yadav *et al.* (2013) have reported that the

addition of rapamycin was not seen to affect the localization of mTOR in HEK293 and HeLa cells.

In addition, a study investigated whether mTOR location changed in response to cellular condition that modulate mTOR signalling has reported that mTOR remained in the perinuclear pattern during rapamycin treatment which inhibited mTOR signal transduction (Drenan *et al.*, 2004). Furthermore, a study using HEK293T and HeLa cells has reported that inhibition of mTORC1 activity with rapamycin does not affect mTORC1 localization (Sancake et al., 2008).

In the present study, HEK293 cells were starved in serum-free media for different periods of time (2, 6 and 24 hours) to induce autophagy through mTOR inhibition by starvation. These experiments were conducted in order to study the behaviour and the subcellular localization of mTOR under the influence of starvation, and compare it with that of rapamycin treatment. As mentioned above, the result demonstrated that there is no difference between the effect of rapamycin treatment or starvation on the subcellular localization of mTOR. The protein remained localized to the mitochondria and did not move to other organelles. This result indicates that starvation also has no effect on the mTOR localisation, which is in agreement with the findings of a study conducted by Drenan *et al.* (2004). They reported that mTOR subcellular localization in HeLa cells did not change under the influence of serum starvation, even for a long period of time. In addition, it has been demonstrated that amino acid starvation does not affect the subcellular localization of mTOR (Yadav *et al.*, 2013).

Apart from the place where mTOR localized, the present result and all the above studies have shown that rapamycin treatment or starvation have no effect on the originally observed subcellular localization of mTOR. It is well known that inhibition of mTOR by rapamycin treatment or starvation is the crucial step in autophagy induction. If mTOR localisation does not change during autophagy, then, how is mTOR

communicating with its partners or substrates that play an important role in the autophagic process? Do they recruit to where mTOR is localized and are then phosphorylated or de-phosphorylated locally?

4.4.2 Regulatory associated protein of mTOR (Raptor)

By using dual label (anti-raptor and anti-mitochondrial antibodies) ICC, the present study has demonstrated that in HEK293 cells raptor diffuses in the cytoplasm and a small portion of the protein might be localized to the mitochondria. The monoclonal rabbit anti-raptor antibody that produced this result was selected from three different anti-raptor antibodies from different suppliers after a characterization process by western blot. The antibody successfully stained bands at the right molecular size of raptor (150 kDa) using proteins from whole cell lysate of three different cell lines (NRK, MCF-7 and HEK293 cells) (Figures 3.23, 3.24 and 3.25).

The results of this study are in agreement with the findings of Yadav *et al.*, (2013). They demonstrated that in HEK293, HeLa and CHO cells raptor expression was observed in the cytoplasm. They studied the subcellular localization of raptor in these three cell lines after a transient transfection of these cells with a vector for DsRed-raptor, while the present study investigated the endogenous protein. Also, Sancak *et al.*, (2008) have reported that raptor localized to the cytoplasm of HEK293T cells.

The present study showed that mTOR is localized to mitochondria in HEK293 cells and after rapamycin treatment or starvation, raptor (mTOR partner) has clearly moved from the cytoplasm toward the perinuclear area with expression pattern was similar to the distribution of mitochondria (Figure 4.8), (Figure 4.9) and (Figure 4.10). mTOR works in a complex called mTORC1 and this complex contains raptor. So, the result suggests that after the induction of autophagy via mTOR inhibition, through either rapamycin treatment or serum starvation, raptor moved to join the mTOR on the mitochondria to

form the mentioned complex. The present study also found that a small portion of raptor might be localized to the mitochondria of HEK293 cells. So, from this result it seems that during autophagy raptor needs to be abundant on the mitochondria.

It has been reported that raptor interacts with mTOR as well as with mTORC1 substrates S6K1 (ribosomal protein S6 kinase 1) and 4EBP1 (eukaryotic initiation factor 4E (eIF4E)-binding protein 1) (Hara *et al.*, 2002; Kim *et al.*, 2002; Loewith *et al.*, 2002; Nojima *et al.*, 2003 and Schalm and Blenis, 2002). Each one of these substrates contains a TOR signaling motif that mediates raptor interaction and their subsequent phosphorylation by mTOR (Nojima *et al.*, 2003 and Schalm *et al.*, 2003). Thus, raptor functions as a scaffolding protein that facilitates the recruitment of substrates to the mTOR kinase (Foster *et al.*, 2010, Wang and Proud, 2010).

Since the present study has shown that mTOR localized to mitochondria under all conditions (un-treated, rapamycin treated and serum starvation in HEK293 cells), and also showed that under the influence of rapamycin treatment or serum starvation (autophagy induction) raptor moved toward the perinuclear area to join mTOR to form with other proteins the mTOR complex 1, and also it has been proved that raptor is responsible for recruitment of mTOR's substrates, suggesting that important autophagic proteins such as ATG-1 and ATG-13 are recruited to the mitochondria via raptor to be phosphorylated or dephosphorylated by mTOR to inhibit or induce autophagy respectively.

In yeast, it has been reported that to induce autophagy, TOR has to dephosphorylate Atg-13 and allow it to bind to Atg-1 to form a complex with Atg-17 to initiate phagophore membrane formatiom which is the first step in autophagic process (Mizushima, 2010; Glick *et al.*, 2010).

TOR signaling also inhibits autophagy (Jung *et al.*, 2010). It seems that phosphorylation of Atg1 (downstream of TOR) decreases the binding of Atg1 to Atg13, impairing

autophagy. Atg13 also appears to be phosphorylated by TOR, and this seems to repress its function (Wang and Proud, 2010).

In mammalian cells, there are some proteins related to Atg1, i.e. ULK1-4. On the basis of data from over expression of wild type or kinase-dead mutants, ULK1-3 seems to have roles in autophagy induction (reviewed in Jung *et al.*, 2010). There appears to be an ortholog of ATG13 in mammalian cells, and an additional protein, FIP200, also connect with ATG13 and ULK1. Moreover, mTORC1 phosphorylates the ATG1 homolouegs ULK1/2 (Ganley *et al.*, 2009; Hosokawa *et al.*, 2009; Jung *et al.*, 2009) and this appears to repress their activities.

It has also been reported that in some cell lines, including HEK293 cells, silencing of ULK1 is sufficient to inhibit autophagy, suggesting that ULK1 could be the major form of ULK (Chan *et al.*, 2007 and Young *et al.*, 2006). However, other aspects of the regulation of the complex differ in mammals for example; inhibition of mTORC1 does not affect ULK1/Atg13 binding (Wang and Proud, 2010). Understanding the control of autophagy in mammalian cells is still very far from complete (Wang and Proud, 2010). Hosokawa et al. (2009) have reported that mTORC1 is incorporated into the large ULK1-mATG13-FIP200 complex upon nutrient stimulation and its recruitment is mediated by the interaction between raptor, a substrate recognition unit of mTORC1, and PS domain of ULK1. This interaction is independent of mAtg13, because a C-terminal deletion mutant of ULK1 that is unable to bind mATG13 remains capable of interacting with raptor (Hosokawa *et al.*, 2009). In addition, both in *vitro* and in *vivo* data suggest that mTORC1 phosphorylates ULK1 and mATG13 under nutrient rich conditions (Ganley *et al.*, 2009; Hosokawa *et al.*, 2009; Jung *et al.*, 2009).

Taken together with the results of the present study, it can be suggested that after rapamycin treatment or serum starvation (autophagy induction), raptor moves from the cytoplasm toward the perinuclear area to join mTOR on the mitochondria. Then, it is

proposed, raptor recruits the autophagic proteins ATG1/ULK1 and mATG13 to the mitochondria to be dephosphorylated by mTORC1 to induce autophagy.

Nevertheless, Yadav et al., (2013) have reported that raptor expression was predominantly within the cytoplasm of HEK293, HeLa and CHO cells and rapamycin treatment or amino acids starvation had no effect on its localisation and distribution.

4.4.3 Microtubule-associated protein 1 light chain 3 (LC3)

By utilizing dual labelling (anti-LC3 and WGA for Golgi apparatus), the present study has shown that in HEK293 cells, LC3 is localized to Golgi apparatus. The monoclonal rabbit anti-LC3 antibody that produced this result was selected from three different anti-LC3 antibodies from different suppliers after a characterization process by western blot. The selected anti-LC3 antibody has succeeded to detect bands of LC3-I and LC3-II forms at the right molecular sizes utilizing whole cell lysate from HEK293 cells treated with 50nM of rapamycin for 16 hours to induce autophagy. To confirm the localization of LC3 on Golgi apparatus, confocal microscope images using Z-stack option were performed and the obtained images have also showed that LC3 was localized to Golgi apparatus.

There are at least three families of mammalian Atg8-related proteins: microtubule-associated protein 1 light chain 3 (LC3); Golgi-associated ATPase enhancer of 16 kDa (GATE16); and γ-aminobutyric-acid-type-A (GABAA)-receptor-associated protein (GABARAP) (Kabeya *et al.*, 2004). Each family has subfamilies, and three human LC3 subfamilies (LC3A, LC3B and LC3C) have been identified (He *et al.*, 2003).

Kabeya et al., (2000) reported that LC3 localizes to the autophagosomal membrane after C-terminal processing. They investigated, using cellular fractionation techniques, both endogenous and exogenous (Myc-tagged LC3-I and II) LC3 in HeLa cells. Based on this result they proposed that LC3 is an orthologue of yeast Atg8, and they also reported

that the precise function and localization of the other two homologues (GATE16 and GABARAP) are unclear (Kabeya *et al.*, 2004). It has been suggested that GABARAP might be involved in the GABAA-receptor clustering (Chen *et al.*, 2000) or transport (Kneussel *et al.*, 2000). GATE16 has been suggested to be an intra-Golgi transport modulator that interacts with *N*-ethylmaleimide-sensitive factor (NSF) and the Golgi v-SNARE GOS-28 (Sagiv *et al.*, 2000).

Kabeya *et al.*, (2000), (2004), did not provide any information about the subcellular localization of un-processed LC3 (in non-autophagic cells). Here, the present study, utilizing confocal microscopy, has shown that in non-autophagic HEK293 cells, the endogenous LC3A/B was localized to Golgi apparatus. Since LC3 and GATE16 are both mammalian homologues of yeast Atg8 and GATE16 was suggested to be an intra-Golgi transport modulator, so this supports the result in the present study suggesting that also LC3 may play a role in Golgi apparatus of non-autophagic HEK293 cells.

To study the behaviour of LC3 protein after autophagy induction, HEK293 cells were treated with 50 nM of rapamycin for 16 hours or serum starved for 24 hours to induce autophagy. As reported previously, rapamycin and serum starvation have the same effect on LC3. The result has shown that a proportion of LC3 has moved from Golgi apparatus toward the cytoplasm in a punctuate pattern. However, most of the LC3 protein remained localized to Golgi apparatus.

Upon autophagy induction, LC3 is cleaved after Gly120 within 6 minutes of synthesis in the cytoplasm (Kabeya *et al.*, 2000). As a result, a cytosolic 18-kDa LC3-I, which lacks the C-terminal 22 amino acid fragment, is produced. Subsequently, a subpopulation of LC3-I is converted to LC3-II, a 16 kDa protein that localizes to autophagosomal membranes (Kabeya *et al.*, 2004). At the autophagosome, LC3-II has been shown to play a role both in selecting cargo for degradation (e.g. interaction of LC3-II with p62/SQTM1 targets-associated protein aggregates for turnover) but has

also been reported to promote membrane tethering and fusion in *vitro* (Nakatogawa, Ichimura and Ohsumi, 2007), supporting a possible role in fusion of other membrane compartments, such as endosomes or even mitochondria with autophagosomes (Barth, Glick and Macleod, 2010).

Taken together, the results suggest that un-processed LC3 localized to Golgi apparatus and immediately after autophagy induction the protein move to the cytoplasm to be cleaved and produce LC3-I, which is then converted to LC3-II which localizes to autophagosomal membrane to perform its function.

4.5 CONCLUSION

This chapter has firstly focused on the subcellular localization of mTOR, raptor and LC3 in non-autophagic HEK293 cells. The results showed that, in non-autophagic cells, mTOR localized to mitochondria, raptor localized to cytoplasm and a fraction might be localized to mitochondria and LC3 localized to Golgi apparatus.

The rationale behind these experiments, was to investigate first the movement of these important proteins when autophagy is induced and secondly to investigate if there is a difference between the effect of rapamycin treatment and the effect of serum starvation on these proteins.

Autophagy was induced by both; rapamycin treatment or serum starvation, and the results showed that there is no change in the subcellular localization of mTOR, but raptor moved from the cytoplasm toward the perinuclear area and had a distribution the same as mitochondria and a fraction of LC3 moved to the cytoplasm in a punctuate pattern, however, most of the protein was still localized to Golgi apparatus. The results have also demonstrated that rapamycin treatment and serum starvation have the same influence on the proteins of interest. The other reason behind these experiments is to

investigate the movement of these proteins inside a cell undergoing autophagy in a normal state (i.e. without any genetic defect).

In the present study, it was hypothesized that during autophagy, mTOR localized to mitochondria and raptor moved from the cytoplasm to mitochondria to join mTOR and other proteins to form the mTORC1 complex. Raptor would be expected to recruit autophagic proteins such as ATG13 to the complex to be de-phosphorylated by mTOR and allow it to bind to ATG-1 to form a complex with ATG-17 to initiate phagophore membrane which is the first step in autophagic process. Also, it is proposed that LC3 moved from Golgi apparatus to the cytoplasm to be cleaved and produce LC3-I and then converted to LC3-II and localized to the phagophore membrane to play a role in the elongation and fusion processes to produce autophagosome and fuse with the lysosome respectively.

In the next chapter HEK293 cells were transiently transfected with truncated PS-1 to investigate if the observed autophagic proteins movement were interrupted by the truncated protein.

Chapter 5

Expression of Truncated PS1-GFP and its effect on the localisation of mTOR, Raptor and LC3

5.1 INTRODUCTION

Presenillin 1 (PS-1) is a ubiquitous transmembrane protein. The protein has diverse putative biological roles in cell adhesion, apoptosis, neurite outgrowth, calcium homeostasis, and synaptic plasticity (Kim and Tanzi, 1997; Shen and Kelleher, 2007). A part of the PS1 holoprotein (45 kDa protein) is cleaved in the ER to produce a two-chain form (Zhang *et al.*, 1998). One of the functions of the cleaved form of PS1 is that it forms the catalytic subunit of the gamma (γ)-secretase enzyme complex, which mediates the intramembranous cleavage of many type 1 membrane proteins, including amyloid precursor protein (APP) and Notch (Citron *et al.*, 1997; De Strooper et al., 1998).

In addition to a role as the catalytic subunit of gamma (γ)-secretase enzyme complex, Strooper and Annaert in 2010, reported that PS plays a role in several diverse cellular processes, including autophagy. Mutated presenillins underlie the majority of FAD cases (Mann *et al.*, 1996; Borchelt *et al.*, 1997; Gomez-Isla *et al.*, 1999).

The first connection between neurodegeneration and autophagy originated from the observation that protein aggregates can be eliminated by autophagy (Yamamoto and Simonsen, 2011; Ravikumar *et al.*, 2002). Growing evidence supports the concept that neurons utilize diverse ways to eliminate pathogenic proteins and that multiple steps of the autophagic process are often affected in a given neurodegenerative disorder. Thus, for example, in the case of Alzheimer's disease (AD), autophagy contributes to the elimination of the toxic product of the APP, amyloid beta (A-β). However, clearance of A-β is compromised as the disease progresses, due to the failure in this autophagic pathway (Yu *et al.*, 2005). Anderson (2003) transiently transfected HEK293 cells with a tPS1-GFP construct to induce autophagy and by using electron microscopy,

demonstrated that autophagosomes were formed and accumulated in the cytoplasm, and did not clear as would be expected in the normal way.

In the present study, this chapter focuses on the transfection of HEK293 cells with the same tPS1-GFP construct used previously (Anderson, 2003) to induce autophagy. Then, investigate the effect of the truncated protein on the behaviour and the subcellular localization of key autophagic process regulators such as mTOR, raptor and LC3 in an attempt to understand the reason behind the autophagic process failure.

5.2 MATERIALS AND METHODS

DNA manipulation, transfection, immunocytochemistry and agarose gel preparation were performed as described in chapter 2.

5.2.1 Plasmid digestion

In order to confirm the presence of the gene of interest, the plasmid was digested into three pieces using *HindIII*, *XhoL* and *EcoR1* sites. The digestion of the first piece was a double digestion and was for *HindIII* and *XhoI*. The reaction was performed as follows: In a 50 µl reaction, 35 µl of distilled water was added to an Eppendorf tube and then 5 µl of 10 x BSA, 500 ng of the plasmid, 5 µl of 10 x NEBuffer 2, 1 µl of *HindIII* enzyme and 1 µl of *XhoI* enzyme were added to the same tube (New England Biolab, UK).

The tube was then incubated in a water bath at 37 °C for 2 hours. Then, the enzymes were inactivated in a water bath at 65 °C for 20 minutes. The second digestion was also a double digestion and was at *EcoRI* and *XhoI* sites. It was exactly as the first digestion reaction, but this time, according to the supplier, *EcoRI* enzyme was used instead of *HindIII* and NEBuffer *EcoRI* was used instead of NEBuffer 2 (New England Biolab, UK).

The third digestion was a sequential digestion and was at *EcoRI* and *HindIII* sites. The protocol was as follows: To an Eppendorf tube, 35 µl of distilled water, 500 ng of the

DNA, NEBuffer 2 and *HindIII* enzyme was added. The tube was incubated in a water bath at 37 °C for 2 hours and then inactivated at 65 °C for 20 minutes. The tube was returned to a water bath at 37 °C for 5 minutes. At this point, 1 µl of the second enzyme *EcoRI* was added to the tube and incubated at 37 °C for another 2 hours. For enzyme inactivation, the tube was incubated again at 65 °C for 20 minutes.

Agarose gel electrophoresis was performed as described above to examine the digestion process. 8 µl of each digestion tube were loaded to 1 % (w/v) agarose gel and the gel was electrophoresed at 100 V for an hour as described in 2.9.5.

5.3 RESULTS

5.3.1 Agarose gel electrophoresis

Upon the transformation step the truncated PS1-GFP construct was extracted from *E-coli* bacteria by QIAprep Spin kit according to the protocol provided by the supplier. Following the extraction, DNA extracts were run on a 1 % (w/v) agarose gel to confirm the presence of the construct and its size. The result confirmed the presence of the construct at 6986 base pairs (Figure 5.1).

To confirm the presence of the gene of interest (PS1-GFP), the construct was digested into three fragments using restriction enzymes (*HindIII*, *Xhol* and *EcoRI*), which are present at the cloning sites provided by the construct supplier (Life Technology, UK). The agarose gel showed a band at 1638 base pairs that represents the size as reported by the construct supplier (Life Technology, UK) (Figure 5.2).

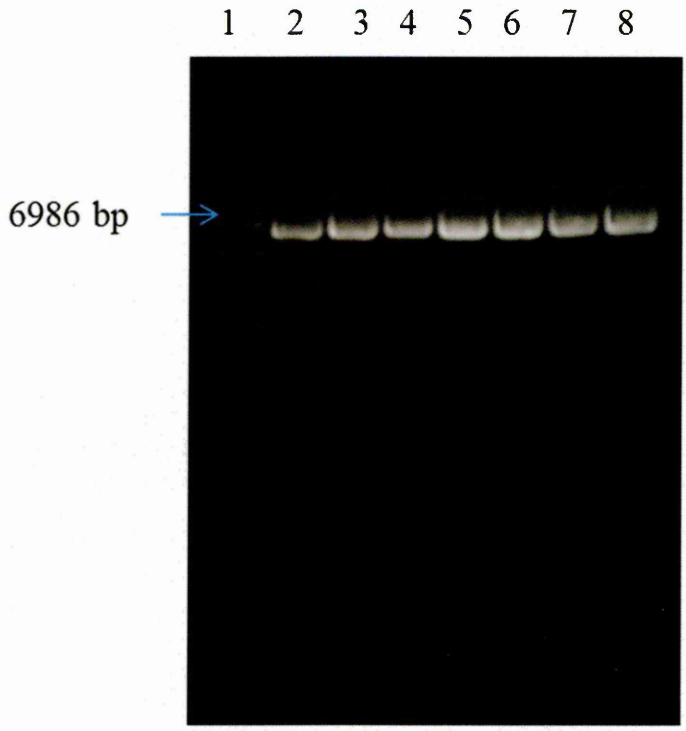

Figure 5.1 Agarose gel electrophoresis of PS1-GFP construct.

Lane (1) ladder GeneRuler 1kb DNA, lanes (2-8) PS1-GFP construct.

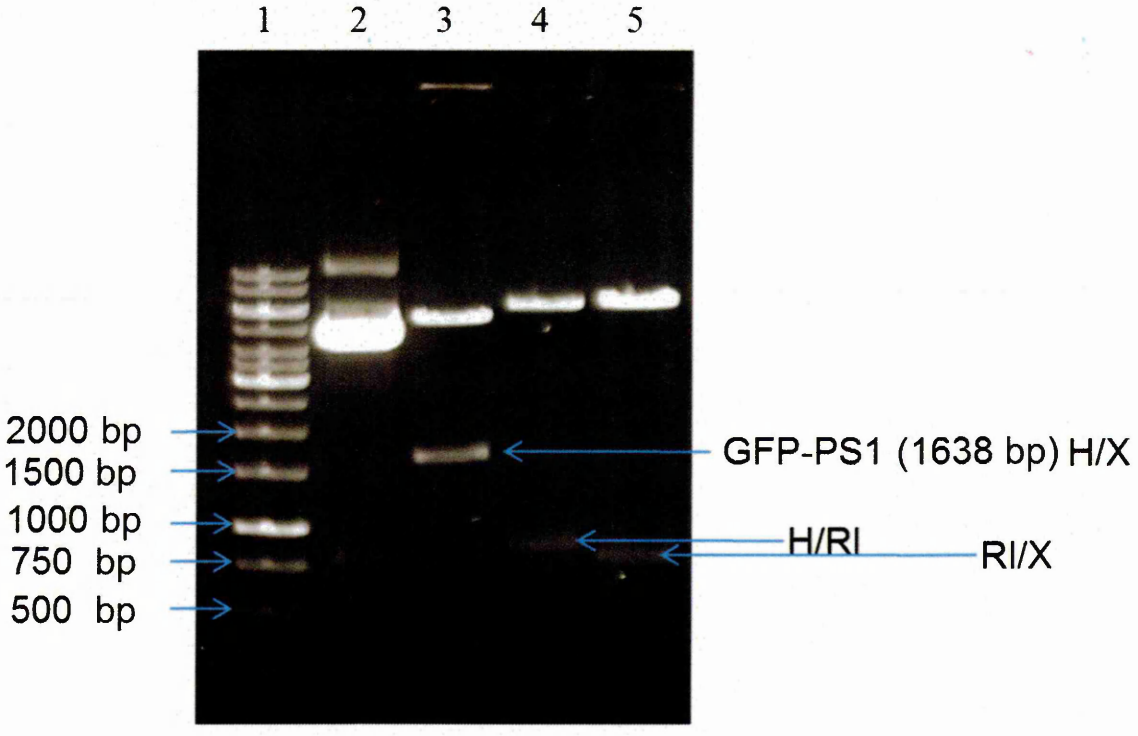

Figure 5.2 Agarose gel electrophoresis of digested PS1-GFP construct.

Lane (1) ladder (GeneRuler 1kb DNA, lane (2) un-digested construct, lane (3) construct digested with HindIII + XhoI (double digestion), lane (4) construct digested with EcoRI + HindIII (sequential digestion), lane (5) construct digested with EcoRI + XhoI (double digestion).

5.3.2 Expression of PS1 (NTF)-GFP in HEK293

Firstly, because stable transfection is more difficult and requires a long time to be achieved with HEK293 cells, the cells were transiently transfected with truncated PS1 conjugated to GFP and monitored by fluorescence microscopy in order to assess how long the construct is able to remain inside before its degradation by the cells. The fluorescence microscopy images show that PS1 (NTF)-GFP- construct was remained in the cells for nine days (Figure 5.3). Based on this result, it was decided that transient transfection was sufficient to study autophagy in the present study.

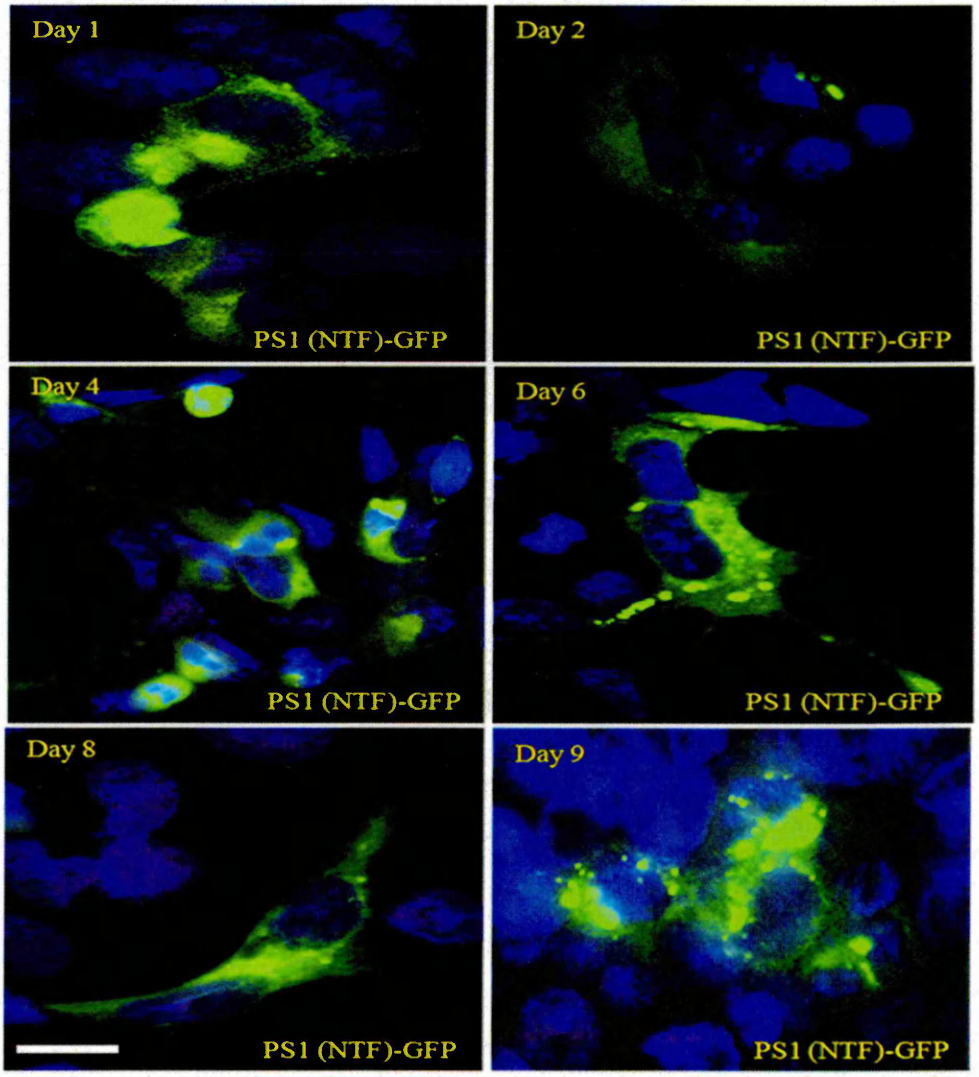

Figure 5.3 HEK293 cells transiently transfected with PS1 (NTF)-GFP upto 9 days post transfection. HEK293 cells transiently transfected with PS1-GFP using X-tremeGENE 9 DNA Transfection Reagent (TR) in a 3:1 ratio (3µl TR: 1µg DNA). Cells were transfected for 24hrs. (x400 magnification). Scale bar: 10µm

5.3.3 Expression of PS1 (NTF)-GFP with mTOR in HEK293 cells

Two 24-well plates of HEK293 cells were transiently transfected with tPS1-GFP construct for 24 hours and then left for two different periods of time before fixation. The first plate was left for 72 hours (3 days), and the other plate was left for 144 hours (6 days). This experiment was performed to induce autophagy in HEK293 cells by tPS1-GFP construct, and study the effect of tPS-1 on the subcellular localization of mTOR during autophagy. The main purpose in using different periods of time before fixation is to be sure that autophagy has initiated and also to give chance for the process to deal with the tPS-1.

Using standard fluorescence and confocal microscopy (Axiovert 200M, laser unit: ZESS LSM 510 Laser Module), the ICC pictures indicate that there is no difference in the observed subcellular localization of mTOR in HEK293 cells transfected for three or six days (Figures 5.4 and 5.5). The confocal images demonstrate that transiently expressed fluorescent protein tPS1-GFP in both cases (3 and 6 days) appear to be co-localized with mTOR protein in a distribution similar to the distribution of mitochondria (Figure 5.6). Controls for mTOR expressed by un-transfected HEK293, HEK293 transfected with transfection reagent alone, HEK293 transfected with DNA alone or HEK293 transfected with complex (DNA+TR) were performed. ICC showed that mTOR had the same distribution in all cases (Figure 5.7). It has been previously reported in chapter 4 that mTOR might be localized to mitochondria in autophagic and non-autophagic HEK293 cells. The result from this experiment has also show that after transfection, the distribution of mTOR is still similar to the mitochondrial distribution. Since tPS1-GFP has been observed appear to be co-localized with mTOR, this suggests that tPS-1 may interact with mTOR complex on the surface of the mitochondria.

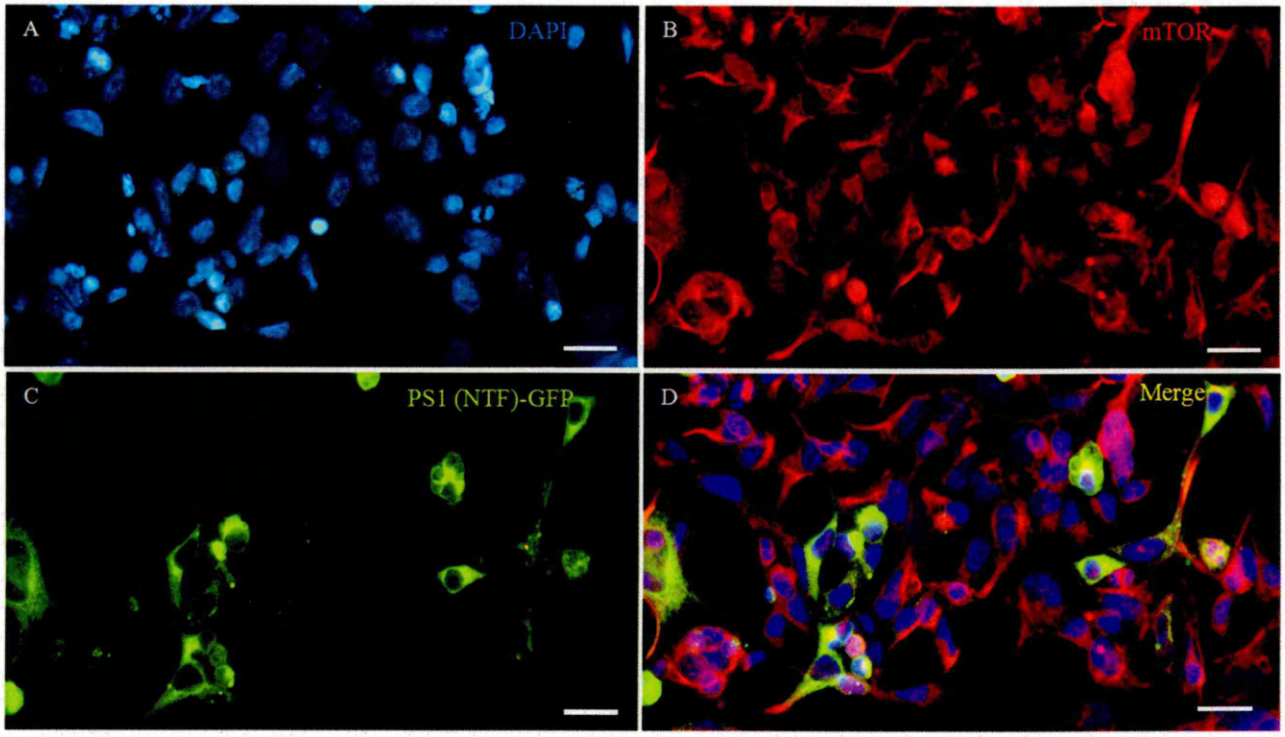

Figure 5.4 Dual label immunofluorescence for mTOR and PS1 (NTF)-GFP in transiently transfected HEK293 cells, (3 days after transfection). Cells were transiently transfected with PS1(NTF)-GFP for 3 days, fixed in cold methanol and labelled for (A) Nuclei were counterstained with DAPI (B) mTOR using primary monoclonal rabbit anti-human mTOR antibody (Millipore, 04-385) and secondary antibody Alexa fluor 594 donkey anti-rabbit IgG (C) PS1(NTF)-GFP (D) Merge. Scale bar: 10μm

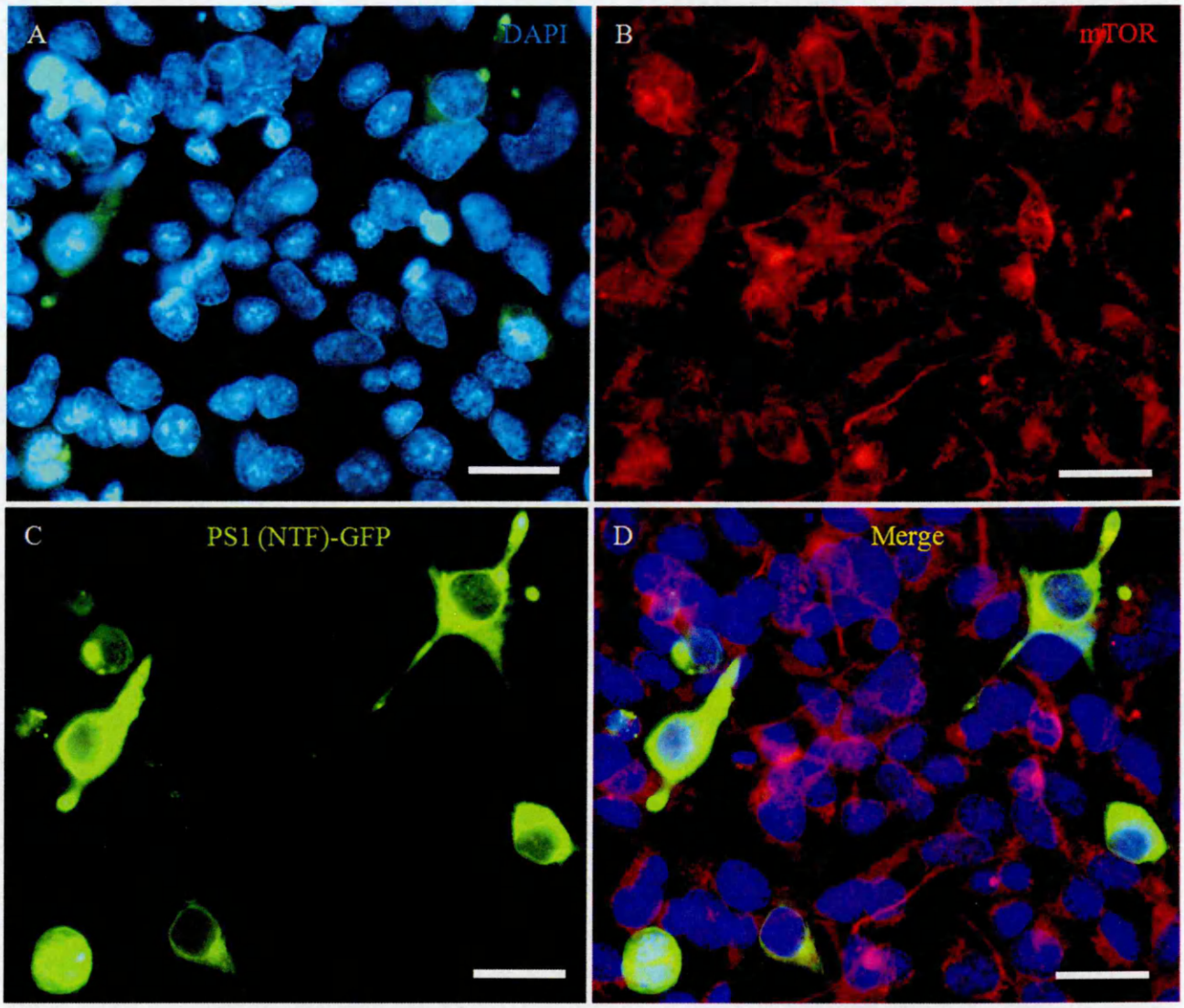

Figure 5.5 Dual label immunofluorescence for mTOR and PS1 (NTF)-GFP in transiently transfected HEK293 cells, (6 days after transfection). Cells were transiently transfected with PS1(NTF)-GFP for 6 days, fixed in cold methanol and labelled for (A) Nuclei were counterstained with DAPI (B) mTOR using primary monoclonal rabbit anti-human mTOR antibody (Millipore, 04-385) and secondary antibody Alexa fluor 594 donkey anti-rabbit IgG (C) PS1 (NTF)-GFP (D) Merge. Scale bar: 10μm

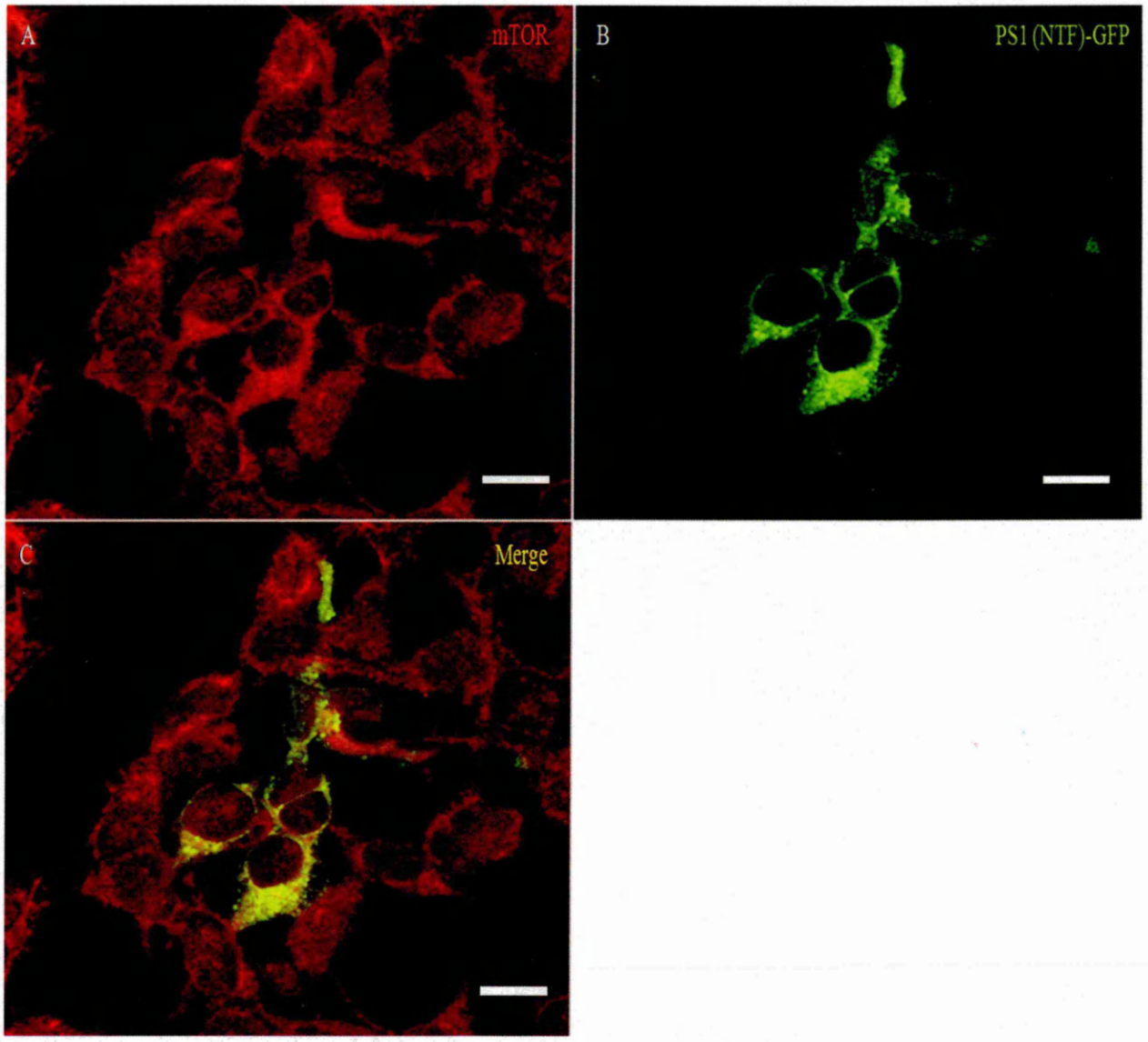

Figure 5.6 Dual label immunofluorescence (Confocal image) for mTOR and PS1 (NTF)-GFP in transiently transfected HEK293 cells, (6 days after transfection). Cells were transiently transfected with PS1(NTF)-GFP for 6 days, fixed in cold methanol and labelled for (A) mTOR using primary monoclonal rabbit anti-human mTOR antibody (Millipore, 04-385) and secondary antibody Alexa fluor 594 donkey anti-rabbit IgG (B) PS1(NTF)-GFP (D) Merge. Scale bar: 10μm

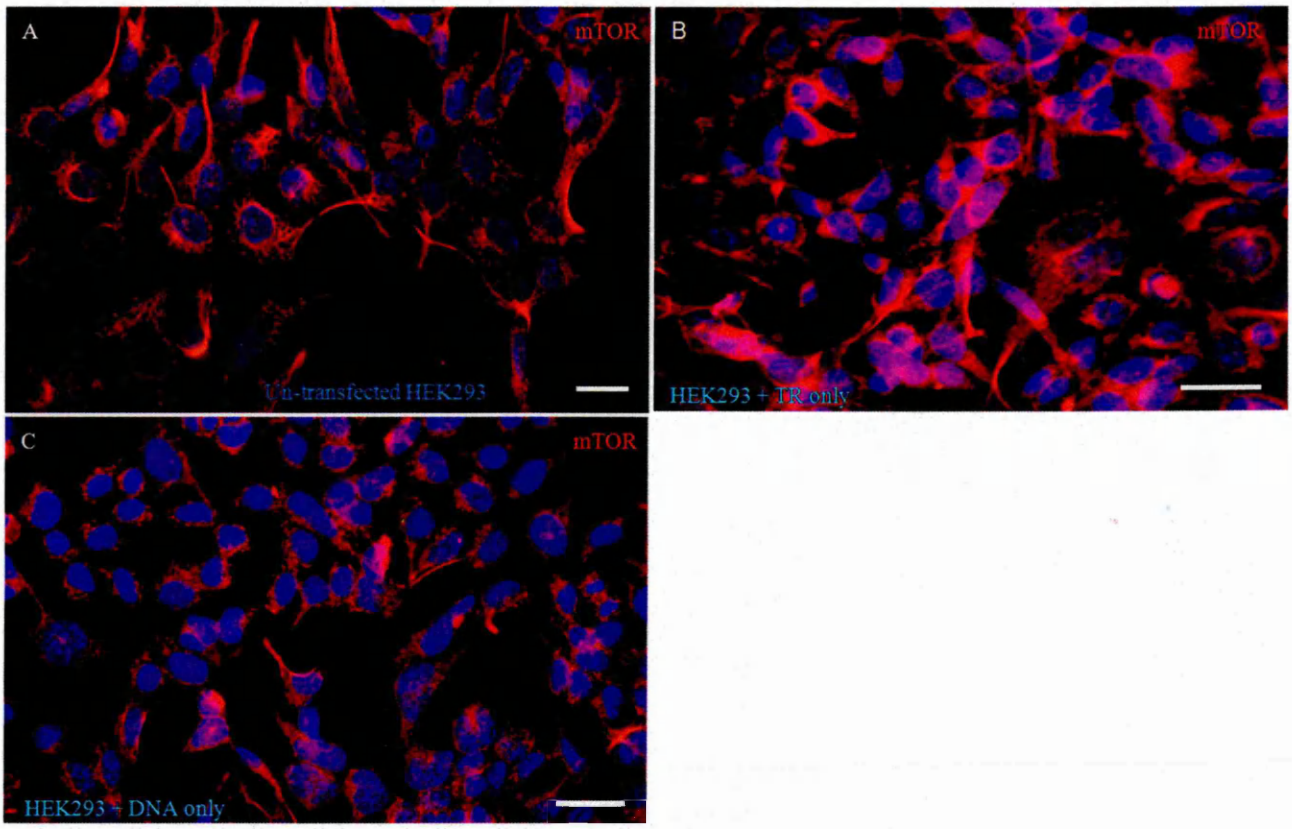

Figure 5.7 Single label immunofluorescence for mTOR in HEK293 cells, (Controls). Cells were fixed in cold methanol and labelled for (A) mTOR in untransfected HEK293 cells (B) mTOR in HEK293 cells transfected with transfection reagent (TR) only (C) mTOR in HEK293 cells transfected with DNA (PS1 (NTF)-GFP) only. In all three merge pictures, mTOR was labelled with primary monoclonal rabbit anti-human mTOR antibody (Millipore, 04-385) and secondary antibody Alexa fluor 594 donkey anti-rabbit IgG. Scale bar: 10μm

5.3.4 Expression of PS1 (NTF)-GFP with raptor in HEK293 cells

In this experiment, in order to detect the subcellular localization of raptor and investigate the effect of truncated PS-1 expression on its location, two groups of HEK293 cells were transiently transfected with the tPS1-GFP construct to induce autophagy for either 3 or 6 days.

Three days after transfection, the ICC images illustrated that there may be an interaction between raptor and the transiently expressed tPS1-GFP construct (Figure 5.8). Also, after 6 days, HEK293 cells demonstrated the same result (Figure 5.9). It appears that raptor and tPS1-GFP are present in the same subcellular location. However, in both cases, although it appears that granular raptor staining was localized with tPS1 expression, the raptor staining was not completely co-localized with it. The other observation in both cases is that it seems that the non-transfected cells have more raptor staining than the transfected cells. Controls were also performed to test for artefactual results and illustrated no non-specific staining. Raptor protein was diffusely stained in the cytoplasm in all cases (Figure 5.10).

Interestingly, the interaction between raptor and tPS1-GFP construct is similar to what has been observed between mTOR and the same construct in the present study. In addition, they have the same intracellular distribution. This similarity in the interaction and the cellular distribution between mTOR, raptor and tPS1-GFP may represent another indication for a direct physical interaction between mTOR and raptor, and the tPS1-GFP construct might be co-localize with the mTORC1 that include mTOR and raptor proteins.

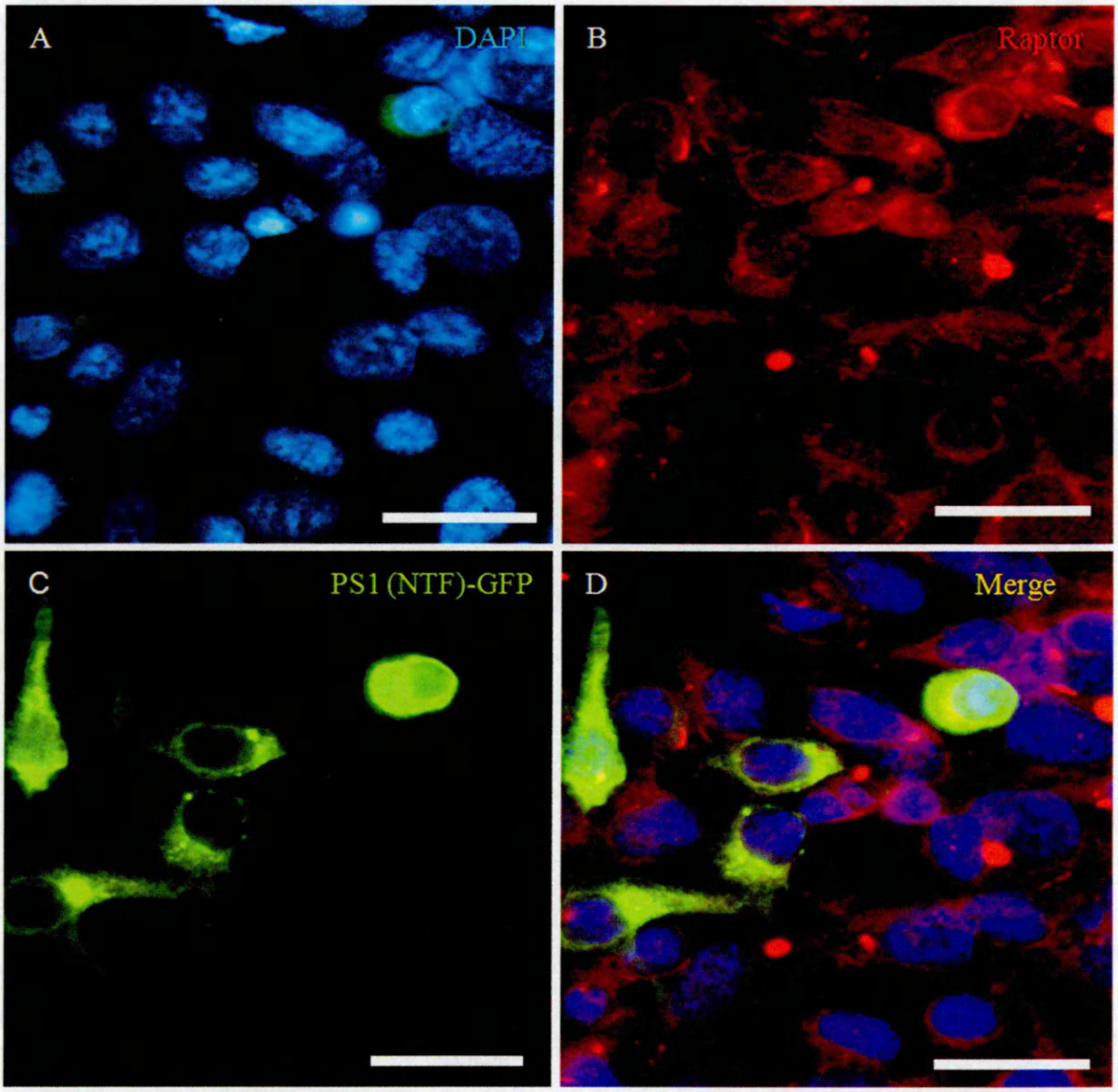

Figure 5.8 Dual label immunofluorescence for raptor and PS1 (NTF)-GFP in transiently transfected HEK293 cells (3 days after transfection). Cells were transiently transfected with PS1(NTF)-GFP for 3 days, fixed in cold methanol and labelled for (A) Nuclei were counterstained with DAPI (B) Raptor using primary monoclonal rabbit anti-human raptor antibody (CellSignaling Technology, 2280) and secondary antibody Alexa fluor 594 donkey anti-rabbit IgG (C) PS1(NTF)-GFP (D) Merge. Scale bar: 10μm

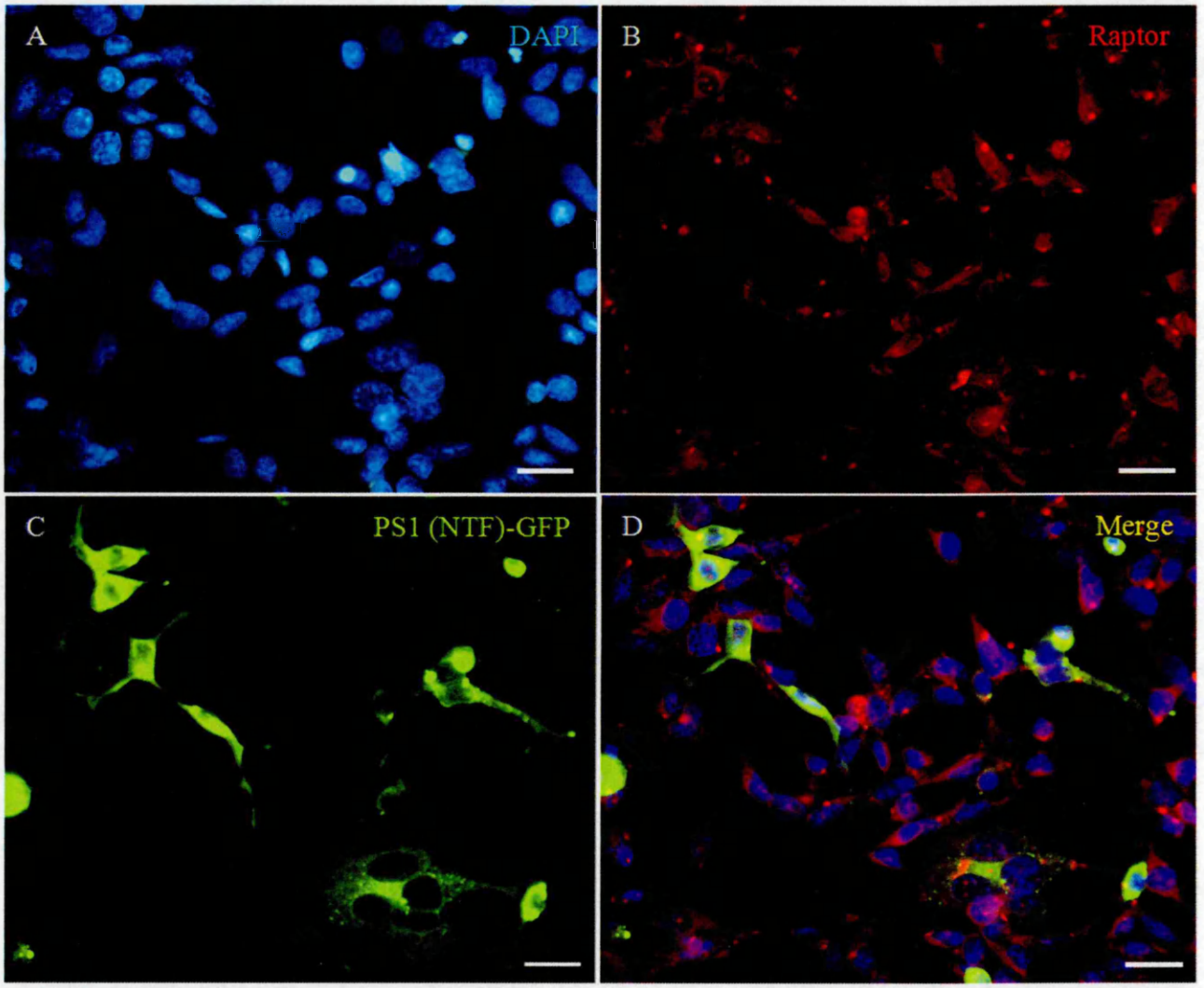

Figure 5.9 Dual label immunofluorescence for raptor and PS1 (NTF)-GFP in transiently transfected HEK293 cells (6 days after transfection). Cells were transiently transfected with PS1(NTF)-GFP for 6 days, fixed in cooled methanol and labelled for (A) Nuclei were counterstained with DAPI (B) raptor using primary monoclonal rabbit anti-human raptor antibody (Cell Signaling Technology, 2280) and secondary antibody Alexa fluor 594 donkey anti-rabbit IgG (C) PS1(NTF)-GFP (D) Merge. Scale bar: 10μm

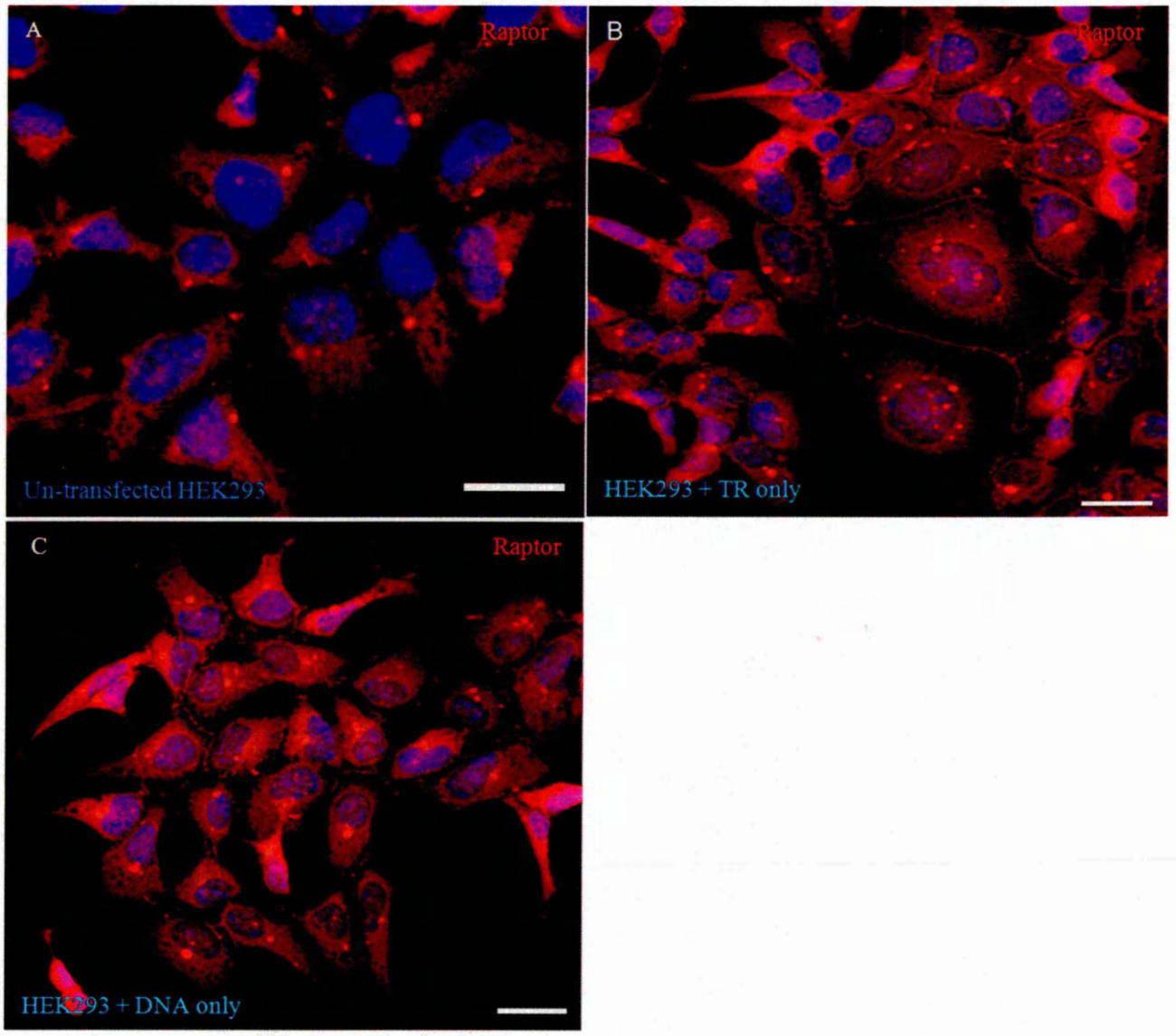

Figure 5.10 Single label immunofluorescence staining for raptor in HEK293 cells (Controls). Cells were fixed in cold methanol and labelled for (A) raptor in untransfected HEK293 cells (B) raptor in HEK293 cells transfected with transfection reagent (TR) only (C) raptor in HEK293 cells transfected with DNA (PS1 (NTF)-GFP) only. In all three images, raptor was labelled with primary monoclonal rabbit anti-human raptor antibody (Cell Signaling Technology, 2280) and secondary antibody Alexa fluor 594 donkey anti-rabbit IgG. Scale bar: 10μm

5.3.5 Expression of PS1 (NTF)-GFP with LC3 in HEK293

HEK293 cells were transiently transfected with truncated PS-1 (PS1-GFP construct) for 3 or 6 days to induce autophagy and to study the behaviour of LC3 under the influence of truncated PS-1.

By fluorescence and confocal microscopy, the ICC images from both groups have shown that the expressed fluorescent protein tPS1-GFP appears to be co-localized with LC3 protein (Figures 5.11 and 5.12). However, it seems that the small amount of LC3 staining that is present over the nucleus is not co-localized with tPS1 as shown clearly in figure 5.12. It has been previously reported in chapter 4 that LC3 appears to localize to the Golgi apparatus in non-autophagic HEK293 cells. However, upon autophagy induction by rapamycin treatment or serum starvation, a small portion of LC3 moved to the cytoplasm, while the majority of the protein remained localized to the Golgi apparatus.

Interestingly, in this experiment, upon autophagy induction by truncated PS-1, the majority of the LC3 protein moved from the Golgi apparatus and appears to be co-localized with tPS1-GFP in the cytoplasm or on other subcellular organelles. However, a small portion of the LC3 protein remained localized to the Golgi apparatus. Figure 5.13 shows confocal images of transiently expressed fluorescent protein tPS1-GFP with LC3 protein in HEK293 cells. As in figure 5.12, figure 3.13 showed that there is not total overlap of staining for tPS1 and LC3. Controls showing subcellular localization of LC3 in transfected and un-transfected HEK293 cells were performed. All three controls showed that the result is not an artefact or due to non specific binding of antibodies. The result suggests that LC3 protein may indeed localize to the Golgi apparatus (Figure 5. 14).

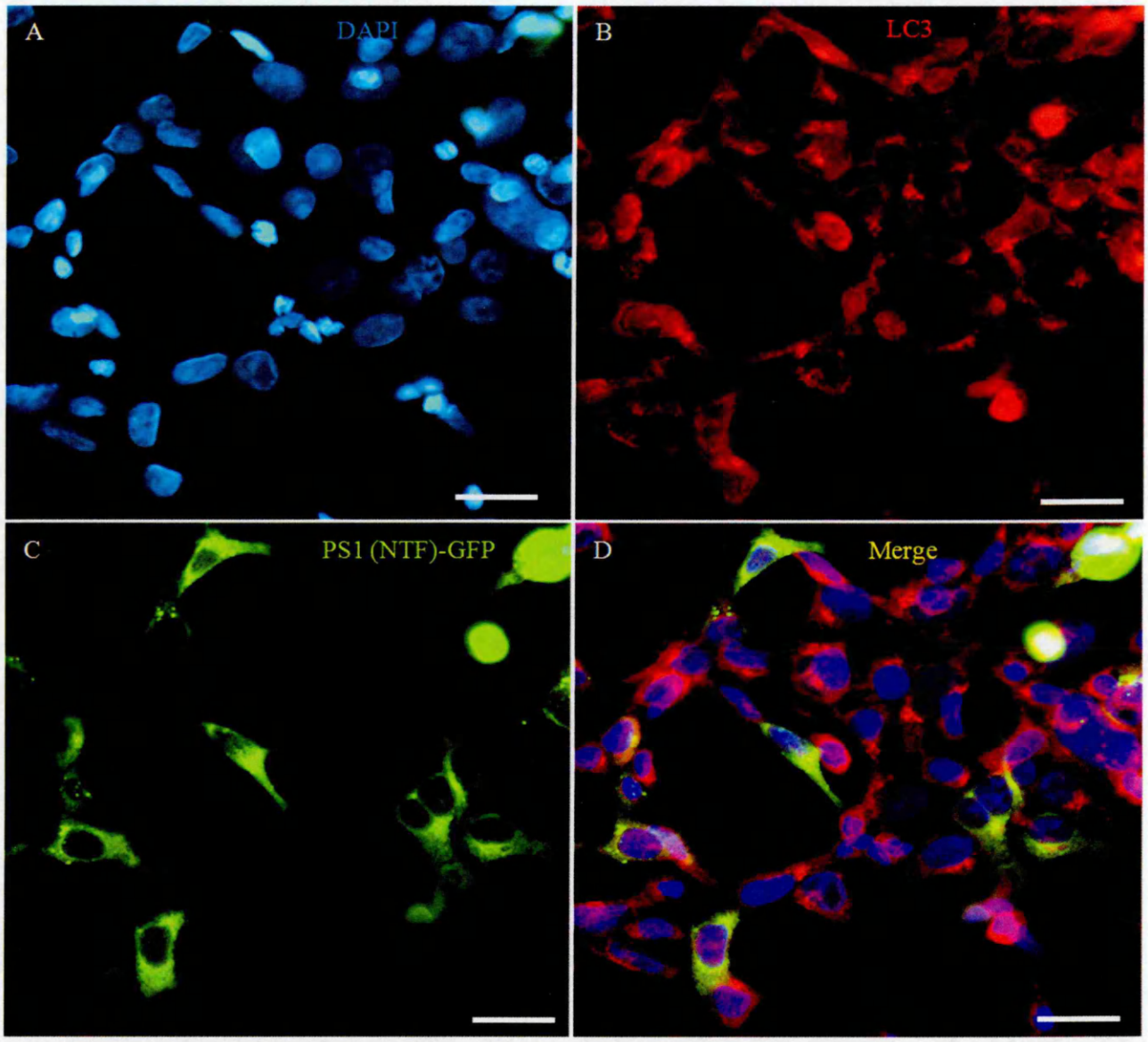

Figure 5.11 Dual label immunofluorescence for LC3 and PS1 (NTF)-GFP in transiently transfected HEK293 cells (3 days after transfection). Cells were transiently transfected with PS1(NTF)-GFP for 3 days, fixed in cold methanol and labelled for (A) Nuclei counterstained with DAPI (B) LC3 using primary monoclonal rabbit anti-human LC3A/B antibody (Millipore, MABC176) and secondary antibody Alexa fluor 594 donkey anti-rabbit IgG (C) PS1(NTF)-GFP (D) Merge. Scale bar: 10μm

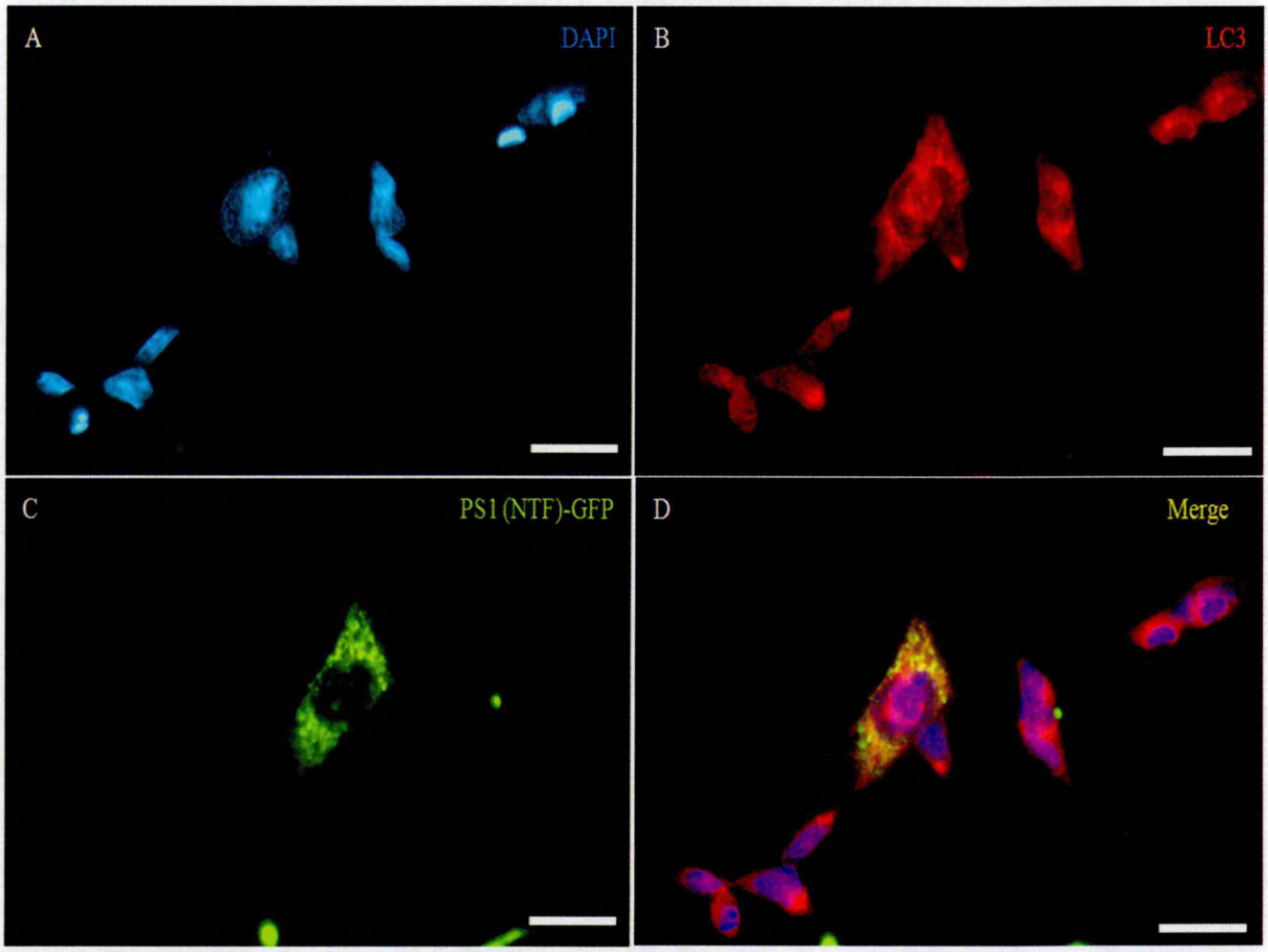

Figure 5.12 Dual label immunofluorescence for LC3 and PS1 (NTF)-GFP in transiently transfected HEK293 cells (6 days after transfection). Cells were transiently transfected with PS1(NTF)-GFP for 6 days, fixed in cold methanol and labelled for (A) Nuclei counterstained with DAPI (B) LC3 using primary monoclonal rabbit anti-human LC3A/B antibody (Millipore, MABC176) and secondary antibody Alexa fluor 594 donkey anti-rabbit IgG (C) PS1(NTF)-GFP (D) Merge. Scale bar: 10μm

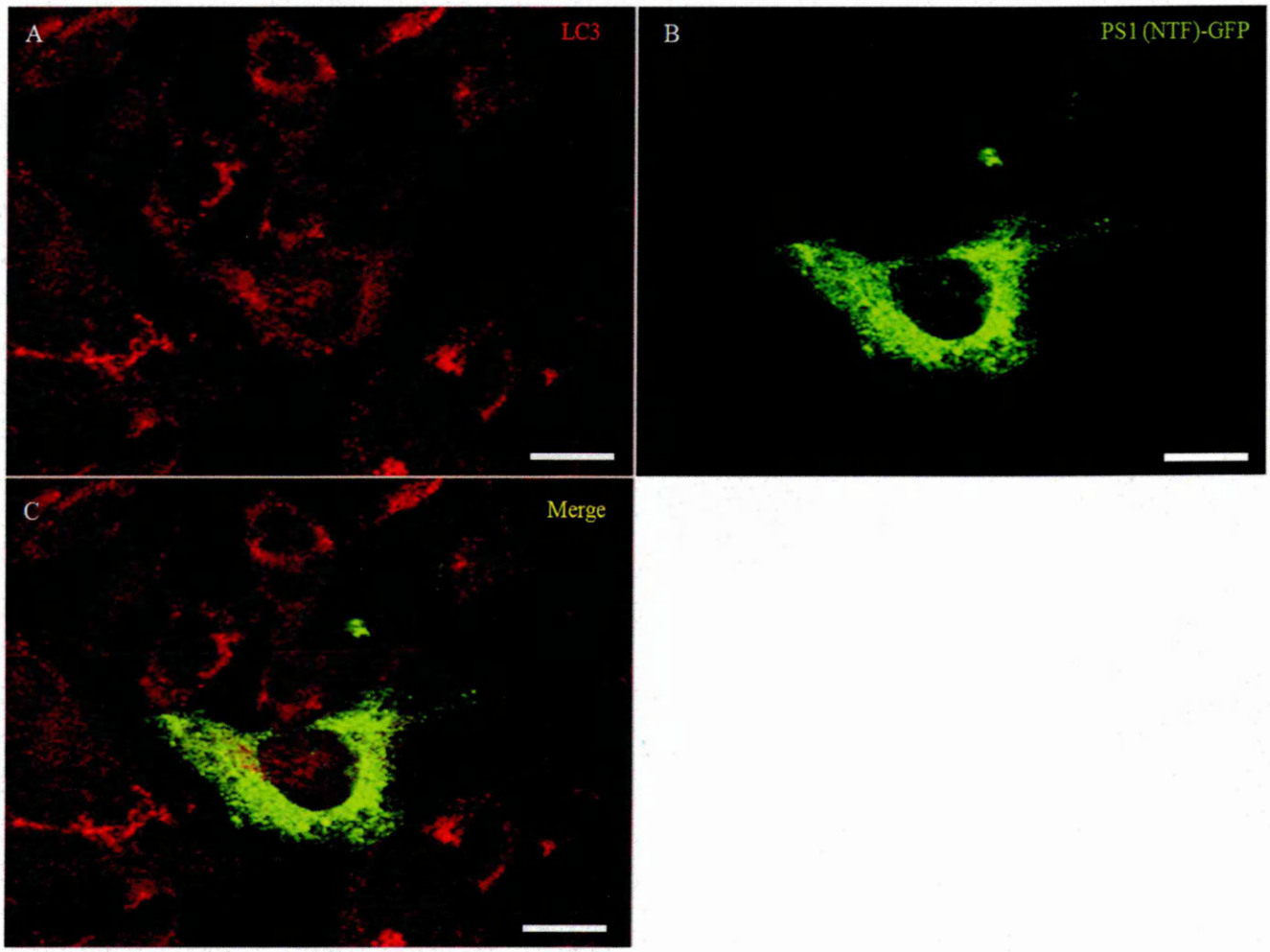

Figure 5.13 Dual label immunofluorescence (Confocal image) for LC3 and PS1 (NTF)-GFP in transiently transfected HEK293 cells (6 days after transfection). Cells were transiently transfected with PS1(NTF)-GFP for 6 days, fixed in cold methanol and labelled for (A) LC3 using primary monoclonal rabbit anti-human LC3A/B antibody (Millipore, MABC176) and secondary antibody Alexa fluor 594 donkey anti-rabbit IgG (B) PS1(NTF)-GFP (C) Merge. Scale bar: 10μm

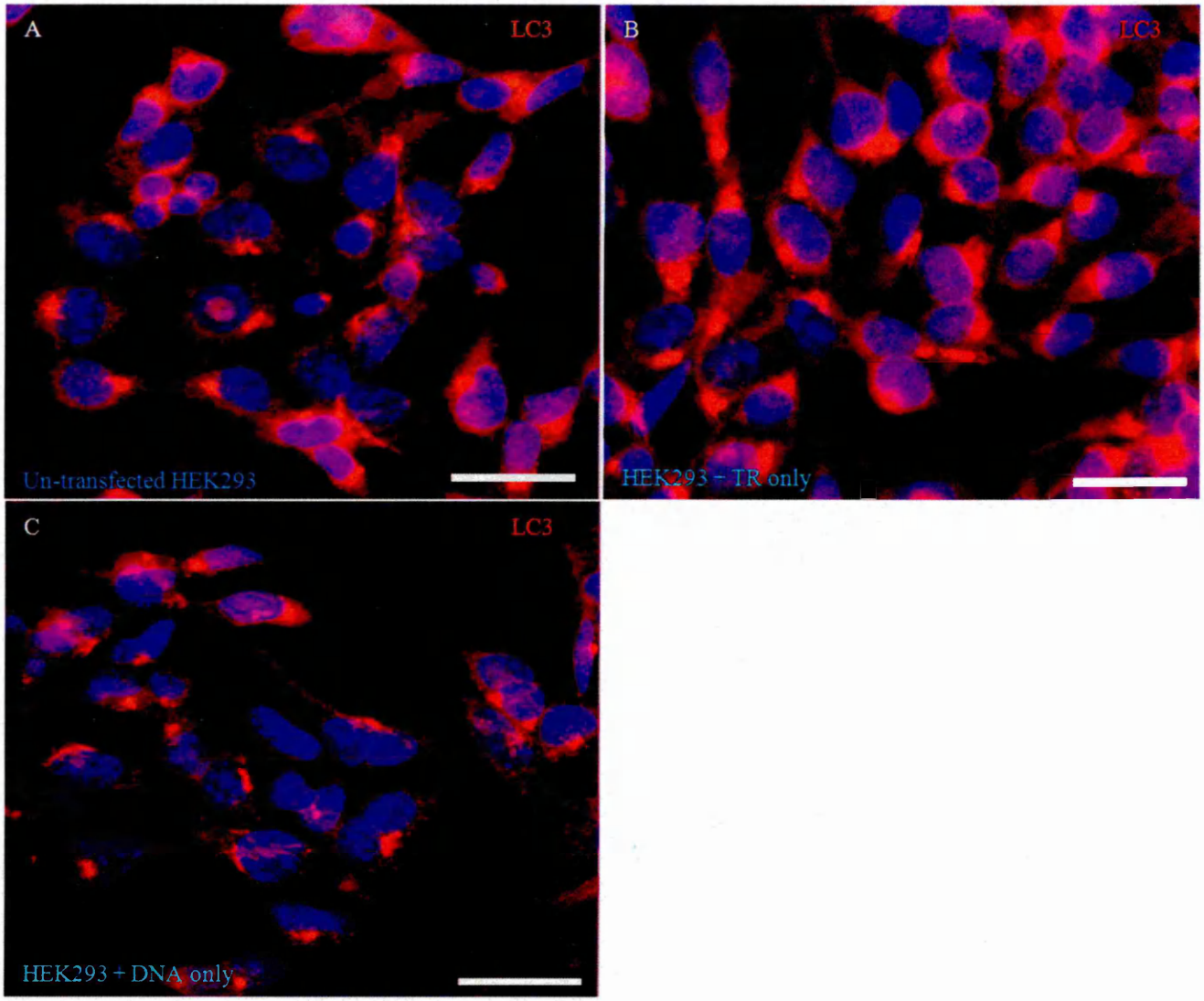

Figure 5.14 Single label immunofluorescence for LC3 in HEK293 cells (Controls). Cells were fixed in cold methanol and labelled for (A) LC3 in untransfected HEK293 cells (B) LC3 in HEK293 cells transfected with transfection reagent (TR) only (C) LC3 in HEK293 cells transfected with DNA (PS1 (NTF)-GFP) only. In all three merge pictures, LC3 was labelled with primary monoclonal rabbit anti-human LC3A/B antibody (Millipore, MABC176) and secondary antibody Alexa fluor 594 donkey anti-rabbit IgG. Scale bar: 10μm

5.4 DISCUSSION

Presenilins are ubiquitous, intramembrane proteins that are known to have crucial functions in many cellular processes including autophagy (Strooper and Annaert, 2010). It has been revealed that lysosomal proteolysis and autophagy require presenilin 1 and are disrupted by Alzheimer related presenilin 1 mutation (Lee *et al.*, 2010b). In addition, Neely *et al.* (2011) demonstrated that presenilin is necessary for efficient proteolysis through the autophagy-lysosome system in a γ-secretase-independent manner. Both studies demonstrated that absence or mutation of presenilin leads to autophagic dysfunction late in the pathway, at the autophagosome-lysosome fusion step.

Lee *et al.* (2010b) attributed the autophagic failure to a deficit in the lysosomal acidification. The authors used PS1 null blastocytes, neurons from mice hypomorphic for PS1 or conditionally deleted of PS1, and show that the substrate proteolysis and autophagosome clearance during macroautophagy are prevented. They concluded that this defect is due to selective impairment of autolysosome acidification and cathepsin activation. Neely *et al.* (2011) have supported Lee's hypothesis but suggested another role for presenilins at the autophagosome-lysosome interaction. Neely *et al.* (2011) have treated PSDKO (presenilin-1 and -2 double knockout mice fibroblasts) cells with the vacuolar ATPase inhibitors, bafilomycin A1 and the microtubule-destabilizing drug nocodazole, both of which will inhibit autophagosome-lysosome fusion. They reported that cells with autophagic defect at the lysosome will lead to a build-up in autophagosomes, and inhibition at the lysosome will not result in an additional increase in LC3-II/autophagosome because the downstream steps of the process are already defective. Interestingly, they have found that PSDKO cells do not have an additional increase in LC3-II when treated with bafilomycin A1 or nocodazole. Based on the results, they concluded that this is a novel function of presenilins in autophagy at the level of autophagosome-lysosome interaction or lysosomal function.

However, a study by Zhang *et al.* (2012) utilizing embryonic stem cells (ES) lacking presenilin 1 (PS1ko-ES) or both presenilin 1 and presenilin 2 (PSko-ES) compared to wild type embryonic stem (WT-ES) cells and also hippocampi of mice with genetic deletions of presenilin 1 and presenilin 2 in excitatory neurons (PScdko mice) compared with their littermate controls has revealed that the absence of presenilins has no significant influence on lysosomal pH.

Anderson (2003) transiently transfected HEK293 cells with truncated presenilin1 construct and demonstrated that autophagy failed to proceed normally. Transfected HEK293 cells with tPS1-GFP construct formed autophagosomes which accumulated in the cytoplasm, observed by electron microscopy and did not clear as would be expected in the normal state. This is another indication that the problem in the autophagic process occurred late in the pathway at the level of autophagosome-lysosome interaction.

The present study repeated and extended the experiments using the same cell line and construct to investigate the reason behind the autophagic dysfunction in terms of the subcellular localization of key autophagic regulator proteins (mTOR, raptor and LC3) and their relation with truncated PS1 localization. In this study, HEK293 cells were transfected for either 3 or 6 days, to compare the results and also to allow time for truncated PS1 to be aggregated and ensure autophagy induction.

The results show that tPS1 persisted in the cells and did not disappear over time at either three or six day experiments and this is an indication that autophagy failed to clear it. In order to study the effect of truncated PS1 on the subcellular localization of the proteins of interest (mTOR, raptor and LC3) and subsequently on the autophagic process, dual label ICC studying the relation between the subcellular localization of truncated PS1 and mTOR, raptor and LC3 localizations was performed.

5.4.1 Intracellular distribution of mTOR and truncated PS1

Intracellular distribution of truncated PS1 is very similar to the intracellular distribution of mTOR protein as seen by ICC, suggestive of co-localisation. The distribution of tPS1 and mTOR is similar to that of mitochondria, as has been demonstrated for mTOR in autophagic, HEK293 cells serum starved or treated with rapamycin, and non-autophagic HEK293 cells. The anti-mitochondrial antibody used in this study detects the surface of the mitochondria, which indicates that truncated PS1 might be co-localized with mTOR in this location.

It has been reported that PS1 modulates autophagy induction (Lee *et al.*, 2010b), which is negatively regulated by mTOR (Wullschleger *et al.*, 2006), suggesting a possible interaction between PS1 and mTOR (Caccamo *et al.*, 2011). If there is a direct or indirect interaction between tPS1 and mTOR protein, so the question is whether PS1 normally interacts with mTOR or mTORC1 during autophagy or whether this interaction occurred incorrectly due to its truncation. If PS1 is required to interact with mTORC1 during autophagy for it to proceed normally, the truncation in this experiment, or the mutations in the case of AD, may alter the normal function of PS1 during autophagy leading to the failure of the process. If the interaction happened incorrectly because of the truncation, so tPS1 may cause dysregulation of the mTOR pathway leading to impairment of autophagy.

As mentioned in chapter four, in yeast, mTOR has the ability to induce and inhibit autophagy. This autophagic induction or inhibition is through dephosphorylation of Atg13 (Mizushima, 2010; Glick *et al.*, 2010) or phosphorylation of Atg1 (Wang and Proud, 2010). Thus, it is proposed that the dysregulation of mTOR pathway by truncated PS1 may result in, for instance, phosphorylation of ATG1 leading to autophagic impairment.

However Lee *et al.* (2010b) and Neely *et al.* (2011) have shown that autophagic dysfunction was late in the pathway, at the autophagosome-lysosome fusion step. Also, before them, Anderson (2003), using electron microscopy, has shown that autophagosomes have formed and accumulated in the cytoplasm of transfected HEK293 cells. However, the autophagic process did not appear to go to completion as would be expected in the normal state, because the PS1 aggregates persisted in the cells and were not removed, and appeared to lead to cell death. Consistent with this, it has been demonstrated that PS1 deletion did not have a significant influence on the major upstream aspects of macroautophagy, including nutrient-dependent regulation of mTOR, a protein kinase-signaling pathway that uses phosphoinositide 3-kinase and protein kinase B (PI3K-AKT) (Sarbassov et al., 2005) and is modulated in part by PS2 (Kang *et al.*, 2005).

It has also been revealed that following autophagy induction in PS1 KO cells, P70S6K was normally dephosphorylated and LC3-positive punctate and autophagic vacuoles were increased. This is an indication of the ability of the cells to form autophagosomes (Lee *et al.*, 2010b). The accumulation of P62 (autophagic substrate) is also an indication that PS1 KO cells have the ability to sequester substrates despite the subsequent degradation impairment (Lee *et al.*, 2010b).

5.4.2 Intracellular distribution of raptor and truncated PS1

Similar to the mTOR protein, ICC illustrates a similarity between the intracellular distribution of raptor and tPS1-GFP construct, suggesting that raptor may interact or co-localize with the tPS1-GFP construct. The present study demonstrated that raptor localised to the cytoplasm of non-autophagic HEK 293 cells and that following autophagy induction by rapamycin treatment or by serum starvation, raptor moved from

the cytoplasm to the perinuclear area which was similar to the distribution of the mitochondria in these cells.

In this study, it was suggested that mTOR localised to the surface of the mitochondria in HEK293, and upon autophagy induction, mTOR remained localized to the mitochondria but raptor has moved from the cytoplasm to be abundant on the mitochondria and join mTOR to form the mTORC1. Based on this, one can suggest that tPS1 may interact with raptor in the cytoplasm first and then they move together to the perinuclear region. The other suggestions are that: tPS1 has co-localized with raptor on the mTORC1, or tPS1 has co-localized with mTOR and not raptor on the mTORC1 (or vice versa) and this is the reason to observe it co-localized with mTOR and raptor at the same time. If the interaction between tPS1 and raptor is true, how can this affect the autophagic process?

Previous studies indicate that raptor may have roles in mediating mTORC1 assembly, recruiting substrates, and regulating mTORC1 activity and subcellular localization (Hara *et al.*, 2002; Kim *et al.*, 2002; Sancak *et al.*, 2008). The strength of the interaction between mTOR and raptor can be modified by nutrients and other signals that regulate the mTORC1 pathway, but how this translates into regulation of the mTORC1 pathway remains elusive (Yip *et al.*, 2010). See also (chapter four: section 4.4.2).

If the PS1 plays a role in normal autophagy via its interaction with raptor, then the truncation of PS1 as in this experiment or the PS1 mutations in the case of FAD may alter or destroy the required normal function of PS1 leading to autophagic impairment. While the abnormal interaction between raptor and tPS1 caused by the protein truncation or mutations, may result in interruption of one of the normal raptor functions. For instance, this abnormal interaction may lead to prevention of mTORC1 assembly or

block substrate recruitment to be phosphorylated or dephosphorylated by mTOR, causing an mTOR pathway dysregulation and subsequently autophagic failure.

However, the formation of phagophore membrane and autophagosomes as proved by Lee *et al.* (2010b) and Neely *et al.* (2011), and also showed by Anderson (2003) gives an indication that there is no defect in the initiation of autophagy. Since mTORC1 is responsible for the initiation of autophagy through mTOR inhibition, it can be suggested that the mTORC1 is not affected by the interaction between tPS1 and raptor, unless this interaction may stimulate another raptor pathway that would stop autophagy late at the fusion step.

5.4.3 Intracellular distribution of LC3 and truncated PS1

Autophagy induced by tPS1-GFP construct in HEK293 cells and the behaviour of endogenous LC3 under the influence of tPS1 during autophagy was investigated. By utilizing fluorescence and confocal microscopy, ICC demonstrated that LC3 changed its subcellular localization and had a similar subcellular localization to truncated PS1. In chapter four, the results showed that in non-autophagic HEK293 cells, it seems that LC3 was localized to the Golgi apparatus and upon autophagy induction by rapamycin treatment or serum starvation, some of the protein diffused in the cytoplasm, while the larger part remained localized to the Golgi apparatus. In comparison, after autophagy induction by tPS1, it's clear from the images that the larger part of the endogenous LC3 was in the cytoplasm and has a similar distribution as tPS1 giving an indication that this might be an interaction between the two proteins upon autophagy induction.

If this interaction between the proteins is true, then does tPS1 move towards the Golgi apparatus first and interact with LC3 and upon autophagy induction they moved together back to the cytoplasm, or has truncated PS1 remained in the cytoplasm or on other cellular organelles, and then LC3 diffused to interact with it and as a result of this

diffusion a new subcellular localization of LC3 was observed. In the present study, because of the limitations in time and resources, it was not possible to view live images of HEK293 cells during transfection. This might have shown the movement of the tPS1 inside the cell.

LC3 is an ubiquitin-like protein that is the mammalian homologue of the autophagy-related Atg8 encoded product in yeast (Kabeya *et al.*, 2000; He *et al.*, 2003). After translation, the unprocessed LC3 is cleaved by Atg4 protease to produce LC3-I form, with a carboxy terminal exposed glycine. Following autophagy induction, the uncovered glycine of LC3-I is conjugated by Atg7, Atg3 and Atg12-Atg5-Atg16 multimers to the highly lipophilic PE moiety to produce LC3-II (Mizushima, 2007; Nakatogawa *et al.*, 2009). The PE group is crucial for the integration of LC3-II into lipid membranes at the phagophore and autophagosomes (Barth *et al.*, 2010). It has been demonstrated that LC3 at the autophagosome plays a role in selecting cargo for degradation. For example; interaction of LC3-II with p62/SQTM1 targets associated protein aggregates for turnover (Pankiv *et al.*, 2007). In addition, it has been reported that LC3 plays an important role in promoting membrane tethering and fusion *in vitro* (Nakatogawa *et al.*, 2007). Based on this, there is the possibility for LC3 plays a role in fusion of autophagosomes with other membrane compartments such as endosomes (Barth *et al.*, 2010).

Based on LC3 function, if the interaction between tPS1 and LC3 is true, this interaction may interrupt the normal function of LC3 leading to autophagic failure. One of the functions of LC3 is to select a cargo for degradation, so when LC3 moved to interact with the cargo to drive it to autophagy, because of the truncation of PS1 in this study, or the mutations of the protein in the AD, this interaction may occurs incorrectly and prevents LC3 protein from fulfilling its normal role in the autophagy process.

Intriguingly, it has been shown that PS1 has a role to play in autophagy at the level of autophagosome-lysosome interaction or lysosome function (Neely *et al.*, 2011). In addition, Lee *et al.* (2010b) and Neely *et al.* (2011) have reported that the autophagic dysfunction is late in the pathway, at the autophagosome-lysosome fusion step. Moreover, LC3 has been proved to play a role in tethering and fusion (Nakatogawa, *et al.*, 2007). Taken together, these results suggest that the interaction between LC3 and the tPS1 may be implicated in the observed autophagic dysfunction.

Nakatogawa *et al.* (2007) used liposomes containing PE incubated with purified Atg7, Atg3 and Atg8 in the presence of ATP and reported that Atg8-PE was efficiently formed. Interestingly, the group demonstrated that aggregates were generated during the production of Atg8-PE and the size of the aggregates appeared to correlate with the amount of Atg8-PE produced. They suggested that these aggregates were clusters of liposomes. After performing some confirmation experiments, they suggested that Atg8-PE molecules function to tether membranes to which they are anchored. Based on these results, one can suggest that the interruption of the lipidation process by tPS1 may have an influence on both: the autophagosome formation and autophagosome-lysosome fusion, as the same group have also found that not only tethering but also fusion of the liposomes was mediated by Atg8-PE.

It has been reported that fusion proceeds via an intermediate state known as hemifusion, in which outer leaflets of two opposed lipid bilayers merge, while inner leaflets remain intact (Chernomordik and Kozlov, 2005). A study revealed that membrane fusion mediated by Atg8-PE is hemifusion and not complete fusion (Nakatogawa *et al.*, 2007). It was also reported by the same group that fusion can be arrested or delayed at the hemifusion state under some conditions. Therefore, it can be suggested that the interaction between tPS1 and LC3 has an undesirable effect on the hemifusion step in the autophagy process.

Nakatogawa *et al.* (2007) have also reported that Atg8 forms a multimer in response to the conjugation with PE. They used immunoelectron microscopy to study liposomes that were clustered by Atg8-PE and demonstrated that Atg8-PE tends to be enriched at the junction between the liposomes. They incubated the same mixture but without ATP. By using the same analytical technique, they realized that the previous observation had disappeared. The group concluded that Atg8-PE is directly involved in the tethering and hemifusion of liposomes. In the same study, the researchers have observed that naked liposomes do not associate with liposomes carrying Atg8-PE, and they suggested that tethering could be achieved by interactions between Atg8-PE molecules on different membranes. Based on this information, if the observed interaction between tPS1 and LC3 in the present study is true, this interaction may interrupt the lipidation step and prevent multimerization or this interaction may block the association between two Atg8-PE molecules on different membranes leading in both cases to prevention of the tethering and fusion steps and subsequently to autophagic failure.

5.5 CONCLUSION

Based on ICC images obtained in this study, it appears that there is an interaction between truncated PS1 and mTOR, raptor and LC3 proteins. If these interactions are true, this suggests that these interactions may be involved in the disruption of the autophagic process in neurodegenerative diseases. The interaction between mTOR and truncated PS1 may dysregulate the mTOR signalling pathway, the interaction between raptor and truncated PS1 may prevent mTORC1 assembly or stop mTOR substrate recruitment and the interaction between LC3 and truncated PS1 may prevent the lipidation process between LC3 and PE or block the connection between two LC3-PE molecules on the membranes of the autophagosome and lysosome and prevent thier fusion. In fact, the most important observation from the present study is the interaction between LC3 and PS1. As previously reported, many studies have revealed that the

defect in the autophagic process occurred late in the pathway at the fusion step. In addition, it has also been reported that PS1 is required in the late autophagic stages, and LC3-PE (LC3-II) was observed to play an important role in tethering and fusion of liposomes. Therefore, the interaction between tPS1 and LC3 should be taken into consideration. It has been reported that the lipidation process between LC3-I and PE is ATP-dependent. So, one can suggest that upon autophagy induction, lipidation process may occur on the mitochondria. So, based on the observation in the present study which suggested that upon autophagy induction, mTOR and raptor might be localized to mitochondria. This may explain why mTOR, raptor and LC3 were observed co-localised with tPS1 in the same location on the surface of the mitochondria.

Chapter 6

Effect of Rapamycin or Serum Starvation on localisation of Truncated PS1-GFP or mTOR, Raptor and LC3

6.1 INTRODUCTION

In the present study, the subcellular localisation of mTOR, raptor and LC3 proteins were investigated in non-autophagic HEK293 cells. Then, the cells were serum starved or treated with rapamycin to induce autophagy and investigate whether the behaviour and subcellular localisation of these proteins have changed during autophagy. The ICC results have shown that the intracellular location of raptor and LC3 proteins has changed, while no change has been observed with mTOR protein. After that, HEK293 cells were transiently transfected with tPS1-GFP construct to induce autophagy (Anderson, 2003), and to study the influence of tPS1 on the behaviour of the proteins of interest. The immunofluoresence and confocal microscopes images have demonstrated that an interaction might occur between the tPS1 and mTOR, raptor and LC3 proteins. However, if the interaction is true, it was difficult to confirm the place where these proteins have interacted. The interaction might be occurring on the mitochondria because mTOR was localized to mitochondria in autophagic and non-autophagic HEK293 cells, while the other two proteins were moved toward the perinuclear area upon autophagy induction.

After the transfection experiment, a question arises: is the tPS1 transfection in this experiment enough to induce autophagy? To overcome this concern, in this chapter, HEK293 cells were serum starved or treated with rapamycin after the transfection to be sure that autophagy has induced. The other purpose from this experiment is to study the effect of serum starvation and rapamycin treatment on the subcellular localization of the truncated PS1 and mTOR, raptor and LC3 proteins after the transfection. In addition, to perform further investigations such as cellular fractionation, transfected HEK293 cells were sorted by a flow cytometer. However, for some reasons, it was not possible to obtain sufficient sorted cells for further experiments.

6.2 MATERIAL AND METHODS

6.2.1 HEK293 cells transfection, rapamycin treatment and starvation:

HEK293 cells were cultured on cover slips in 24-well plates. Then, the cells were transfected with tPS1 (see section 2.10.1). After that, the cells were treated with three different concentrations of rapamycin (50, 200 and 500 nM) for 16 hours. The concentration of DMSO (rapamycin solvent) was 0.05% at all three rapamycin concentrations. The cells were treated in the same way as reported in chapter 4: section 4.2.2. The cells were serum starved after transfection in serum free EMEM media (Lonza, UK) for 24 hours as described in section 4.2.3.

6.2.2 Immunocytochemistry:

The HEK293 cells were fixed by cold methanol and the rest of the experiment was performed exactly as reported in section 2.7.1.

6.2.3 Flow cytometry and fluorescence activated cell sorting (FACS):

Transiently transfected HEK293 cells were sorted by a flow cytometer in the Medical School at the University of Sheffield. HEK293 cells were cultured in EMEM complete media using T25 flask and left in the incubator at 37 °C to be confluent. Then, the complete media was removed and replaced with antibiotics free media and the cells transfected with truncated PS1 at ratio 3:1 (3 µl transfection reagent: 1µg DNA) according to the protocol provided by Roche company. The cells were left for 24 hours and then the transfection reagent containing media was removed and replaced by complete media for cells recovery. The transfected cells were left for another 24 hours in the complete media and then the flask was taken to the flow cytometry staff in Sheffield University and the transfected cells were sorted by flow cytometer and FACS machine (BD FACSAriaTM llu, BD FACSAriaTM Cell Sorter) and collected.

6.3 RESULTS

HEK293 cells were transfected with tPS1-GFP and then treated with three different concentrations (50, 200 and 500 nM) of rapamycin for 16 hours. ICC was performed to investigate the subcellular localisations of tPS1-GFP, mTOR, raptor and LC3 for each rapamycin concentration. The dual label ICC images for mTOR and tPS1-GFP show the same results as observed in the previous chapter. Rapamycin treatment of the cells after transfection had no effect on the subcellular localisation of tPS1 when compared with the previous results (chapter 5). ICC demonstrated that tPS1 still persisted in the cell and might be interacting with mTOR in a distribution similar to the distribution of the mitochondria (Figures 6.1, 6.2 and 6.3). However, mTOR staining was not completely co-localized with the tPS1 and this is observed clearly in figures (6.1, 6.2 and 6.3). In addition, the result revealed that there was no difference observed between the three rapamycin concentrations used in the experiment.

In regard to raptor, the result also revealed that rapamycin treatment after transfection had no effect on the expression of either tPS1 or raptor protein, as observed in chapter 5. An interaction between truncated PS1 and raptor might be occurred during autophagy (Figures 6.4, 6.5 and 6.6). However, some raptor staining present in the perinuclear region was not co-localized with tPS1 staining. Also, the three different rapamycin concentrations have produced the same results. In the case of LC3A/B result, no change has been observed in the subcellular localisations of tPS1 and LC3 when HEK293 cells treated with rapamycin after the transfection.

As observed in chapter 5, the majority of the LC3 staining moved from the Golgi apparatus to interact with tPS1 in the same subcellular distribution, whilst a small portion of the LC3 protein remained localized to the Golgi apparatus. In addition, there were some small tPS1 bulbs not co-localized with the LC3 protein. The same result was

observed under the influence of the different rapamycin concentrations (Figures 6.7, 6.8 and 6.9).

HEK293 cells were serum starved after transfection in serum-free media for 24 hours. Then, dual label ICC was performed to investigate the influence of starvation on the expression of tPS1 and on the subcellular localizations of mTOR, raptor and LC3 after transfection. The obtained immunofluorescence images revealed that starvation had no effect on the subcellular localization of tPS1. The result was the same as what has been observed in chapter 5. It seems that tPS1 might be interacting with mTOR, raptor and LC3 upon autophagy induction.

However, in the case of mTOR staining, some small tPS1 bulb staining was not co-localized with mTOR protein, and also, some mTOR stained spots were not co-localized with tPS1. In regard to raptor, the perinuclear raptor spots were not co-localized with tPS1, and also, the small bulbs of tPS1 were not co-localized with the raptor protein. The majority of LC3 protein moved from the Golgi apparatus and co-localized with tPS1. However, some small bulbs of tPS1 were not co-localized with LC3 protein (Figures 6.10, 6.11 and 6.12).

Transient transfection produces a mixture of transfected and non-transfected cells. In the present study, to perform further investigation such as cellular fractionation using transiently transfected cells only, transfected HEK293 cells were sorted by flow cytometry at the University of Sheffield. The cells were sorted more than five times in order to obtain pure, live and uncontaminated transfected cells. But, it was difficult to handle the sorted cells. In the first attempts, after the sorting process, the cells were re-cultured in complete media, but, the cells did not attached to the bottom of the flasks and then died within 24 hrs. After that, the plan was to deal immediately with the sorted

transfected HEK293 cells, but this time the cells had bacterial contamination after the sorting process.

Figures (6.13A, 6.13B and 6.13C) show the graphs of the last attempt of the sorting process. In this case, immediately after the sorting process, the cells were poured into a well of a 6-well plate and pictures were taken using an inverted microscope (Olympus, IX2-UCB) to be sure that the well contained transfected cells only (Figure 6.14a and 6.14b). However, it was not possible to obtain sufficient sorted cells for further experiments.

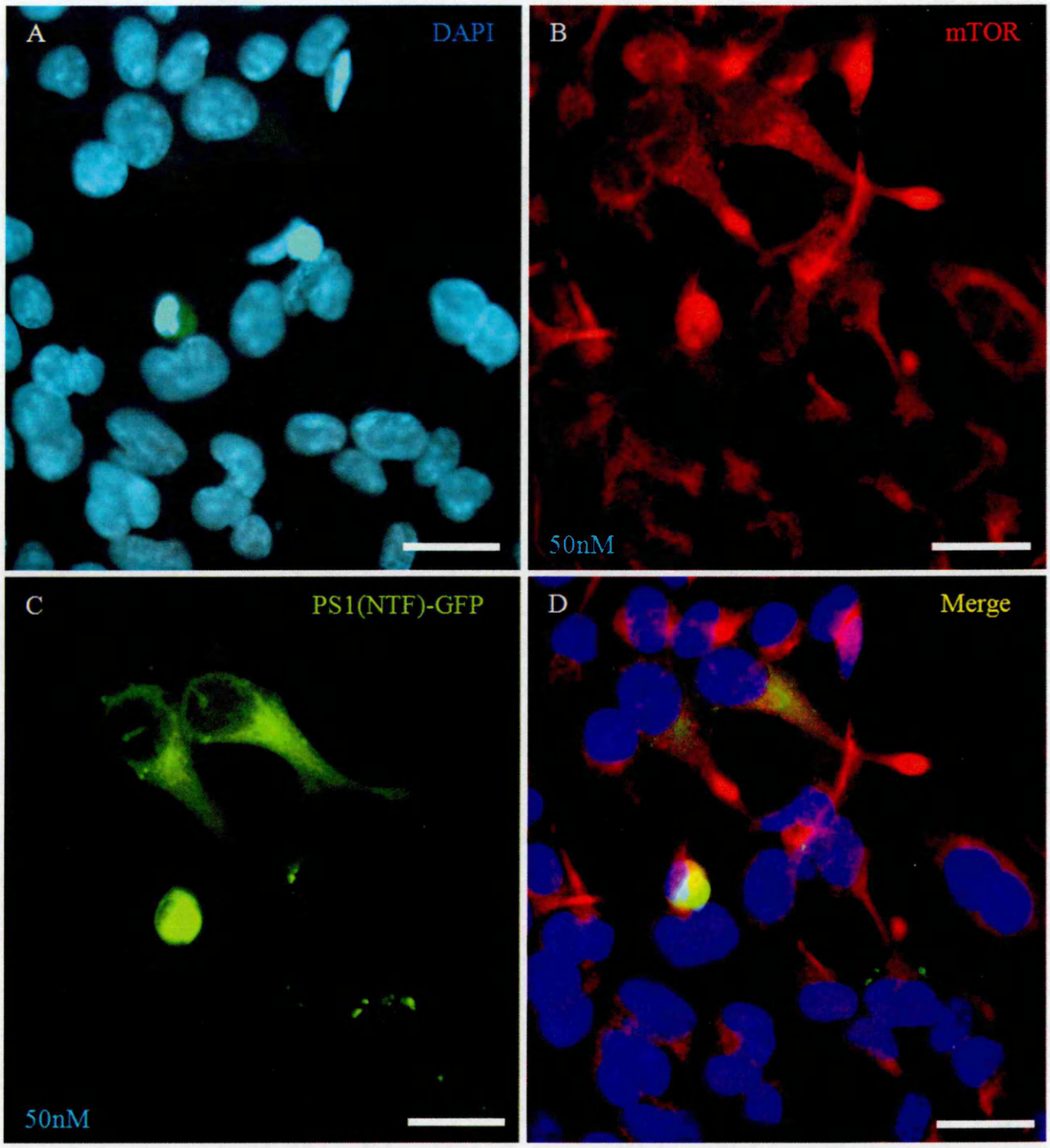

Figure 6.1 Dual label immunofluorescence for mTOR and PS1 (NTF)-GFP in transiently transfected HEK293 cells after 50nM rapamycin treatment for 16 hrs. Cells were transiently transfected with PS1(NTF)-GFP first and then treated with 50 nM rapamycin for 16 hrs and then fixed in cooled methanol and labelled for (A) Nuclei were counterstained with DAPI (B) mTOR using primary monoclonal rabbit anti-human mTOR antibody (Millipore, 04-385) and secondary antibody Alexa fluor 594 donkey anti-rabbit IgG (C) Green fluorescence of GFP conjugated to PS1 (NTF) (D) Merge. Scale bar: 10μm

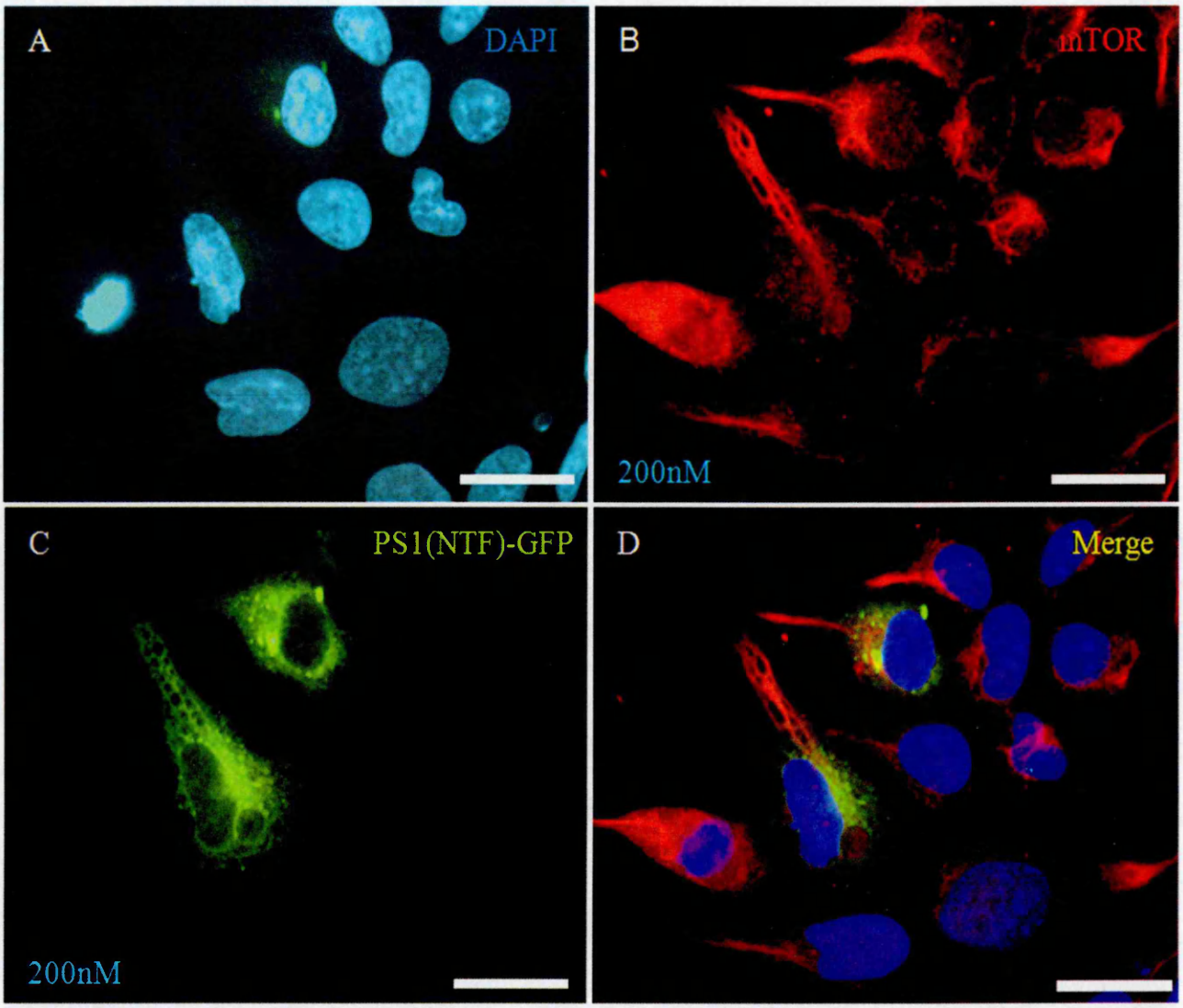

Figure 6.2 Dual label immunofluorescence for mTOR and PS1 (NTF)-GFP in transiently transfected HEK293 cells after 200nM rapamycin treatment for 16 hrs. Cells were transiently transfected with PS1 (NTF)-GFP first and then treated with 200 nM rapamycin for 16 hrs and then fixed in cooled methanol and labelled for (A) Nuclei were counterstained with DAPI (B) mTOR using primary monoclonal rabbit anti-human mTOR antibody (Millipore, 04-385) and secondary antibody Alexa fluor 594 donkey anti-rabbit IgG (C) Green fluorescence of GFP conjugated to PS1 (NTF) (D) Merge. Scale bar: 10μm

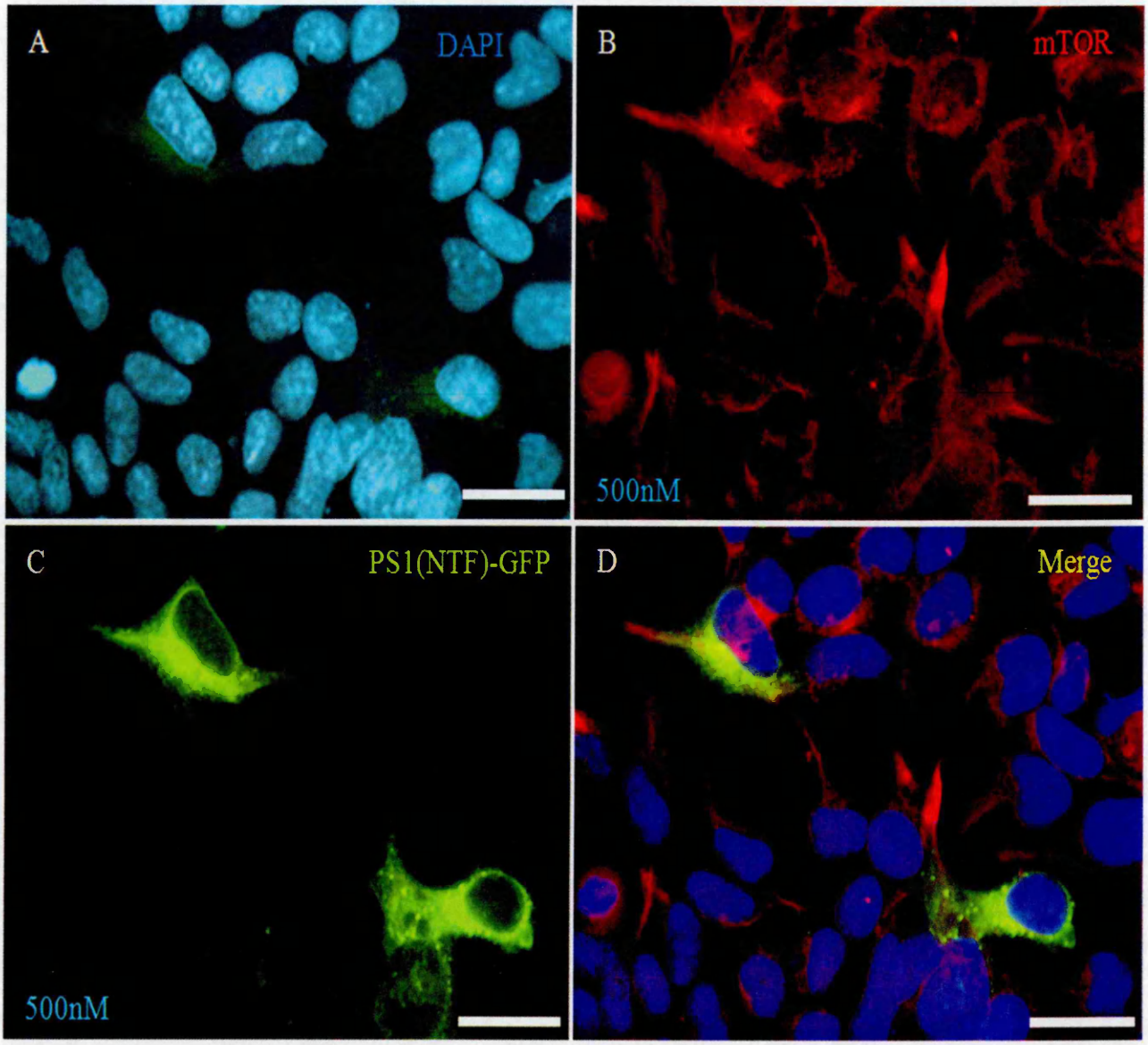

Figure 6.3 Dual label immunofluorescence for mTOR and PS1 (NTF)-GFP in transiently transfected HEK293 cells after 500nM rapamycin treatment for 16 hrs. Cells were transiently transfected with PS1 (NTF)-GFP first and then treated with 500 nM rapamycin for 16 hrs and then fixed in cooled methanol and labelled for (A) Nuclei were counterstained with DAPI (B) mTOR using primary monoclonal rabbit anti-human mTOR antibody (Millipore, 04-385) and secondary antibody Alexa fluor 594 donkey anti-rabbit IgG (C) Green fluorescence of GFP conjugated to PS1 (NTF) (D) Merge. Scale bar: 10μm

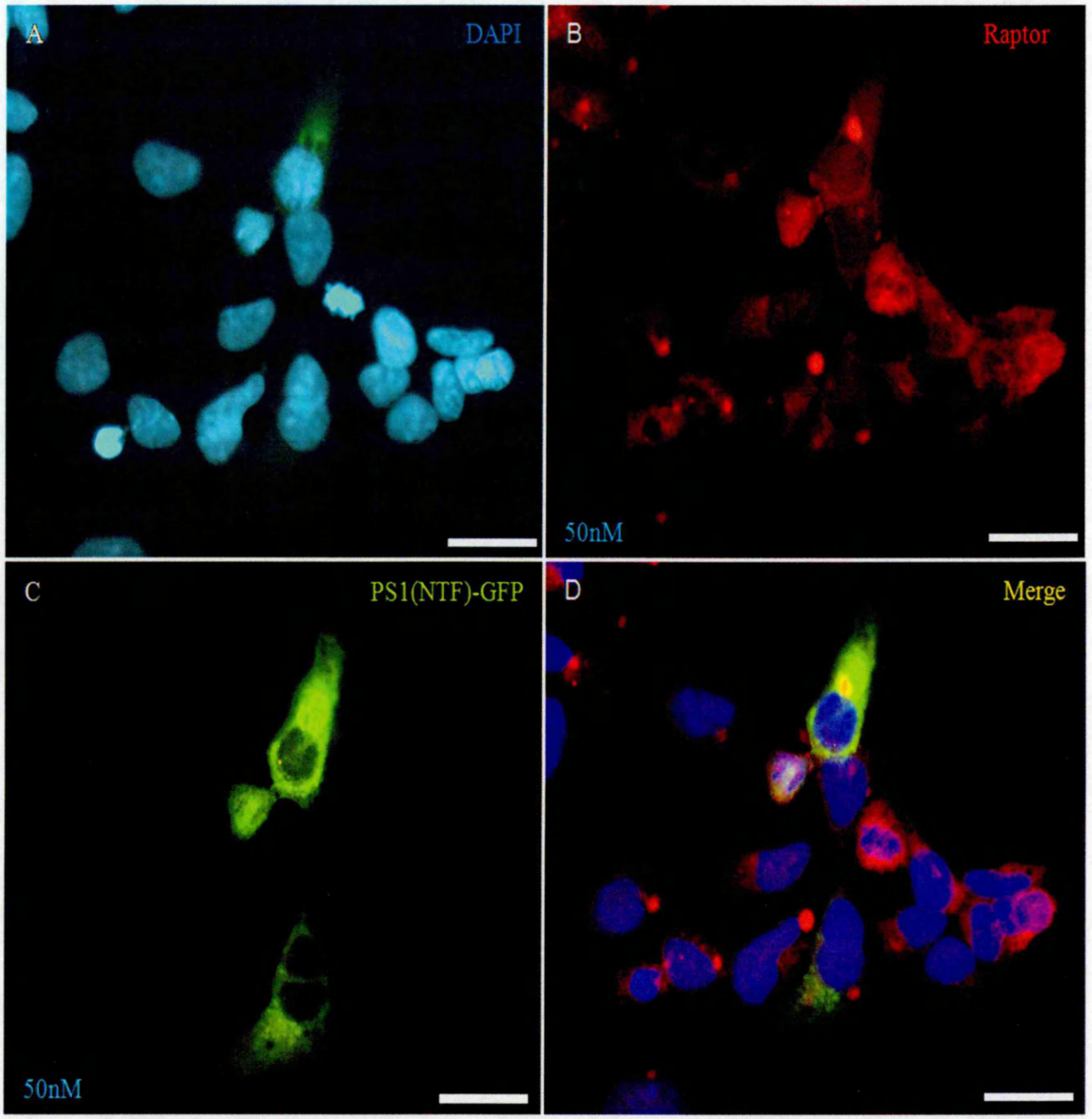

Figure 6.4 Dual label immunofluorescence for raptor and PS1 (NTF)-GFP in transiently transfected HEK293 cells after 50nM rapamycin treatment for 16 hrs. Cells were transiently transfected with PS1 (NTF)-GFP first and then treated with 50 nM rapamycin for 16 hrs and then fixed in cooled methanol and labelled for (A) Nuclei were counterstained with DAPI (B) raptor using primary monoclonal rabbit anti-human raptor antibody (CellSignaling Technology, 2280) and secondary antibody Alexa fluor 594 donkey anti-rabbit IgG (C) Green fluorescence of GFP conjugated to PS1 (NTF) (D) Merge. Scale bar: 10μm

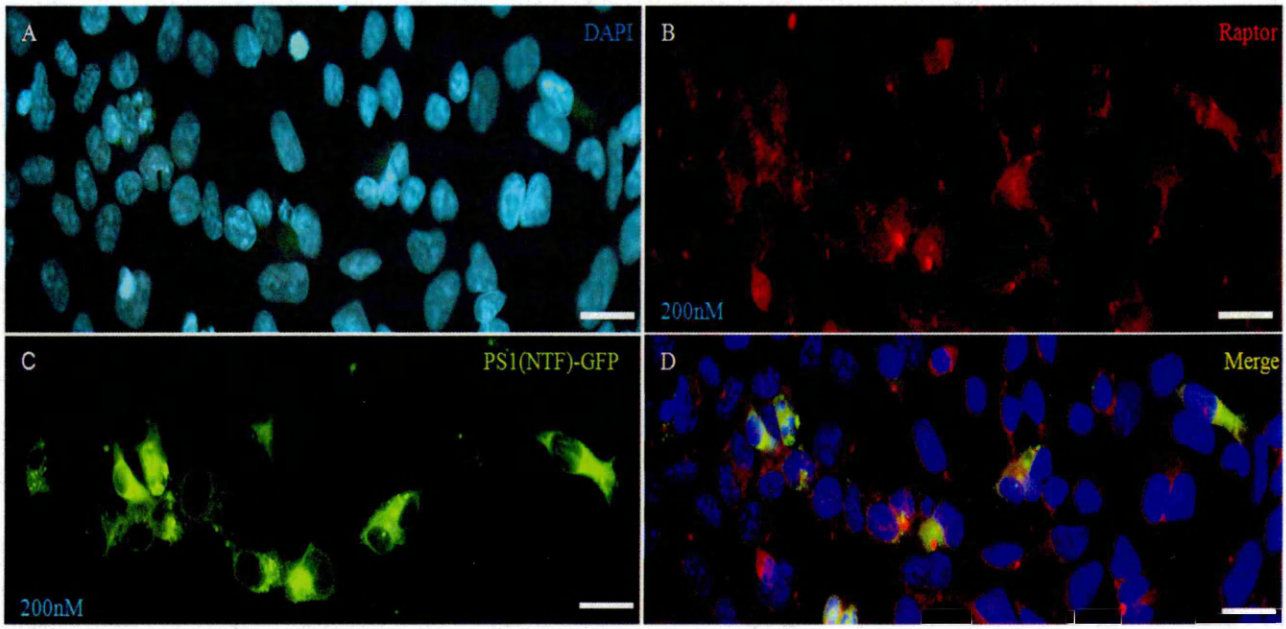

Figure 6.5 Dual label immunofluorescence for raptor and PS1 (NTF)-GFP in transiently transfected HEK293 cells after 200nM rapamycin treatment for 16 hrs. Cells were transiently transfected with PS1(NTF)-GFP first and then treated with 200 nM rapamycin for 16 hrs and then fixed in cooled methanol and labelled for (A) Nuclei were counterstained with DAPI (B) raptor using primary monoclonal rabbit anti-human raptor antibody (CellSignaling Technology, 2280) and secondary antibody Alexa fluor 594 donkey anti-rabbit IgG (C) Green fluorescence of GFP conjugated to PS1 (NTF) (D) Merge. Scale bar: 10μm

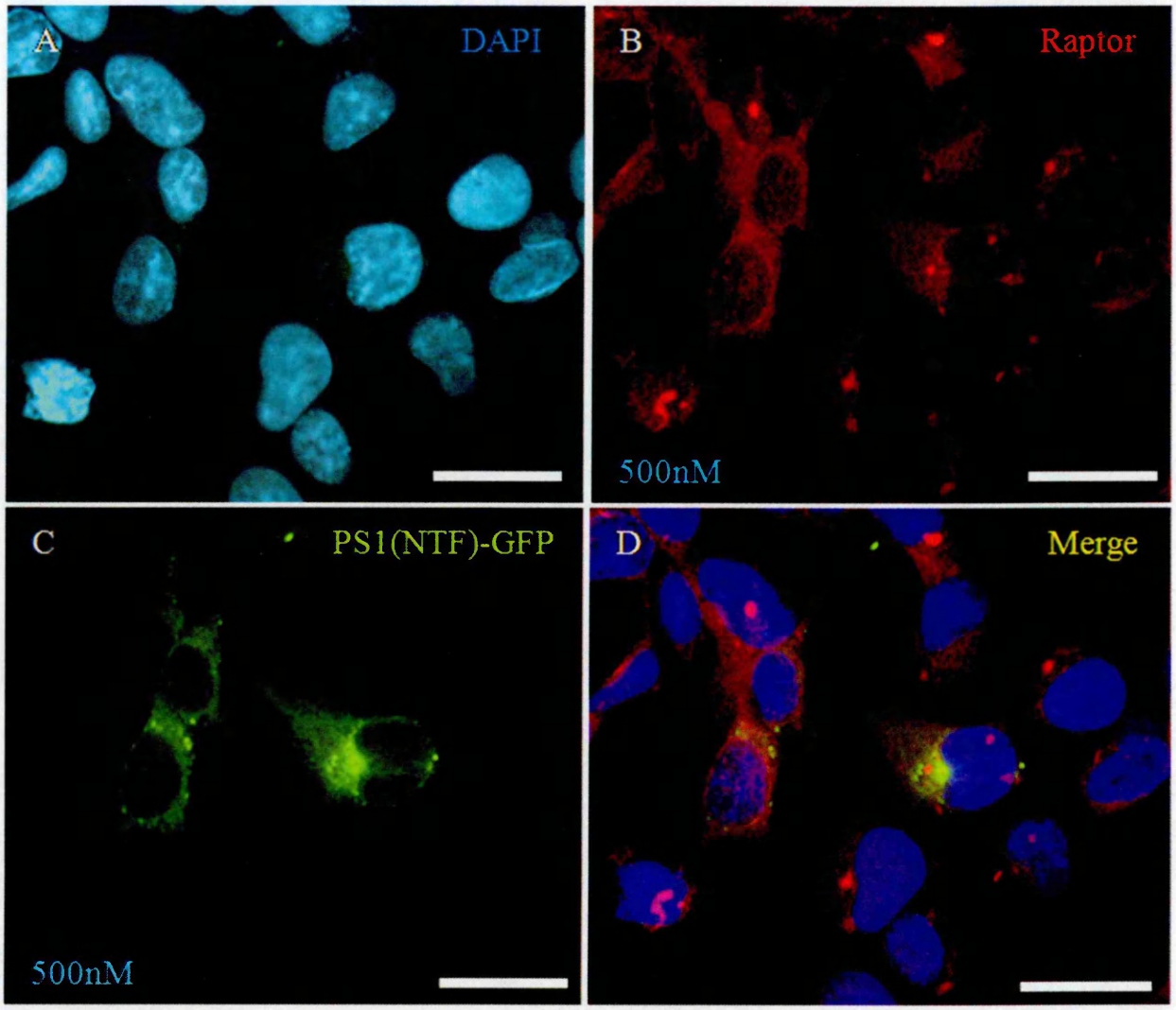

Figure 6.6 Dual label immunofluorescence for raptor and PS1 (NTF)-GFP in transiently transfected HEK293 cells after 500nM rapamycin treatment for 16 hrs. Cells were transiently transfected with PS1(NTF)-GFP first and then treated with 500 nM rapamycin for 16 hrs and then fixed in cooled methanol and labelled for (A) Nuclei were counterstained with DAPI (B) raptor using primary monoclonal rabbit anti-human raptor antibody (CellSignaling Technology, 2280) and secondary antibody Alexa fluor 594 donkey anti-rabbit IgG (C) Green fluorescence of GFP conjugated to PS1 (NTF) (D) Merge. Scale bar: 10μm

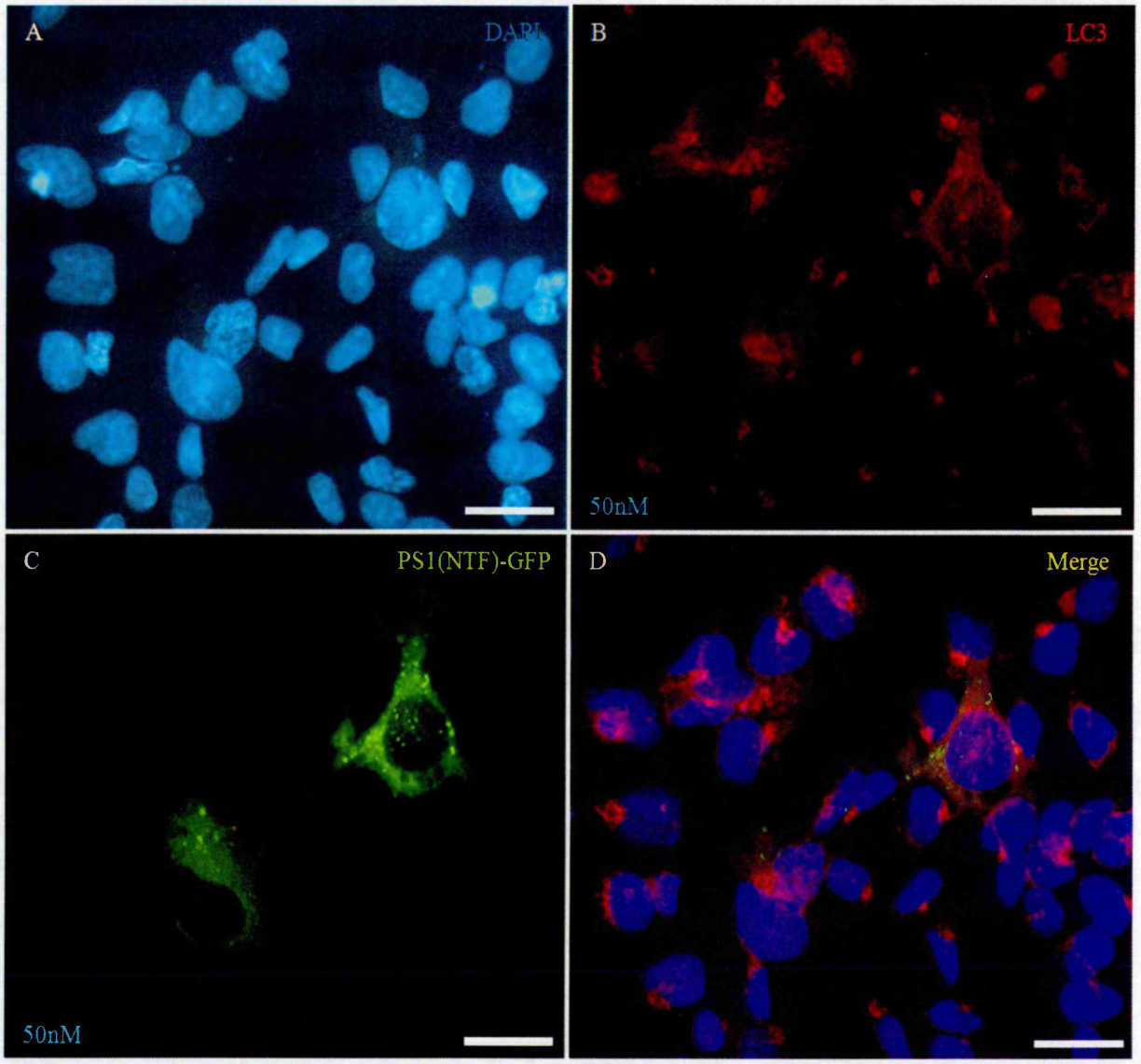

Figure 6.7 Dual label immunofluorescence for LC3 and PS1 (NTF)-GFP in transiently transfected HEK293 cells after 50nM rapamycin treatment for 16 hrs. Cells were transiently transfected with PS1(NTF)-GFP first and then treated with 50 nM rapamycin for 16 hrs and then fixed in cooled methanol and labelled for (A) Nuclei were counterstained with DAPI (B) LC3 using primary monoclonal rabbit anti-human LC3A/B antibody (Millipore, MABC176) and secondary antibody Alexa fluor 594 donkey anti-rabbit IgG (C) Green fluorescence of GFP conjugated to PS1 (NTF) (D) Merge. Scale bar: 10μm

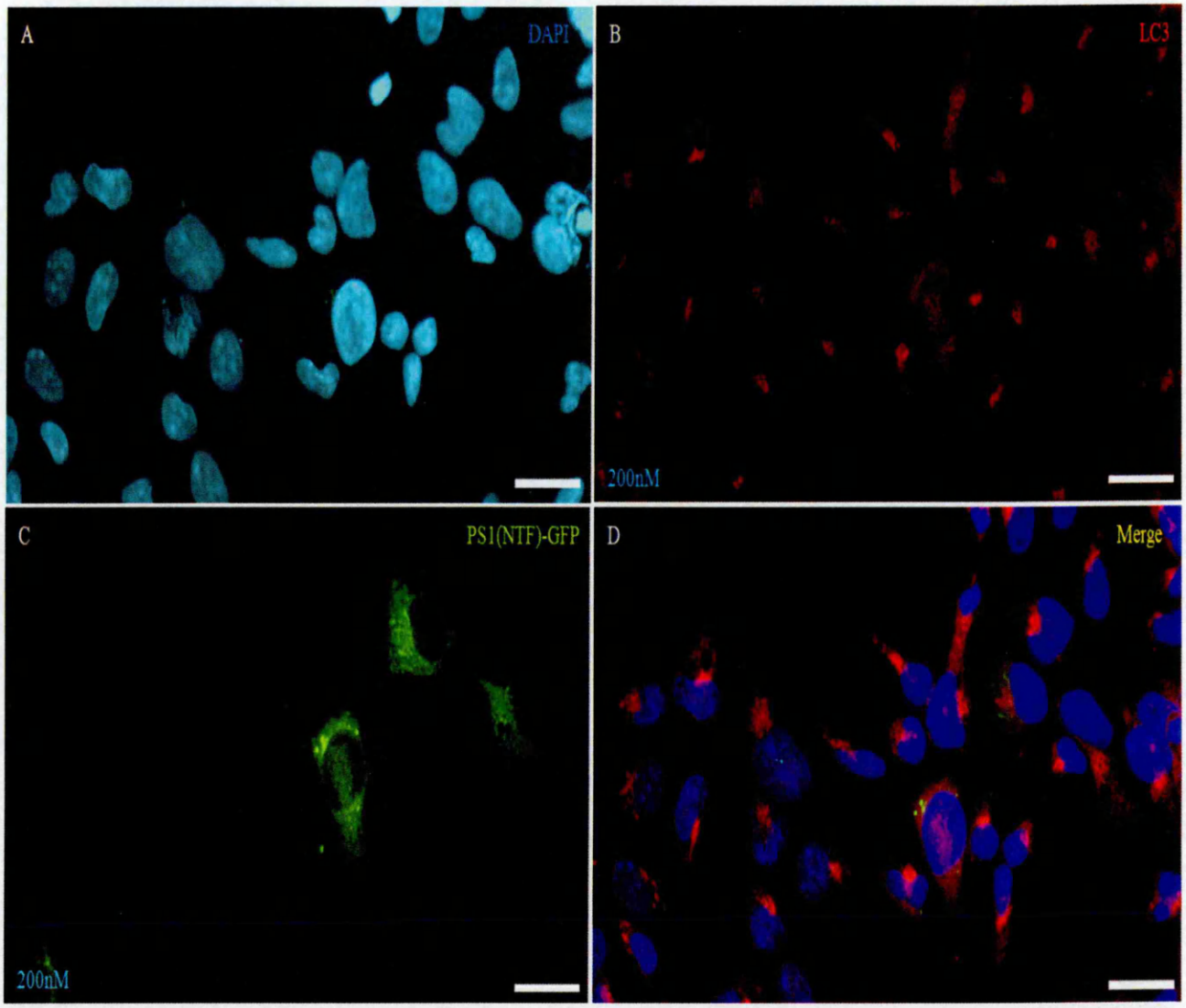

Figure 6.8 Dual label immunofluorescence for LC3 and PS1 (NTF)-GFP in transiently transfected HEK293 cells after 200nM rapamycin treatment for 16 hrs. Cells were transiently transfected with PS1(NTF)-GFP first and then treated with 200 nM rapamycin for 16 hrs and then fixed in cooled methanol and labelled for (A) Nuclei were counterstained with DAPI (B) LC3 using primary monoclonal rabbit anti-human LC3A/B antibody (Millipore, MABC176) and secondary antibody Alexa fluor 594 donkey anti-rabbit IgG (C) Green fluorescence of GFP conjugated to PS1 (NTF) (D) Merge. Scale bar: 10μm

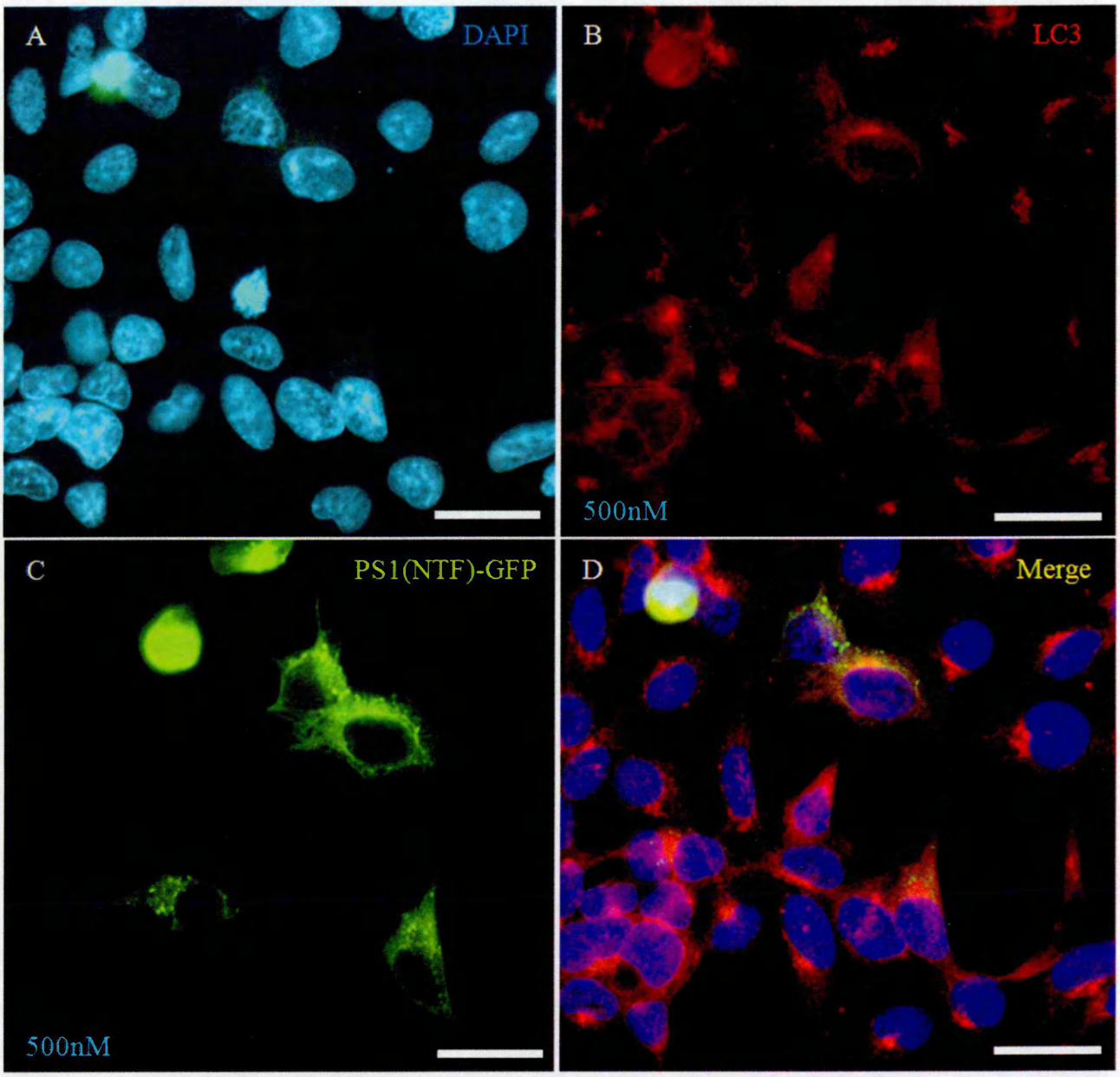

Figure 6.9 Dual label immunofluorescence for LC3 and PS1 (NTF)-GFP in transiently transfected HEK293 cells after 500nM rapamycin treatment for 16 hrs. Cells were transiently transfected with PS1(NTF)-GFP first and then treated with 500 nM rapamycin for 16 hrs and then fixed in cooled methanol and labelled for (A) Nuclei were counterstained with DAPI (B) LC3 using primary monoclonal rabbit anti-human LC3A/B antibody (Millipore, MABC176) and secondary antibody Alexa fluor 594 donkey anti-rabbit IgG (C) Green fluorescence of GFP conjugated to PS1 (NTF) (D) Merge. Scale bar: 10μm

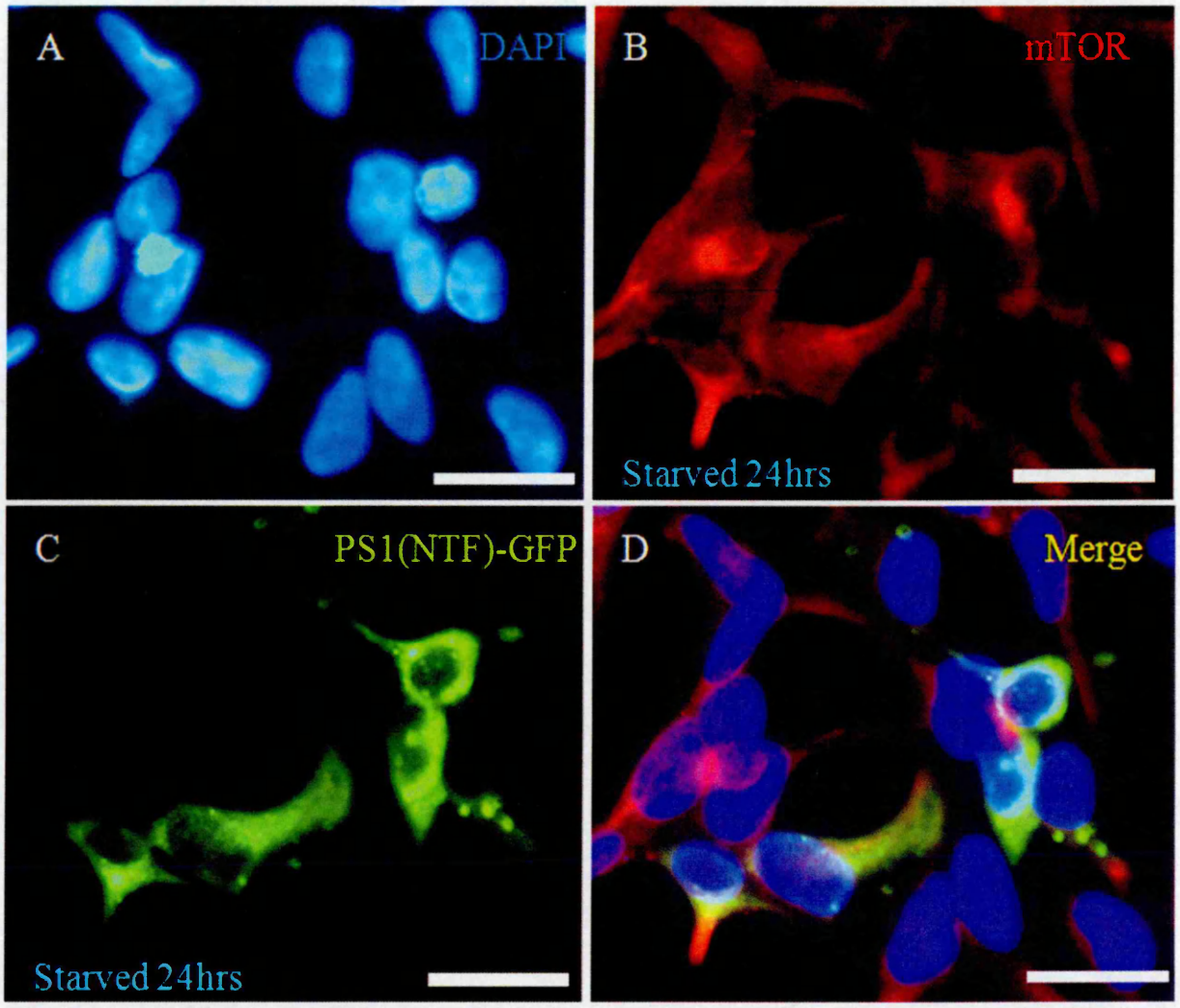

Figure 6.10 Dual label immunofluorescence for mTOR and PS1 (NTF)-GFP in transiently transfected HEK293 cells after serum starvation for 24 hrs. Cells were transiently transfected with PS1(NTF)-GFP first and then starved in serum free media for 24 hrs, and then fixed in cooled methanol and labelled for (A) Nuclei were counterstained with DAPI (B) mTOR using primary monoclonal rabbit anti-human mTOR antibody (Millipore, 04-385) and secondary antibody Alexa fluor 594 donkey anti-rabbit IgG (C) Green fluorescence of GFP conjugated to PS1 (NTF) (D) Merge. Scale bar: 10μm

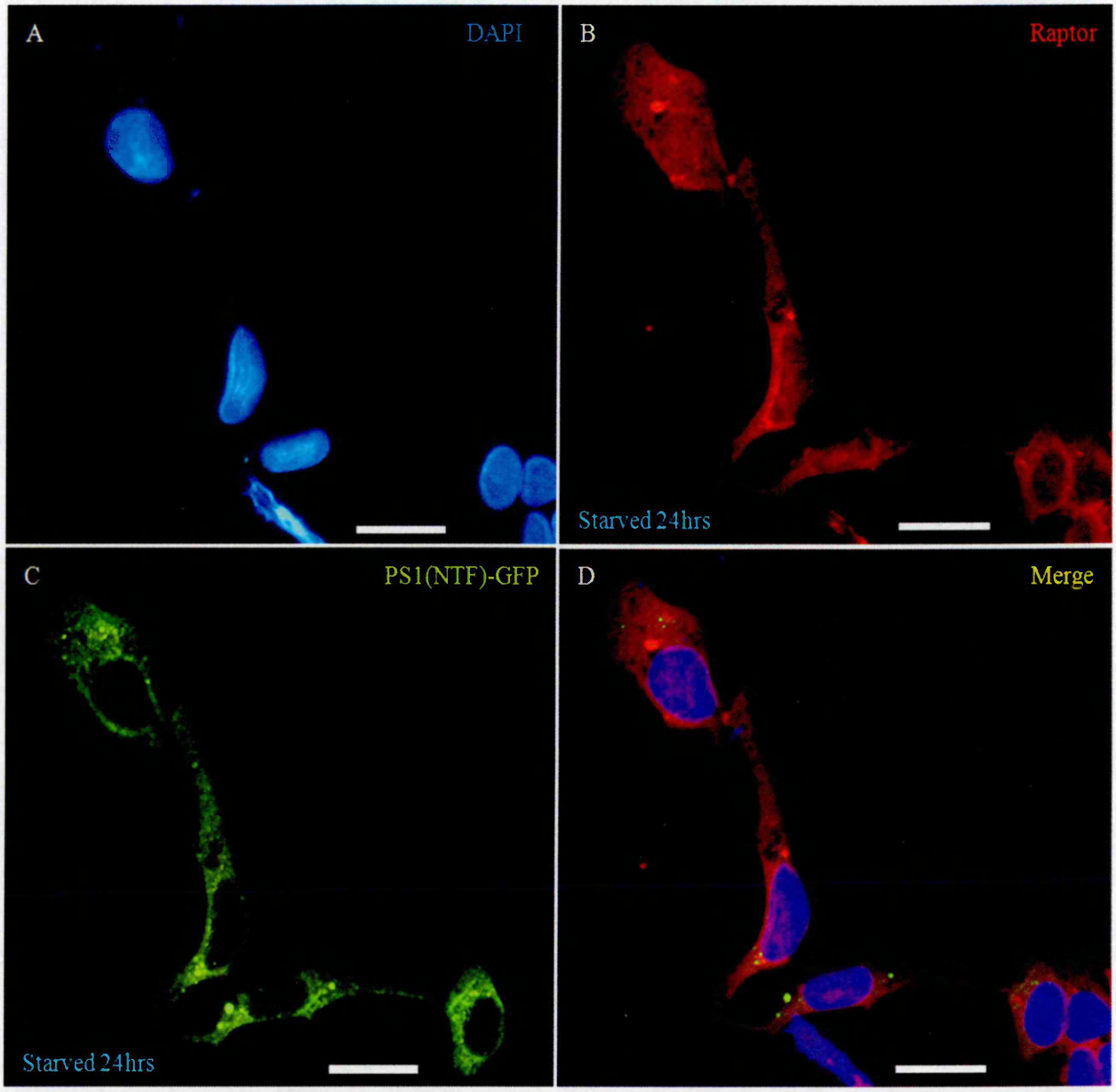

Figure 6.11 Dual label immunofluorescence for raptor and PS1 (NTF)-GFP in transiently transfected HEK293 cells after serum starvation for 24 hrs. Cells were transiently transfected with PS1(NTF)-GFP first and then starved in serum free media for 24 hrs, and then fixed in cooled methanol and labelled for (A) Nuclei were counterstained with DAPI (B) raptor using primary monoclonal rabbit anti-human raptor antibody (CellSignaling Technology, 2280) and secondary antibody Alexa fluor 594 donkey anti-rabbit IgG (C) Green fluorescence of GFP conjugated to PS1 (NTF) (D) Merge. Scale bar: 10μm

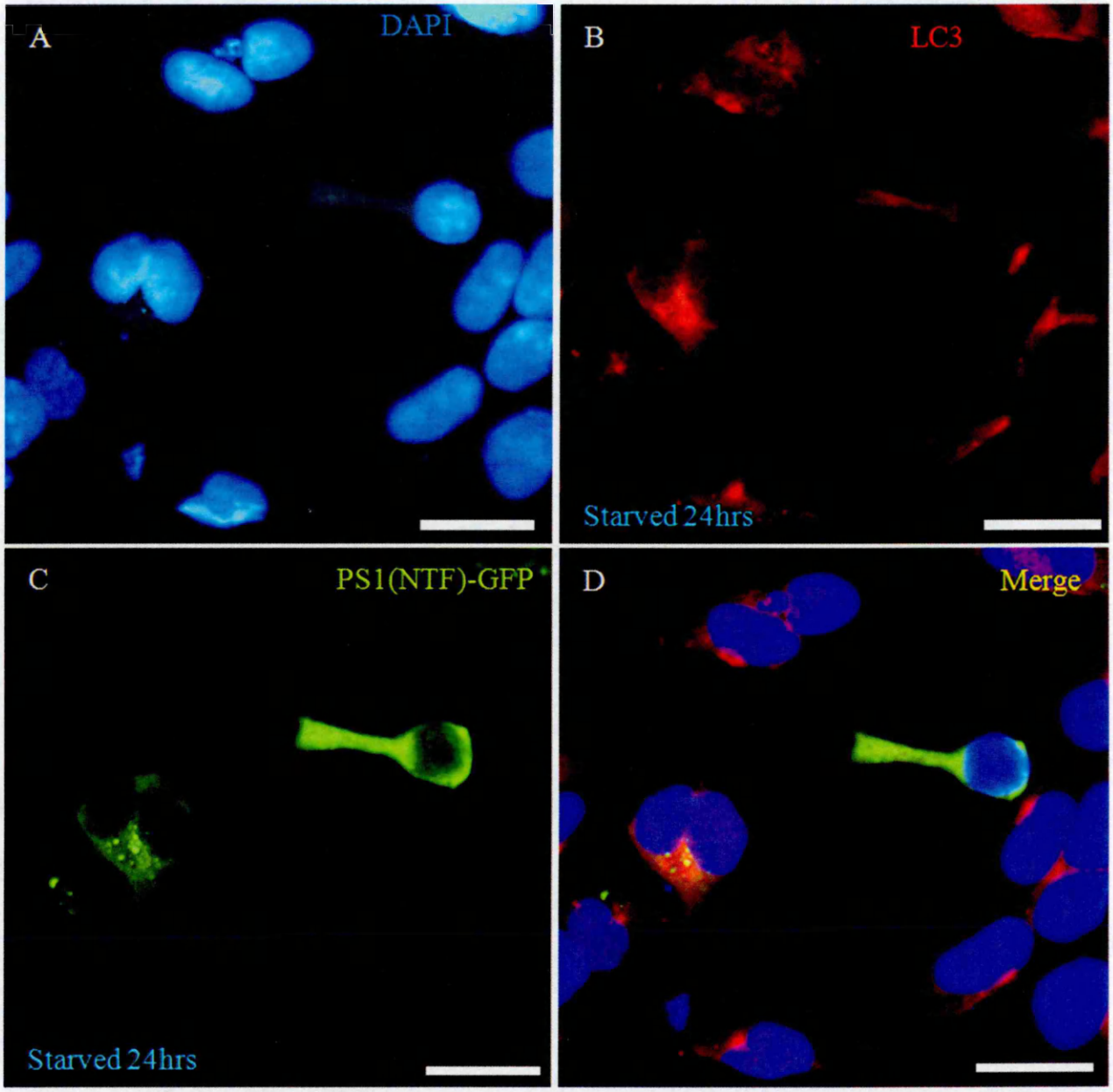

Figure 6.12 Dual label immunofluorescence for LC3 and PS1 (NTF)-GFP in transiently transfected HEK293 cells after serum starvation for 24 hrs. Cells were transiently transfected with PS1(NTF)-GFP first and then starved in serum free media for 24 hrs, and then fixed in cooled methanol and labelled for (A) Nuclei were counterstained with DAPI (B) LC3 using primary monoclonal rabbit anti-human LC3A/B antibody (Millipore, MABC176) and secondary antibody Alexa fluor 594 donkey anti-rabbit IgG (C) Green fluorescence of GFP conjugated to PS1 (NTF) (D) Merge. Scale bar: 10μm

A

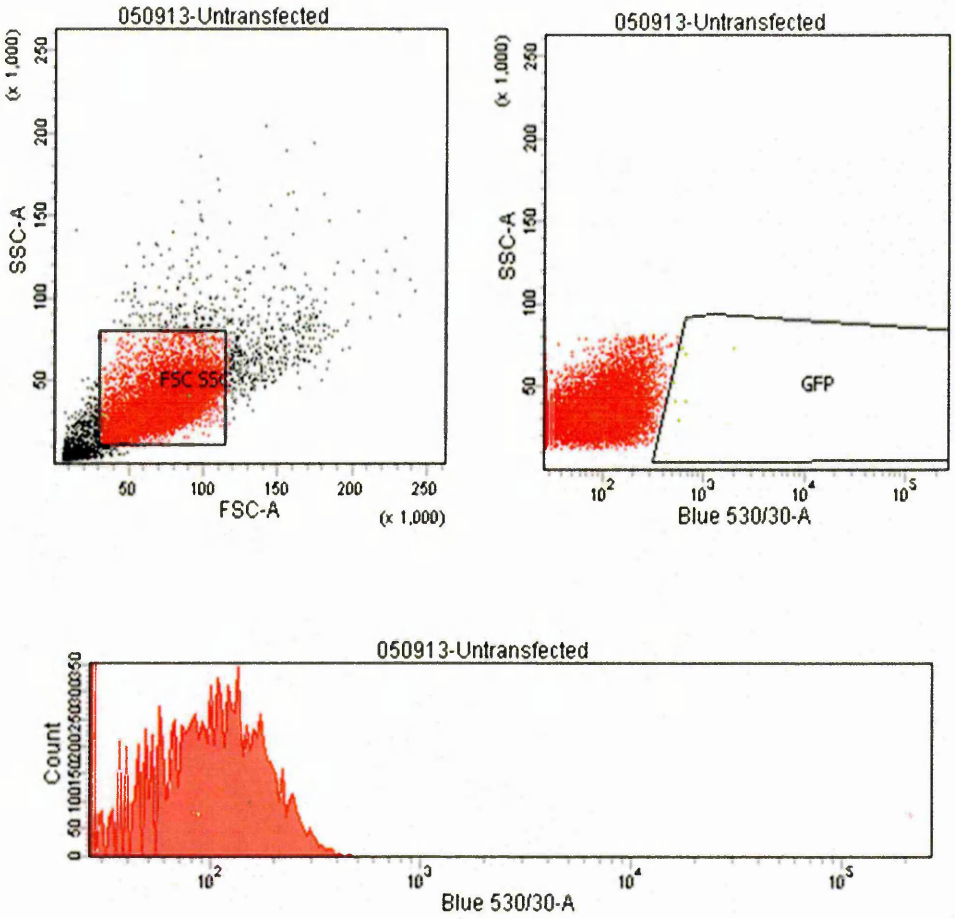

Tube: Untransfected

Population	#Events	%Parent	%Total
All Events	16,287	####	100.0
FSC SSC	13,455	82.6	82.6
GFP	9	0.1	0.1

Sorting of HEK293 cells by flow cytometry. (A) un-transfected HEK293 cells

B

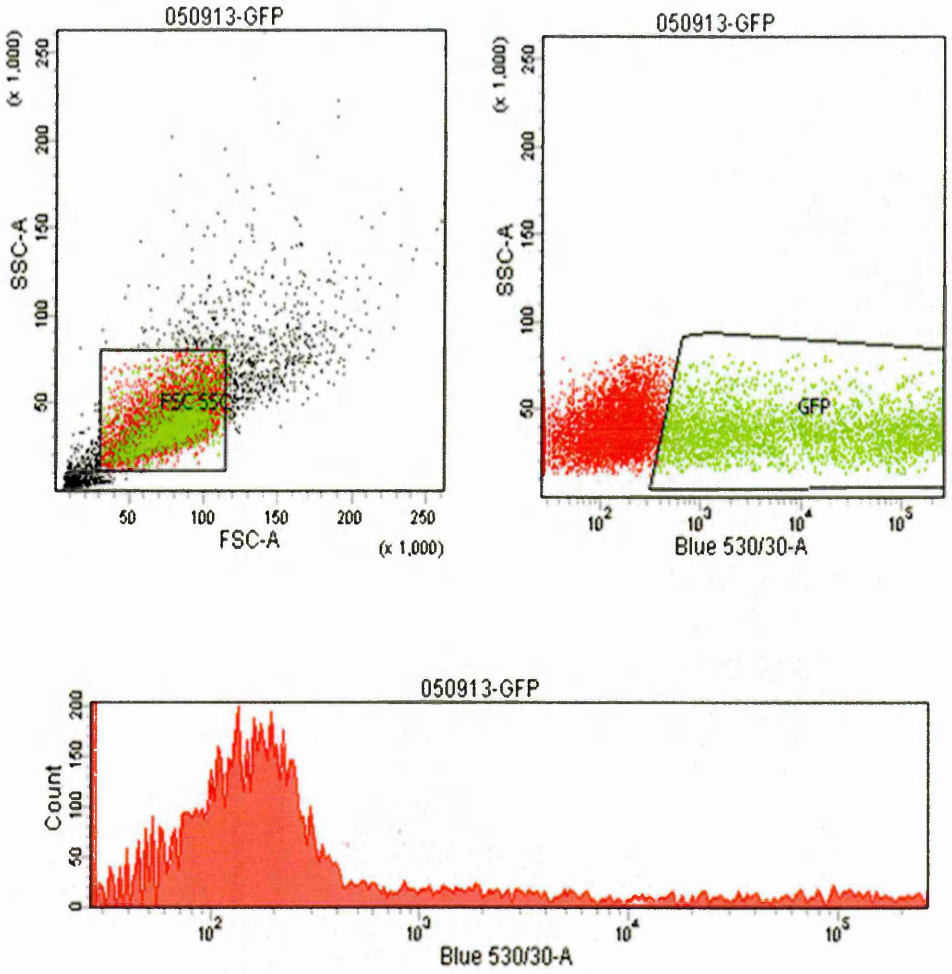

Tube: GFP

Population	#Events	%Parent	%Total
All Events	11,662	####	100.0
FSC SSC	10,000	85.7	85.7
GFP	2,609	26.1	22.4

Sorting of transfected HEK293 cells by flow cytometry. (B) GFP

C

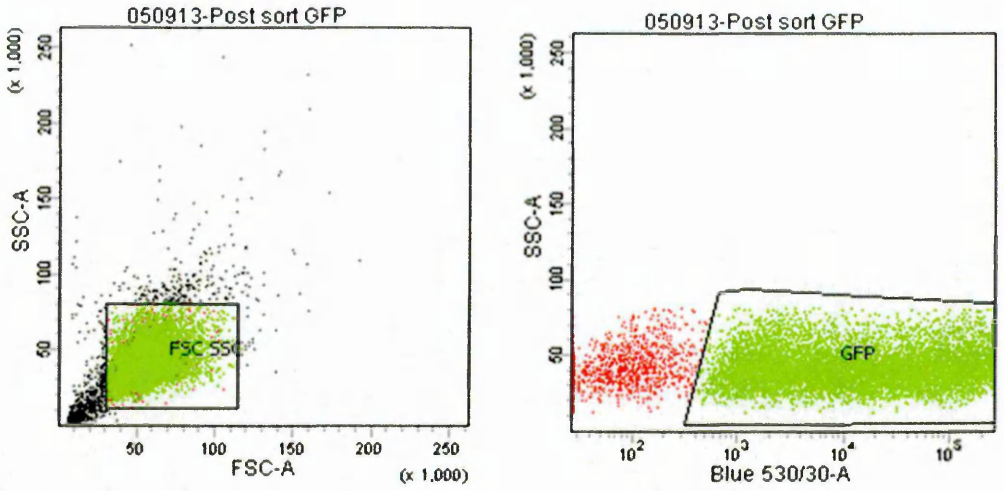

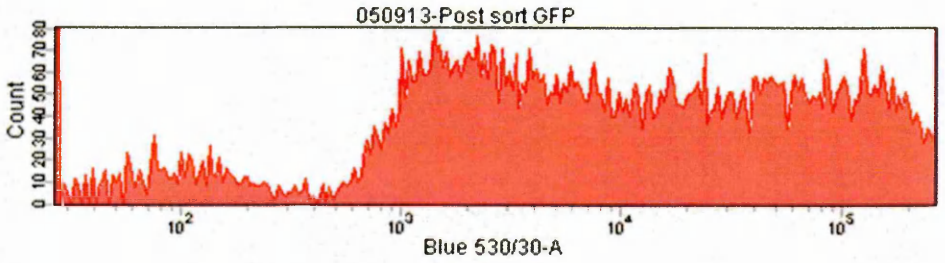

Tube: Post sort GFP

Population	#Events	%Parent	%Total
All Events	11,137	####	100.0
FSC SSC	10,000	89.8	89.8
GFP	9,042	90.4	81.2

Figure 6.13 Sorting of transfected HEK293 cells by flow cytometry. (A) un-transfected HEK293 cells. **(B)** GFP **(C)** Post sort GFP.

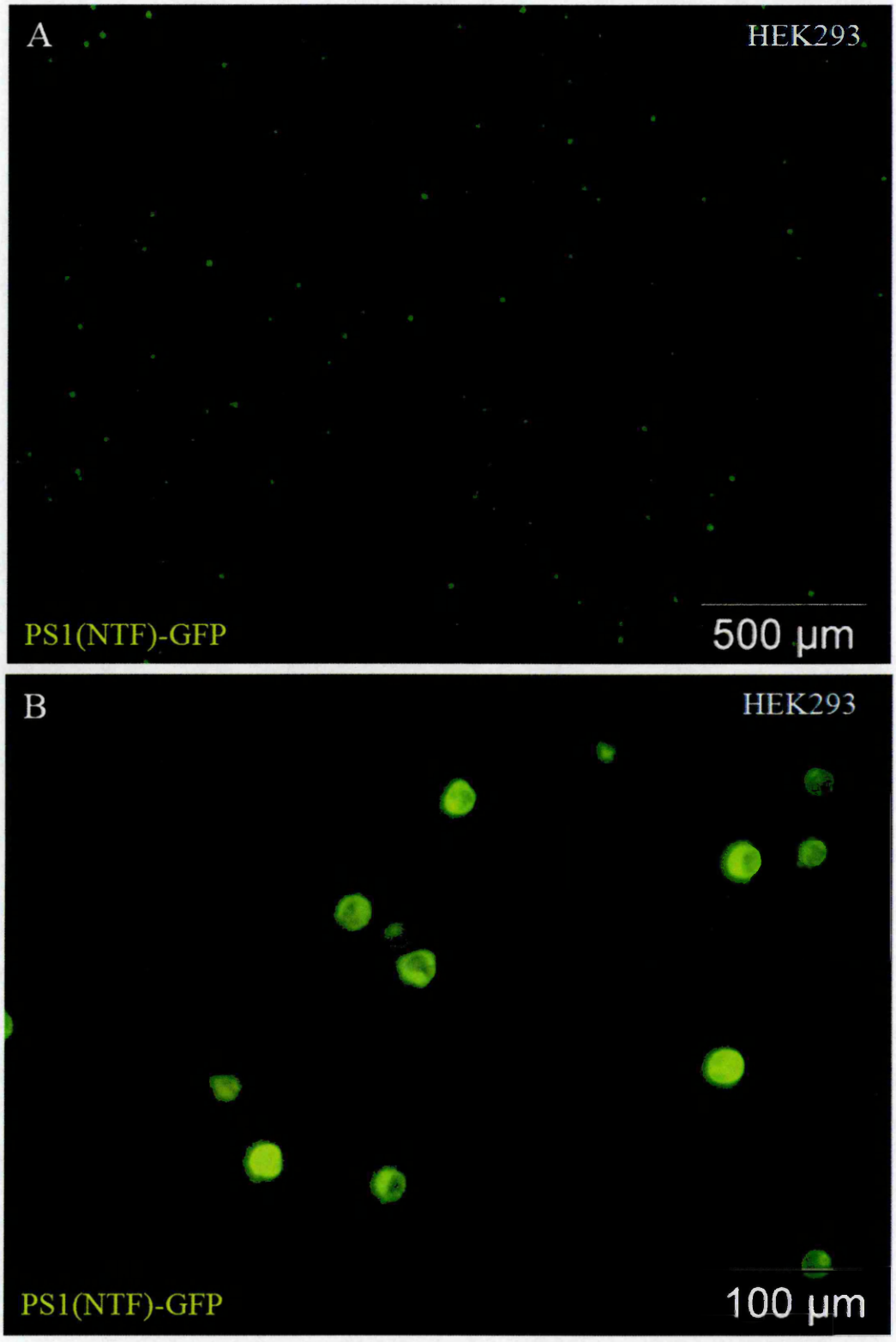

Figure 6.14 Sorted PS1 (NTF)-GFP construct transfected HEK293 cells. (A) Scale bar 500µm **(B)** Scale bar 100µm.

6.4 DISCUSSION

From the results presented in this chapter, it is clear that tPS1 protein persisted in the cells and was not removed even when autophagy was induced with rapamycin treatment or serum starvation after transfection. The similarity between the results in chapter five and in this chapter suggests that tPS1 has the ability to induce autophagy and indicates that autophagy has failed to proceed normally even when induced by rapamycin or serum starvation. In addition, the result has revealed that rapamycin treatment has as the same influence as serum starvation on the subcellular localization of tPS1 and the autophagy associated proteins studied in this project.

In chapter three, it was shown that the rapamycin concentrations (50, 200 and 500nM) for 16 hours were able to induce autophagy. The anti-LC3A/B antibody has succeeded in staining the two forms of LC3 (LC3-I and LC3-II) (autophagic markers) using proteins extracted from HEK293 cells treated with these concentrations of rapamycin. So, the same rapamycin concentrations and times were used in this experiment to be sure that autophagy has really induced after the transfection of the cells with tPS1.

It is clear that the results obtained in this chapter are the same as what was observed in chapter 5. The results suggest that there might be some interaction between tPS1 and mTOR, raptor and LC3 proteins. These suggested interactions may somehow interrupt the autophagy process.

A limitation of this current study is that only HEK293 cell line was investigated. Previous studies investigating different cell lines have shown that the autophagy proteins of interest can be present at different subcellular localizations.

Chapter 7

Conclusion and Recommendations

7.1 CONCLUSION

The research reported in this thesis has investigated, in terms of subcellular localization, the effect of tPS1 on the autophagy proteins: mTOR, raptor and LC3 and subsequently on the autophagy process. Evidence presented here suggests that some interactions between tPS1 and mTOR, raptor and LC3 take place. These interactions may have a deleterious influence on the performance of these autophagy proteins, leading to autophagic impairment. *In vitro* studies on different cell lines using truncated or mutated PS1 have proved to lead to the formation of autophagosomes, and also that autophagy failed to remove these autophagosomes. This suggests that the autophagic defect might be at the late stage of the process (fusion step). Based on this, it is unlikely that mTORC1, which contains mTOR and raptor, are responsible for the autophagosome initiation to be the cause of this problem. However, it has been demonstrated that mTOR localization to the lysosomes is an important regulator of autophagosomal–lysosomal fusion, and inhibition of mTOR by Torin1 stimulates fusion (Zhou *et al.*, 2013). So, the proposed interaction between mTOR and tPS1 in this study may prevent the localisation of mTOR to the lysosome.

LC3 protein, which is importantly involved in selecting cargo and in the fusion step of autophagy, might be aggregated with the truncated or mutant PS1 protein, leading to loss of its normal function and thus may be implicated in the autophagic defect. This is not specific for truncated or mutant PS1, as the same defect has been observed with other neurodegenerative diseases such as PD and HD in the presence of normal PS1 protein (Martinez-Vincente *et al.*, 2008; 2010).

Analysis of the binding interaction between tPS1 and the autophagy proteins of interest especially LC3 protein, would provide some insight into the nature of this interaction at the molecular level and the protein domains involved in the binding process. This may

present an interesting, alternative entry point for motivating further research and novel therapeutic approaches in neurodegenerative diseases caused by protein aggregates.

7.2 FUTURE WORK

Although conflicting results were found, accumulating evidence suggests a role for mTOR, raptor, LC3 and tPS-1 proteins in the defective autophagy process in the pathogenesis of degenerative diseases such as AD, and warrants further investigation. It is important that future research focuses on why the autophagy proteins: mTOR, raptor, LC3 and tPS-1, have the same subcellular localization. Are they actually bound to each other after autophagy induction by the transfected protein or just present in the same organelle? Further investigations that use biochemical methods such as isolation of subcellular organelles will need to be done with homogenous populations, since the transient transfection with tPS1 has resulted in mixed cell populations; some expressing tPS1 and some not.

Investigation of the interaction between the truncated PS-1 and the proteins of interest should be undertaken using protein-protein interaction methods, for example: co-immunoprecipitation assays. In addition, the failure in having live images during the transfection of HEK293 cells with tPS-1 needs adressing. It would also be useful to have live images during transfection to determine the movement of truncated PS-1 inside the cells.

There are no publications, in terms of subcellular localization, investigating the relationship between PS-1 and the autophagy proteins of interest (mTOR, raptor and LC3) or any other autophagy proteins; therefore it would be useful to further investigate these relationships. The studies should be repeated with different cell lines including neuronal cells in order to compare the results and provide more relvant detail to AD.

REFERENCES

Amaravadi, R. K., Yu, D., Lum, J. J., Bui, T., Christophorou, M. A., Evan, G. I,Thompson, C. B. (2007). Autophagy inhibition enhances therapy-induced apoptosis in a myc-induced model of lymphoma. *The Journal of Clinical Investigation, 117* (2), 326-336.

Anderson, D. (2003). Effect of the cellular factors on the generation of beta-amyloid. *PhD thesis.*

Axe, E. L., Walker, S. A., Manifava, M., Chandra, P., Roderick, H. L., Habermann, A., Ktistakis, N. T. (2008). Autophagosome formation from membrane compartments enriched in phosphatidylinositol 3-phosphate and dynamically connected to the endoplasmic reticulum. *The Journal of Cell Biology, 182* (4), 685-701.

Backer, J. (2008). The regulation and function of class III PI3Ks: Novel roles for Vps34. *Biochem.J, 410*, 1-17.

Bai, X., Ma, D., Liu, A., Shen, X., Wang, Q. J., Liu, Y., & Jiang, Y. (2007). Rheb activates mTOR by antagonizing its endogenous inhibitor, FKBP38. *Science, 318* (5852), 977-980.

Bar-Peled, L., Schweitzer, L. D., Zoncu, R., & Sabatini, D. M. (2012). Ragulator is a GEF for the rag GTPases that signal amino acid levels to mTORC1. *Cell, 150* (6), 1196-1208.

Barth, S., Glick, D., & Macleod, K. F. (2010). Autophagy: Assays and artifacts. *The Journal of Pathology, 221* (2), 117-124.

Basel-Vanagaite, L., Muncher, L., Straussberg, R., Pasmanik-Chor, M., Yahav, M., Rainshtein, L., Drasinover, V. (2006). Mutated nup 62 causes autosomal recessive infantile bilateral striatal necrosis. *Annals of Neurology, 60* (2), 214-222.

Bendiske, J., & Bahr, B. A. (2003). Lysosomal activation is a compensatory response against protein accumulation and associated synaptopathogenesis—an approach for slowing alzheimer disease? *Journal of Neuropathology & Experimental Neurology, 62* (5), 451-463.

Benjamin, D., Colombi, M., Moroni, C., & Hall, M. N. (2011). Rapamycin passes the torch: A new generation of mTOR inhibitors. *Nature Reviews Drug Discovery, 10* (11), 868-880.

Berger, Z., Ravikumar, B., Menzies, F. M., Oroz, L. G., Underwood, B. R., Pangalos, M. N., Rubinsztein, D. C. (2006). Rapamycin alleviates toxicity of different aggregate-prone proteins. *Human Molecular Genetics, 15* (3), 433-442.

Betz, C., & Hall, M. N. (2013). Where is mTOR and what is it doing there? *The Journal of Cell Biology, 203* (4), 563-574.

Bhaskar, P. T., & Hay, N. (2007). The two TORCs and AKT. *Developmental Cell, 12* (4), 487-502.

Bhutia, S. K., Kegelman, T. P., Das, S. K., Azab, B., Su, Z. Z., Lee, S. G., Fisher, P. B. (2010). Astrocyte elevated gene-1 induces protective autophagy. *Proceedings of the National Academy of Sciences of the United States of America, 107* (51), 22243-22248.

Bohn, G., Allroth, A., Brandes, G., Thiel, J., Glocker, E., Schäffer, A. A., Zeidler, C. (2007). A novel human primary immunodeficiency syndrome caused by deficiency of the endosomal adaptor protein p14. *Nature Medicine, 13* (1), 38-45.

Boland, B., Kumar, A., Lee, S., Platt, F. M., Wegiel, J., Yu, W. H., & Nixon, R. A. (2008). Autophagy induction and autophagosome clearance in neurons: Relationship to autophagic pathology in Alzheimer's disease. *The Journal of Neuroscience: The Official Journal of the Society for Neuroscience, 28* (27), 6926-6937.

Borchelt, D. R., Ratovitski, T., van Lare, J., Lee, M. K., Gonzales, V., Jenkins, N. A., Sisodia, S. S. (1997). Accelerated amyloid deposition in the brains of transgenic mice coexpressing mutant presenilin 1 and amyloid precursor proteins.*Neuron, 19* (4), 939-945.

Bordeaux, J., Welsh, A., Agarwal, S., Killiam, E., Baquero, M., Hanna, J., Rimm, D. (2010). Antibody validation. *Biotechniques, 48* (3), 197-209.

Bratton, D. L., & Henson, P. M. (2005). Autoimmunity and apoptosis: Refusing to go quietly. *Nature Medicine, 11* (1), 26-27.

Bredesen, D. E., Rao, R. V., & Mehlen, P. (2006). Cell death in the nervous system. *Nature, 443* (7113), 796-802.

Buchwalow, I., Samoilova, V., Boecker, W., & Tiemann, M. (2011). Non-specific binding of antibodies in immunohistochemistry: Fallacies and facts. *Scientific Reports, 1*

Caccamo, A., Majumder, S., Richardson, A., Strong, R., & Oddo, S. (2010). Molecular interplay between mammalian target of rapamycin (mTOR), amyloid-beta, and tau: Effects on cognitive impairments. *The Journal of Biological Chemistry, 285* (17), 13107-13120.

Caccamo, A., Maldonado, M. A., Majumder, S., Medina, D. X., Holbein, W., Magri, A., & Oddo, S. (2011). Naturally secreted amyloid-beta increases mammalian target of rapamycin (mTOR) activity via a PRAS40-mediated mechanism. *The Journal of Biological Chemistry, 286* (11), 8924-8932.

Cadwell, K., Liu, J. Y., Brown, S. L., Miyoshi, H., Loh, J., Lennerz, J. K., Hunt, S. (2008). A key role for autophagy and the autophagy gene Atg16l1 in mouse and human intestinal paneth cells. *Nature, 456* (7219), 259-263.

Chacinska, A., Koehler, C. M., Milenkovic, D., Lithgow, T., & Pfanner, N. (2009). Importing mitochondrial proteins: Machineries and mechanisms. *Cell, 138* (4), 628-644.

Chahine, M. N., & Pierce, G. N. (2009). Therapeutic targeting of nuclear protein import in pathological cell conditions. *Pharmacological Reviews, 61* (3), 358-372.

Chan, E. Y., Kir, S., & Tooze, S. A. (2007). siRNA screening of the kinome identifies ULK1 as a multidomain modulator of autophagy. *The Journal of Biological Chemistry, 282* (35), 25464-25474.

Chan, E. Y., Longatti, A., McKnight, N. C., & Tooze, S. A. (2009). Kinase-inactivated ULK proteins inhibit autophagy via their conserved C-terminal domains using an Atg13-independent mechanism. *Molecular and Cellular Biology, 29* (1), 157-171.

Chen, L., Wang, H., Vicini, S., & Olsen, R. W. (2000). The γ-aminobutyric acid type A (GABAA) receptor-associated protein (GABARAP) promotes GABAA receptor clustering and modulates the channel kinetics. *Proceedings of the National Academy of Sciences, 97* (21), 11557-11562.

Cheong, H., Yorimitsu, T., Reggiori, F., Legakis, J. E., Wang, C. W., & Klionsky, D. J. (2005). Atg17 regulates the magnitude of the autophagic response.*Molecular Biology of the Cell, 16* (7), 3438-3453.

Chernomordik, L. V., & Kozlov, M. M. (2005). Membrane hemifusion: Crossing a chasm in two leaps. *Cell, 123* (3), 375-382.

Cheung, Z. H., & Ip, N. Y. (2011). Autophagy deregulation in neurodegenerative diseases–recent advances and future perspectives. *Journal of Neurochemistry, 118* (3), 317-325.

Chou, K. (2013). Some remarks on predicting multi-label attributes in molecular biosystems.*Mol.BioSyst., 9* (6), 1092-1100.

Chu, C. T. (2006). Autophagic stress in neuronal injury and disease. *Journal of Neuropathology and Experimental Neurology, 65* (5), 423-432.

Ciechanover, A. (2005). Proteolysis: From the lysosome to ubiquitin and the proteasome. *Nature Reviews Molecular Cell Biology, 6* (1), 79-87.

Citron, M., Westaway, D., Xia, W., Carlson, G., Diehl, T., Levesque, G., Davis, A. (1997). Mutant presenilins of Alzheimer's disease increase production of 42-residue amyloid β-protein in both transfected cells and transgenic mice. *Nature Medicine, 3* (1), 67-72.

Couchman, J. R. (2009). Commercial antibodies: The good, bad, and really ugly. *The Journal of Histochemistry and Cytochemistry: Official Journal of the Histochemistry Society, 57* (1), 7-8.

Cuervo, A. M., Stefanis, L., Fredenburg, R., Lansbury, P. T., & Sulzer, D. (2004). Impaired degradation of mutant alpha-synuclein by chaperone-mediated autophagy. *Science (New York, N.Y.), 305* (5688), 1292-1295.

De Strooper, B., & Annaert, W. (2010).Novel research horizons for presenilins and γ-secretases in cell biology and disease. *Annual Review of Cell and Developmental Biology, 26*, 235-260.

De Strooper, B., Saftig, P., Craessaerts, K., Vanderstichele, H., Guhde, G., Annaert, W., Van Leuven, F. (1998). Deficiency of presenilin-1 inhibits the normal cleavage of amyloid precursor protein. *Nature, 391* (6665), 387-390.

Degenhardt, K., Mathew, R., Beaudoin, B., Bray, K., Anderson, D., Chen, G., Fan, Y. (2006). Autophagy promotes tumor cell survival and restricts necrosis, inflammation, and tumorigenesis. *Cancer Cell, 10* (1), 51-64.

Desai, B. N., Myers, B. R., & Schreiber, S. L. (2002). FKBP12-rapamycin-associated protein associates with mitochondria and senses osmotic stress via mitochondrial dysfunction.*Proceedings of the National Academy of Sciences, 99* (7), 4319-4324.

Deter, R. L., & De Duve, C. (1967). Influence of glucagon, an inducer of cellular autophagy, on some physical properties of rat liver lysosomes. *The Journal of Cell Biology, 33* (2), 437-449.

Djordjevic, S., Zhang, X., Bartlam, M., Ye, S., Rao, Z., & Danpure, C. J. (2010). Structural implications of a G170R mutation of alanine: Glyoxylate aminotransferase that is associated with peroxisome-to-mitochondrion mistargeting. *Acta Crystallographica Section F: Structural Biology and Crystallization Communications, 66* (3), 233-236.

Drenan, R. M., Liu, X., Bertram, P. G., & Zheng, X. S. (2004). FKBP12-rapamycin-associated protein or mammalian target of rapamycin (FRAP/mTOR) localization in the endoplasmic reticulum and the golgi apparatus. *Journal of Biological Chemistry, 279* (1), 772-778.

Dreuillet, C., Harper, M., Tillit, J., Kress, M., & Ernoult-Lange, M. (2008). Mislocalization of human transcription factor MOK2 in the presence of pathogenic mutations of lamin A/C. *Biology of the Cell, 100* (1), 51-61.

Dunlop, E. A., Hunt, D. K., Acosta-Jaquez, H. A., Fingar, D. C., & Tee, A. R. (2011). ULK1 inhibits mTORC1 signaling, promotes multisite raptor phosphorylation and hinders substrate binding. *Autophagy, 7* (7), 737-747.

Efeyan, A., Zoncu, R., & Sabatini, D. M. (2012). Amino acids and mTORC1: From lysosomes to disease. *Trends in Molecular Medicine, 18* (9), 524-533.

English, L., Chemali, M., Duron, J., Rondeau, C., Laplante, A., Gingras, D., Lippé, R. (2009). Autophagy enhances the presentation of endogenous viral antigens on MHC class I molecules during HSV-1 infection. *Nature Immunology, 10* (5), 480-487.

Eskelinen, E. (2005). Maturation of autophagic vacuoles in mammalian cells. *Autophagy, 1* (1), 1-10.

Eskelinen, E. (2006). Roles of LAMP-1 and LAMP-2 in lysosome biogenesis and autophagy. *Molecular Aspects of Medicine, 27* (5), 495-502.

Eskelinen, E. (2008). To be or not to be? examples of incorrect identification of autophagic compartments in conventional transmission electron microscopy of mammalian cells.*Autophagy, 4* (2), 257-260.

Fimia, G. M., Stoykova, A., Romagnoli, A., Giunta, L., Di Bartolomeo, S., Nardacci, R., Schwartz, P. (2007). Ambra1 regulates autophagy and development of the nervous system. *Nature, 447* (7148), 1121-1125.

Foster, K. G., Acosta-Jaquez, H. A., Romeo, Y., Ekim, B., Soliman, G. A., Carriere, A., Fingar, D. C. (2010). Regulation of mTOR complex 1 (mTORC1) by raptor Ser 863 and multisite phosphorylation. *Journal of Biological Chemistry, 285* (1), 80-94.

Fu, L., Cheng, Y., & Liu, B. (2013). Beclin-1: Autophagic regulator and therapeutic target in cancer. *The International Journal of Biochemistry & Cell Biology, 45* (5), 921-924.

Funakoshi, T., Matsuura, A., Noda, T., & Ohsumi, Y. (1997). Analyses of < i> APG13 < /i> gene involved in autophagy in yeast, < i> saccharomyces cerevisiae </i>. *Gene, 192* (2), 207-213.

Ganley, I. G., Lam, D. H., Wang, J., Ding, X., Chen, S., & Jiang, X. (2009). ULK1· ATG13· FIP200 complex mediates mTOR signaling and is essential for autophagy. *Journal of Biological Chemistry, 284* (18), 12297-12305.

García-Arencibia, M., Hochfeld, W. E., Toh, P. P., & Rubinsztein, D. C. (2010). Autophagy, a guardian against neurodegeneration.*Seminars in Cell & Developmental Biology, , 21* (7) 691-698.

Garcia-Martinez, J., & Alessi, D. (2008). mTOR complex 2 (mTORC2) controls hydrophobic motif phosphorylation and activation of serum-and glucocorticoid-induced protein kinase 1 (SGK1). *Biochem.J, 416*, 375-385.

Geng, J., & Klionsky, D. J. (2008). The Atg8 and Atg12 ubiquitin-like conjugation systems in macroautophagy. *EMBO Reports, 9* (9), 859-864.

Glick, D., Barth, S., & Macleod, K. F. (2010). Autophagy: Cellular and molecular mechanisms. *The Journal of Pathology, 221* (1), 3-12.

Gómez-Isla, T., Growdon, W. B., McNamara, M. J., Nochlin, D., Bird, T. D., Arango, J. C., Cairns, N. J. (1999). The impact of different presenilin 1 andpresenilin 2 mutations on amyloid deposition, neurofibrillary changes and neuronal loss in the familial Alzheimer's disease brain evidence for other phenotype-modifying factors. *Brain, 122* (9), 1709-1719.

Gong, C., Bauvy, C., Tonelli, G., Yue, W., Delomenie, C., Nicolas, V.,Tharinger, H. (2013). Beclin 1 and autophagy are required for the tumorigenicity of breast cancer stem-like/progenitor cells. *Oncogene, 32* (18), 2261-2272.

Gordy, C., & He, Y. (2012). The crosstalk between autophagy and apoptosis: Where does this lead? *Protein & Cell, 3* (1), 17-27.

Guertin, D. A., & Sabatini, D. M. (2007). Defining the role of mTOR in cancer. *Cancer Cell, 12* (1), 9-22.

Gutierrez, M. G., Munafo, D. B., Beron, W., & Colombo, M. I. (2004). Rab7 is required for the normal progression of the autophagic pathway in mammalian cells. *Journal of Cell Science, 117* (Pt 13), 2687-2697.

Gwinn, D. M., Shackelford, D. B., Egan, D. F., Mihaylova, M. M., Mery, A., Vasquez, D. S., Shaw, R. J. (2008). AMPK phosphorylation of raptor mediates a metabolic checkpoint. *Molecular Cell, 30* (2), 214-226.

Hampe, J., Franke, A., Rosenstiel, P., Till, A., Teuber, M., Huse, K., Briggs, J. (2007). A genome-wide association scan of nonsynonymous SNPs identifies a susceptibility variant for crohn disease in ATG16L1. *Nature Genetics, 39* (2), 207-211.

Hands, S. L., Proud, C. G., & Wyttenbach, A. (2009).mTOR's role in ageing: Protein synthesis or autophagy? *Aging, 1* (7), 586-597.

Hara, K., Maruki, Y., Long, X., Yoshino, K., Oshiro, N., Hidayat, S.,Yonezawa, K. (2002). Raptor, a binding partner of target of rapamycin (TOR), mediates TOR action. *Cell, 110* (2), 177-189.

Hara, K., Yonezawa, K., Weng, Q. P., Kozlowski, M. T., Belham, C., & Avruch, J. (1998). Amino acid sufficiency and mTOR regulate p70 S6 kinase and eIF-4E BP1 through a common effector mechanism. *The Journal of Biological Chemistry, 273* (23), 14484-14494.

Hara, T., Nakamura, K., Matsui, M., Yamamoto, A., Nakahara, Y., Suzuki-Migishima, R., Okano, H. (2006). Suppression of basal autophagy in neural cells causes neurodegenerative disease in mice. *Nature, 441* (7095), 885-889.

Hara, T., Takamura, A., Kishi, C., Iemura, S., Natsume, T., Guan, J. L., & Mizushima, N. (2008). FIP200, a ULK-interacting protein, is required for autophagosome formation in mammalian cells. *The Journal of Cell Biology, 181* (3), 497-510.

Hashimoto, M., & Masliah, E. (1999). Alpha-synuclein in lewy body disease and Alzheimer's disease. *Brain Pathology, 9* (4), 707-720.

Hayat, M.Introduction to autophagy: Cancer, other pathologies, inflammation, immunity, infection, and aging, volume 5.

He, C., & Klionsky, D. J. (2009). Regulation mechanisms and signaling pathways of autophagy. *Annual Review of Genetics, 43*, 67-93.

He, H., Dang, Y., Dai, F., Guo, Z., Wu, J., She, X.,Wu, C. (2003). Post-translational modifications of three members of the human MAP1LC3 family and detection of a novel type of modification for MAP1LC3B. *Journal of Biological Chemistry, 278* (31), 29278-29287.

Heitman, J., Movva, N. R., & Hall, M. N. (1991). Targets for cell cycle arrest by the immunosuppressant rapamycin in yeast. *Science (New York, N.Y.), 253*(5022), 905-909.

Hosokawa, N., Hara, T., Kaizuka, T., Kishi, C., Takamura, A., Miura, Y.,Yamada, N. (2009). Nutrient-dependent mTORC1 association with the ULK1–Atg13–FIP200 complex required for autophagy. *Molecular Biology of the Cell, 20* (7), 1981-1991.

Hosokawa, N., Sasaki, T., Iemura, S., Natsume, T., Hara, T., & Mizushima, N. (2009). Atg101, a novel mammalian autophagy protein interacting with Atg13. *Autophagy, 5* (7), 973-979.

Hung, M. C., & Link, W. (2011). Protein localization in disease and therapy. *Journal of Cell Science, 124* (Pt 20), 3381-3392.

Hung, S. Y., Huang, W. P., Liou, H. C., & Fu, W. M. (2009). Autophagy protects neuron from abeta-induced cytotoxicity. *Autophagy, 5* (4), 502-510.

Inoki, K., Li, Y., Zhu, T., Wu, J., & Guan, K. (2002). TSC2 is phosphorylated and inhibited by akt and suppresses mTOR signalling. *Nature Cell Biology, 4* (9), 648-657.

Inoki, K., Zhu, T., & Guan, K. (2003). TSC2 mediates cellular energy response to control cell growth and survival. *Cell, 115* (5), 577-590.

Jaeger, P. A., Pickford, F., Sun, C., Lucin, K. M., Masliah, E., & Wyss-Coray, T. (2010).Regulation of amyloid precursor protein processing by the beclin 1 complex. *PLoS One, 5* (6), e11102.

Jager, S., Bucci, C., Tanida, I., Ueno, T., Kominami, E., Saftig, P., & Eskelinen, E. L. (2004). Role for Rab7 in maturation of late autophagic vacuoles. *Journal of Cell Science, 117* (Pt 20), 4837-4848.

Jahreiss, L., Menzies, F. M., & Rubinsztein, D. C. (2008). The itinerary of autophagosomes: From peripheral formation to kiss-and-run fusion with lysosomes. *Traffic, 9* (4), 574-587.

Jamur, M. C., & Oliver, C. (2010). Permeabilization of cell membranes. *Immunocytochemical methods and protocols* (pp. 63-66) Springer.

Johansen, T., & Lamark, T. (2011). Selective autophagy mediated by autophagic adapter proteins. *Autophagy, 7* (3), 279-296.

Jung, C. H., Jun, C. B., Ro, S., Kim, Y., Otto, N. M., Cao, J., Kim, D. (2009). ULK-Atg13-FIP200 complexes mediate mTOR signaling to the autophagy machinery. *Molecular Biology of the Cell, 20* (7), 1992-2003.

Jung, C. H., Ro, S., Cao, J., Otto, N. M., & Kim, D. (2010). mTOR regulation of autophagy. *FEBS Letters, 584* (7), 1287-1295.

Kabeya, Y., Kamada, Y., Baba, M., Takikawa, H., Sasaki, M., & Ohsumi, Y. (2005). Atg17 functions in cooperation with Atg1 and Atg13 in yeast autophagy.*Molecular Biology of the Cell, 16* (5), 2544-2553.

Kabeya, Y., Mizushima, N., Ueno, T., Yamamoto, A., Kirisako, T., Noda, T.,Yoshimori, T. (2000). LC3, a mammalian homologue of yeast Apg8p, is localized in autophagosome membranes after processing. *The EMBO Journal, 19* (21), 5720-5728.

Kabeya, Y., Mizushima, N., Yamamoto, A., Oshitani-Okamoto, S., Ohsumi, Y., & Yoshimori, T. (2004). LC3, GABARAP and GATE16 localize to autophagosomal membrane depending on form-II formation. *Journal of Cell Science, 117* (13), 2805-2812.

Kabeya, Y., Noda, N. N., Fujioka, Y., Suzuki, K., Inagaki, F., & Ohsumi, Y. (2009). Characterization of the Atg17–Atg29–Atg31 complex specifically required for starvation-induced autophagy in< i> saccharomyces cerevisiae</i>. *Biochemical and Biophysical Research Communications, 389* (4), 612-615.

Kamada, Y., Funakoshi, T., Shintani, T., Nagano, K., Ohsumi, M., & Ohsumi, Y. (2000). Tor-mediated induction of autophagy via an Apg1 protein kinase complex. *The Journal of Cell Biology, 150* (6), 1507-1513.

Kamada, Y., Yoshino, K., Kondo, C., Kawamata, T., Oshiro, N., Yonezawa, K., & Ohsumi, Y. (2010). Tor directly controls the Atg1 kinase complex to regulate autophagy. *Molecular and Cellular Biology, 30* (4), 1049-1058.

Kang, D. E., Yoon, I. S., Repetto, E., Busse, T., Yermian, N., Ie, L., & Koo, E. H. (2005). Presenilins mediate phosphatidylinositol 3-kinase/AKT and ERK activation via select signaling receptors. Selectivity of PS2 in platelet-derived growth factor signaling. *The Journal of Biological Chemistry, 280* (36), 31537-31547.

Kang, R., Zeh, H., Lotze, M., & Tang, D. (2011). The beclin 1 network regulates autophagy and apoptosis. *Cell Death & Differentiation, 18* (4), 571-580.

Karim, M. R., Kanazawa, T., Daigaku, Y., Fujimura, S., Miotto, G., & Kadowaki, M. (2007). Cytosolic LC3 ratio as a sensitive index of macroautophagy in isolated rat hepatocytes and H4-II-E cells. *Autophagy, 3* (6), 553-560.

Kau, T. R., Way, J. C., & Silver, P. A. (2004). Nuclear transport and cancer: From mechanism to intervention. *Nature Reviews Cancer, 4* (2), 106-117.

Kawamata, T., Kamada, Y., Kabeya, Y., Sekito, T., & Ohsumi, Y. (2008). Organization of the pre-autophagosomal structure responsible for autophagosome formation. *Molecular Biology of the Cell, 19* (5), 2039-2050.

Kim, D., Sarbassov, D. D., Ali, S. M., King, J. E., Latek, R. R., Erdjument-Bromage, H., Sabatini, D. M. (2002). mTOR interacts with raptor to form a nutrient-sensitive complex that signals to the cell growth machinery. *Cell, 110* (2), 163-17

Kim, E., Goraksha-Hicks, P., Li, L., Neufeld, T. P., & Guan, K. (2008). Regulation of TORC1 by rag GTPases in nutrient response. *Nature Cell Biology, 10* (8), 935-945.

Kim, I., Rodriguez-Enriquez, S., & Lemasters, J. J. (2007). Selective degradation of mitochondria by mitophagy. *Archives of Biochemistry and Biophysics, 462* (2), 245-253.

Kim, J., Kundu, M., Viollet, B., & Guan, K. (2011). AMPK and mTOR regulate autophagy through direct phosphorylation of Ulk1. *Nature Cell Biology, 13* (2), 132-141.

Kim, T., & Tanzi, R. E. (1997). Presenilins and Alzheimer's disease. *Current Opinion in Neurobiology, 7* (5), 683-688.

Kirisako, T., Baba, M., Ishihara, N., Miyazawa, K., Ohsumi, M., Yoshimori, T., Ohsumi, Y. (1999). Formation process of autophagosome is traced with Apg8/Aut7p in yeast. *The Journal of Cell Biology, 147* (2), 435-446.

Kirisako, T., Ichimura, Y., Okada, H., Kabeya, Y., Mizushima, N., Yoshimori, T., Ohsumi, Y. (2000). The reversible modification regulates the membrane-binding state of Apg8/Aut7 essential for autophagy and the cytoplasm to vacuole targeting pathway. *The Journal of Cell Biology, 151* (2), 263-276.

Kiriyama, T., Hirano, M., Asai, H., Ikeda, M., Furiya, Y., & Ueno, S. (2008). Restoration of nuclear-import failure caused by triple A syndrome and oxidative stress. *Biochemical and Biophysical Research Communications, 374* (4), 631-634.

Kirkegaard, K., Taylor, M. P., & Jackson, W. T. (2004). Cellular autophagy: Surrender, avoidance and subversion by microorganisms. *Nature Reviews Microbiology, 2* (4), 301-314.

Kirkin, V., McEwan, D. G., Novak, I., & Dikic, I. (2009). A role for ubiquitin in selective autophagy. *Molecular Cell, 34* (3), 259-269.

Klionsky, D. J. (2007). Autophagy: From phenomenology to molecular understanding in less than a decade. *Nature Reviews Molecular Cell Biology, 8* (11), 931-937.

Klionsky, D. J., Cuervo, A. M., & Seglen, P. O. (2007). Methods for monitoring autophagy from yeast to human.*Autophagy, 3* (3), 181.

Kneussel, M., Haverkamp, S., Fuhrmann, J. C., Wang, H., Wässle, H., Olsen, R. W., & Betz, H. (2000). The γ-aminobutyric acid type A receptor (GABAAR)-associated protein GABARAP interacts with gephyrin but is not involved in receptor anchoring at the synapse. *Proceedings of the National Academy of Sciences, 97* (15), 8594-8599.

Koike, M., Shibata, M., Waguri, S., Yoshimura, K., Tanida, I., Kominami, E., Mizushima, N. (2005). Participation of autophagy in storage of lysosomes in neurons from mouse models of neuronal ceroid-lipofuscinoses (batten disease). *The American Journal of Pathology, 167* (6), 1713-1728.

Komatsu, M., Waguri, S., Chiba, T., Murata, S., Iwata, J., Tanida, I., Kominami, E. (2006). Loss of autophagy in the central nervous system causes neurodegeneration in mice.*Nature, 441* (7095), 880-884.

Kraft, C., Kijanska, M., Kalie, E., Siergiejuk, E., Lee, S. S., Semplicio, G., Hansmann, I. (2012). Binding of the Atg1/ULK1 kinase to the ubiquitin-like protein Atg8 regulates autophagy. *The EMBO Journal, 31* (18), 3691-3703.

Kragh, C. L., Ubhi, K., Wyss-Corey, T., & Masliah, E. (2012). Autophagy in dementias. *Brain Pathology, 22* (1), 99-109.

Kundu, M., Lindsten, T., Yang, C. Y., Wu, J., Zhao, F., Zhang, J., Thompson, C. B. (2008). Ulk1 plays a critical role in the autophagic clearance of mitochondria and ribosomes during reticulocyte maturation. *Blood, 112* (4), 1493-1502.

Kurien, B. T., & Scofield, R. H. (2006).Western blotting. *Methods, 38* (4), 283-293.

Kuroyanagi, H., Yan, J., Seki, N., Yamanouchi, Y., Suzuki, Y., Takano, T., Shirasawa, T. (1998). Human ULK1, a novel Serine/Threonine kinase related to UNC-51 kinase of< i> caenorhabditis elegans : < /i> cDNA cloning, expression, and chromosomal assignment. *Genomics, 51* (1), 76-85.

Laemmli, U. K. (1970).Cleavage of structural proteins during the assembly of the head of bacteriophage T4. *Nature, 227* (5259), 680-685.

Laplante, M., & Sabatini, D. M. (2009). mTOR signaling at a glance. *Journal of Cell Science, 122* (Pt 20), 3589-3594.

Lee, J. (2012). Neuronal autophagy: A housekeeper or a fighter in neuronal cell survival? *Experimental Neurobiology, 21* (1), 1-8.

Lee, J. W., Park, S., Takahashi, Y., & Wang, H. (2010a). The association of AMPK with ULK1 regulates autophagy. *PloS One, 5* (11), e15394.

Lee, J., Yu, W. H., Kumar, A., Lee, S., Mohan, P. S., Peterhoff, C. M., Sovak, G. (2010b). Lysosomal proteolysis and autophagy require presenilin 1 and are disrupted by alzheimer-related PS1 mutations. *Cell, 141* (7), 1146-1158.

Lee, S. B., Kim, S., Lee, J., Park, J., Lee, G., Kim, Y., Chung, J. (2007). ATG1, an autophagy regulator, inhibits cell growth by negatively regulating S6 kinase. *EMBO Reports, 8* (4), 360-365.

Levine, B., & Klionsky, D. J. (2004). Development by self-digestion: Molecular mechanisms and biological functions of autophagy. *Developmental Cell, 6* (4), 463-477.

Levine, B., & Kroemer, G. (2008).Autophagy in the pathogenesis of disease. *Cell, 132* (1), 27-42.

Liang, C., Feng, P., Ku, B., Dotan, I., Canaani, D., Oh, B., & Jung, J. U. (2006).Autophagic and tumour suppressor activity of a novel Beclin1-binding protein UVRAG. *Nature Cell Biology, 8* (7), 688-698.

Liang, X. H., Jackson, S., Seaman, M., Brown, K., Kempkes, B., Hibshoosh, H., & Levine, B. (1999). Induction of autophagy and inhibition of tumorigenesis by beclin 1. *Nature, 402* (6762), 672-676.

Loewith, R., Jacinto, E., Wullschleger, S., Lorberg, A., Crespo, J. L., Bonenfant, D., Hall, M. N. (2002). Two TOR complexes, only one of which is rapamycin sensitive, have distinct roles in cell growth control. *Molecular Cell, 10* (3), 457-468.

Lu, J., He, L., Behrends, C., Araki, M., Araki, K., Wang, Q. J., Fiel, M. I. (2014). NRBF2 regulates autophagy and prevents liver injury by modulating Atg14L-linked phosphatidylinositol-3 kinase III activity. *Nature Communications, 5*

Lünemann, J., & Münz, C. (2009). Autophagy in CD4 & plus; T-cell immunity and tolerance. *Cell Death & Differentiation, 16* (1), 79-86.

Ma, D., Bai, X., Guo, S., & Jiang, Y. (2008). The switch I region of rheb is critical for its interaction with FKBP38. *Journal of Biological Chemistry, 283* (38), 25963-25970.

Maiuri, M. C., Le Toumelin, G., Criollo, A., Rain, J. C., Gautier, F., Juin, P., Kroemer, G. (2007). Functional and physical interaction between bcl-X (L) and a BH3-like domain in beclin-1. *The EMBO Journal, 26* (10), 2527-2539.

Major, S. M., Nishizuka, S., Morita, D., Rowland, R., Sunshine, M., Shankavaram, U., Kane, D. (2006). AbMiner: A bioinformatic resource on available monoclonal antibodies and corresponding gene identifiers for genomic, proteomic, and immunologic studies.*BMC Bioinformatics, 7* (1), 192.

Mak, S. K., McCormack, A. L., Manning-Bog, A. B., Cuervo, A. M., & Di Monte, D. A. (2010).Lysosomal degradation of alpha-synuclein in vivo. *The Journal of Biological Chemistry, 285* (18), 13621-13629.

Mammucari, C., Milan, G., Romanello, V., Masiero, E., Rudolf, R., Del Piccolo, P., Zhao, J. (2007). FoxO3 controls autophagy in skeletal muscle in vivo. *Cell Metabolism, 6* (6), 458-471.

Mann, D., Iwatsubo, T., Cairns, N., Lantos, P., Nochlin, D., Sumi, S., Hutton, M. (1996). Amyloid β protein (Aβ) deposition in chromosome 14–linked Alzheimer's disease: Predominance of Aβ42 (43). *Annals of Neurology, 40* (2), 149-156.

Mann, S. S., & Hammarback, J. A. (1994). Molecular characterization of light chain 3. A microtubule binding subunit of MAP1A and MAP1B. *The Journal of Biological Chemistry, 269* (15), 11492-11497.

Manning, B. D., Tee, A. R., Logsdon, M. N., Blenis, J., & Cantley, L. C. (2002).Identification of the tuberous sclerosis complex-2 tumor suppressor gene product tuberin as a target of the phosphoinositide 3-kinase/akt pathway. *Molecular Cell, 10* (1), 151-162.

Martinez-Vicente, M., Talloczy, Z., Kaushik, S., Massey, A. C., Mazzulli, J., Mosharov, E. V., Cuervo, A. M. (2008). Dopamine-modified alpha-synuclein blocks chaperone-mediated autophagy. *The Journal of Clinical Investigation, 118* (2), 777-788.

Martinez-Vicente, M., Talloczy, Z., Wong, E., Tang, G., Koga, H., Kaushik, S., Sulzer, D. (2010). Cargo recognition failure is responsible for inefficient autophagy in Huntington's disease. *Nature Neuroscience, 13* (5), 567-576.

Matsunaga, K., Saitoh, T., Tabata, K., Omori, H., Satoh, T., Kurotori, N., Isobe, T. (2009). Two beclin 1-binding proteins, Atg14L and Rubicon, reciprocally regulate autophagy at different stages. *Nature Cell Biology, 11* (4), 385-396.

Matsuura, A., Tsukada, M., Wada, Y., & Ohsumi, Y. (1997). Apg1p, a novel protein kinase required for the autophagic process in< i> saccharomyces cerevisiae </i>.*Gene, 192* (2), 245-250.

Meijer, W. H., van der Klei, Ida J, Veenhuis, M., & Kiel, J. (2007). ATG genes involved in non-selective autophagy are conserved from yeast to man, but the selective cvt and pexophagy pathways also require organism-specific genes.*Autophagy, 3* (2), 106.

Meister, G., & Tuschl, T. (2004). Mechanisms of gene silencing by double-stranded RNA. Nature, *431* (7006), 343-349.

Menon, S., Dibble, C. C., Talbott, G., Hoxhaj, G., Valvezan, A. J., Takahashi, H., Manning, B. D. (2014). Spatial control of the TSC complex integrates insulin and nutrient regulation of mTORC1 at the lysosome. *Cell, 156* (4), 771-785.

Mercer, C. A., Kaliappan, A., & Dennis, P. B. (2009). A novel, human Atg13 binding protein, Atg101, interacts with ULK1 and is essential for macroautophagy. *Autophagy, 5* (5), 649-662.

Meredith, G., Totterdell, S., Petroske, E., Santa Cruz, K., Callison Jr, R., & Lau, Y. (2002). Lysosomal malfunction accompanies alpha-synuclein aggregation in a progressive mouse model of Parkinson's disease. *Brain Research, 956* (1), 156-165.

Mizushima, N. (2004). Methods for monitoring autophagy. *The International Journal of Biochemistry & Cell Biology, 36* (12), 2491-2502.

Mizushima, N. (2007). Autophagy: Process and function. *Genes & Development, 21* (22), 2861-2873.

Mizushima, N. (2010). The role of the Atg1/ULK1 complex in autophagy regulation. *Current Opinion in Cell Biology, 22* (2), 132-139.

Mizushima, N., & Yoshimori, T. (2007). How to interpret LC3 immunoblotting.*Autophagy, 3* (6), 542.

Mizushima, N., Levine, B., Cuervo, A. M., & Klionsky, D. J. (2008). Autophagy fights disease through cellular self-digestion. *Nature, 451* (7182), 1069-1075.

Mukhopadhyay, D., & Riezman, H. (2007). Proteasome-independent functions of ubiquitin in endocytosis and signaling. *Science (New York, N.Y.), 315*(5809), 201-205.

Nakajima, T., Takauchi, S., Ohara, K., Kokai, M., Nishii, R., Maeda, S., Seki, M. (2005). α-Synuclein-positive structures induced in leupeptin-infused rats. *Brain Research, 1040* (1), 73-80.

Nakatogawa, H., Ichimura, Y., & Ohsumi, Y. (2007). Atg8, a ubiquitin-like protein required for autophagosome formation, mediates membrane tethering and hemifusion. *Cell, 130* (1), 165-178.

Nakatogawa, H., Suzuki, K., Kamada, Y., & Ohsumi, Y. (2009). Dynamics and diversity in autophagy mechanisms: Lessons from yeast. *Nature Reviews Molecular Cell Biology, 10* (7), 458-467.

Nanni, L., & Lumini, A. (2008). A reliable method for cell phenotype image classification.*Artificial Intelligence in Medicine, 43* (2), 87-97.

Nazio, F., Strappazzon, F., Antonioli, M., Bielli, P., Cianfanelli, V., Bordi, M., Fimia, G. M. (2013). mTOR inhibits autophagy by controlling ULK1 ubiquitylation, self-association and function through AMBRA1 and TRAF6. *Nature Cell Biology, 15* (4), 406-416.

Neely, K. M., Green, K. N., & LaFerla, F. M. (2011). Presenilin is necessary for efficient proteolysis through the autophagy-lysosome system in a gamma-secretase-

independent manner. *The Journal of Neuroscience: The Official Journal of the Society for Neuroscience, 31* (8), 2781-2791.

Nixon, R. A. (2007). Autophagy, amyloidogenesis and Alzheimer disease. *Journal of Cell Science, 120* (Pt 23), 4081-4091.

Nixon, R. A., Wegiel, J., Kumar, A., Yu, W. H., Peterhoff, C., Cataldo, A., & Cuervo, A. M. (2005). Extensive involvement of autophagy in alzheimer disease: An immuno-electron microscopy study. *Journal of Neuropathology & Experimental Neurology, 64* (2), 113-122.

Noda, T., & Ohsumi, Y. (1998). Tor, a phosphatidylinositol kinase homologue, controls autophagy in yeast.*The Journal of Biological Chemistry, 273* (7), 3963-3966.

Nojima, H., Tokunaga, C., Eguchi, S., Oshiro, N., Hidayat, S., Yoshino, K., Yonezawa, K. (2003). The mammalian target of rapamycin (mTOR) partner, raptor, binds the mTOR substrates p70 S6 kinase and 4E-BP1 through their TOR signaling (TOS) motif. *Journal of Biological Chemistry, 278* (18), 15461-15464.

Pan, T., Kondo, S., Le, W., & Jankovic, J. (2008). The role of autophagy-lysosome pathway in neurodegeneration associated with Parkinson's disease.*Brain: A Journal of Neurology, 131* (Pt 8), 1969-1978.

Pankiv, S., Clausen, T. H., Lamark, T., Brech, A., Bruun, J. A., Outzen, H., Johansen, T. (2007). P62/SQSTM1 binds directly to Atg8/LC3 to facilitate degradation of ubiquitinated protein aggregates by autophagy. *The Journal of Biological Chemistry, 282* (33), 24131-24145.

Pattingre, S., Espert, L., Biard-Piechaczyk, M., & Codogno, P. (2008). Regulation of macroautophagy by mTOR and beclin 1 complexes. *Biochimie, 90* (2), 313-323.

Pattingre, S., Tassa, A., Qu, X., Garuti, R., Liang, X. H., Mizushima, N., Levine, B. (2005). Bcl-2 antiapoptotic proteins inhibit beclin 1-dependent autophagy. *Cell, 122* (6), 927-939.

Peterson, T. R., Laplante, M., Thoreen, C. C., Sancak, Y., Kang, S. A., Kuehl, W. M., Sabatini, D. M. (2009). DEPTOR is an mTOR inhibitor frequently overexpressed in multiple myeloma cells and required for their survival. *Cell, 137* (5), 873-886.

Pirkmajer, S., & Chibalin, A. V. (2011). Serum starvation: Caveat emptor.*American Journal of Physiology-Cell Physiology, 301* (2), C272-C279.

Polson, H. E., de Lartigue, J., Rigden, D. J., Reedijk, M., Urbé, S., Clague, M. J., & Tooze, S. A. (2010). Mammalian Atg18 (WIPI2) localizes to omegasome-anchored phagophores and positively regulates LC3 lipidation. *Autophagy, 6* (4), 506-522.

Portier, B. P., & Taglialatela, G. (2006). Bcl-2 localized at the nuclear compartment induces apoptosis after transient overexpression. *Journal of Biological Chemistry, 281* (52), 40493-40502.

Qu, X., Zou, Z., Sun, Q., Luby-Phelps, K., Cheng, P., Hogan, R. N., Levine, B. (2007). Autophagy gene-dependent clearance of apoptotic cells during embryonic development. *Cell, 128* (5), 931-946.

Ralston, S. H. (2008). Pathogenesis of Paget's disease of bone.*Bone, 43* (5), 819-825.

Ramanathan, A., & Schreiber, S. L. (2009). Direct control of mitochondrial function by mTOR. *Proceedings of the National Academy of Sciences, 106* (52), 22229-22232.

Ramos-Vara, J. A. (2005). Technical aspects of immunohistochemistry. *Veterinary Pathology, 42* (4), 405-426.

Randall-Demllo, S., Chieppa, M., & Eri, R. (2013). Intestinal epithelium and autophagy: Partners in gut homeostasis. *Frontiers in Immunology, 4*

Rapoport, T. A. (2007). Protein translocation across the eukaryotic endoplasmic reticulum and bacterial plasma membranes. *Nature, 450* (7170), 663-669.

Ravikumar, B., Acevedo-Arozena, A., Imarisio, S., Berger, Z., Vacher, C., O'Kane, C. J., Rubinsztein, D. C. (2005). Dynein mutations impair autophagic clearance of aggregate-prone proteins. *Nature Genetics, 37* (7), 771-776.

Ravikumar, B., Duden, R., & Rubinsztein, D. C. (2002). Aggregate-prone proteins with polyglutamine and polyalanine expansions are degraded by autophagy. *Human Molecular Genetics, 11* (9), 1107-1117.

Ravikumar, B., Vacher, C., Berger, Z., Davies, J. E., Luo, S., Oroz, L. G., O'Kane, C. J. (2004). Inhibition of mTOR induces autophagy and reduces toxicity of polyglutamine expansions in fly and mouse models of Huntington disease. *Nature Genetics, 36* (6), 585-595.

Reggiori, F., & Klionsky, D. J. (2013). Autophagic processes in yeast: Mechanism, machinery and regulation. *Genetics, 194* (2), 341-361.

Rhodes, K. J., & Trimmer, J. S. (2006). Antibodies as valuable neuroscience research tools versus reagents of mass distraction. *The Journal of Neuroscience: The Official Journal of the Society for Neuroscience, 26* (31), 8017-8020.

Rideout, H. J., Lang-Rollin, I., & Stefanis, L. (2004). Involvement of macroautophagy in the dissolution of neuronal inclusions. *The International Journal of Biochemistry & Cell Biology, 36* (12), 2551-2562.

Rioux, J. D., Xavier, R. J., Taylor, K. D., Silverberg, M. S., Goyette, P., Huett, A., Datta, L. W. (2007). Genome-wide association study identifies new susceptibility loci for crohn disease and implicates autophagy in disease pathogenesis. *Nature Genetics, 39* (5), 596-604.

Rockenstein, E., Schwach, G., Ingolic, E., Adame, A., Crews, L., Mante, M., Masliah, E. (2005). Lysosomal pathology associated with α-synuclein accumulation in transgenic models using an eGFP fusion protein. *Journal of Neuroscience Research, 80* (2), 247-259.

Rogov, V., Dötsch, V., Johansen, T., & Kirkin, V. (2014). Interactions between autophagy receptors and ubiquitin-like proteins form the molecular basis for selective autophagy. *Molecular Cell, 53* (2), 167-178.

Rosner, M., & Hengstschläger, M. (2008). Cytoplasmic and nuclear distribution of the protein complexes mTORC1 and mTORC2: Rapamycin triggers dephosphorylation

and delocalization of the mTORC2 components rictor and sin1. *Human Molecular Genetics, 17* (19), 2934-2948.

Rubinsztein, D. C. (2006). The roles of intracellular protein-degradation pathways in neurodegeneration. *Nature, 443* (7113), 780-786.

Sagiv, Y., Legesse-Miller, A., Porat, A., & Elazar, Z. (2000). GATE-16, a membrane transport modulator, interacts with NSF and the golgi v-SNARE GOS-28. *The EMBO Journal, 19* (7), 1494-1504.

Salmena, L., & Pandolfi, P. P. (2007). Changing venues for tumour suppression: Balancing destruction and localization by monoubiquitylation. *Nature Reviews Cancer, 7* (6), 409-413.

Sancak, Y., Bar-Peled, L., Zoncu, R., Markhard, A. L., Nada, S., & Sabatini, D. M. (2010). Ragulator-rag complex targets mTORC1 to the lysosomal surface and is necessary for its activation by amino acids. *Cell, 141* (2), 290-303.

Sancak, Y., Peterson, T. R., Shaul, Y. D., Lindquist, R. A., Thoreen, C. C., Bar-Peled, L., & Sabatini, D. M. (2008). The rag GTPases bind raptor and mediate amino acid signaling to mTORC1. *Science, 320* (5882), 1496-1501.

Sancak, Y., Thoreen, C. C., Peterson, T. R., Lindquist, R. A., Kang, S. A., Spooner, E., Sabatini, D. M. (2007). PRAS40 is an insulin-regulated inhibitor of the mTORC1 protein kinase. *Molecular Cell, 25* (6), 903-915.

Saper, C. B. (2005). An open letter to our readers on the use of antibodies. *Journal of Comparative Neurology, 493* (4), 477-478.

Saper, C. B., & Sawchenko, P. E. (2003). Magic peptides, magic antibodies: Guidelines for appropriate controls for immunohistochemistry. *Journal of Comparative Neurology, 465* (2), 161-163.

Sarbassov, d. D., Ali, S. M., & Sabatini, D. M. (2005).Growing roles for the mTOR pathway. *Current Opinion in Cell Biology, 17* (6), 596-603.

Sarbassov, D. D., Ali, S. M., Kim, D., Guertin, D. A., Latek, R. R., Erdjument-Bromage, H., Sabatini, D. M. (2004). Rictor, a novel binding partner of mTOR, defines a

rapamycin-insensitive and raptor-independent pathway that regulates the cytoskeleton. *Current Biology, 14* (14), 1296-1302.

Sarbassov, D. D., Ali, S. M., Sengupta, S., Sheen, J., Hsu, P. P., Bagley, A. F., Sabatini, D. M. (2006). Prolonged rapamycin treatment inhibits mTORC2 assembly and Akt/PKB. *Molecular Cell, 22* (2), 159-168.

Sarbassov, D. D., Guertin, D. A., Ali, S. M., & Sabatini, D. M. (2005). Phosphorylation and regulation of Akt/PKB by the rictor-mTOR complex. *Science (New York, N.Y.), 307* (5712), 1098-1101.

Saucedo, L. J., Gao, X., Chiarelli, D. A., Li, L., Pan, D., & Edgar, B. A. (2003). Rheb promotes cell growth as a component of the insulin/TOR signalling network. *Nature Cell Biology, 5* (6), 566-571.

Schägger, H., & Von Jagow, G. (1987).Tricine-sodium dodecyl sulfate-polyacrylamide gel electrophoresis for the separation of proteins in the range from 1 to 100 kDa. *Analytical Biochemistry, 166* (2), 368-379.

Schalm, S. S., & Blenis, J. (2002). Identification of a conserved motif required for mTOR signaling. *Current Biology, 12* (8), 632-639.

Schalm, S. S., Fingar, D. C., Sabatini, D. M., & Blenis, J. (2003).TOS motif-mediated raptor binding regulates 4E-BP1 multisite phosphorylation and function. *Current Biology, 13* (10), 797-806.

Schieke, S. M., Phillips, D., McCoy, J. P., Aponte, A. M., Shen, R., Balaban, R. S., & Finkel, T. (2006). The mammalian target of rapamycin (mTOR) pathway regulates mitochondrial oxygen consumption and oxidative capacity. *Journal of Biological Chemistry, 281*(37), 27643-27652.

Scott, J. D., & Pawson, T. (2009). Cell signaling in space and time: Where proteins come together and when they're apart. *Science (New York, N.Y.), 326* (5957), 1220-1224.

Scott, R. C., Juhász, G., & Neufeld, T. P. (2007). Direct induction of autophagy by Atg1 inhibits cell growth and induces apoptotic cell death. *Current Biology, 17* (1), 1-11.

Scott, R. C., Schuldiner, O., & Neufeld, T. P. (2004). Role and regulation of starvation-induced autophagy in the < i> Drosophila </i> fat body. *Developmental Cell, 7* (2), 167-178.

Sekito, T., Kawamata, T., Ichikawa, R., Suzuki, K., & Ohsumi, Y. (2009). Atg17 recruits Atg9 to organize the pre-autophagosomal structure. *Genes to Cells, 14* (5), 525-538.

Shen, J., & Kelleher, R. J. (2007). The presenilin hypothesis of Alzheimer's disease: Evidence for a loss-of-function pathogenic mechanism. *Proceedings of the National Academy of Sciences, 104* (2), 403-409.

Shirane, M., & Nakayama, K. I. (2003). Inherent calcineurin inhibitor FKBP38 targets bcl-2 to mitochondria and inhibits apoptosis. *Nature Cell Biology, 5* (1), 28-37.

Sofer, A., Lei, K., Johannessen, C. M., & Ellisen, L. W. (2005).Regulation of mTOR and cell growth in response to energy stress by REDD1. *Molecular and Cellular Biology, 25* (14), 5834-5845.

Solache, R., Brockett, T., Chuang, D. R., Clark, R. D., Fisher, A., & Yang, C. (2013). Evolving strategies for application-specific validation of research use antibodies. *Drug Discovery,*, 89.

Son, J. H., Shim, J. H., Kim, K., Ha, J., & Han, J. Y. (2012).Neuronal autophagy and neurodegenerative diseases. *Experimental & Molecular Medicine, 44* (2), 89-98.

Spencer, B., Potkar, R., Trejo, M., Rockenstein, E., Patrick, C., Gindi, R., Masliah, E. (2009). Beclin 1 gene transfer activates autophagy and ameliorates the neurodegenerative pathology in alpha-synuclein models of Parkinson's and lewy body diseases. *The Journal of Neuroscience: The Official Journal of the Society for Neuroscience, 29* (43), 13578-13588.

Spicer, S. S., Spivey, M. A., Ito, M., & Schulte, B. A. (1994). Some ascites monoclonal antibody preparations contain contaminants that bind to selected Golgi zones or mast cells. *The Journal of Histochemistry and Cytochemistry: Official Journal of the Histochemistry Society, 42* (2), 213-221.

Sridhar, S., Botbol, Y., Macian, F., & Cuervo, A. M. (2012). Autophagy and disease: Always two sides to a problem. *The Journal of Pathology, 226* (2), 255-273.

Stefanis, L., Larsen, K. E., Rideout, H. J., Sulzer, D., & Greene, L. A. (2001). Expression of A53T mutant but not wild-type alpha-synuclein in PC12 cells induces alterations of the ubiquitin-dependent degradation system, loss of dopamine release, and autophagic cell death. *The Journal of Neuroscience: The Official Journal of the Society for Neuroscience, 21* (24), 9549-9560.

Stocker, H., Radimerski, T., Schindelholz, B., Wittwer, F., Belawat, P., Daram, P., Hafen, E. (2003). Rheb is an essential regulator of S6K in controlling cell growth in drosophila. *Nature Cell Biology, 5* (6), 559-566.

Straub, M., Bredschneider, M., & Thumm, M. (1997). AUT3, a serine/threonine kinase gene, is essential for autophagocytosis in saccharomyces cerevisiae. *Journal of Bacteriology, 179* (12), 3875-3883.

Suzuki, K., Kubota, Y., Sekito, T., & Ohsumi, Y. (2007). Hierarchy of atg proteins in pre-autophagosomal structure organization. *Genes to Cells, 12* (2), 209-218.

Takeuchi, H., Kondo, Y., Fujiwara, K., Kanzawa, T., Aoki, H., Mills, G. B., & Kondo, S. (2005). Synergistic augmentation of rapamycin-induced autophagy in malignant glioma cells by phosphatidylinositol 3-kinase/protein kinase B inhibitors.*Cancer Research, 65* (8), 3336-3346.

Tanaka, Y., Guhde, G., Suter, A., Eskelinen, E., Hartmann, D., Lüllmann-Rauch, R., Saftig, P. (2000). Accumulation of autophagic vacuoles and cardiomyopathy in LAMP-2-deficient mice. *Nature, 406* (6798), 902-906.

Tanida, I., Sou, Y. S., Ezaki, J., Minematsu-Ikeguchi, N., Ueno, T., & Kominami, E. (2004). HsAtg4B/HsApg4B/autophagin-1 cleaves the carboxyl termini of three human Atg8 homologues and delipidates microtubule-associated protein light chain 3- and GABAA receptor-associated protein-phospholipid conjugates. *The Journal of Biological Chemistry, 279* (35), 36268-36276.

Tanida, I., Ueno, T., & Kominami, E. (2008). LC3 and autophagy.*Autophagosome and phagosome* (pp. 77-88) Springer.

Tanida, I., Ueno, T.,& Kominami, E. (2004). LC3 conjugation system in mammalian autophagy. *The International Journal of Biochemistry & Cell Biology, 36* (12), 2503-2518.

Tellez-Nagel, I., Johnson, A. B., . Terry, R. D. (1974). Studies on brain biopsies of patients with Huntington's chorea. *Journal of Neuropathology & Experimental Neurology, 33* (2), 308-332.

Tooze, S. A., Jefferies, H. B., Kalie, E., Longatti, A., Mcalpine, F. E., Mcknight, N. C., Robinson, D. J. (2010). Trafficking and signaling in mammalian autophagy. *IUBMB Life, 62* (7), 503-508.

Vander Haar, E., Lee, S., Bandhakavi, S., Griffin, T. J., & Kim, D. (2007). Insulin signalling to mTOR mediated by the Akt/PKB substrate PRAS40. *Nature Cell Biology, 9* (3), 316-323.

Vassar, R., Bennett, B. D., Babu-Khan, S., Kahn, S., Mendiaz, E. A., Denis, P., Citron, M. (1999). Beta-secretase cleavage of Alzheimer's amyloid precursor protein by the transmembrane aspartic protease BACE. *Science (New York, N.Y.), 286* (5440), 735-741.

Vergne, I., Roberts, E., Elmaoued, R. A., Tosch, V., Delgado, M. A., Proikas-Cezanne, T., Deretic, V. (2009). Control of autophagy initiation by phosphoinositide 3-phosphatase jumpy. *The EMBO Journal, 28* (15), 2244-2258.

Vingtdeux, V., Giliberto, L., Zhao, H., Chandakkar, P., Wu, Q., Simon, J. E., Marambaud, P. (2010). AMP-activated protein kinase signaling activation by resveratrol modulates amyloid-beta peptide metabolism. *The Journal of Biological Chemistry, 285* (12), 9100-9113.

Vogiatzi, T., Xilouri, M., Vekrellis, K., & Stefanis, L. (2008). Wild type alpha-synuclein is degraded by chaperone-mediated autophagy and macroautophagy in neuronal cells. *The Journal of Biological Chemistry, 283* (35), 23542-23556.

Wang, H., Ma, J., Tan, Y., Wang, Z., Sheng, C., Chen, S., & Ding, J. (2010). Amyloid-β 1-42 induces reactive oxygen species-mediated autophagic cell death in U87 and SH-SY5Y cells. *Journal of Alzheimer's Disease, 21* (2), 597-610.

Wang, L., Harris, T. E., Roth, R. A., & Lawrence, J. C., Jr. (2007). PRAS40 regulates mTORC1 kinase activity by functioning as a direct inhibitor of substrate binding. *The Journal of Biological Chemistry, 282* (27), 20036-20044.

Wang, S., & Hung, M. (2005). Cytoplasmic/nuclear shuttling and tumor progression. *Annals of the New York Academy of Sciences, 1059* (1), 11-15.

Wang, X., & Proud, C. G. (2011).mTORC1 signaling: What we still don't know. *Journal of Molecular Cell Biology, 3* (4), 206-220.

Wang, Y., Martinez-Vicente, M., Kruger, U., Kaushik, S., Wong, E., Mandelkow, E. M., Mandelkow, E. (2009). Tau fragmentation, aggregation and clearance: The dual role of lysosomal processing. *Human Molecular Genetics, 18* (21), 4153-4170.

Webb, J. L., Ravikumar, B., & Rubinsztein, D. C. (2004). Microtubule disruption inhibits autophagosome-lysosome fusion: Implications for studying the roles of aggresomes in polyglutamine diseases. *The International Journal of Biochemistry & Cell Biology, 36* (12), 2541-2550.

Webb, J. L., Ravikumar, B., Atkins, J., Skepper, J. N., & Rubinsztein, D. C. (2003). Alpha-synuclein is degraded by both autophagy and the proteasome. *The Journal of Biological Chemistry, 278* (27), 25009-25013.

Wei, Y., Pattingre, S., Sinha, S., Bassik, M., & Levine, B. (2008). JNK1-mediated phosphorylation of bcl-2 regulates starvation-induced autophagy. *Molecular Cell, 30* (6), 678-688.

Whitney, M. L., Jefferson, L. S., & Kimball, S. R. (2009). ATF4 is necessary and sufficient for ER stress-induced upregulation of REDD1 expression. *Biochemical and Biophysical Research Communications, 379* (2), 451-455.

Wilkinson, K. D. (2005). The discovery of ubiquitin-dependent proteolysis. *Proceedings of the National Academy of Sciences of the United States of America, 102* (43), 15280-15282.

Wirth, M., Joachim, J., & Tooze, S. A. (2013).Autophagosome formation—the role of ULK1 and Beclin1–PI3KC3 complexes in setting the stage.*Seminars in Cancer Biology,, 23* (5) 301-309.

Woo, S. Y., Kim, D. H., Jun, C. B., Kim, Y. M., Haar, E. V., Lee, S. I., Kim, D. H. (2007). PRR5, a novel component of mTOR complex 2, regulates platelet-derived growth factor receptor beta expression and signaling. *The Journal of Biological Chemistry, 282* (35), 25604-25612.

Wullschleger, S., Loewith, R., & Hall, M. N. (2006).TOR signaling in growth and metabolism. *Cell, 124* (3), 471-484.

Xie, Z., & Klionsky, D. J. (2007). Autophagosome formation: Core machinery and adaptations. *Nature Cell Biology, 9* (10), 1102-1109.

Xilouri, M., Vogiatzi, T., Vekrellis, K., Park, D., & Stefanis, L. (2009). Abberant α-synuclein confers toxicity to neurons in part through inhibition of chaperone-mediated autophagy. *PloS One, 4* (5), e5515.

Yadav, R. B., Burgos, P., Parker, A. W., Iadevaia, V., Proud, C. G., Allen, R. A., Botchway, S. W. (2013). mTOR direct interactions with rheb-GTPase and raptor: Sub-cellular localization using fluorescence lifetime imaging.*BMC Cell Biology, 14* (1), 3.

Yamamoto, A., & Simonsen, A. (2011). The elimination of accumulated and aggregated proteins: A role for aggrephagy in neurodegeneration. *Neurobiology of Disease, 43* (1), 17-28.

Yan, J., Kuroyanagi, H., Kuroiwa, A., Matsuda, Y., Tokumitsu, H., Tomoda, T., Muramatsu, M. (1998). Identification of mouse ULK1, a novel protein kinase structurally related to < i> C. elegans </i> UNC-51. *Biochemical and Biophysical Research Communications, 246* (1), 222-227.

Yan, J., Kuroyanagi, H., Tomemori, T., Okazaki, N., Asato, K., Matsuda, Y., Muramatsu, M. (1999). Mouse ULK2, a novel member of the UNC-51-like protein kinases: Unique features of functional domains. *Oncogene, 18* (43), 5850-5859.

Yip, C. K., Murata, K., Walz, T., Sabatini, D. M., & Kang, S. A. (2010). Structure of the human mTOR complex I and its implications for rapamycin inhibition. *Molecular Cell, 38* (5), 768-774.

Ylä-Anttila, P., Vihinen, H., Jokitalo, E., & Eskelinen, E. (2009). 3D tomography reveals connections between the phagophore and endoplasmic reticulum. *Autophagy, 5* (8), 1180-1185.

Yonezawa, K., Tokunaga, C., Oshiro, N., & Yoshino, K. (2004).Raptor, a binding partner of target of rapamycin. *Biochemical and Biophysical Research Communications, 313* (2), 437-441.

Young, A. R., Chan, E. Y., Hu, X. W., Köchl, R., Crawshaw, S. G., High, S., Tooze, S. A. (2006). Starvation and ULK1-dependent cycling of mammalian Atg9 between the TGN and endosomes. *Journal of Cell Science, 119* (18), 3888-3900.

Young, A. R., Narita, M., Ferreira, M., Kirschner, K., Sadaie, M., Darot, J. F., Narita, M. (2009). Autophagy mediates the mitotic senescence transition. *Genes & Development, 23* (7), 798-803.

Yousefi, S., Perozzo, R., Schmid, I., Ziemiecki, A., Schaffner, T., Scapozza, L., Simon, H. (2006). Calpain-mediated cleavage of Atg5 switches autophagy to apoptosis.*Nature Cell Biology, 8* (10), 1124-1132.

Yu, W. H., Cuervo, A. M., Kumar, A., Peterhoff, C. M., Schmidt, S. D., Lee, J., Tjernberg, L. O. (2005). Macroautophagy—a novel β-amyloid peptide-generating pathway activated in Alzheimer's disease. *The Journal of Cell Biology, 171* (1), 87-98.

Zhang, J., Kang, D. E., Xia, W., Okochi, M., Mori, H., Selkoe, D. J., & Koo, E. H. (1998).Subcellular distribution and turnover of presenilins in transfected cells. *Journal of Biological Chemistry, 273* (20), 12436-12442.

Zhang, X., Garbett, K., Veeraraghavalu, K., Wilburn, B., Gilmore, R., Mirnics, K., & Sisodia, S. S. (2012). A role for presenilins in autophagy revisited: Normal acidification of lysosomes in cells lacking PSEN1 and PSEN2. *The Journal of Neuroscience: The Official Journal of the Society for Neuroscience, 32* (25), 8633-8648.

Zhang, X., Qi, L., Wu, J., & Qin, Z. (2013). DRAM1 regulates autophagy flux through lysosomes. *PloS One, 8* (5), e63245.

Zhao, J., Brault, J. J., Schild, A., Cao, P., Sandri, M., Schiaffino, S., Goldberg, A. L. (2007). FoxO3 coordinately activates protein degradation by the autophagic/lysosomal and proteasomal pathways in atrophying muscle cells. *Cell Metabolism, 6* (6), 472-483.

Zhao, Y., Yang, J., Liao, W., Liu, X., Zhang, H., Wang, S., Zhu, W. (2010). Cytosolic FoxO1 is essential for the induction of autophagy and tumour suppressor activity. *Nature Cell Biology, 12* (7), 665-675.

Zhou, J., Tan, S., Nicolas, V., Bauvy, C., Yang, N., Zhang, J., Shen, H. (2013). Activation of lysosomal function in the course of autophagy via mTORC1 suppression and autophagosome-lysosome fusion. *Cell Research, 23* (4), 508-523.